

5-11-2018


# Environmental Dynamics of Dissolved Organic Matter and Dissolved Black Carbon in Fluvial Systems: Effects of Biogeochemistry and Land Use

J. Alan Roebuck Jr.

*Southeast Environmental Research Center and Department of Chemistry and Biochemistry, Florida International University,*  
jroeb002@fiu.edu

**DOI:** 10.25148/etd.FIDC006880

Follow this and additional works at: <https://digitalcommons.fiu.edu/etd>

 Part of the [Biogeochemistry Commons](#), [Environmental Chemistry Commons](#), and the [Hydrology Commons](#)

---

## Recommended Citation

Roebuck, J. Alan Jr., "Environmental Dynamics of Dissolved Organic Matter and Dissolved Black Carbon in Fluvial Systems: Effects of Biogeochemistry and Land Use" (2018). *FIU Electronic Theses and Dissertations*. 3755.  
<https://digitalcommons.fiu.edu/etd/3755>

This work is brought to you for free and open access by the University Graduate School at FIU Digital Commons. It has been accepted for inclusion in FIU Electronic Theses and Dissertations by an authorized administrator of FIU Digital Commons. For more information, please contact [dcc@fiu.edu](mailto:dcc@fiu.edu).

FLORIDA INTERNATIONAL UNIVERSITY

Miami, Florida

ENVIRONMENTAL DYNAMICS OF DISSOLVED ORGANIC MATTER AND  
DISSOLVED BLACK CARBON IN FLUVIAL SYSTEMS: EFFECTS OF  
BIOGEOCHEMISTRY AND LAND USE

A dissertation submitted in partial fulfillment of

the requirements for the degree of

DOCTOR OF PHILOSOPHY

in

CHEMISTRY

by

Jesse Alan Roebuck, Jr.

2018

To: Dean Michael R. Heithaus  
College of Arts, Sciences and Education

This dissertation, written by Jesse Alan Roebuck, Jr., and entitled Environmental Dynamics of Dissolved Organic Matter and Dissolved Black Carbon in Fluvial Systems: Effects of Biogeochemistry and Land Use, having been approved in respect to style and intellectual content, is referred to you for judgment.

We have read this dissertation and recommend that it be approved.

---

Yong Cai

---

Piero Gardinali

---

Anthony DeCaprio

---

John Kominoski

---

Rudolf Jaffé, Major Professor

Date of Defense: May 11, 2018

The dissertation of Jesse Alan Roebuck, Jr. is approved.

---

Dean Michael R. Heithaus  
College of Arts, Sciences and Education

---

Andrés G. Gil  
Vice President for Research and Economic Development  
and Dean of the University Graduate School

Florida International University, 2018

© Copyright 2018 by Jesse Alan Roebuck, Jr.

All rights reserved.

## DEDICATION

To my family for your love and continued support of my academic pursuits

&

To Kirk Sydney – It has been an amazing four years and I cannot wait for more adventures to come...I love you to the moon and back.

## ACKNOWLEDGMENTS

I would first like to thank my major advisor, Rudolf Jaffé. I am humbled to have been a part of your lab these past four years. You have been a constant motivator and positive support system in both my academic and personal endeavors. I am lucky to have an advisor with a strong dedication to science and the academic success of his students. I am forever grateful for the opportunities you have provided and doors you have opened for me to meet and collaborate with new people. You continue to inspire me to ask more questions, push myself to new limits, and continue in pursuits to discover the undiscovered...even if it involves the side of a bridge in Georgia with 18-wheelers passing by full steam head. I am truly honored to be your last student.

I would also like to thank my committee members John Kominoski, Piero Gardinali, Yong Cai, and Anthony DeCaprio for your constructive comments and suggestions during committee meetings. I would also like to acknowledge our many collaborators who have contributed to this research. In particular to Michael Gonsior for providing Amazon River samples, Patricia Medeiros (and her lab group) for collecting monthly samples in the Altamaha River, as well as Thorsten Dittmar, Michael Seidel, and David Podgorski for collecting mass spec data on a number of samples. Appreciation is extended to both Patricia Medeiros and Aron Stubbins for providing lab space during a week of sampling in Altamaha River. Special thanks to Nicolas Jaffé for assistance with GIS programs, Phoebe Zito and Kaelin Cawley for teaching me to build PARAFAC models, and Sasha Wagner for training me with the black carbon method.

I would like to thank the Department of Chemistry and Biochemistry for providing salary support through teaching assistantships. I would also like to thank the

National Science Foundation and the Florida Coastal Everglades Long Term Ecological Research program as well as the Southeast Environmental Research Center's George Barley Endowment (awarded to Rudolf Jaffé) for providing additional salary support, funding for sample collection and processing, and travel support to attend a number of workshops and conferences.

I have had the fortunate privilege of sharing the lab with a number of Jaffé group alumni and am grateful to them for making time in the lab fun and enjoyable: Sasha Wagner, Kaelin Cawley, Wenxi Huang, Oliva Pisani, and Helen Du. Special thanks to Peter Regier, who continues to be my travel buddy and always knew the whereabouts of free food. I would like to thank Heather Black for keeping me motivated during my final year in an empty lab. Thanks to all of my friends for making time outside of the lab in Miami an enjoyable experience and for making my Christmas party a success each year!

I would like to thank my family (Hi, Molly) for your unconditional love, support and encouragement, as well as additional financial assistance from time to time. To Kirk Sydney – you have been my rock to lean on and I am grateful to have gone on this journey with you by my side. To many other friends and family who have shown encouragement and support over the years, I am truly grateful.

ABSTRACT OF THE DISSERTATION  
ENVIRONMENTAL DYNAMICS OF DISSOLVED ORGANIC MATTER AND  
DISSOLVED BLACK CARBON IN FLUVIAL SYSTEMS: EFFECTS OF  
BIOGEOCHEMISTRY AND LAND USE

by

Jesse Alan Roebuck, Jr.

Florida International University, 2018

Miami, Florida

Professor Rudolf Jaffé, Major Professor

Black carbon (BC) is an organic residue formed primarily from biomass burning (e.g., wildfires) and fossil fuel combustion. Until recently, it was understood that BC was highly recalcitrant and stabilized in soils over millennial scales. However, a fraction of the material can be solubilized and transported in fluvial systems as dissolved BC (DBC), which represents on average 10% of the global export of dissolved organic carbon (DOC) from rivers to coastal systems. The composition of DBC controls its reactivity, and it has been linked with a variety of in-stream processes that induce both carbon sequestration and evasion of CO<sub>2</sub> from aquatic systems, which suggest DBC may have a significant contribution within the global carbon cycle.

The primary objectives for the thesis were to elucidate environmental factors that control the fate and transport of DBC in fluvial systems. Ultra-high resolution mass spectrometry was used to characterize DBC on a molecular scale whereas benzenepolycarboxylic acids were used to quantify and characterize BC in both dissolved and particulate phases (PBC). Sinks for polycondensed DBC were linked to a series of in-



stream biogeochemical processes (e.g., photodegradation, metal interactions); whereas photooxidation of particulate charcoal led to production of DBC, suggesting photodissolution as a previously unrecognized source of DBC to fluvial systems. Coupling of DBC with PBC, however, was hydrologically constrained with sources varying over temporal scales and land use regimes. For DBC in particular, an enrichment of heteroatomic functionality was observed as a function of anthropogenic land use. Furthermore, land use coupled with stream order (a proxy for in-stream processing as defined by the River Continuum Concept) could explain significant spatial variability in organic matter (e.g., DOC) composition within an anthropogenically impacted system.

With an increase in wildfire frequency projected with on-going climate change trends, parallel projections for increases in BC production are also expected. Furthermore, conversion of natural landscapes for urban and agricultural practices is also expected to continue in the coming decades. Thus, it is imperative to reach a comprehensive understanding of processes regulating the transport of DBC in fluvial systems with efforts to constrain future BC budgets and climate change models.

## TABLE OF CONTENTS

CHAPTER	PAGE
I. INTRODUCTION.....	1
1.1 Introduction.....	2
1.2 References.....	8
II. ENVIRONMENTAL DYNAMICS OF DISSOLVED BLACK CARBON IN THE AMAZON RIVER.....	11
2.1 Abstract.....	12
2.2 Introduction.....	13
2.3 Methods.....	16
2.3.1 Sample Collection.....	16
2.3.2 Isolation and Quantification of DBC.....	17
2.3.3 Ultra-High Resolution Mass Spectrometry.....	18
2.3.4 Incubation of DOM with Mineral Clays.....	18
2.3.5 Incubation of DOM with Iron.....	19
2.4 Results and Discussion.....	19
2.4.1. DBC Composition in Amazonian Tributaries.....	19
2.4.2 Adsorption of DBC to Mineral Clays.....	23
2.4.3 Selective Co-precipitation of DBC with Iron.....	24
2.4.4 Ultra-High Resolution Mass Spectrometry.....	26
2.5 Conclusions.....	27
2.6 References.....	28
III. PHOTODISSOLUTION OF CHARCOAL AND FIRE-IMPACTED SOIL AS A POTENTIAL SOURCE OF DISSOLVED BLACK CARBON IN AQUATIC ENVIRONMENTS.....	33
3.1 Abstract.....	34
3.2 Introduction.....	34
3.3 Methods.....	36
3.3.1 Sample Collection.....	36
3.3.2 Experimental Setup.....	37
3.3.3 Quantification of DBC.....	38
3.3.4 Ultra-High Resolution Mass Spectrometry.....	39
3.4 Results.....	39
3.4.1 Photoproduction of DBC.....	39
3.4.2 Photoproduction of DOC.....	40
3.4.3 Ultra-High Resolution Mass Spectrometry.....	42
3.5 Discussion.....	44
3.5.1 Photoproduction of DOC and DBC.....	44
3.5.2 Mobilization of BC.....	49
3.6 Conclusions.....	50
3.7 References.....	51

IV. HYDROLOGICAL CONTROLS ON THE SEASONAL VARIABILITY OF DISSOLVED AND PARTICULATE BLACK CARBON IN THE ALTAMAHA RIVER, GA.....	55
4.1 Abstract.....	56
4.2 Introduction.....	57
4.3 Methods.....	61
4.3.1 Altamaha River Watershed Description .....	61
4.3.2 Sample Collection and Processing.....	62
4.3.2.1 Collection.....	62
4.3.2.2 Bulk Analyses.....	63
4.3.2.3 Optical Analyses.....	64
4.3.2.4 Hydrological Data.....	64
4.3.3 Quantification of DBC and PBC.....	65
4.4 Results.....	67
4.4.1 Watershed Hydrology.....	67
4.4.2 Seasonal Distribution of Dissolved and Particulate Organic Carbon.....	67
4.4.3 Seasonal Distribution of Dissolved and Particulate Black Carbon...69	
4.4.4 Organic Matter Fluxes from the Altamaha River .....	71
4.5 Discussion.....	72
4.5.1 Temporal Controls on Sources and Export of DOC .....	72
4.5.2 Sources and Export of DBC during Low Flow Regimes.....	73
4.5.3 Sources and Export of DBC during High Flow Regimes .....	75
4.5.4 Decoupling Between DOC and DBC .....	79
4.5.5 Hydrological Controls on the Export of POC and PBC .....	80
4.5.6 Seasonal Variability in PBC Source .....	83
4.5.7 Seasonal Coupling of PBC and DBC.....	86
4.6 Conclusion .....	88
4.7 References.....	90
V. LAND USE CONTROLS ON THE SPATIAL VARIABILITY OF DISSOLVED BLACK CARBON IN A SUBTROPICAL WATERSHED .....	99
5.1 Abstract.....	100
5.2 Introduction.....	101
5.3 Methods.....	104
5.3.1 Site Description.....	104
5.3.2 Sample Collection.....	105
5.3.3 Dissolved Black Carbon Analysis .....	107
5.3.4 Development of Conservative Mixing Model for the Altamaha River .....	108
5.3.5 Ultra-High Resolution Mass Spectrometry.....	109
5.3.6 Statistical Analysis.....	110
5.4 Results.....	112

5.5 Discussion.....	113
5.5.1 DBC Fluxes and Conservative Mixing Along the Altamaha River Continuum.....	113
5.5.2 Land Use Controls on DBC Concentration and Composition.....	116
5.5.3 Land Use Controls on Molecular Composition of DBC.....	120
5.5.4 Environmental Implications and Future Directions.....	125
5.6References.....	126
VI. CHARACTERIZATION OF DISSOLVED ORGANIC MATTER ALONG A RIVER CONTINUUM: LINKING WATERSHED LAND USE TO THE RIVER CONTINUUM CONCEPT.....	133
6.1 Abstract.....	134
6.2 Introduction.....	135
6.3 Methods.....	138
6.3.1 Sample Locations and Collection .....	138
6.3.2 Water Quality Analyses .....	140
6.3.3 Optical Properties and Parallel Factor Analysis .....	141
6.3.4 Ultra-High Resolution Mass Spectrometry.....	141
6.3.5 Statistical Analysis and Land Use.....	142
6.4 Results.....	143
6.5 Discussion.....	148
6.5.1 Identification of PARAFAC Components.....	148
6.5.2 Shifts in DOM Composition along the Altamaha River Continuum.....	151
6.5.3 Land Use Controls on DOM Composition .....	155
6.5.4 Spatial Variability in DOM Composition: Land Use vs Stream Order (RCC).....	158
6.6 References.....	163
VII. CONCLUSIONS.....	174
APPENDICES.....	179
VITA.....	197

LIST OF TABLES

TABLE	PAGE
2.1 BPCA and FTICR-MS information for the respective Amazonian tributaries.....	21
2.2 Results of a 24 hour DBC adsorption experiment with common mineral clays found within the Amazon basin .....	24
3.1 Photodissolution experimental data .....	41
3.2 FTICR-MS information for light exposed samples and dark controls at 2 and 7 days .....	43
6.1 Pearson’s product-moment correlation coefficient (r) showing correlations between watershed land use with water quality parameters, EEM-PARAFAC components, and FTICR-MS molecular compound classes that are significant a $p < 0.01$ and $p < 0.05$ .....	146

## LIST OF FIGURES

FIGURE	PAGE
1.1 Black carbon combustion continuum.....	3
1.2 Recent global black carbon budget.....	4
2.1 Map of Amazon River drainage basin .....	16
2.2 Graphs displaying respective results for a 24 hour DBC co-precipitation experiment with iron using (a) SRFA and (b) SRHA.....	25
3.1 Graph showing change in amount of photoproducted DBC over the 7 days photoincubation.....	45
3.2 FTICR-MS data in the form of van Krevelen diagrams displaying (a) unique molecular formulae identified as a comparison of light samples at 2 and 7 days, and (b) unique molecular formulae identified as a comparison between the light exposed char and the dark controls at 7 days.....	48
4.1 Map of Altamaha River Watershed with monthly sampling and USGS information.....	63
4.2 Water discharge (a) and daily rain data collected at USGS monitoring stations in (b) the South River – Atlanta, GA, (c) the Oconee River – Dublin, GA, and (d) the Altamaha River – Doctortown, GA.....	65
4.3 Seasonal patterns of DOC and POC related parameters in the Altamaha River .....	68
4.4 Seasonal patterns of DBC and PBC related parameters in the Altamaha River.....	70
5.1 Map of Altamaha River watershed displaying the 41 sample locations primarily from the Oconee River drainage basin.....	106
5.2 Map displaying land cover characteristics throughout the Altamaha River watershed .....	111
5.3 Spatial distribution of (a) DBC and (b) DBC composition (BPCA ratio) within the Altamaha River .....	114
5.4 A principal component analysis of the intensity mean-centered DBC molecular formulae as determined by FTICR-MS analysis.....	122

6.1 Map of Altamaha River (a) land use and (b) sample locations categorized by stream order .....	139
6.2 A 5-component PARAFAC model for the Altamaha River .....	149
6.3 Distribution of EEM-PARAFAC components and FTICR-MS molecular compound classes as a function of stream order in the Altamaha River .....	150
6.4 Redundancy analysis using stream order (i.e., RCC) and land use as predictor variables for the spatial distribution of EEM-PARAFAC components in the Altamaha River .....	160
6.5 Redundancy analysis using stream order (i.e., RCC) and land use as predictor variables for the spatial distribution of FTICR-MS molecular compound classes in the Altamaha River watershed.....	161

## CHAPTER I

### INTRODUCTION



## 1.1 Introduction

Dissolved organic matter (DOM) is an important component of fluvial systems and can greatly influence river dynamics and ecosystem functions. Among its many functions include controls on river primary production through light attenuation (Zhang et al., 2007), transport of metals (Yamashita and Jaffé, 2008), and serving as an energy source for residing heterotrophic communities (Kaplan et al., 2008). Dissolved organic matter is heterogeneous by nature and its role in ecosystem functions are significantly influenced by its source material (terrestrial inputs versus in-stream primary production).

A useful model that has been used to predict changing DOM dynamics during downstream transport is the River Continuum Concept (RCC, Vannote et al. (1980)). The RCC predicts enhanced inputs of molecularly complex DOM in small headwater streams. As stream order increases, molecular complexity of DOM decreases as selective labile components are removed from the system. While the RCC was developed specifically for undisturbed systems, it does not account for an increase in anthropogenic activities such as land use that may significantly alter the DOM characteristics. For instance, an increase in agricultural land use can supply local rivers with nutrients thereby fueling microbial activity and in-stream production of DOM (Carpenter et al., 1998; Williams et al., 2010; Wilson and Xenopoulos, 2008). While others have also suggested increasing DOM complexity with increasing agricultural land use (Graeber et al., 2012), the effects of land use may be variable in different fluvial systems and regulation of DOM may compete with a river's biogeochemical properties as determined by stream order, for example. In any case, it is commonly assumed that DOM composition is not only related to in-stream processes, but also to the composition of soil organic matter (SOM) in the watershed. As

such, land use change commonly modifies SOM composition, which can be reflected within the DOM exported within the watershed (Chantigny, 2003).

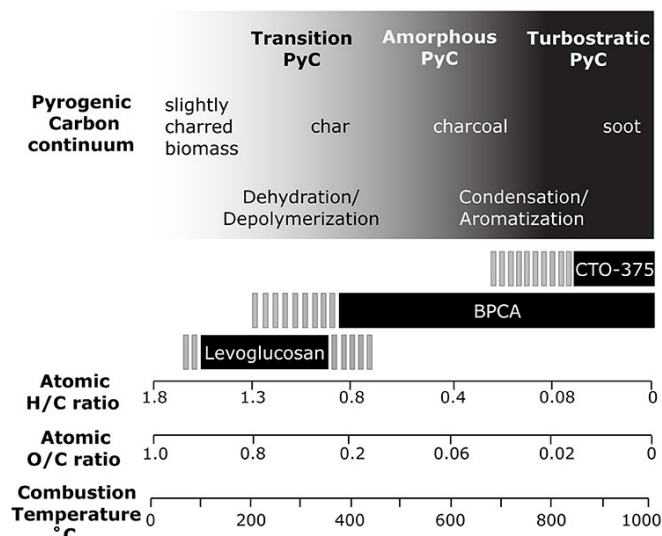


**Figure 1.1:** Black carbon combustion continuum (Myers-Pigg et al., 2017)

Another significant component of SOM is black carbon (BC). Black carbon is an important, but often overlooked, component of the global carbon cycle that is formed through incomplete combustion of biomass during wildfires and fossil fuel burning (Goldberg, 1985). The nature and composition of BC can be best described using a combustion continuum (Figure 1.1), which defines BC as a heterogeneous mixture organic material ranging from slightly charred biomass formed at lower combustion temperatures to soot particles from high temperature combustion (Masiello, 2004). While slightly charred materials may keep some functionalities of its original source material, the nature of the BC formed can be an indication of source material and formation conditions as increasing charring temperatures amplify production of more refractory BC material with an enhanced polycondensed signature (Baldock and Smernik, 2002; Schneider et al., 2010).

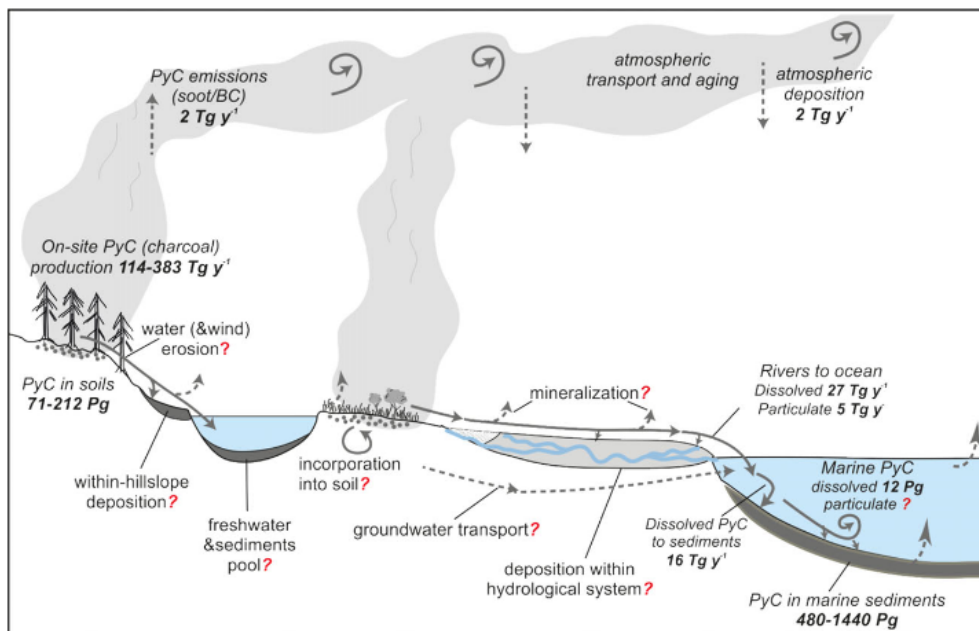


**Figure 1.2:** Recent global black carbon budget (Santín et al., 2016)

It is estimated that up to 383 Tg of BC is produced annually from vegetation fires (Figure 1.2). A small portion of BC (2 Tg y<sup>-1</sup>) is emitted to the atmosphere whereas a significant portion (212 Tg y<sup>-1</sup>) remains local and becomes incorporated in the soil matrix (Santín et al., 2016). Because BC composition is believed to largely consist of pyrolyzed, condensed aromatic material, it has commonly been considered highly refractory and expected to have soil residence times of millennia, and thus has been considered a global carbon sink (Bird et al., 2015). However, if BC is indeed very refractory, it has been estimated that it should represent up to 125% of soil matrices assuming production of BC has been consistent over the past tens of thousands of years (Masiello, 2004). Yet the BC content of soils and sediments is estimated on the order of 5-15% of the total organic carbon (Hockaday et al., 2007). The imbalance in the BC budget suggests there exist a significant labile portion of BC that can mobilized out of the

soil matrix, which may then be further translocated to other environmental compartments (such as the aqueous phase) and undergo additional biogeochemical processing.

Recent studies suggest that BC turnover rates in soils can vary over short to long time scales. For instance, Zimmerman (2010) has shown that a small portion of BC is respired to CO<sub>2</sub>. Particulate BC (PBC) can be mobilized and transported in fluvial systems as a result of increased post-wildfire soil erosion (Wagner et al., 2015a). In addition, BC stored in soils can undergo microbial oxidation processes, which can facilitate a small short-term loss (< 3%) of BC through respiration to CO<sub>2</sub> (Zimmerman, 2010). However, in the long-term, microbial oxidation can also facilitate the translocation and transport of dissolved BC (DBC) in fluvial systems by increasing its polar functionality (Abiven et al., 2011; Hockaday et al., 2006). Dissolved black carbon is an important component of riverine dissolved organic carbon (DOC) with an estimated 26.5 million metric tons exported to the oceans annually (Jaffé et al., 2013). Globally, riverine export of DBC and DOC are also highly correlated suggesting that similar mechanisms controlling the release and transport of DBC from soils is similar to that of DOC (Jaffé et al., 2013).

During transport to the ocean, DBC may undergo significant transformations that may affect its mobility and stability throughout a fluvial system. For instance, similar to DOC, high molecular weight DBC can be selectively removed from aquatic systems through photodegradation processes (Stubbins et al., 2012). However, photochemical processes have also been shown to increase production of DOC through photodissolution of particulate organic carbon (POC) (Mayer et al., 2006; Mayer et al., 2012; Pisani et al., 2011). Thus, it may also be expected that DBC can be generated through

photodissolution of char, though this has yet to be determined. Dissolved black carbon may also be susceptible to other environmental processes known to affect downstream transport of DOC, such as flocculation or sorption to clay minerals (Gu et al., 1995; Kothawala et al., 2012; Riedel et al., 2012).

Despite our current understanding of BC mobility, little is known about the systematic and physical processes regulating DBC in fluvial systems (Figure 1.2). The biogeochemical processes regulating DOM and associated DBC in rivers are often reflective of changing river dynamics and the landscapes that they drain. Thus, DOM characteristics can be reflective of changes in watershed activity, such as wildfires or shifts to anthropogenically impacted landscapes (Parr et al., 2015; Wagner et al., 2015b; Wilson and Xenopoulos, 2008). Similar patterns of compositional change in the DBC could be reflective of land use variations, but have not been reported in the literature. However, while Wagner et al. (2015a) have shown a post wildfire increase in export of PBC, the coupling between DBC and PBC appeared to be minimal in the small river setting they studied. Surprisingly, there have been no direct correlations of increasing DBC export because of increased fire activity (Ding et al., 2013; Wagner et al., 2015a), but DBC is still exported from rivers even decades after the most recent burn activity in the surrounding watershed (Dittmar et al., 2012). The long-term export of DBC may in fact complicate the establishment of a correlation between DBC character with fire history and/or land use. However, differences in DBC source, namely wildfire vs. fossil fuels, have been determined in different environments (Khan et al., 2016; Ding et al., 2015), and as such DBC composition may be affected by urban runoff. In addition, Wagner et al. (2015b) has shown that an increase in nitrogen containing DBC in world

rivers was correlated with an increase in watershed anthropogenic activity. Others have also shown that DBC in areas likely affected by fossil fuel combustion is less polycondensed in character in comparison to what is expected from wildfire derived DBC (Ding et al., 2015; Khan et al., 2016). However, no direct correlations between changing landscapes and DBC distribution have been observed in fluvial systems.

The goal of the current research is to elucidate biogeochemical and physical parameters that promote changes in DBC and DOM distribution in fluvial systems. This was performed by analyzing DBC distribution in a variety of biogeochemically unique river settings from one large basin that is expected to have a significant source of wildfire derived DBC (Chapter 1). These processes include sorption and coprecipitation along with photochemical processes. However, though DBC can be removed from aquatic systems through a variety of biogeochemical processes, DBC may also be generated photochemically through dissolution of char and soils (Chapter 2). Considering processes that may induce translocation of BC from the particulate to dissolved phase, it would be expected that significant coupling between DBC and PBC would be observed in river systems. However, Wagner et al. (2015a) has shown that in a small system recently affected by wildfire, there is no direct relationship between DBC and PBC. That relationship however warrants further investigation on a larger scale (Chapter 3). To investigate the potential effects of land use and stream order on DOM and DBC composition and flux, DOM and DBC was quantified throughout a large river system and directly compared to the subsequent watershed land cover (Chapter 4 & 5). In an effort to constrain future BC budgets and understand the potentially important role of BC in global

carbon cycling, it is important to elucidate the above-described environmental drivers (both natural and anthropogenic) on the fate and export of BC from fluvial systems.

## 1.2 References

- Abiven, S., Hengartner, P., Schneider, M.P.W., Singh, N., Schmidt, M.W.I., 2011. Pyrogenic carbon soluble fraction is larger and more aromatic in aged charcoal than in fresh charcoal. *Soil Biology and Biochemistry* 43, 1615-1617.
- Baldock, J.A., Smernik, R.J., 2002. Chemical composition and bioavailability of thermally altered *Pinus resinosa* (Red pine) wood. *Organic Geochemistry* 33, 1093-1109.
- Bird, M.I., Wynn, J.G., Saiz, G., Wurster, C.M., McBeath, A., 2015. The Pyrogenic Carbon Cycle. *Annual Review of Earth and Planetary Sciences* 43, 273-298.
- Carpenter, S.R., Caraco, N.F., Correll, D.L., Howarth, R.W., Sharpley, A.N., Smith, V.H., 1998. Nonpoint Pollution of Surface Waters with Phosphorus and Nitrogen. *Ecological Applications* 8, 559-568.
- Chantigny, M.H., 2003. Dissolved and water-extractable organic matter in soils: a review on the influence of land use and management practices. *Geoderma* 113, 357-380.
- Ding, Y., Yamashita, Y., Dodds, W.K., Jaffé, R., 2013. Dissolved black carbon in grassland streams: Is there an effect of recent fire history? *Chemosphere* 90, 2557-2562.
- Ding, Y., Yamashita, Y., Jones, J., Jaffé, R., 2015. Dissolved black carbon in boreal forest and glacial rivers of central Alaska: assessment of biomass burning versus anthropogenic sources. *Biogeochemistry* 123, 15-25.
- Dittmar, T., de Rezende, C.E., Manecki, M., Niggemann, J., Coelho Ovalle, A.R., Stubbins, A., Bernardes, M.C., 2012. Continuous flux of dissolved black carbon from a vanished tropical forest biome. *Nature Geoscience* 5, 618-622.
- Goldberg, E.D., 1985. *Black Carbon in the Environment: Properties and Distribution*, 1 ed. John Wiley & Sons Inc, New York.
- Graeber, D., Gelbrecht, J., Pusch, M.T., Anlanger, C., von Schiller, D., 2012. Agriculture has changed the amount and composition of dissolved organic matter in Central European headwater streams. *Science of The Total Environment* 438, 435-446.
- Gu, B., Schmitt, J., Chen, Z., Liang, L., McCarthy, J.F., 1995. Adsorption and desorption of different organic matter fractions on iron oxide. *Geochimica et Cosmochimica Acta* 59, 219-229.

- Hockaday, W.C., Grannas, A.M., Kim, S., Hatcher, P.G., 2007. The transformation and mobility of charcoal in a fire-impacted watershed. *Geochimica et Cosmochimica Acta* 71, 3432-3445.
- Jaffé, R., Ding, Y., Niggemann, J., Vähätalo, A.V., Stubbins, A., Spencer, R.G.M., Campbell, J., Dittmar, T., 2013. Global Charcoal Mobilization from Soils via Dissolution and Riverine Transport to the Oceans. *Science* 340, 345-347.
- Kaplan, L.A., Wiegner, T.N., Newbold, J.D., Ostrom, P.H., Gandhi, H., 2008. Untangling the complex issue of dissolved organic carbon uptake: a stable isotope approach. *Freshwater Biology* 53, 855-864.
- Khan, A.L., Jaffé, R., Ding, Y., McKnight, D.M., 2016. Dissolved black carbon in Antarctic lakes: Chemical signatures of past and present sources. *Geophysical Research Letters* 43, 5750-5757.
- Kothawala, D.N., Roehm, C., Blodau, C., Moore, T.R., 2012. Selective adsorption of dissolved organic matter to mineral soils. *Geoderma* 189–190, 334-342.
- Masiello, C. A. 2004. New directions in black carbon organic geochemistry. *Marine Chemistry* 92 (1-4), 201-213.
- Mayer, L.M., Schick, L.L., Skorko, K., Boss, E., 2006. Photodissolution of particulate organic matter from sediments. *Limnology and Oceanography* 51, 1064-1071.
- Mayer, L.M., Thornton, K.R., Schick, L.L., Jastrow, J.D., Harden, J.W., 2012. Photodissolution of soil organic matter. *Geoderma* 170, 314-321.
- Myers-Pigg, A.N., Louchouart, P., Teisserenc, R., 2017. Flux of dissolved and particulate low-temperature pyrogenic carbon from two high-latitude rivers across the spring freshet hydrograph. *Frontiers in Marine Science* 4 (38), doi: 10.3389/fmars.2017.00038
- Parr, T.B., Cronan, C.S., Ohno, T., Findlay, S.E.G., Smith, S.M.C., Simon, K.S., 2015. Urbanization changes the composition and bioavailability of dissolved organic matter in headwater streams. *Limnology and Oceanography* 60, 885-900.
- Pisani, O., Yamashita, Y., Jaffé, R., 2011. Photodissolution of flocculent, detrital material in aquatic environments: Contributions to the dissolved organic matter pool. *Water Research* 45, 3836-3844.
- Riedel, T., Biester, H., Dittmar, T., 2012. Molecular fractionation of dissolved organic matter with metal salts. *Environmental Science & Technology* 46, 4419-4426.



- Santín, C., Doerr, S.H., Kane, E.S., Masiello, C.A., Ohlson, M., de la Rosa, J.M., Preston, C.M., Dittmar, T., 2016. Towards a global assessment of pyrogenic carbon from vegetation fires. *Global Change Biology* 22, 76-91.
- Schneider, M. P. W., Hilf, M., Vogt, U., Schmidt, M. W. I., 2010. The benzenepolycarboxylic acid (BPCA) pattern of wood pyrolyzed between 200 °C and 1000 °C. *Organic Geochemistry* 41 (10), 1082-1088.
- Stubbins, A., Niggemann, J., Dittmar, T., 2012. Photolability of deep ocean dissolved black carbon. *Biogeosciences* 9, 1661-1670.
- Vannote, R.L., Minshall, G.W., Cummins, K.W., Sedell, J.R., Cushing, C.E., 1980. The River Continuum Concept. *Canadian Journal of Fisheries and Aquatic Sciences* 37, 130-137.
- Wagner, S., Cawley, K., Rosario-Ortiz, F., Jaffé, R., 2015a. In-stream sources and links between particulate and dissolved black carbon following a wildfire. *Biogeochemistry* 124, 145-161.
- Wagner, S., Riedel, T., Niggemann, J., Vähätalo, A.V., Dittmar, T., Jaffé, R., 2015b. Linking the Molecular Signature of Heteroatomic Dissolved Organic Matter to Watershed Characteristics in World Rivers. *Environmental Science & Technology* 49, 13798-13806
- Williams, C.J., Yamashita, Y., Wilson, H.F., Jaffé, R., Xenopoulos, M.A., 2010. Unraveling the role of land use and microbial activity in shaping dissolved organic matter characteristics in stream ecosystems. *Limnology and Oceanography* 55, 1159-1171.
- Wilson, H.F., Xenopoulos, M.A., 2008. Effects of agricultural land use on the composition of fluvial dissolved organic matter. *Nature Geoscience* 2, 37-41.
- Yamashita, Y., Jaffé, R., Maie, N., Tanoue, E., 2008. Assessing the dynamics of dissolved organic matter (DOM) in coastal environments by excitation emission matrix fluorescence and parallel factor analysis (EEM-PARAFAC). *Limnology and Oceanography* 53, 1900-1908.
- Zhang, Y.L., Zhang, E.L., Liu, M.L., Wang, X., Qin, B.Q., 2007. Variation of chromophoric dissolved organic matter and possible attenuation depth of ultraviolet radiation in Yunnan Plateau lakes. *Limnology* 8, 311-319.
- Zimmerman, A.R., 2010. Abiotic and Microbial Oxidation of Laboratory-Produced Black Carbon (Biochar). *Environmental Science & Technology* 44, 1295-1301.

## CHAPTER II

# ENVIRONMENTAL DYNAMICS OF DISSOLVED BLACK CARBON IN THE AMAZON RIVER

## 2.1 Abstract

Dissolved black carbon (DBC) is ubiquitous in fluvial systems and represents about 10% of the dissolved organic carbon (DOC) exported from rivers annually. During riverine transport, DOC is subject to a number of biogeochemical transformations because of processes such as photo- and bio-degradation and interactions with particles and polyvalent metals. The coupling between DBC and DOC often observed in aquatic systems suggest the systematic processes regulating the fate and transport of DOC in rivers would also be similar for DBC. However, little is known about biogeochemical controls on DBC during transport within terrestrial systems. To further investigate the influence of river biogeochemistry on the fate and transport of DBC in fluvial systems, DBC was characterized using the benzenepolycarboxylic acid method along with ultra high resolution mass spectrometry in three unique tributaries of the Amazon River, which provides the greatest export of freshwater discharge to coastal systems. These tributaries were unique in their biogeochemical character ranging from clear water rivers, highly turbid white water rivers, and black water rivers. In comparison to the black water river, DBC was compositionally less polycondensed and lower in molecular weight in both the clear water river, as evident by photodegradation, and the white water river, suggesting selective loss of DBC through interaction with mineral clays and polyvalent metal species. To confirm the hypothesis, we show through laboratory incubation experiments that coprecipitation with iron is a reasonable mechanism for selective removal of high molecular weight DBC from fluvial systems. Collectively, the data reported in this study show that local river biochemistry may have a significant impact on the fate and transport of DBC from rivers to coastal systems.

## 2.2 Introduction

Black carbon (BC) is a heterogeneous collection of thermogenically altered organic material formed through incomplete combustion of biomass (e.g., such as from wildfires) and fossil fuel combustion (Goldberg, 1985). The nature to which BC is formed is dependent on source material and charring conditions, with BC becoming enriched in high molecular weight, polycondensed aromatic compounds as charring temperature increases (Masiello, 2004). Because of this high degree of polycondensed aromaticity, it is expected that BC is highly recalcitrant and after postproduction incorporation into soils, can have mean residence times upwards of millennia (Bird et al., 2015). However, a fraction of the BC pool incorporated into soils can be altered through microbial oxidation processes, thereby increasing the polar functionality of these polycondensed aromatic compounds and promoting their release from soils as dissolved BC (DBC; Hockaday et al., 2006). Dissolved black carbon becomes integrated within the dissolved organic matter pool where it accounts for ~10% of the total dissolved organic carbon (DOC) exported globally from fluvial networks to the ocean (Jaffé et al., 2013). The reason why such a strong correlation between DOC and DBC exists globally is currently unknown and has raised concerns about alternative sources of DBC. However, no alternative sources that can explain high levels of dissolved condensed aromatic compounds in aquatic systems have been identified to date.

The relationship between DOC and DBC is complex and not well understood. However, the coupling between DOC and DBC throughout the aquatic environment suggests that the systematic biogeochemical processes involved in regulating DOC during riverine transport may be similar for DBC. For instance, photochemical

degradation can be a sink for both high molecular weight DBC and DOC (Stubbins et al., 2012). However, biogeochemical processes, such as sorption/desorption with minerals (Kothawala et al., 2012) and interactions with polyvalent metal species (Gu et al., 1995), that have been shown to remove DOC from aquatic environments and alter DOM composition, have not been fully explored quantitatively for DBC. Thus, local river biogeochemistry may play a pivotal role in the cycling of DBC.

Global river systems are responsible for significant export of DOC to coastal oceans (Raymond and Spencer, 2015). The Amazon River basin in particular is a globally important system as it is responsible for nearly 20% of the global freshwater discharge and exports an estimated 36 Tg of organic carbon into the ocean annually (Moreira-Turcq et al., 2003a; Richey et al., 1990). However, the Amazon River basin, which is still comprised predominately of its pristine natural cover, is subjected to regularly occurring natural wildfires along with frequent slash and burn events (Cochrane and Schulze, 1998; Sanford et al., 1985), making it a significant regional source of DBC to the coastal ocean (Jaffe et al., 2013).

The Amazon River basin is also unique as the DOC in its fluvial network is supplied from a variety of tributaries representative of a wide array of biogeochemical characteristics. The three major types of rivers that comprise the Amazon River basin, named for their ability to mediate light availability, are black, white, and clear water rivers (Moreira-Turcq et al., 2003a). The “black water” rivers are rich in chromophoric DOM (CDOM) and have the ability to absorb copious amounts of light and limit light penetration beneath the surface (Mounier et al., 1999). Similarly, light penetration is inhibited in “white water” rivers as well because of increased suspended sediment

concentrations (Guyot et al., 2007), which are made up of primarily suspended mineral clays and particulate species of polyvalent metals (such as aluminum and iron). On the contrary, the “clear water” rivers have increased light availability because of the low turbidity (Richey et al., 1990). Considering the distinct biogeochemical characteristics of Amazonian tributaries, it may be expected that the combination of light penetration, sorption/desorption and co-precipitation might be reflected in the local DBC signatures among these tributaries, highlighting the influence of local river biogeochemistry on the fate and transport of DBC.

To explore the hypothesis further, DBC was characterized using the benzenepolycarboxylic acid (BPCA) method and ultra high-resolution mass spectrometry in three major Amazonian tributaries, each representative of a clear, white, or black water conditions. We hypothesize that DOM would contain higher DBC levels and of a more condensed aromatic signature in the black and white water rivers because of potential shielding effects from photochemical degradation. However, in the highly turbid white water rivers, which are rich in mineral clays and polyvalent metal species, selective removal of high molecular weight DOM would result in lower DBC concentrations and a less polycondensed DBC signature relative to the black water river. To explore the potential effects on DBC composition and abundance through sorption onto clay minerals and co-precipitation with iron hydroxides, controlled laboratory experiments were performed. Characterization of *in situ* DBC within the Amazon River basin along with the previously described experiments provides a better understanding of how local biogeochemistry may influence the fate and transport of DBC within the aquatic environment.

## 2.3 Methods

### 2.3.1 Sample Collection

Dissolved organic matter samples analyzed from the Amazon River for the present study have been previously described by Gonsior et al. (2016). Samples were collected from the main stems and adjacent flooded lakes of the Rio Negro (n = 11), Rio Madeira (n = 10), and Rio Tapajos (n = 4, Figure 2.1) using 1 L precombusted (500 °C, 5 hr) Pyrex glass bottles in May 2013.

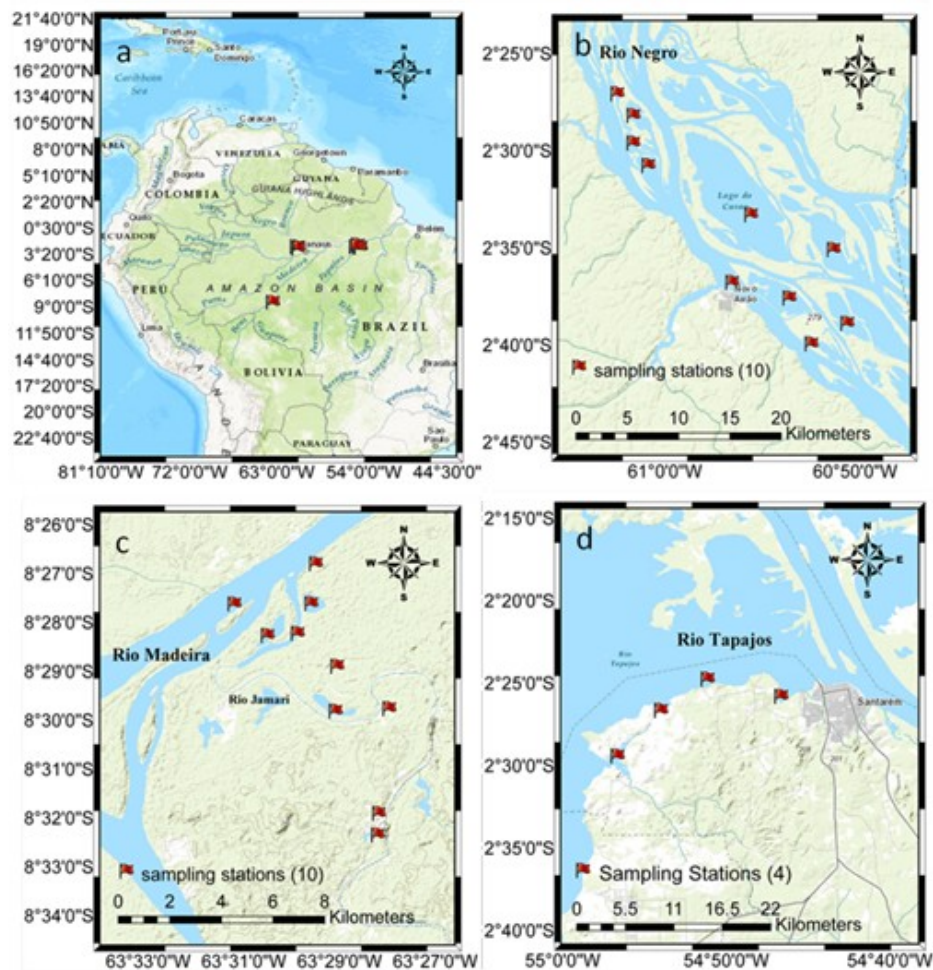


**Figure 2.1:** Map of the Amazon River drainage basin. (a) General location of sampling regions within the Amazon Basin. (b) Sampling locations within the Rio Negro region. (c) Sampling locations within the Rio Madeira region. (d) Sampling locations within the Rio Tapaós.

### 2.3.2 Isolation and Quantification of DBC

All samples collected were passed through a 0.7  $\mu\text{m}$  precombusted (500 °C, 5hrs) Whatman glass fiber filter (GFF) and acidified to pH 2 with formic acid. Bulk DOM was isolated from the samples using a solid phase extraction (SPE) technique previously described by Dittmar et al. (2008). Briefly, acidified samples were gravity-fed through Agilent Bond Elut PPL SPE cartridges (1g PPL resin, 6 mL volume) preconditioned with methanol and rinsed with acidified ultra-pure water. Upon completion of sample loading, SPE cartridges were further washed with acidified ultra pure water, dried, and eluted with 10 mL methanol.

The DBC isolated by SPE was quantified using the benzenepolycarboxylic acid (BPCA) method previously described by Dittmar (2008). The BPCA method is primarily used for quantification of the condensed aromatic portion of the total pyrogenic carbon spectrum. The DBC is thermally oxidized into polysubstituted benzene carboxylic acids in which a greater proportion of the more substituted BPCAs (B5CA & B6CA) in relation to the less substituted BPCAs (B3CA & B4CA) imply the represented DBC contains a more condensed aromatic signature.

Methanol aliquots containing roughly 0.25 mg C were dried under a stream of  $\text{N}_2$  gas in 2 mL glass ampoules and oxidized with 0.5 mL nitric acid at 160 °C for 6 hours (Ding et al., 2013). The remaining BPCAs were re-dissolved in mobile phase buffer and quantified by high performance liquid chromatography (HPLC) coupled with a diode array detector (Surveyor, Thermo Scientific). Chromatographic conditions for separation and quantification of BPCAs are previously described in detail by Dittmar, 2008. The DBC oxidation was performed in triplicate (CV < 5%).



### *2.3.3 Ultra-High Resolution Mass Spectrometry*

Details for the characterization of this data set by FTICR-MS have been previously described by Gonsior et al., 2016 with more detailed FTICR-MS protocols described by Hertkorn et al., 2013. Briefly, DOM samples isolated by SPE were diluted (1:20) in methanol and analyzed with a Bruker Solarix ultra high resolution mass spectrometer (Helmholtz Zentrum Munich, Germany) connected to a 12 Tesla superconducting magnet. Samples were infused into the ionization source (negative mode) at a flow rate of 120  $\mu\text{L}/\text{min}$ . For each sample, 500 scans were averaged and calibrated to a list of known DOM calibrants. Molecular formulae were assigned over a mass range up to an  $m/z$  of 800 Da. For our analysis, a mass resolution of 500,000 was documented at  $m/z$  400 Da and a mass accuracy of less than 0.2 ppm was achieved. A modified aromaticity index ( $AI_{\text{mod}}$ ) was calculated for each molecular mass as described by Koch and Dittmar (2006, 2016). Condensed aromatic compounds (i.e. DBC) were defined with an  $AI_{\text{mod}} \geq 0.67$  and molecular formulae containing only carbon, hydrogen, and oxygen.

### *2.3.4 Incubation of DOM with Mineral Clays*

In triplicates, three mineral clays (Montmorillonite, Kaolinite, and Illite) were each suspended at 250 mg/L in a 10 ppm DOM solution prepared in synthetic freshwater (Smith et al., 2002) with Suwannee River Fulvic Acid (SRFA) obtained as International Humic Substances (IHSS) reference material (2R101N). After 24 hours of shaking at 100 RPM, samples were filtered through a 0.7  $\mu\text{m}$  GFF and the DOM and associated DBC were isolated and quantified to determine if high molecular weight DBC selectively adsorbed to the respective mineral clays.

### *2.3.5 Incubation of DOM with Iron*

Using IHSS reference standards, two sets of DOM solutions were prepared with SRFA and Suwannee River Humic Acid (SRHA, 2S101H) at a concentration of 10 ppm. These DOM solutions were separated into four sets of triplicates each. Using  $\text{Fe}(\text{NO}_3)_3 \cdot 9\text{H}_2\text{O}$ , two sets of triplicates for each DOM solution were brought to a 60  $\mu\text{M}$  iron concentration and two sets were brought to 12  $\mu\text{M}$  iron concentration. One set representative of each iron concentration was then adjusted to pH 4 and pH 7.5 and then shaken at 100 RPM. After 24 hours, the samples were filtered through a 0.2  $\mu\text{m}$  membrane filter (Millipore) and the DOC and associated DBC were isolated by SPE (method described above) and quantified using the BPCA method to determine if selective high molecular weight DBC is removed from solution as a result of co-precipitation with iron. However, for samples at pH 7.5, further precipitation was observed upon acidification for DBC isolation by SPE. This additional precipitation was not observed for samples prepared at pH 4. Because there is a high probability that more DBC was lost upon acidification of samples prepared at pH 7.5, the data for these samples were omitted from this dataset as they are likely not reflective of the true DBC concentration and composition at the conclusion of the 24 hour experiments.

## **2.4 Results and Discussion**

### *2.4.1 DBC Composition in Amazonian Tributaries*

The DBC concentrations were highly variable among the three main tributaries sampled in the Amazon basin. Of these, DBC was highest in the black water Rio Negro with an average concentration of  $0.47 \pm 0.05$  ppm. The clear water Rio Tapajós followed with an average concentration of  $0.11 \pm 0.01$  ppm, while the white water Rio Madeira

had the lowest DBC concentration at  $0.05 \pm 0.02$  ppm. These DBC concentrations are in general agreement with concentrations ranges previously reported throughout the Amazon River main stem from Óbidos to Macapá (Medeiros et al., 2015).

The DOC concentrations for the sample set have been previously reported by (Gonsior et al., 2016). The Rio Negro region had the highest DOC concentration averaging roughly 10 ppm, nearly two-fold that of the Rio Madeira and Rio Tapajós, which ranged from 1.9 - 5.8 ppm. The DBC was significantly correlated with DOC in both the Rio Negro ( $p < 0.05$ ) and Rio Tapajós ( $p < 0.05$ ), a relationship consistent with previous reports that these two variables are correlated in wide array of fluvial networks (Ding et al., 2014; Dittmar et al., 2012; Jaffé et al., 2013; Wagner et al., 2015). The biogeochemical drivers leading to the linear relationship between DBC and DOC (Jaffe et al., 2013) are still not well understood. In the current study, while the relative abundance of DBC as percent of DOC fell within the range of previously reported values (Jaffe et al., 2013), it was below the average global distribution (10% of DOC) in both the Rio Tapajós and the Rio Negro (DBC = ~4.5% DOC), and even lower in the Rio Madeira (1.8%). The differences in the relative abundance of DBC in the overall DOC pool between these river systems is unclear, but could be related to selective removal mechanisms of DBC in the Rio Madeira, such as through stronger associations with the high suspended solids loads (sorption) or co-precipitation within the high molecular weight DOC fractions (Chen et al., 2014) via the formation of iron hydroxide precipitates. This hypothesis for DBC-iron interactions is discussed in further detail below.

**Table 2.1:** BPCA and FT-ICR-MS information in the respective Amazonian tributaries. Errors represent 1 standard deviation from the mean.

<b>Sample Area</b>	<b>DBC (ppm)</b>	<b>BPCA Ratio</b>	<b>Avg. Mol. Weight</b>	<b>No. BC Formula</b>
<b>Rio Tapajós</b>	0.11 ± 0.01	0.69 ± 0.02	322 ± 8	225 ± 72
<b>Rio Negro</b>	0.47 ± 0.05	0.90 ± 0.10	353 ± 10	322 ± 20
<b>Rio Madeíá</b>	0.05 ± 0.02	0.70 ± 0.07	331 ± 2	228 ± 20

Dissolved black carbon is likely comprised of a collection of condensed aromatic compounds. While the condensed aromatic nature of DBC has in part been related to its source material and combustion conditions (Schneider et al., 2010), it has been reported that the aromatic character of DBC can be reduced through photo-exposure (Stubbins et al., 2012). Thus, in order to assess the impact of stream biogeochemistry on the degree of DBC aromaticity throughout the Amazon River basin, BPCA ratios were used and compared between ecosystems with different degrees of light penetration (as determined by CDOM and turbidity). The BPCA ratio used herein was defined as the ratio of  $(B5CA+B6CA)/(B3CA+B4CA)$ , where a higher ratio implies a more polycondensed DBC character of the sample.

The BPCA ratio was not significantly different between the Rio Tapajós and the Rio Madeira ( $p < 0.05$ ). However, both were significantly lower compared to the Rio Negro ( $p < 0.05$ , Table 2.1). The higher BPCA ratio in the Rio Negro would imply a higher degree of polycondensation for DBC compared to the other two tributaries. Photochemical degradation of DOC is highly prevalent within Amazonian clear waters (Amado et al., 2006) and thus, the lower BPCA ratio in the Rio Tapajós could be driven by higher degrees of photodegradation. In contrast, the Rio Negro is rich in CDOM that may shield DBC from associated photodegradation processes leading to a more preserved

pool of DBC. The Rio Madeira on the other hand had the lowest DBC concentrations as well as a low degree of condensed aromaticity (low BPCA ratio) in comparison to the Rio Negro. However, the highly turbid waters of the Rio Madeira make it unlikely that photochemical degradation can justify the low degree of condensed aromaticity in this system. High suspended sediment loads in the Rio Madeira are rich in clay minerals, such as montmorillonite, kaolinite, and illite (Guyot et al., 2007). Its surface waters and sediments are also rich in abundance of polyvalent metals, such as iron (Conrad et al., 2014). For instance, the Rio Madeira has total iron concentration of up to 256  $\mu\text{M}$ , of which 12.8  $\mu\text{M}$  is in the dissolved phase (Bergquist and Boyle, 2006; Poitrasson et al., 2014). The interactions between bulk DOC and mineral clays as well as with iron in aquatic systems have been previously established. Kothawala et al. (2012) has shown that high molecular weight DOC is selectively removed from solution through adsorption to mineral soils. Gu et al. (1995) has shown that presence of iron oxides will induce the loss of high molecular weight DOC. It has been estimated that between 4 and 40% of DOM is lost when the black waters of the Rio Negro converge with the highly turbid waters of the Rio Solimões (Aucour et al., 2003; Moreira-Turcq et al., 2003b). Considering that DBC associates most predominately with the high molecular weight fraction of DOC (Wagner and Jaffé, 2015), we hypothesize that the presence of clay minerals and iron will induce the selective removal of highly condensed DBC from the water column. Evidence to support this hypothesis has been previously presented by (Riedel et al., 2013), who have shown by FTICR/MS that there is a loss of condensed aromatic structures at redox interfaces in soils. Furthermore, Riedel et al. (2012) also reported the loss of condensed

aromatic structures in solutions containing peat derived DOM that was enriched with iron.

Although strong evidence is available to support significant DBC-iron interactions within the aquatic environment as well as the adsorption to mineral clays considering their interaction with DOC, direct quantitative measures have yet to be employed to confirm the importance of these processes in removing DBC from the dissolved phase. In the present study, experiments were performed to investigate the interactions of DBC with mineral clays and with iron to confirm if selective removal of high molecular weight DBC is indeed possible.

#### *2.4.2 Adsorption of DBC to Mineral Clays*

To test the above-mentioned hypotheses, a sorption experiment was designed to determine if there is significant loss of DBC in the presence of clays minerals. Montmorillonite and kaolinite were used because of their ubiquity throughout the Amazon River system, and illite was chosen because of its high abundance in the Rio Madeira (Guyot et al., 2007). As observed in Table 2.2, there was no significant loss of DBC after 24 hour incubation of SRFA with each clay. Thus, the hypothesis that additional polycondensed DBC would be removed from solution through adsorption (Kothawala et al., 2012) could not be confirmed. It should be noted that soils, such as luvisol and gleysol, were used for the work reported by Kothawala and coworkers. The difference in soil properties and mineral characteristics likely plays a key role in the adsorptive properties with DOM. Thus, it is possible that DBC may interact differently with mineral soils found within the Amazon River basin. However, on the basis of the

results reported here, it seems unlikely this process induces significant removal of DBC throughout the Amazon basin and the Rio Madeira.

**Table 2.2:** Results of a 24 hour DBC adsorption experiment with common mineral clays found in the Amazon basin. Error represents 1 standard deviation from the mean.

	<b>DBC (ppm)</b>	<b>BPCA Ratio</b>
<b>Initial</b>	1.32 ± 0.04	1.94 ± 0.03
<b>Montmorillonite</b>	1.25 ± 0.02	1.95 ± 0.02
<b>Kaolinite</b>	1.39 ± 0.01	1.91 ± 0.02
<b>Illite</b>	1.33 ± 0.13	1.93 ± 0.05

#### 2.4.3 Selective Co-precipitation of DBC with Iron

To further explore interactions between DBC and iron as a potential mechanism for loss of more polycondensed DBC in the Rio Madeira, 24 hour incubations were performed using SRFA and SRHA as a natural DBC substrate to determine if selective coprecipitation of more polycondensed DBC is removed from solution with varying iron concentrations. These experiments were carried out at pH 4 and pH 7.5. However, samples at pH 7.5 were omitted as a consequence of an experimental defect with respect to these samples (see methods section).

After the 24 hour incubation, a significant loss of DBC was observed in both the SRFA (Figure 2.2a) and SRHA (Figure 2.2b) experiments. The most significant loss of DBC for both SRFA and SRHA was in samples containing 60  $\mu\text{M}$  dissolved iron (Figure 2.2a,b), with each losing more than 60% of the DBC present in the original samples. These losses in DBC abundance were coupled with a decrease in the BPCA ratio (Figure 2.2a,b), suggesting the selective removal of more polycondensed DBC during coprecipitation with iron hydroxide. In samples containing 12  $\mu\text{M}$  dissolved iron,

a loss in DBC was also observed, but was much less significant than what was observed in samples with 60  $\mu\text{M}$  iron concentrations (Figure 2.2a,b). For SRFA, the decrease in DBC was 13% with a decrease of 34% in SRHA samples. The more extensive loss of DBC in samples with 60  $\mu\text{M}$  dissolved iron is on par with other studies involving bulk DOC in which coprecipitation is enhanced when there is a higher proportion of iron with respect to DOC (Nierop et al., 2002).

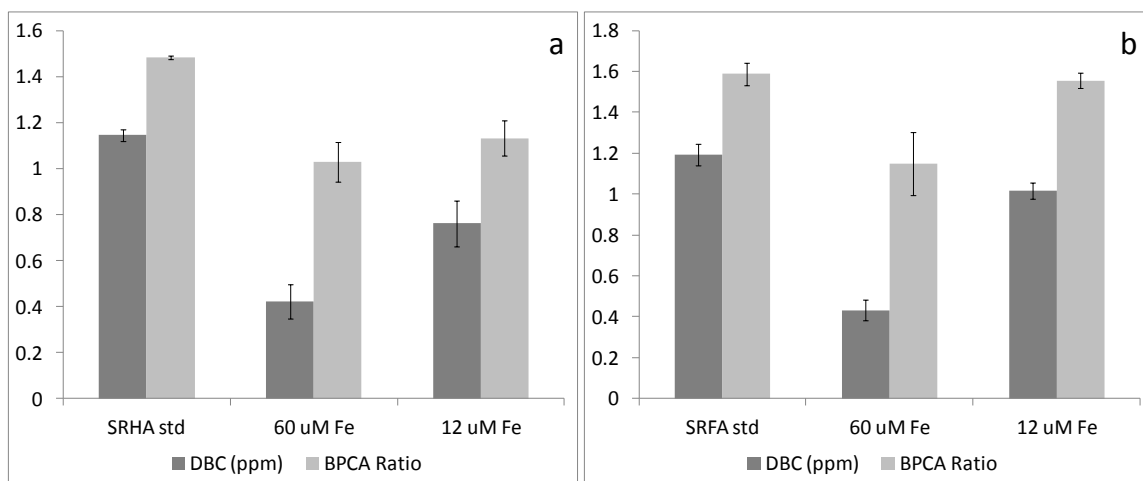


**Figure 2.2:** Graphs displaying respective results for a 24 hour DBC co-precipitation experiment with iron using (a) SRFA and (b) SRHA. The y-axis is representative of both DBC (ppm) and the BPCA ratio. Error bars represent 1 standard deviation from the mean.

While a significant decrease in the BPCA ratio was observed for the SRHA samples both with 60 and 12  $\mu\text{M}$  iron and the SRFA sample with 60  $\mu\text{M}$  iron, a decrease in the BPCA ratio was less obvious for the SRFA sample with 12  $\mu\text{M}$  iron (Figure 2.2a). The reason a decrease in the BPCA ratio in the SRFA sample with 12  $\mu\text{M}$  iron is currently unclear. However, the bulk humic acid fraction of the DOM pool is higher in molecular weight than to fulvic acids (Beckett et al., 1987) and can be separated from fulvic acids through selective coprecipitation at low iron concentrations (Hiraide et al., 1987). The increased affinity for the humic acid fraction to coprecipitation with iron at



low concentrations may provide some insight into the selective removal of polycondensed DBC in the low iron SRHA sample versus the low iron SRFA sample. In addition, DBC was reported to associate with high molecular weight DOM fractions that are enriched in humic-like substances (Wagner and Jaffe, 2015). Nevertheless, we show that in general, the more polycondensed fraction of the DBC pool can be selectively removed from aquatic systems through iron coprecipitation processes leaving a less polycondensed DBC signature.

The DBC-iron interactions described above may have important implications for cycling of BC in aquatic systems as these processes may induce carbon sequestration and storage in soils as well as enhance the movement of BC in the particulate phase. About 21% of organic matter in sediments is directly bound to reactive iron (Lalonde et al., 2012), and in the Amazon basin, BC in soils has been reported as high as 35% with significant portions being bound within iron oxide clusters (Glaser et al., 2000). The ability for iron to sequester BC further highlights the importance of DBC coprecipitation with iron as a likely explanation for the lower DBC levels and low BPCA ratios in the Rio Madeira.

#### *2.4.4 Ultra-High Resolution Mass Spectrometry*

Amazon DOM samples were characterized on the molecular level using FTICR-MS. The highest number of DBC compounds was detected in the Rio Negro samples, which may be expected when considering DBC in this region may be less impacted by photochemical degradation, in comparison to the Rio Tapajós or from removal through interactions with metals, which is hypothesized to occur in the Rio Madeira. The DBC detected in the Rio Negro also had the highest intensity weighted

average molecular weight (MW) at 354 Da in comparison to the other two tributaries sampled (Table 2.1). This is consistent with the overall bulk DOM as well in which the Rio Negro exhibited the highest mass among the three tributaries sampled (Gonsior et al., 2016). The number of detected DBC compounds and their average MW however were not significantly different ( $p > 0.05$ ) between the Rio Tapajós and the Rio Madeira (Table 2.1). Although the lower number of detected compounds in the Rio Tapajós and the Rio Madeira may be expected when considering potential sinks for more polycondensed DBC in these regions, FTICR-MS may also be discriminating against DBC in general because of an assumed low ionization efficiency of these compounds and thus, making it rather difficult to observe clear trends. In addition, the low average molecular weight of the compounds detected in these two tributaries (Table 2.1) correlates with the variation in BPCA ratios, further suggesting that DBC compounds are both lower in both molecular weight and polycondensed character within the Rio Tapajós and the Rio Madeira. In summary, FTICR-MS was in general agreement with BPCA method suggesting the more polycondensed DBC (noted by higher BPCA ratios) in the Rio Negro was accompanied with a higher average molecular weight, and the less condensed DBC observed in the Rio Tapajós and Rio Madeira was lower in molecular weight (Table 2.1).

## **2.5 Conclusions**

The results of the study suggest that local river biogeochemistry may have significant impacts on the systematic processing of DBC in fluvial networks. The BPCA ratios in the Rio Tapajós indicate that photochemistry may play a pivotal role in altering DBC composition as has been previously alluded to in the marine environment (Stubbins

et al., 2012). The clear waters of the Rio Tapajós may allow significant photodegradation of DBC, whereas the high light absorbing capacity of CDOM in the Rio Negro shields DBC from significant photochemical alteration. The DBC from the Rio Madeira on the other hand is also less likely to be influenced photochemically because of the highly turbid environment, however; the increased suspended sediment load and high iron content make this region prime for DBC adsorption interactions or coprecipitation with iron. While we were unable to demonstrate that adsorption of DBC to common clay minerals is a significant geochemical process affecting DBC in aquatic environments, laboratory experiments show that high molecular weight DBC is co-precipitated when copious amounts of iron are present, as is the case in the Rio Madeira. The FTICR-MS data were generally in agreement with BPCA data where the Rio Negro region had a greater number of detectable DBC compounds that are higher in average molecular weight in comparison to the Rio Tapajós and the Rio Madeira. While the cycling of DBC throughout fluvial networks is still not well understood, the present study emphasizes the importance of stream-specific biogeochemical characteristics in driving the fate and transport of DBC in aquatic environments.

## 2.6 References

- Amado, A.M., Farjalla, V.F., Esteves, F.d.A., Bozelli, R.L., Roland, F., Enrich-Prast, A., 2006. Complementary pathways of dissolved organic carbon removal pathways in clear-water Amazonian ecosystems: photochemical degradation and bacterial uptake. *FEMS Microbiology Ecology* 56, 8-17.
- Aucour, A.M., Tao, F.X., Moreira-Turcq, P., Seyler, P., Sheppard, S., Benedetti, M.F., 2003. The Amazon River: behaviour of metals (Fe, Al, Mn) and dissolved organic matter in the initial mixing at the Rio Negro/Solimões confluence. *Chemical Geology* 197, 271-285.

- Beckett, R., Jue, Z., Giddings, J.C., 1987. Determination of molecular weight distributions of fulvic and humic acids using flow field-flow fractionation. *Environmental Science & Technology* 21, 289-295.
- Bergquist, B.A., Boyle, E.A., 2006. Iron isotopes in the Amazon River system: Weathering and transport signatures. *Earth and Planetary Science Letters* 248, 54-68.
- Bird, M.I., Wynn, J.G., Saiz, G., Wurster, C.M., McBeath, A., 2015. The pyrogenic carbon cycle. *Annual Review of Earth and Planetary Sciences* 43, 273-298.
- Chen, C., Dynes, J.J., Wang, J., Sparks, D.L., 2014. Properties of Fe-organic matter associations via coprecipitation versus adsorption. *Environmental Science & Technology* 48, 13751-13759.
- Cochrane, M.A., Schulze, M.D., 1998. Forest fires in the Brazilian Amazon. *Conservation Biology* 12, 948-950.
- Conrad, R., Ji, Y., Noll, M., Klose, M., Claus, P., Enrich-Prast, A., 2014. Response of the methanogenic microbial communities in Amazonian oxbow lake sediments to desiccation stress. *Environmental Microbiology* 16, 1682-1694.
- Ding, Y., Cawley, K.M., da Cunha, C.N., Jaffé, R., 2014. Environmental dynamics of dissolved black carbon in wetlands. *Biogeochemistry* 119, 259-273.
- Ding, Y., Yamashita, Y., Dodds, W.K., Jaffé, R., 2013. Dissolved black carbon in grassland streams: Is there an effect of recent fire history? *Chemosphere* 90, 2557-2562.
- Dittmar, T., 2008. The molecular level determination of black carbon in marine dissolved organic matter. *Organic Geochemistry* 39, 396-407.
- Dittmar, T., de Rezende, C.E., Manecki, M., Niggemann, J., Coelho Ovalle, A.R., Stubbins, A., Bernardes, M.C., 2012. Continuous flux of dissolved black carbon from a vanished tropical forest biome. *Nature Geoscience* 5, 618-622.
- Dittmar, T., Koch, B., Hertkorn, N., Kattner, G., 2008. A simple and efficient method for the solid-phase extraction of dissolved organic matter (SPE-DOM) from seawater. *Limnology and Oceanography: Methods* 6, 230-235.
- Glaser, B., Balashov, E., Haumaier, L., Guggenberger, G., Zech, W., 2000. Black carbon in density fractions of anthropogenic soils of the Brazilian Amazon region. *Organic Geochemistry* 31, 669-678.
- Goldberg, E.D., 1985. *Black Carbon in the Environment: Properties and Distribution*, 1 ed. John Wiley & Sons Inc, New York.

- Gonsior, M., Valle, J., Schmitt-Kopplin, P., Hertkorn, N., Bastviken, D., Luek, J., Harir, M., Bastos, W., Enrich-Prast, A., 2016. Chemodiversity of dissolved organic matter in the Amazon Basin. *Biogeosciences* 13, 4279-4290.
- Gu, B., Schmitt, J., Chen, Z., Liang, L., McCarthy, J.F., 1995. Adsorption and desorption of different organic matter fractions on iron oxide. *Geochimica et Cosmochimica Acta* 59, 219-229.
- Guyot, J.L., Jouanneau, J.M., Soares, L., Boaventura, G.R., Maillet, N., Lagane, C., 2007. Clay mineral composition of river sediments in the Amazon Basin. *CATENA* 71, 340-356.
- Hertkorn, N., Harir, M., Koch, B.P., Michalke, B., Schmitt-Kopplin, P., 2013. High-field NMR spectroscopy and FTICR mass spectrometry: powerful discovery tools for the molecular level characterization of marine dissolved organic matter. *Biogeosciences* 10, 1583-1624.
- Hiraide, M., Ren, F.-L., Tamura, R., Mizuike, A., 1987. Rapid separation of humic acid in fresh waters by coprecipitation and flotation. *Microchimica Acta* 92, 137-142.
- Hockaday, W.C., Grannas, A.M., Kim, S., Hatcher, P.G., 2006. Direct molecular evidence for the degradation and mobility of black carbon in soils from ultrahigh-resolution mass spectral analysis of dissolved organic matter from a fire-impacted forest soil. *Organic Geochemistry* 37, 501-510.
- Jaffé, R., Ding, Y., Niggemann, J., Vähätalo, A.V., Stubbins, A., Spencer, R.G.M., Campbell, J., Dittmar, T., 2013. Global charcoal mobilization from soils via dissolution and riverine transport to the oceans. *Science* 340, 345-347.
- Koch, B.P., Dittmar, T., 2006. From mass to structure: an aromaticity index for high-resolution mass data of natural organic matter. *Rapid Communications in Mass Spectrometry* 20, 926-932.
- Koch, B.P., Dittmar, T., 2016. From mass to structure: an aromaticity index for high-resolution mass data of natural organic matter. *Rapid Communications in Mass Spectrometry* 30, 250-250.
- Kothawala, D.N., Roehm, C., Blodau, C., Moore, T.R., 2012. Selective adsorption of dissolved organic matter to mineral soils. *Geoderma* 189–190, 334-342.
- Lalonde, K., Mucci, A., Ouellet, A., Gelinas, Y., 2012. Preservation of organic matter in sediments promoted by iron. *Nature* 483, 198-200.
- Masiello, C.A., 2004. New directions in black carbon organic geochemistry. *Marine Chemistry* 92, 201-213.

- Medeiros, P.M., Seidel, M., Ward, N.D., Carpenter, E.J., Gomes, H.R., Niggemann, J., Krusche, A.V., Richey, J.E., Yager, P.L., Dittmar, T., 2015. Fate of the Amazon River dissolved organic matter in the tropical Atlantic Ocean. *Global Biogeochemical Cycles* 29, 677-690.
- Moreira-Turcq, P., Seyler, P., Guyot, J.L., Etcheber, H., 2003a. Exportation of organic carbon from the Amazon River and its main tributaries. *Hydrological Processes* 17, 1329-1344.
- Moreira-Turcq, P.F., Seyler, P., Guyot, J.L., Etcheber, H., 2003b. Characteristics of organic matter in the mixing zone of the Rio Negro and Rio Solimões of the Amazon River. *Hydrological Processes* 17, 1393-1404.
- Mounier, S., Braucher, R., Benaïm, J.Y., 1999. Differentiation of organic matter's properties of the Rio Negro basin by cross-flow ultra-filtration and UV-spectrofluorescence. *Water Research* 33, 2363-2373.
- Nierop, K.G.J.J., Jansen, B., Verstraten, J.M., 2002. Dissolved organic matter, aluminium and iron interactions: precipitation induced by metal/carbon ratio, pH and competition. *Science of The Total Environment* 300, 201-211.
- Poitrasson, F., Cruz Vieira, L., Seyler, P., Márcia dos Santos Pinheiro, G., Santos Mulholland, D., Bonnet, M.-P., Martinez, J.-M., Alcantara Lima, B., Resende Boaventura, G., Chmeleff, J., Dantas, E.L., Guyot, J.-L., Mancini, L., Martins Pimentel, M., Ventura Santos, R., Sondag, F., Vauchel, P., 2014. Iron isotope composition of the bulk waters and sediments from the Amazon River Basin. *Chemical Geology* 377, 1-11.
- Raymond, P.A., Spencer, R.G.M., 2015. Riverine DOM, in: Hansell, D., Carlson, C. (Eds.), *Biogeochemistry of Marine Dissolved Organic Matter*, pp. 509-533.
- Richey, J.E., Hedges, J.I., Devol, A.H., Quay, P.D., Victoria, R., Martinelli, L., Forsberg, B.R., 1990. Biogeochemistry of carbon in the Amazon River. *Limnology and Oceanography* 35, 352-371.
- Riedel, T., Biester, H., Dittmar, T., 2012. Molecular fractionation of dissolved organic matter with metal salts. *Environmental Science & Technology* 46, 4419-4426.
- Riedel, T., Zak, D., Biester, H., Dittmar, T., 2013. Iron traps terrestrially derived dissolved organic matter at redox interfaces. *Proceedings of the National Academy of Sciences* 110, 10101-10105.
- Sanford, R.L., Jr., Saldarriaga, J., Clark, K.E., Uhl, C., Herrera, R., 1985. Amazon rain-forest fires. *Science* 227, 53-55.
- Schneider, M.P.W., Hilf, M., Vogt, U.F., Schmidt, M.W.I., 2010. The benzene polycarboxylic acid (BPCA) pattern of wood pyrolyzed between 200 °C and 1000 °C. *Organic Geochemistry* 41, 1082-1088.

Smith, E.J., Davison, W., Hamilton-Taylor, J., 2002. Methods for preparing synthetic freshwaters. *Water Research* 36, 1286-1296.

Stubbins, A., Niggemann, J., Dittmar, T., 2012. Photo-lability of deep ocean dissolved black carbon. *Biogeosciences* 9, 1661-1670.

Wagner, S., Cawley, K., Rosario-Ortiz, F., Jaffé, R., 2015. In-stream sources and links between particulate and dissolved black carbon following a wildfire. *Biogeochemistry* 124, 145-161.

Wagner, S., Jaffé, R., 2015. Effect of photodegradation on molecular size distribution and quality of dissolved black carbon. *Organic Geochemistry* 86, 1-4.

## CHAPTER III

### PHOTODISSOLUTION OF CHARCOAL AND FIRE-IMPACTED SOIL AS A POTENTIAL SOURCE OF DISSOLVED BLACK CARBON IN AQUATIC ENVIRONMENTS

(Modified from *Roebuck et al. 2017, Organic Geochemistry*)



### **3.1 Abstract**

This study investigates the effect of photodissolution on the production of dissolved black carbon (DBC) from particulate charcoal and a fire-impacted soil. A soil sample and char sample were collected within the burn vicinity of the 2012 Cache La Poudre River wildfire and irradiated in deionized water with artificial sunlight. Photoexposure of the suspended char and soil significantly enhanced production of DBC after 7 days of continuous exposure to the simulated sunlight. The increase was coupled with an increase in the DBC polycondensed character. In agreement with this, molecular characterization using Fourier transform-ion cyclotron resonance mass spectrometry (FTICR-MS) showed an increase in the number of DBC molecular formulae detected and in their average molecular weight, suggesting that increasing photoexposure is required for dissolution of larger, more polycondensed DBC compounds. An increase in molecular signatures with lower H/C ratio and higher O/C ratio after 7 days photoexposure suggest increasing functionality of newly produced DBC with irradiation time, and therefore photooxidation as a potential mechanism for the photodissolution of BC. The photoproduct DBC was also strongly coupled with the photoproduct bulk dissolved organic carbon (DOC). The results suggest that photodissolution may be a significant and previously unrecognized mechanism of DBC translocation to aquatic systems.

### **3.2 Introduction**

Black carbon (BC) is an organic residue formed through incomplete combustion of biomass and is ubiquitous in the environment (Goldberg, 1985; Schmidt and Noack, 2000). BC is heterogenic by nature, and includes wide array of compounds comprising a

continuum of lightly charred biomolecules to highly condensed aromatic material formed from high temperature combustion. Roughly 80% of BC deposited in soils is in the form of char, where it can remain for up to a millennium due to its recalcitrant nature (Preston and Schmidt, 2006). However, a significant portion of the BC pool can be translocated to the aqueous phase as dissolved BC (DBC). Using benzene polycarboxylic acid (BPCA) markers as tracers for DBC comprised predominately of condensed aromatic units, a recent study found that on a global scale, DBC accounts for roughly 10% of dissolved organic carbon (DOC) in river systems (Jaffé et al., 2013). This coupling of DBC with DOC suggests that biogeochemical mechanisms controlling the release of DBC to aquatic ecosystems are similar to those of DOC.

While the translocation of BC from particulate charcoal to the dissolved phase is not well understood, it has been suggested that, like the generation of DOC from soil organic matter (OM), long term microbial oxidation is a major factor in the release of DBC from charcoal in soils (Hockaday et al., 2006). On the other hand, photodissolution of particulate organic carbon (POC) to DOC has also been shown to be a significant process in the generation of DOC in aquatic systems (Mayer et al., 2006, 2012; Pisani et al., 2011; Shank et al., 2011), which might then be further photodegraded once in solution (Mopper et al., 1991). While there is currently only limited information on the photochemical transformation of DBC, photodegradation has been shown to preferentially remove DBC relative to bulk DOC (Stubbins et al., 2012; Wagner and Jaffé, 2015). Due to the highly aromatic nature of BC, it is expected that charcoal might also be prone to follow similar photochemical transformation pathways as soil OM,

leading to the potential translocation of particulate black carbon (PBC) to DBC in aquatic systems.

The ubiquity and stability of BC in the environment may have an important impact on the global biogeochemical cycling of organic carbon as significant amounts of BC may not be only sequestered in soils, but further mobilized and transported throughout the environment. An understanding of biogeochemical processes involved in the mobilization of BC is therefore of increasing importance. The goal of the present study was to investigate the potential photochemical release of DBC from two particulate sample types: fire-impacted soil and wood char formed during a wildfire event. We hypothesized that significant photodissolution of BC would occur upon irradiation of both soil and char. It was further hypothesized that the photochemical oxidation of BC would be a driving mechanism for the photodissolution of BC, as observed for bulk DOC (Estapa and Mayer, 2010). These hypotheses were tested by quantifying DBC (using the BCPA method) photoproduced from suspensions of soil and char in water and exposed to simulated sunlight. Light-exposed and dark control samples were also characterized using Fourier transform-ion cyclotron resonance mass spectrometry (FTICR-MS) to observe molecular level changes in DOC and DBC composition during irradiation.

### **3.3 Methods**

#### *3.3.1 Sample Collection*

The soil and char samples were collected within a burned area of the Cache La Poudre River watershed near Fort Collins, Colorado, which was described by Wagner et al. (2015). The burn occurred in June of 2012, encompassing roughly 350 km<sup>2</sup> of the total watershed (< 10%) and samples were collected roughly 1 year after the burn. Soil BC

concentrations have been reported as high as 33.83 g/kg in highly burned areas of the Poudre River watershed (Boot et al. 2015). The char sample was collected by physically scraping surface char from the burned surface layer of a pine tree trunk at a height of about 1 m above ground. The soil sample was collected in an area near burned shrub-like vegetation within the vicinity of the tree from which the char sample was collected. Samples were stored in the dark at -20 °C until processing.

### *3.3.2 Experimental Setup*

Samples were dried for 48 h before being ground and passed through a 30 mesh sieve. The soil and char samples were mixed with deionized water in pre-combusted quartz flasks at a final concentration of 3.33 g/l (0.5 g in 150 ml). Each individual sample flask was representative of a single measurement. Flasks containing light exposed samples were covered with quartz plates and flasks containing dark controls were covered with Al foil and wrapped in black plastic bags. All samples were placed in a circulating water bath kept at 25 °C, with vigorous shaking at 100 RPM to induce suspension of particulates for the duration of the experiment. The samples were incubated in a solar simulator (Suntest XLS+, Atlas Material Testing Technology LLC) set at 765 W/m<sup>2</sup>, which provided exposure conditions equivalent to roughly 4 days natural sunlight per 24 h photoincubation period in the solar simulator. The highly turbid nature of these samples was expected to shield newly generated DOC (Pisani et al., 2011) and DBC from further photochemical degradation (Stubbins et al. 2012) throughout the photoincubation period. Triplicate light and dark samples were removed from the solar simulator at 2, 4 and 7 days (equivalent to 8, 16, & 32 days natural sunlight) and filtered through a pre-combusted 0.7 µm GFF filter. A deionized water blank was also analyzed and recorded

as time zero. Samples were analyzed for DOC with a Shimadzu TOC-V CSH total organic carbon analyzer after acidification and purging with CO<sub>2</sub> free air to remove inorganic carbon.

### 3.3.3 *Quantification of DBC*

Samples were quantified at each time point for DBC using the BPCA method described by Dittmar (2008). This method is based on the thermo-chemical oxidation of the condensed aromatic compounds into polysubstituted benzene carboxylic acids, whose distribution patterns provide an indication into the overall condensed aromaticity of the DBC represented.

To describe the method, briefly, the DOM was extracted using solid phase extraction (SPE) with Varian Bond Elut PPL cartridges (Dittmar et al., 2008). Aliquots of the methanol SPE eluent containing *ca.* 0.2 mg DOC were dried under N<sub>2</sub> in combusted 2 ml glass ampoules. The DOC was then oxidized with 0.5 mL HNO<sub>3</sub> for 6 h at 160 °C (Ding et al., 2013). The samples were then dried under N<sub>2</sub> gas and the remaining BPCAs redissolved in mobile phase buffer and quantified using a high performance liquid chromatography (HPLC) instrument coupled with diode array detection (Surveyor, Thermo Scientific). Separation of BPCAs was carried on a Sunfire C<sub>18</sub> reversed phase column (3.1 µm, 2.1 x 150 mm; Waters Corporation) using a elution gradient containing mobile phase A (50 mM sodium acetate, 4 mM tertbutylammonium bromide, 10 % methanol) and mobile phase B (100% methanol). These conditions have been further described in detail by Dittmar (2008). BPCA oxidation and analysis were performed for each individual sample in triplicates. The average coefficient of variation for these analytical triplicates was less than 5%.

### 3.3.4 Ultra-High Resolution Mass Spectrometry

Each SPE extract was diluted with methanol to 50 µg C/ ml and analyzed using negative-ion electrospray ionization coupled with a custom-built 9.4 Tesla FTICR-MS instrument at the National High Magnetic Field Laboratory (Tallahassee, FL; Blakney et al., 2011; Kaiser et al., 2011). Samples were introduced into the electrospray source at 400 nL/min with 200 scans being accumulated with a mass window up to 800 Da. A “walking” internal calibration was applied to each mass spectrum (Savory et al., 2011) prior to the assignment of molecular formulae with software developed at the NHMFL. Samples were analyzed in triplicate with a 3% average standard deviation in the number of assigned molecular formulae across all samples.

## 3.4 Results

### 3.4.1 Photoproduction of DBC

Photoexposure of the soil and char significantly enhanced the production of DBC ( $n = 3$ ,  $p < 0.05$ ; Table 3.1). Normalized to initial POC concentration, photoexposed char and soil produced up to  $1.63 \pm 0.16$  mg/l/g C and  $4.6 \pm 0.1$  mg/l/g C of DBC respectively over the 7 day photoincubation period. These abundances were significantly greater ( $n = 3$ ,  $p < 0.05$ ) than the DBC in the dark controls for both the char ( $0.67 \pm 0.01$  mg/l/g C) and soil ( $1.22 \pm 0.03$  mg/l/g C) over the same period. By subtracting DBC concentration of the control sample from the light exposed sample, the amount of additional DBC produced from photodissolution (p-DBC) at 7 days was  $0.96 \pm 0.15$  mg/l/g C and  $3.42 \pm 0.13$  mg/l/g C for the char and soil respectively (Figure 3.1). While this was significantly greater than the amount of p-DBC produced at

two days for each sample, it appears in each case the p-DBC may be reaching an equilibrium after approximately 4 days (Figure 3.1).

The BPCA ratio  $[(B5CA+B6CA)/(B3CA+B4CA)]$  was used to monitor changes in DBC character during the photoincubation period. The ratio is used to describe condensed aromaticity of DBC where a higher relative abundance of B5CA and B6CAs compared to B3CA and B4CAs implies a greater degree of polycondensed DBC. The light exposed char and soil samples each showed a significant increase ( $n = 3, p < 0.05$ ) in the BPCA ratio throughout the photoincubation period (Table 3.1). The BPCA ratio from DBC generated from the char increased from  $0.50 \pm 0.03$  to  $0.85 \pm 0.04$  from 2 to 7 days light exposure. An increase in BPCA ratio from  $0.59 \pm 0.03$  to  $0.77 \pm 0.01$  was also observed for DBC generated from the photoexposed soil sample from 2 to 7 days irradiation. For the char dark control samples, the BPCA ratio increased only slightly from  $0.49 \pm 0.02$  to  $0.58 \pm 0.04$  from 2 to 7 days, and there was no overall net change in the ratio from the dark control soil samples at 2 ( $0.44 \pm 0.02$ ) and 7 days ( $0.47 \pm 0.01$ ).

#### *3.4.2 Photoproduction of DOC*

Patterns of photochemical changes in the bulk DOC varied between the char and soil. For the char, a significantly greater amount of DOC was produced in light exposed samples ( $16.89 \pm 0.53$  mg/l/g C) compared with the dark controls ( $13.52 \pm 0.36$  mg/l/g C) after two days irradiation ( $n = 3, p < 0.05$ ). However, unlike the p-DBC, no significant increase was observed for the photodissolved DOC (p-DOC) throughout the photoincubation (Table 3.1). The molar proportion of p-DBC to p-DOC (p-DBC%) for the char sample increased from  $10.34 \pm 2.12\%$  to  $24.91 \pm 13.42\%$  from 2 to 7 days.

**Table 3.1:** Photodissolution experimental data. (nd = not detected, a (-) indicates value was not calculated because of a nd response). p-DBC and p-DOC were calculated by subtracting the dark DBC and DOC concentrations from the light DBC and DOC concentrations, respectively. Errors represent 1 standard deviation from the mean

Time (days)	Char										
	DOC (mg/l/g C)			DBC (mg/l/g C)			BPCA ratio		DBC (%)		
	Light	Dark	p-DOC	Light	Dark	p-DBC	Light	Dark	Light	Dark	p-DBC(%)
0 (blank)	0.2 ± 0.2		-	Nd		-	-		-		
2	16.89 ± 0.53	13.52 ± 0.36	3.36 ± 0.64	1.15 ± 0.01	0.81 ± 0.02	0.35 ± 0.02	0.50 ± 0.03	0.49 ± 0.02	6.85 ± 0.21	5.98 ± 0.24	10.34 ± 2.12
4	15.29 ± 0.64	10.37 ± 0.60	4.92 ± 0.87	1.42 ± 0.12	0.62 ± 0.03	0.80 ± 0.12	0.65 ± 0.03	0.44 ± 0.06	9.28 ± 0.92	4.23 ± 2.10	16.37 ± 3.96
7	16.07 ± 1.82	12.20 ± 0.78	3.87 ± 1.98	1.63 ± 0.16	0.67 ± 0.01	0.96 ± 0.15	0.85 ± 0.04	0.58 ± 0.04	10.16 ± 1.51	4.97 ± 0.67	24.91 ± 13.42
Time	Soil										
	DOC (mg/l/g C)			DBC (mg/l/g C)			BPCA ratio		DBC%		
	Light	Dark	p-DOC	Light	Dark	p-DBC	Light	Dark	Light	Dark	p-DBC%
0 (blank)	0.067 ± 0.005		-	Nd		-	-		-		
2	22.46 ± 0.67	10.28 ± 0.38	12.1 ± 0.77	2.52 ± 0.11	0.74 ± 0.02	1.79 ± 0.12	0.59 ± 0.03	0.44 ± 0.02	11.25 ± 0.60	7.17 ± 0.33	14.71 ± 1.31
4	33.17 ± 1.31	10.42 ± 0.33	22.7 ± 1.35	4.19 ± 0.12	1.00 ± 0.02	3.19 ± 0.13	0.69 ± 0.02	0.46 ± 0.01	12.64 ± 0.63	9.62 ± 0.38	14.03 ± 1.00
7	38.45 ± 2.48	12.48 ± 0.76	26.0 ± 2.59	4.63 ± 0.12	1.22 ± 0.03	3.42 ± 0.13	0.77 ± 0.01	0.47 ± 0.01	12.06 ± 0.84	9.78 ± 0.65	13.15 ± 1.41



For the soil sample exposed to light, the bulk DOC increased significantly ( $n = 3$ ,  $p < 0.05$ ) in concert with the DBC. The DOC produced in light exposed samples ( $22.46 \pm 0.67$  mg/l/g C) was more than 2x that of the DOC in the dark control ( $10.28 \pm 0.38$  mg/l/g C) at 2 days and increased in the light exposed sample to  $38.45 \pm 2.48$  mg/l/g C at seven days. The DOC in the control sample increased slightly to  $12.48 \pm 0.76$  mg/l/g C at 7 days. Thus, the amount of p-DOC generated from the soil was  $25.96 \pm 2.59$  mg/l/g C after a 7 days exposure (Table 3.1). Unlike the char sample, there was no significant change in p-DBC% for the light exposed soil sample, which averaged  $13.96 \pm 0.72\%$  throughout the photoincubation.

### *3.4.3 Ultra-High Resolution Mass Spectrometry*

FTICR-MS is a unique analytical technique that can be used to obtain structural information about complex DOM matrices (Kujawinski, 2002; Sleighter and Hatcher, 2007). It provides high resolution separation of sample compounds with a mass accuracy error of  $< 1$  ppm (Stenson et al., 2003). A molecular formula can be assigned to resolved peaks based on the molecular mass and detailed structural information for each sample matrix can be obtained using the elemental compositions of assigned peaks. Here, FTICR-MS was used for molecular characterization of the DOC produced from the samples throughout the photoincubation. Compounds detected containing C, H, and O were assigned a molecular formula and molecular weight (MW). The total number of assigned formulas varied with each sample and ranged from 8,700 to 12,500 (Table 3.2). A modified aromatic index, calculated using only the assigned molecular formula, was used to identify condensed aromatic structures (DBC) detected with FTICR-MS (Koch and Dittmar, 2006; Spencer et al., 2014). The DBC detected with FTICR-MS was defined

as molecular formulae with a calculated modified aromatic index greater than or equal to 0.67 (Koch and Dittmar, 2006).

Irradiation of the char for 2 days produced  $980 \pm 41$  unique DBC compounds, which was not significantly different from the number of DBC compounds in the dark controls ( $935 \pm 17$ ). However, the average MW of DBC compounds for the light exposed samples was slightly larger than that for the dark control samples (Table 3.2). With increasing irradiation time, the number of DBC compounds detected at seven days increased to  $1339 \pm 44$ , concomitant with an increase in their average MW vs. the dark control samples (Table 3.2).

**Table 3.2:** FTICR-MS information for light exposed samples and dark controls at 2 and 7 days. Errors represent 1 standard deviation from the mean.

Sample	Assigned Formulae	Assigned BC Formulae	Average BC MW .
Char Dark 2 days	$9267 \pm 170$	$935 \pm 17$	$398 \pm 1$
Char Light 2 days	$8789 \pm 316$	$980 \pm 41$	$407 \pm 3$
Char Dark 7 days	$10804 \pm 384$	$1106 \pm 28$	$419 \pm 4$
Char Light 7 days	$9127 \pm 152$	$1339 \pm 43$	$453 \pm 4$
Soil Dark 2 days	$9039 \pm 228$	$1936 \pm 69$	$428 \pm 1$
Soil Light 2 days	$12016 \pm 1018$	$2498 \pm 242$	$460 \pm 7$
Soil Dark 7 days	$12501 \pm 379$	$2901 \pm 85$	$458 \pm 2$
Soil Light 7 days	$11933 \pm 268$	$2789 \pm 27$	$457 \pm 2$

For the soil, the number of DBC formulae detected at 2 days was  $2489 \pm 242$  in the light vs.  $1936 \pm 69$  in the dark, with the average MW for the light exposed samples also being significantly higher ( $n = 3$ ,  $p < 0.05$ ; Table 3.2). Despite the significant increase in DBC concentration during photoincubation, no significant increase in the number of detected BC compounds or average MW was observed with increasing irradiation time for the soil samples.

### 3.5 Discussion

#### 3.5.1 Photoproduction of DOC and DBC

Production of DOC through photodissolution of POC has been well studied for soils from many different environments (Kieber et al., 2006; Mayer et al., 2006, 2012; Pisani et al., 2011; Shank et al., 2011). However, information regarding the photoinduced release of DOC from particulate charcoal and recently fire-impacted soils is unavailable. Our results show that photodissolution accounted for up to  $4.92 \pm 0.87$  mg/l/g C of the DOC produced from the char sample and up to  $25.96 \pm 2.59$  mg/l/g C of the DOC produced from the soil sample. Photoproduction of DOC from the soil sample is also greater than the DOC photoproduced from marine sediments in Florida Bay (4 mg/l/g C; Shank et al., 2011) and from organic rich estuarine sediments in the Cape Fear River, North Carolina (3 mg/l/g C; Kieber et al., 2006)]. It is also greater than the DOC produced from sediments in a Texas estuary (up to 6.62 mg C/l/g C; Liu and Shank, 2015) and from a number of soils described by Mayer et al. (2012), however; it is significantly less than the DOC produced from Everglades floc (259 mg C/l/g C; Pisani et al., 2011). It is likely these differences can be attributed to use of different source material, and also from different experimental conditions with higher POC loadings of 3.33 mg/l here when compared with other studies, such as the 1-2 mg/l used by Shank et al. (2011) and Kieber et al. (2006) and 24 mg/l by Pisani et al. (2011).

As observed for the soil, the p-DOC was expected to increase throughout photoincubation. However, no significant net change in p-DOC for the char sample was observed from 2 to 7 days, suggesting an equilibrium between photodissolution and photodegradation may have been reached (Table 3.1). Santín et al. (2015) have shown

that > 50% of carbon in wood samples from a post Canadian wildfire is retained as pyrogenic carbon, compared with roughly 25% in soil. Thus, it would be expected that the bulk OC in the char is more recalcitrant and less water soluble than the soil sample. Thus, the more recalcitrant nature of the char sample may explain why the DOC did not continue to increase throughout photoincubation when compared with the soil sample.

Contrary to the bulk DOC from the char, an increase in p-DBC was observed throughout the 7 day photoincubation period, which was coupled with an increase in the apparent condensed aromaticity of DBC as evidenced by an increase in BPCA ratio (Table 3.1). A similar increase in both p-DBC and BPCA ratio was observed for the soil sample. This would suggest that larger, more polycondensed BC compounds are entering the dissolved phase with increasing light exposure time.

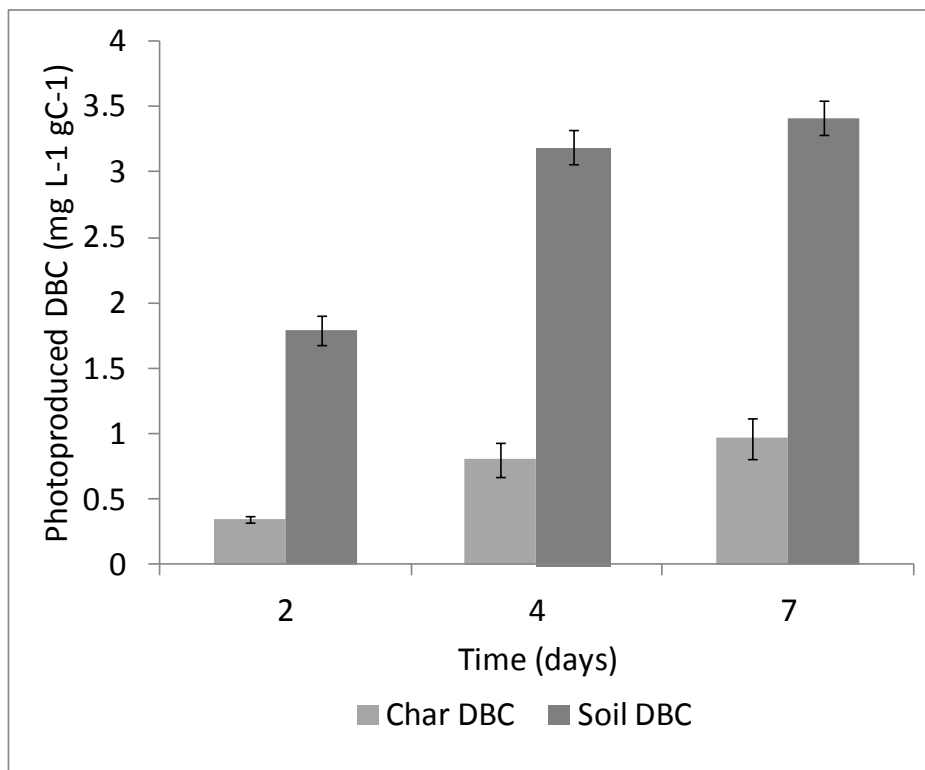


**Figure 3.1:** Graph showing change in amount of photoproduced DBC over the 7 days photoincubation. Error bars represent 1 standard deviation from the mean.

Estapa and Mayer (2010) have shown evidence that DOC became more oxygenated as it was photodissolved. Thus, an increase in BPCA ratio with light exposure would not be unexpected, as larger BC compounds would presumably need to become more functionalized (i.e. oxygenated) to increase their polarity before they are soluble enough to be transferred to the dissolved phase. It has been suggested that under unique environmental conditions (low pH, high Fe and high DOC), new 'BC like' compounds are formed from irradiation of terrestrial OM and flocculated in the form of POC (Chen et al., 2014). However, analysis of these new FTICR-MS based 'BC like' compounds has yet to be performed through quantitative means, such as the BPCA method. Additionally, evidence for the photoproduction of DBC from DOC has not been observed in other studies (Stubbins et al., 2012; Wagner and Jaffé, 2015). This study provides proof of concept that the production of DBC can occur photochemically from char and soils, likely following similar mechanisms as those described by Estapa and Mayer (2010) for DOC generated from soil OM.

The char and soil photoincubations at 2 and 7 days exposure were characterized using FTICR-MS with molecular formulae and MW being assigned for greater than 8,500 compounds in each of the samples. Van Krevelen diagrams were created using the H/C and O/C ratios of assigned molecular formulae to show differences in molecular composition between samples. Figure 3.2a shows example van Krevelen diagrams for the char sample exposed to light at 2 and 7 days respectively. These van Krevelen diagrams represent the unique molecular formulas detected with respect to each sample in comparison to its counterpart. All molecular formulas common to the two samples were removed to emphasize the major compositional changes for each sample between two

and seven day treatments. As observed in Figure 3.2a, a general shift to lower H/C values and higher O/C values is apparent with a longer photoincubation time suggesting the bulk DOC becomes more oxygenated with increasing light exposure. This observation is supported by an increase in both the number and average MW of identified BC compounds after 7 days exposure (Table 3.2). The latter further supports the hypothesis that more extensive light exposure is required for the oxidation of larger BC compounds prior to their transfer to the dissolved phase. Comparison of the unique molecular formula for light and dark samples at 7 days (Figure 3.2b), presented in a similar format as those in Figure 3.2a, supports the trend of increasing DBC in the light-exposed samples to be a consequence of photoexposure rather than resulting from a leaching process. The lower H/C values in Figure 3.2b, along with increasing number of BC molecular formulae and their average MW (Table 3.2) in the light vs. dark samples, suggest that the BC actively undergoes photodissolution.

The trend of simultaneous increases in DBC concentration and BPCA ratio is consistent between the soil and char samples. However, the molecular composition of the soil sample was expectedly more complex than the char sample (based on FTICR-MS, with the total number of *ca.* 12,000 molecular formulas for light exposed samples for the soil vs. *ca.* 9,000 for the char; Table 1). No significant changes in the number of detected DBC molecular formulas or average MW were observed for the light exposed soil sample at 7 days compared to the light exposed sample at 2 days (Table 3.2). This is in contrast to the trend observed for the char sample. In addition, there was roughly twice the number of assigned BC compounds detected in any soil sample vs. the char samples. This would suggest that the soil BC might have already been further degraded/oxidized vs. the

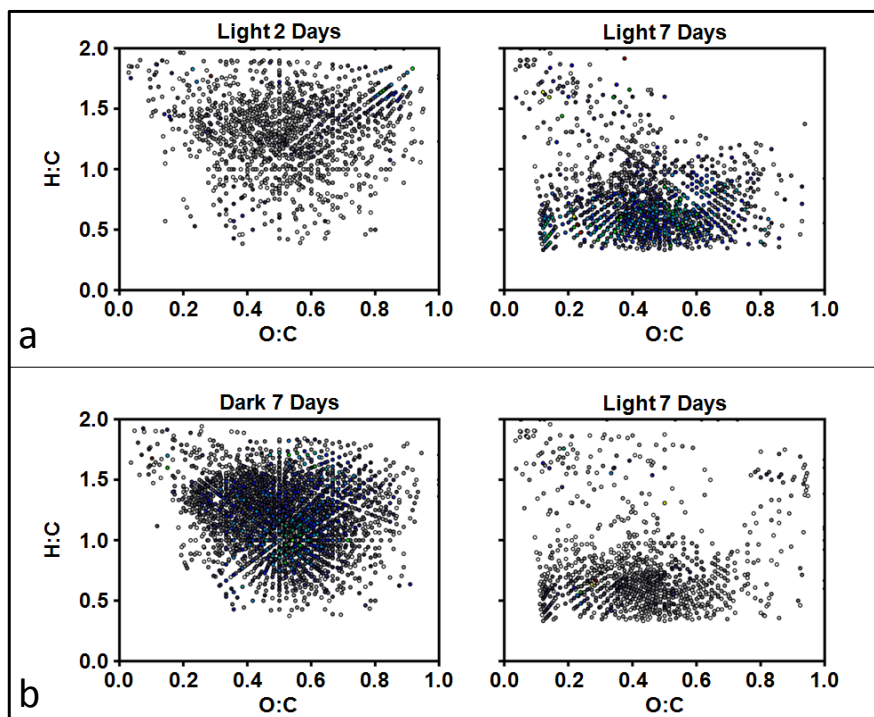


**Figure 3.2:** FTICR-MS data in the form of van Krevelen diagrams displaying (a) unique molecular formulae identified as a comparison of light samples at 2 and 7 days, and (b) unique molecular formulae identified as a comparison between the light exposed char and the dark controls at 7 days. Note: The unique molecular formulae are defined as those that are not detected in the comparison sample (i.e., all molecular formulae that were detected in both samples were removed from the van Krevelen diagrams).

char sample, or that the soil sample also contained charcoal from older fires in the region.

This is supported by strong coupling of DBC and DOC for the soil where 14% of the p-DOC was represented as p-DBC consistently throughout the photoincubation period.

With aged BC in soils being more oxidized and water soluble (Abiven et al., 2011), the increase in p-DBC from the soil sample is likely from continuous production of more similar DBC compounds throughout the photoincubation, thereby explaining the lack of new DBC compounds detected with time. This is in contrast to the PBC for the char, which has not likely experienced such weathering conditions as PBC in the soil. Thus the

char has a clearer path of photodissolution via photooxidation resulting in the continuous production of new, unique DBC compounds throughout the photoincubation period vs. the soil sample.

### *3.5.2 Mobilization of BC*

BC is considered highly recalcitrant, yet current estimates suggest that 26.5 million metric tons is annually transported from rivers to the ocean in dissolved form (Jaffé et al., 2013). This mobilization of BC in rivers is best understood to be the result of long-term microbial oxidation of charcoal in soils before it is released in the dissolved phase. For instance, using FTICR-MS, Hockaday et al. (2006) observed an increase in aromatic structures enriched with O-containing functional groups in water soluble soil products that had experienced a century of degradation in a forest environment. Abiven et al. (2011) also reported increased aromaticity and oxidation in the soluble products from aged charcoal. It has also been shown in a Brazilian tropical biome that DBC is still mobilized from soils even decades after the most recent burn event (Dittmar et al., 2012). While enhanced solubilization due to long term biotic processing of char in soils might be a critical factor in determining the mobility of BC from soils to aquatic systems, results from this study show that photochemical processes may also contribute to the mobilization of soil BC. In fact, a significant portion of the photoproducts comprised of DBC (up to 25% for light exposed char and on average 14% for light exposed soil). This coupling behavior between DBC and DOC clearly suggest that these carbon pools are photodissolved through similar mechanisms. While these preliminary experiments provide ‘proof of concept’ for photodissolution as a potential mechanism in the mobilization of BC from soils to water, the process may likely be most prominent for



surface soils (Mayer et al., 2012) in shallow aquatic systems and in systems with high sediment resuspension. At this point, however, the relative contributions of abiotic vs. biotic processes in mobilization of DBC in aquatic systems remain to be explored.

### **3.6 Conclusions**

This is the first report to show photodissolution as a potential source of DBC in the aquatic environment. Photoproduced DBC increased significantly in the photoexposed soil and char samples. The increase in DBC concentration and polycondensed aromatic character in the char sample was complemented with FTICR-MS data showing an increase in the number of BC compounds detected and their average MW. A shift toward lower H/C and higher OC values in van Krevelen diagrams also showed photooxidation as a potential pathway in the photodissolution of BC.

DBC accounted for up to 25% of the photoproduced DOC for the char and 14% for the soil suggesting photodissolution may be a significant, short-term mechanism for mobilization of BC from freshly charred biomass and from older, more degraded charcoal particles. The coupling between DBC and DOC is consistent with the literature (Jaffé et al., 2013) and may imply that photochemical processes regulating the fate and transport of DBC and DOC in aquatic systems are related. While the overall extent to which photodissolution accounts for production of DBC in the aquatic environment remains unknown, it is expected that the mobilization of BC through photodissolution would be most prominent in near shore shallow environments with increased light penetration or in areas with a high amount of suspended sediment. For instance, resuspension of soils from alluvial fans in Colorado may provide a continuous long-term supply of DBC produced from photodissolution as pyrogenic carbon has historically

accumulated in these areas (Cotrufo et al. 2016). However, in order to extrapolate the results from this study on photodissolution of BC into environmental applications on a global scale, future research should focus on the quantitative assessment of photodissolution from different types of soils and chars over a wide range sources and PBC content and under a variety of environmental conditions. In addition, photodissolution kinetics and mass balances should be used to further investigate the relationship between PBC and p-DBC including the mineralization of PBC during photoexposure as well as the further degradation of the newly generated DBC (Stubbins et al. 2012). The data presented here are proof of concept that photodissolution of PBC may be a previously unrecognized and potentially significant source of DBC in aquatic systems, which merits further study.

### 3.7 References

- Abiven, S., Hengartner, P., Schneider, M.P.W., Singh, N., Schmidt, M.W.I., 2011. Pyrogenic carbon soluble fraction is larger and more aromatic in aged charcoal than in fresh charcoal. *Soil Biology and Biochemistry* 43, 1615-1617.
- Blakney, G.T., Hendrickson, C.L., Marshall, A.G., 2011. Predator data station: A fast data acquisition system for advanced FT-ICR MS experiments. *International Journal of Mass Spectrometry* 306, 246-252.
- Boot, C.M., Haddix, M., Paustian, K., Cotrufo, M. F., 2015. Distribution of black carbon in ponderosa pine forest floor and soils following the High Park wildfire. *Biogeosciences* 12, 3029-3039.
- Chen, H., Abdulla, H.A.N., Sanders, R.L., Myneni, S.C.B., Mopper, K., Hatcher, P.G., 2014. Production of black carbon-like and aliphatic molecules from terrestrial dissolved organic matter in the presence of sunlight and iron. *Environmental Science & Technology Letters* 1, 399-404.
- Cotrufo, M. F., Boot, C. M., Kampf, S., Nelson, P. A., Brogan, D. J., Covino, T., Haddix, M. L., MacDonald, L. H., Rathburn, S., Ryan-Bukett, S., Schmeer, S., Hall, E., 2016. Redistribution of pyrogenic carbon from hillslopes to stream corridors following a large montane wildfire. *Global Biogeochemical Cycles* 30, 1348-1355

- Ding, Y., Yamashita, Y., Dodds, W.K., Jaffé, R., 2013. Dissolved black carbon in grassland streams: Is there an effect of recent fire history? *Chemosphere* 90, 2557-2562.
- Dittmar, T., 2008. The molecular level determination of black carbon in marine dissolved organic matter. *Organic Geochemistry* 39, 396-407.
- Dittmar, T., de Rezende, C.E., Manecki, M., Niggemann, J., Coelho Ovalle, A.R., Stubbins, A., Bernardes, M.C., 2012. Continuous flux of dissolved black carbon from a vanished tropical forest biome. *Nature Geoscience* 5, 618-622.
- Dittmar, T., Koch, B., Hertkorn, N., Kattner, G., 2008. A simple and efficient method for the solid-phase extraction of dissolved organic matter (SPE-DOM) from seawater. *Limnology and Oceanography: Methods* 6, 230-235.
- Estapa, M.L., Mayer, L.M., 2010. Photooxidation of particulate organic matter, carbon/oxygen stoichiometry, and related photoreactions. *Marine Chemistry* 122, 138-147.
- Goldberg, E.D., 1985. *Black Carbon in the Environment: Properties and Distribution*, 1 ed. John Wiley & Sons Inc, New York.
- Hockaday, W.C., Grannas, A.M., Kim, S., Hatcher, P.G., 2006. Direct molecular evidence for the degradation and mobility of black carbon in soils from ultrahigh-resolution mass spectral analysis of dissolved organic matter from a fire-impacted forest soil. *Organic Geochemistry* 37, 501-510.
- Jaffé, R., Ding, Y., Niggemann, J., Vähätalo, A.V., Stubbins, A., Spencer, R.G.M., Campbell, J., Dittmar, T., 2013. Global charcoal mobilization from soils via dissolution and riverine transport to the oceans. *Science* 340, 345-347.
- Kaiser, N.K., Quinn, J.P., Blakney, G.T., Hendrickson, C.L., Marshall, A.G., 2011. A Novel 9.4 Tesla FTICR Mass Spectrometer with improved sensitivity, mass resolution, and mass range. *Journal of The American Society for Mass Spectrometry* 22, 1343-1351.
- Kieber, R.J., Whitehead, R.F., Skrabal, S.A., 2006. Photochemical production of dissolved organic carbon from resuspended sediments. *Limnology and Oceanography* 51, 2187-2195.
- Koch, B.P., Dittmar, T., 2006. From mass to structure: an aromaticity index for high-resolution mass data of natural organic matter. *Rapid Communications in Mass Spectrometry* 20, 926-932.
- Kujawinski, E.B., 2002. Electrospray Ionization Fourier Transform Ion Cyclotron Resonance Mass Spectrometry (ESI FT-ICR MS): Characterization of complex environmental mixtures. *Environmental Forensics* 3, 207-216.

- Liu, Q., Shank, G.C., 2015. Solar radiation-enhanced dissolution (photodissolution) of particulate organic matter in Texas estuaries. *Estuaries and Coasts* 38, 2172-2184.
- Mayer, L.M., Schick, L.L., Skorko, K., Boss, E., 2006. Photodissolution of particulate organic matter from sediments. *Limnology and Oceanography* 51, 1064-1071.
- Mayer, L.M., Thornton, K.R., Schick, L.L., Jastrow, J.D., Harden, J.W., 2012. Photodissolution of soil organic matter. *Geoderma* 170, 314-321.
- Mopper, K., Zhou, X., Kieber, R.J., Kieber, D.J., Sikorski, R.J., Jones, R.D., 1991. Photochemical degradation of dissolved organic carbon and its impact on the oceanic carbon cycle. *Nature* 353, 60-62.
- Pisani, O., Yamashita, Y., Jaffé, R., 2011. Photo-dissolution of flocculent, detrital material in aquatic environments: Contributions to the dissolved organic matter pool. *Water Research* 45, 3836-3844.
- Preston, C.M., Schmidt, M.W.I., 2006. Black (pyrogenic) carbon: a synthesis of current knowledge and uncertainties with special consideration of boreal regions. *Biogeosciences* 3, 397-420.
- Santín, C., Doerr, S.H., Preston, C.M., González-Rodríguez, G., 2015. Pyrogenic organic matter production from wildfires: a missing sink in the global carbon cycle. *Global Change Biology* 21, 1621-1633.
- Savory, J.J., Kaiser, N.K., McKenna, A.M., Xian, F., Blakney, G.T., Rodgers, R.P., Hendrickson, C.L., Marshall, A.G., 2011. Parts-Per-Billion Fourier Transform Ion Cyclotron Resonance mass measurement accuracy with a “walking” calibration equation. *Analytical Chemistry* 83, 1732-1736.
- Schmidt, M.W.I., Noack, A.G., 2000. Black carbon in soils and sediments: Analysis, distribution, implications, and current challenges. *Global Biogeochemical Cycles* 14, 777-793.
- Shank, G.C., Evans, A., Yamashita, Y., Jaffé, R., 2011. Solar radiation-enhanced dissolution of particulate organic matter from coastal marine sediments. *Limnology and Oceanography* 56, 577-588.
- Sleighter, R.L., Hatcher, P.G., 2007. The application of electrospray ionization coupled to ultrahigh resolution mass spectrometry for the molecular characterization of natural organic matter. *Journal of Mass Spectrometry* 42, 559-574.
- Spencer, R.G.M., Guo, W., Raymond, P.A., Dittmar, T., Hood, E., Fellman, J., Stubbins, A., 2014. Source and biolability of ancient dissolved organic matter in glacier and lake ecosystems on the Tibetan Plateau. *Geochimica et Cosmochimica Acta* 142, 64-74.

Stenson, A.C., Marshall, A.G., Cooper, W.T., 2003. Exact masses and chemical formulas of individual Suwannee River fulvic acids from ultrahigh resolution Electrospray ionization Fourier transform ion cyclotron resonance mass spectra. *Analytical Chemistry* 75, 1275-1284.

Stubbins, A., Niggemann, J., Dittmar, T., 2012. Photo-lability of deep ocean dissolved black carbon. *Biogeosciences* 9, 1661-1670.

Wagner, S., Cawley, K., Rosario-Ortiz, F., Jaffé, R., 2015. In-stream sources and links between particulate and dissolved black carbon following a wildfire. *Biogeochemistry* 124, 145-161.

Wagner, S., Jaffé, R., 2015. Effect of photodegradation on molecular size distribution and quality of dissolved black carbon. *Organic Geochemistry* 86, 1-4.

Ward, C.P., Sleighter, R.L., Hatcher, P.G., Cory, R.M., 2014. Insights into the complete and partial photooxidation of black carbon in surface waters. *Environmental Science: Processes & Impacts* 16, 721-731.

## CHAPTER IV

# HYDROLOGICAL CONTROLS ON THE SEASONAL VARIABILITY OF DISSOLVED AND PARTICULATE BLACK CARBON IN THE ALTAMAHA RIVER, GA

(Submitted to *Journal of Geophysical Research: Biogeosciences*, 2018)

#### 4.1 Abstract

Rivers play a critical role in the annual transport of organic material from terrestrial to marine environments. A significant portion of this material is black carbon (BC), a thermogenic residue formed from incomplete combustion of biomass and fossil fuel combustion. Black carbon is mobilized in fluvial systems as both particulate BC (PBC) and dissolved BC (DBC) and the export of BC to coastal environments may have significant implications for carbon cycling in marine environments. However, while little is known regarding the potential connectivity between riverine export of PBC and DBC, current knowledge suggests that fluvial export of PBC and DBC are decoupled in small fire-impacted watersheds. The present study aims to further address the subject, but on a watershed scale. For this study, thirteen monthly samples were collected (Sept. 2015 - Sept. 2016) near the mouth of the Altamaha River, Georgia. Particulate black carbon and DBC were characterized using the benzenepolycarboxylic acid method. We show that seasonal hydrology and regional shifts in high intensity storm events play a pivotal role for both PBC and DBC export during high flow months. During baseflow, groundwater transports DBC derived from deep-soil charcoal, whereas evidence of seasonal salt-water intrusions suggest an additional estuarine contribution of PBC at the sampling location. An apparent coupling between DBC and PBC was observed during baseflow, although the association was disrupted during high flow periods. While this is the first report of potential coupling between DBC and PBC, environmental drivers controlling this association between DBC and PBC remain to be constrained.

## 4.2 Introduction

Rivers export around 0.5 Pg of organic carbon (OC) to oceans annually making them an important link between terrestrial and aquatic ecosystems (Cai, 2011). This carbon pool can be exported from the terrestrial environment in dissolved (DOC) and particulate (POC) forms, both of which play pivotal roles in ecosystem function and carbon cycling (Spencer et al., 2016). The mobility of OC is closely linked to watershed hydrology, where often the greatest export is observed during periods of high water flow that can be directly related to storm events as well as spring snow melts in high-latitude climates (Holmes et al., 2012; Spencer et al., 2010). In fact, singular high intensity storm events over a few days can be responsible for nearly half of the annual OC exported from a watershed (Jeong et al., 2012; Yoon & Raymond, 2012). These high precipitation events promote the flushing of near-stream organic rich soils leading to increased DOC fluxes (Inamdar et al., 2011), whereas increased POC export can be related to soil erosion and overland runoff (Dhillon & Inamdar, 2014). The shift in OC sources during high flow events can also be coupled with a shift in OC composition. During high flow events, surface soil flushing and overland runoff generates OC mainly derived from allochthonous sources, such as humic and fulvic acids generated from decomposed leaf and plant debris (Bianchi et al., 2004; Hedges et al., 1994) and specific biomarkers derived from the primary vegetation (e.g., conifers; Medeiros et al., 2012). In contrast, during baseflow, groundwater sources depleted of highly aromatic dissolved organic matter (DOM) and rich in microbial and protein-like character contribute primarily to streamflow (Hood et al., 2006; Inamdar et al., 2011; Raymond & Spencer, 2015).



Organic matter (OM) sources and composition throughout a watershed cannot only be linked to hydrology, but can also be influenced by watershed land use (Williams et al., 2010; Wilson & Xenopoulos, 2008), forest management strategies (Yamashita et al., 2011), and natural processes, such as fire activity (Santín et al., 2016). Fire activity in particular is becoming increasingly common as a result of forest and agricultural management practices (U.S. EPA, 1998; Sanberg et al., 2002). However, higher intensity wildfire events are also becoming more frequent as a result of rising global temperatures and are expected to become more prevalent with continued climate change (Flannigan et al., 2009; Krawchuck et al., 2009). Whether through management practices or climate-induced wildfires, fire activity within a watershed can significantly alter the OC pool. Biomass burning as well as anthropogenic activities (such as fossil fuel combustion) thermogenically alter organic matter to generate a combustion derived carbon pool with a heat-induced molecular signature, otherwise known as pyrogenic carbon (PyC; Goldberg, 1985). Pyrogenic carbon is represented across a combustion continuum from low temperature derived anhydrosugars to highly condensed polycyclic aromatic soot particles formed at higher combustion temperatures (Masiello, 2004). This condensed aromatic fraction of the PyC spectrum is more commonly referred to as black carbon (BC; Masiello, 2004; Preston & Schmidt, 2006).

Post fire activity, BC becomes incorporated into soils and due to its highly aromatic nature, is expected to be largely refractory and remain on millennial time scales (Bird et al., 2015). However, a fraction of this material can be partially oxidized and mobilized in aquatic environments as dissolved BC (DBC; Abiven et al., 2011; Hockaday et al., 2006; Roebuck et al., 2017). The relative proportion of BC translocated from the

particulate to the dissolved phase is still relatively unknown, however; DBC has been reported to be coupled to the bulk DOC pool and represents about 10% of the global DOC flux from the terrestrial to coastal systems (Jaffé et al., 2013). Similar to DOC, the export of DBC has been closely linked to watershed hydrology where storm events and spring snow melt lead to flushing of DBC from organic rich upper soil horizons leading to an enrichment of DBC under high flow conditions (Dittmar et al., 2012; Stubbins et al., 2015). The link between DBC concentration and watershed hydrology has also been observed in a watershed with recent wildfire activity (Wagner et al., 2015a). However, surprisingly there appears to be no clear link between recent fire activity and DBC export (Ding et al., 2013; Myers-Pigg et al., 2015; Wagner et al., 2015a). On the contrary, mobilization of the pyrogenic carbon in the form of particulate BC (PBC) is enhanced in fire-impacted watersheds (Moody & Martin, 2001; Wagner et al., 2015a; Pyle et al., 2017), and rivers may be a significant contributor of PBC to coastal environments (Santín et al., 2016; Leorri et al., 2014).

Particulate black carbon may also enter aquatic systems through a variety of other mechanisms such as aeolian transport followed by dry or wet deposition (Bird et al., 2015). Further sources of PBC in aquatic systems may also be a function of DBC through sorption onto suspended solids and particulate organic material (Coppola et al., 2014; Zigah et al., 2012). While local hydrology can mobilize both PBC and DBC, there has been no indication that DBC and PBC exported from fluvial systems are directly coupled (Wagner et al., 2015a; Wang et al., 2016). Although PBC and DBC can be linked biogeochemically during fluvial transport (e.g., sorption processes, photochemistry), seasonal shifts in BC sources have been noted in anthropogenically impacted watersheds

(Wang et al., 2016). A combination of seasonal differences in sources, biogeochemical processing, as well as the variability in wildfire influence on BC export likely limits the establishment of a correlation between DBC and PBC. However, the available information in the literature is quite limited (Wagner et al., 2015a; Wang et al., 2016).

To our knowledge, there are currently only a few studies in which simultaneous measurements of both DBC and PBC are compared (Wagner et al., 2015a; Wang et al., 2016; Xu et al., 2016). Thus, additional information is needed to elucidate the potential inter-relationship between DBC and PBC in fluvial systems. Considering a forecasted increase in pyrogenic carbon production with on-going climate change, it is increasingly important to elucidate the biogeochemical processes and environmental drivers controlling the land-to-river transfers of BC with efforts to constrain current BC budgets and understand its importance on global carbon cycling. In this study, DBC and PBC were measured monthly in tandem and compared over a year-long sampling regime in the Altamaha River, Georgia. The major objectives of this study were to compare the primary hydrological drivers of DBC and PBC export and to determine if a link between these two BC phase exists on a large watershed scale. We hypothesized that watershed hydrology would play a pivotal role in the seasonal export of both DBC and PBC in the Altamaha River. Furthermore, we hypothesized that the relationship between DBC and PBC on a large watershed scale may be different in comparison to the decoupled relationship observed on localized scales (Wagner et al., 2015a) as bulk OM becomes homogenized during transport downstream (Creed et al. 2015).

## 4.3 Methods

### 4.3.1 Altamaha River Watershed Description

The Altamaha River watershed is located within the southeastern United States and drains roughly 36,000 km<sup>2</sup> (25%) of Georgia's land mass (Figure 4.1). Its main tributaries, namely the Ocmulgee and Oconee Rivers, both have their source in the Georgia piedmonts and converge near Lumber City to form the Altamaha River. These two tributaries contribute about 75% of the water flow to the Altamaha River, which has an average annual water discharge of 400 m<sup>3</sup>/s to the Atlantic Ocean. Water discharge reaches annual maxima in winter/early spring (Dai & Sun, 2007). The upper watershed primarily in the Georgia Piedmonts can be characterized by rolling hills and soils primarily characterized as ultisols, which are relatively acidic, highly weathered soils characterized by sub-soils enriched with clay particles including kaolinite and iron-oxides (US Department of Agriculture). In contrast, the lower Altamaha River lies in the nearly flat southern Georgia coastal plains with a diversity of soils including both ultisols and spodosols. Similar to ultisols, spodosols form from weathering processes, but are typically formed in sandy parent materials and are quite porous due to their highly coarse texture. Each soil type consist of relatively similar soil organic carbon contents ranging from *ca.* 5 to 25 kg/m<sup>2</sup> (Buringh 1984).

Anthropogenic activity is generally highest in the upper Altamaha River watershed where a significant portion of the Atlanta Metropolitan Area is drained primarily by means of the Ocmulgee River, with a small fraction also drained by the Oconee River (Figure 4.1). Fossil-fuel combustions is highest during winter months in Georgia (U.S. EIA, 2017) with coal representing ~30% of Georgia's energy consumption

in 2015 (Georgia Environmental Finance Authority, 2016). Notable seasonal variations in atmospheric fine particulate matter (PM<sub>2.5</sub>), polycondensed aromatic hydrocarbons, and elemental carbon (i.e. BC) have been recorded in the Atlanta region with the highest atmospheric concentrations during cooler months of November to February (Li et al., 2009). Agricultural activity is also highest within the upper Oconee River sub-basin and while still sporadic throughout the remainder of the watershed, generally declines downstream (Weston et al., 2009). Agriculture generally consists of poultry, beef, soy, and hay production (Schaefer & Alber, 2007). The lower watershed can be characterized as having a higher degree of pristine wetland and natural forested areas (Weston et al., 2009) primarily consisting of a mix between deciduous and evergreen forests. In addition, forest fires in the southeastern United States contribute about 20% of PM<sub>2.5</sub>, with more than one million acres being subjected to prescribed burning annually in Georgia alone (Lee et al., 2005).

#### *4.3.2 Sample Collection and Processing*

##### *4.3.2.1 Collection*

Thirteen monthly samples were collected at the mouth of the Altamaha River near Darien, Georgia (31.3378, -81.4501, Figure 4.1) from September 2015 to September 2016 (Appendix 4.1). Immediately after collection, ~ 4 L of riverine samples were filtered (0.7 µm Whatman GF/F filters pre-combusted at 450 °C for 5 h), and aliquots were collected for DOC analysis. Filters were stored at -20 °C until further POC and PBC analysis. Filtrates (1-2 L) were acidified to pH 2 (using concentrated HCl), and DOM was isolated using solid phase extraction (SPE) cartridges (Agilent Bond Elut PPL) and then

eluted with methanol as described in Dittmar et al. (2008) for DBC analysis (see subsection 2.3). The PPL extraction efficiency across all samples was  $73 \pm 8\%$ .

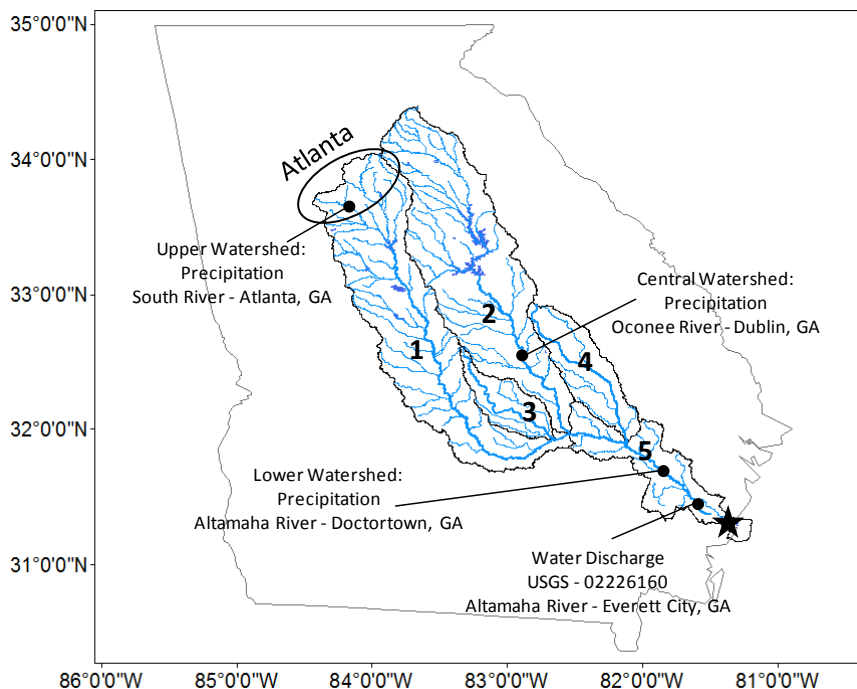


**Figure 4.1:** Map of Altamaha River Watershed with monthly sampling and USGS information. Respective sub-basins are 1) Ocmulgee River, 2) Oconee River, 3) Little Ocmulgee River, 4) Ohoopsee River, and 5) Altamaha River. The black star notes the monthly sampling station. The portion of the watershed draining from the Atlanta Metropolitan Area is enclosed in a black circle. The locations of 4 USGS monitoring stations used to collect precipitation (Atlanta, Dublin, & Doctortown) and water discharge (Everett City) are displayed as black circles.

#### 4.3.2.2 Bulk Analyses

After acidification and purging to remove inorganic carbon, filtered river samples were analyzed for DOC using a Shimadzu TOC-V CSH total organic carbon analyzer. TOC Quality control standards from ERA (Demand, WasteWarR, Lot#516, ERA) were used to determine accuracy, which was 100.3%, with the analytical precision (as RSD) of less than 5%. The POC and  $\delta^{13}\text{C}$  (POC only) analyses were performed on a Carlo Erba elemental analyzer coupled to a Delta XP Thermo Finnigan isotope ratio mass

spectrometer, following fumigation with concentrated HCl to remove carbonates.

Isotopic values are expressed relative to the Vienna PeeDee Belemnite (VPDB) standard.

The analytical precision as RSD was < 2% for POC measurements and  $\pm 0.1\%$  or better (standard deviation) for  $\delta^{13}\text{C}$  signatures.

#### 4.3.2.3 Optical Analyses

Absorbance and fluorescence measurements were obtained simultaneously using an Aqualog (Horiba Scientific) equipped with a 150-W continuous output Xenon lamp. Fluorescence spectra were corrected for inner filter effects as described by Ohno (2002) and normalized to Raman scatter units. The specific UV absorbance (SUVA), an indicator of DOM aromaticity, was calculated by dividing the decadic absorbance at 254 nm by DOC concentration (Weishaar et al., 2003). Units are reported in liters per milligram of carbon per meter. A higher SUVA indicates a more aromatic DOM pool whereas a lower SUVA indicates DOM that is less aromatic. The biological index (BIX), a measure of recent autochthonous DOM contributions, was calculated as a ratio of fluorescence intensity (excitation 310 nm; emission 380nm/430) previously reported by Huguet et al. (2009). BIX values greater than 1 generally indicate recently produced/fresh DOM whereas values less than 0.7 indicate low degrees of in-situ DOM production.

#### 4.3.2.4 Hydrological Data

Water discharge data were obtained from the United States Geological Survey (USGS) for each sampling period at the nearest monitoring station (Everett City, 02226160) roughly 20 km upstream from the sampling site. Seasonal precipitation information was also collected from three USGS locations (Figure 4.1) to observe general rainfall patterns throughout the watershed. These locations include the upper watershed

within the South River in Atlanta, Georgia (USGS 02203900), the middle watershed in the Oconee River near Dublin, Georgia (USGS 02223500), and the lower watershed near Doctortown (USGS 02226000, Figure 4.1).

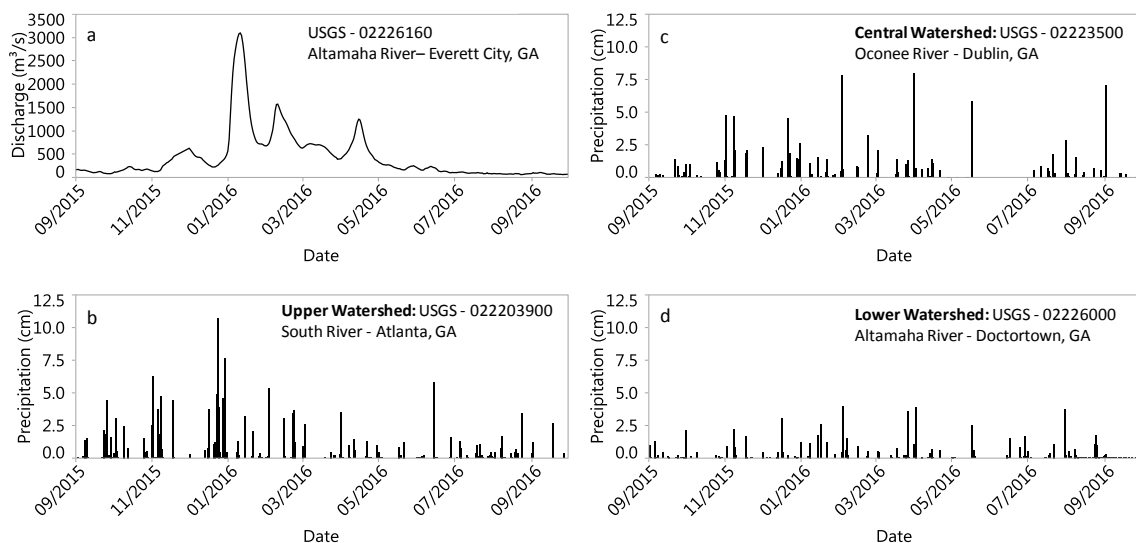


**Figure 4.2:** Water discharge (a) and daily rain data collected at USGS monitoring stations in (b) the South River – Atlanta, GA, (c) the Oconee River – Dublin, GA, and (d) the Altamaha River – Doctortown, GA

#### 4.3.3 Quantification of DBC and PBC

Both DBC and PBC were characterized using benzenepolycarboxylic acids as chemical markers for the highly condensed aromatic components of the pyrogenic carbon spectrum. The individual monthly samples collected were analyzed in triplicate for BC analysis. For DBC, a small amount of DOM extract (isolated by PPL cartridges and eluted in methanol), containing ~0.2 mg of DOC was dried under a stream of nitrogen gas in pre-combusted (500 °C, 5.5 hours) 2 mL glass ampoules. The dried extract was re-dissolved in 0.5 mL concentrated nitric acid and thermo-chemically oxidized at 160 °C for 6 hours to yield a suite of tri- to hexa-substituted BPCAs (Ding et al., 2013; Dittmar, 2008). Excess nitric acid was removed by a stream of nitrogen gas before quantification.



The PBC oxidation was carried out in a similar manner to DBC; however, additional clean up steps were required to remove potential metals and particulates that interfere with the BPCA analysis (Wiedemeier et al., 2013). Briefly, filter papers containing particulate organic material were added to 20 mL glass ampoules containing 2 mL concentrated nitric acid. Samples were heated at 160 °C for 6 hours to form BPCAs, from which the sample was then passed through a pre-rinsed 0.7 µm Whatman GF/F filter, followed by a cation exchange resin to remove metals. The eluent containing BPCAs was collected and freeze-dried. The BPCAs were then re-dissolved in 1:1 methanol/water and again passed through a C<sub>18</sub> SPE cartridge (Supelco) for removal of apolar compounds. The BPCA containing eluent was again collected and freeze-dried.

For both DBC and PBC, BPCAs were separated and quantified using high performance liquid chromatography (HPLC) coupled with photodiode array detection (Surveyor, Thermo Scientific). Briefly, for both DBC and PBC, the extracted BPCAs were redissolved in mobile phase A (50 mM sodium acetate, 4 mM tert-butylammonium bromide, 10% methanol) and were separated on a Sunfire C<sub>18</sub> reverse phase column (3.1 µm, 2.1 x 150 mm, Waters Corporation) using an elution gradient consisting of mobile phase buffer A and mobile phase B (100% methanol). Chromatographic separation conditions are reported by Dittmar (2008). The analytical uncertainty for this method was less than 5% for DBC and less than 10% for PBC. A conversion factor of  $33.4[0.5(B3CA + B4CA) + B5CA + B6CA]$  was used to determine the BC concentrations from individual BPCAs as reported by Dittmar (2008).

## 4.4 Results

### 4.4.1 Watershed Hydrology

Water discharge data collected from the mouth of the Altamaha River between September 2015 and September 2016 suggest the existence of two primary hydrological seasons within the watershed (Figure 4.2a). These consisted of a dry season (May to November) characterized by moderate rain activity and low water discharge, and a wet season (December to April) characterized by heavy rain events and high water discharge. Heavy rainfall and storm events were highly variable throughout the wet season in the watershed (Figure 4.2b-d) and led to three distinct high discharge events during the study period (Figure 4.2a). The highest water discharge was observed in January 2016 peaking at *ca.* 3200 m<sup>3</sup>/s and is driven by heavy rainfall events within the upper anthropogenically impacted regions of the watershed (Figure 4.1, 4.2a-b). Two other prominent peaks in discharge observed in February 2016 (*ca.* 1500 m<sup>3</sup>/s) and April 2016 (*ca.* 1250 m<sup>3</sup>/s) are linked to heavy rainfall events within the central region of the watershed where there is a higher proportion of natural land cover (Figure 4.1, 4.2a,c; Weston et al. 2009). Heavy rain events were minimal in the lower watershed (Figure 4.1, 4.2a,d) indicating that high discharge peaks observed during the wet season were primarily driven by rainfall events within the upper and central regions of the watershed. During periods of baseflow, increases in salinity suggested estuarine intrusion at the sampling location (Appendix 4.1)

### 4.4.2 Seasonal Distribution of Dissolved and Particulate Organic Carbon

The DOC concentrations ranged from 6.1 to 12.6 ppm (Figure 4.3a) and were positively correlated with water discharge ( $r = 0.75$ ,  $p < 0.01$ ). However, while the most significant high discharge event was observed in January 2016, DOC peaked in

April 2016 with concentrations more than 20% greater than that observed in January 2016 (Figure 4.3a). The SUVA values generally ranged between 3 and 6 and peaked during periods of high flow (Figure 4.3c), whereas BIX generally ranged from 0.45 to 0.65 and peaked under baseflow conditions (Figure 4.3c).

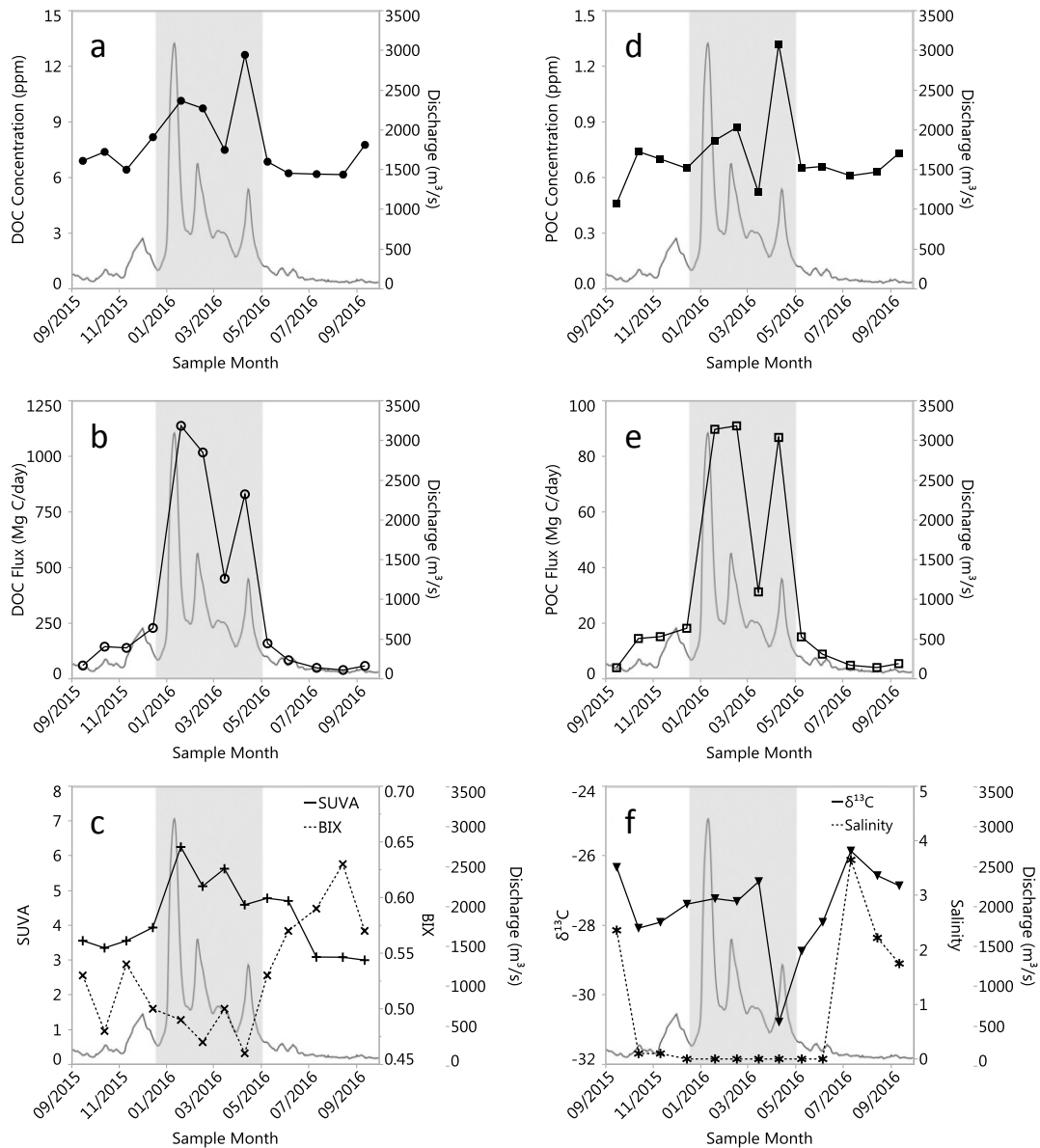


**Figure 4.3:** Seasonal patterns of DOC and POC related parameters in the Altamaha River. (a) DOC concentration, (b) DOC flux, (c) BIX and SUVA, (d) POC concentration, (e) POC flux, and (f)  $\delta^{13}\text{C}$  and salinity. The shaded region designates the wet season. Water discharge is represented as a solid gray line.

The POC displayed a similar seasonal pattern as DOC with the highest concentrations observed in the wet season (up to 1.32 ppm, Figure 4.3d) compared to the dry season (*ca.* 0.7 ppm). However, contrary to the DOC, a statistically significant correlation between POC concentration and water discharge was not observed ( $r = 0.48$ ,  $p > 0.05$ ). Throughout the sampling period, bulk  $\delta^{13}\text{C}$  generally ranged between -26 and -28‰ (Figure 4.3f) and was not statistically significantly correlated with POC concentration ( $r = 0.40$ ,  $p > 0.05$ ). However, a decrease in  $\delta^{13}\text{C}$  from -26.74‰ to -30.78‰ was observed from March 2016 to April 2016 coinciding with an increase in POC concentration from 0.52 ppm to 1.32 ppm.

#### *4.4.3 Seasonal Distribution of Dissolved and Particulate Black Carbon*

Seasonal parameters for DBC and PBC are presented in Figure 4.4 (a-c: DBC related, d-f: PBC related). Seasonal DBC concentrations (Figure 4.4a) were highly variable ranging from 0.27 to 0.45 ppm and were not correlated to either water discharge ( $r = 0.15$ ,  $p > 0.15$ ) or DOC concentration ( $r = 0.00$ ,  $p > 0.05$ ). Unlike for DOC, DBC concentrations exhibited a seasonal maximum in February 2016 (0.47 ppm) with a minimum during the highest flow period in January 2016 (0.28 ppm; Figure 4.4a). Under baseflow conditions however, DBC was present in higher concentrations reaching near maximum values (*ca.* 0.43 ppm) in both pre- and post-high discharge months of October 2015 and August 2016 (Figure 4.4a).

Seasonal shifts in DBC composition were determined using the distribution of BPCAs generated during the chemical oxidation of DBC (Dittmar, 2008). The BPCA ratio is defined as the ratio of more substituted BPCAs (B5CA and B6CA) to less substituted BPCAs (B3CA and B4CA). A greater proportion of B5CAs and B6CAs

relative to B3CAs and B4CAs, and thus a higher BPCA ratio, is an indication DBC with a more polycondensed signature (Ziolkowski et al., 2011). The BPCA ratio for DBC (Figure 4.4c) was relatively consistent ( $1.1 \pm 0.1$ ) through the sampling period with the exception of the high flow months when less polycondensed DBC signatures were observed: January 2016 - BPCA Ratio: 0.53 and April 2016 - BPCA Ratio: 0.69.

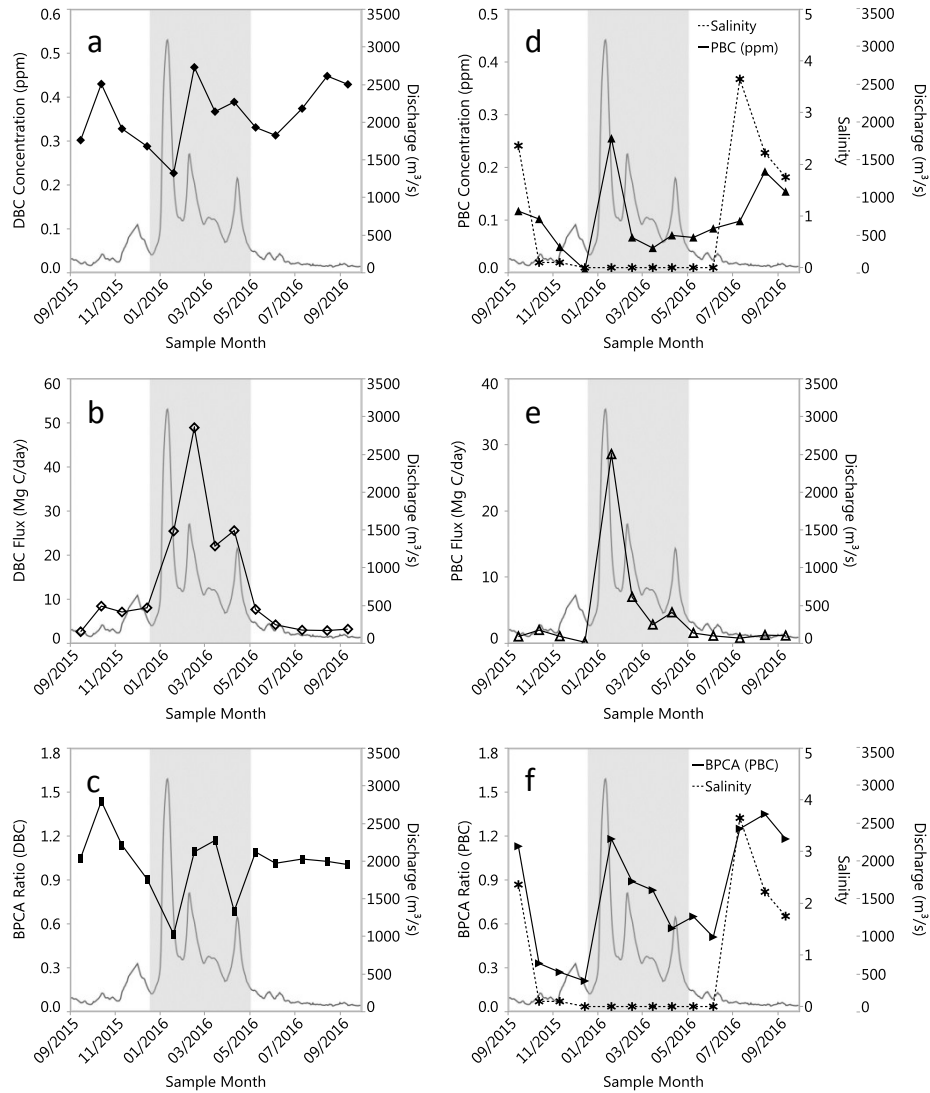


**Figure 4.4:** Seasonal patterns of DBC and PBC related parameters within the Altamaha River. (a) DBC concentration, (b) DBC flux, (c) BPCA ratio (DBC), (d) PBC concentration and salinity, (e) PBC flux, and (f) BPCA ratio (PBC) and salinity. The shaded area designates the wet season. Water discharge is represented as a solid gray line.

The PBC concentrations reached a maximum during the high flow period in January 2016 (0.25 ppm), at which point concentrations remained consistently low throughout the remainder of the high flow season ( $< 0.1$  ppm) until baseflow conditions were reached and concentrations began to rise again (Figure 4.4d). PBC and POC were not significantly correlated ( $r = 0.00$ ,  $p > 0.05$ ). Consistent with previous reports (Wagner et al., 2015a; Wang et al., 2016), DBC and PBC were also not significantly coupled ( $r = 0.07$ ,  $p > 0.05$ ). However, when considering samples only taken at low flow (excluding January to April 2016) a positive correlation between DBC and PBC ( $r = 0.78$ ,  $p < 0.05$ ) is observed suggesting potential coupling of these two parameters under baseflow conditions. The BPCA ratio (calculated in the same manner as DBC), commonly used to assess PBC character (Wiedemeier et al., 2015), was highly variable for PBC (Figure 4.4f) with the most polycondensed PBC signature observed during both winter storm events and during periods of baseflow where estuarine intrusion (noted by increase in salinity) was evident (Figure 4.4f).

#### *4.4.4 Organic Matter Fluxes from the Altamaha River*

As expected, fluxes of DOC, POC, DBC, and PBC were predominately driven by water discharge and thus, the highest fluxes were observed during the rainy season of January to April 2016 (DOC & POC: Figure 4.3b,e; DBC & PBC: Figure 4.4b,e). DOC fluxes ranged from *ca.* 40 Mg/day during baseflow to *ca.* 1100 Mg/day during the wet season (peaking in January 2016), and POC fluxes ranged from *ca.* 4 Mg/day at baseflow to *ca.* 90 Mg/day during the wet season (peaking in January 2016). PBC fluxes ranged from less than 1 Mg/day during baseflow to *ca.* 29 Mg/day also peaking in January 2016. For DBC, fluxes were *ca.* 3 Mg/day at baseflow, however; peak DBC fluxes were

observed in February 2016 (49 Mg/day) compared to other parameters (i.e. DOC, POC, and PBC), which peaked during the highest discharge event in January 2016. DBC fluxes were notably lower in January 2016 as the lowest concentrations were observed during this time (Figure 4.4a). By integrating the area under the flux curves using Riemann sums, we were able to estimate the yearly flux of DOC from the Altamaha River to the Atlantic Ocean to be 128 Gg/yr with DBC accounting for roughly 4% of the total DOC export at 4.9 Gg/yr. PBC export (1.6 Gg/yr) represented roughly 13% of the total POC export (11.4 Gg/yr) from the Altamaha River.

## **4.5 Discussion**

### *4.5.1 Temporal Controls on Sources and Export of DOC*

Water discharge and DOC were positively correlated ( $r = 0.75$ ,  $p < 0.01$ ) in the present study suggesting that seasonal hydrology has a significant role in the export of DOC from the Altamaha River. This observation strengthens the evidence for this DOC-discharge relationship that has been previously reported for a variety of climatic conditions, including in Arctic systems (Holmes et al., 2012), tropical climates (Spencer et al., 2010) and rivers draining temperate to subtropical climates (Bianchi et al. 2004). Storm runoff events generally lead to flushing of upper soil layers that represent a source of more aromatic, humic-rich DOM to rivers (Fellman et al., 2009; Hood et al., 2006; Inamdar et al., 2011; Raymond & Saiers, 2010). This trend is also observed in the Altamaha River where DOC concentrations increase in response to significant rainfall during the wet season as observed in Figure 4.3a. An increase in SUVA from 3.94 to 6.25 from December 2015 to January 2016 further indicates the contribution of aromatic DOC to the Altamaha River in response to the heavy rain events and flushing of organic-rich

upper soil layers (Hood et al., 2006). Upon returning to baseflow after the April 2016 storm events, DOC concentrations decrease from 12.62 ppm and consistently remain around 6.20 ppm. The decrease in DOC concentration is concurrent with a decrease in SUVA (Figure 4.3c) and an increase in the BIX (Figure 4.3c) indicating a shift of sources from mostly allochthonous derived DOM during winter soil flushing to an enrichment in autochthonously derived DOM during summer baseflow conditions. Similar observations have been reported in response to storm events in a forested watershed where SUVA values peak around 6 during high discharge events (Inamdar et al. 2011). These results are also consistent with other reports which indicate that rivers primarily sourced from groundwater at baseflow have reduced contributions of highly aromatic humic like DOM and larger contributions of autochthonous DOM sources and protein like fluorescence (Hood et al., 2006; Inamdar et al., 2011; Shen et al., 2015).

#### *4.5.2 Sources and Export of DBC during Low Flow Regimes*

Selective fractionation, potentially as a consequence of sorption processes and microbial processing of DOM, has also been linked to groundwater sources that are low in highly aromatic and humic-rich DOM components (Maurice et al., 2002; Qualls & Haines, 1991; Ussiri & Johnson, 2004). Thus, because of its associations with high molecular weight DOM fractions (Wagner & Jaffé, 2015), we would have expected low DBC concentrations under baseflow conditions, which would be consistent with previous studies suggesting low DBC concentrations at baseflow in both arctic (Stubbins et al., 2015) and tropical rivers (Dittmar et al., 2012; Marques et al. 2017). While our data is generally in agreement with these observations, DBC peaked three times throughout the monthly sampling regime, twice during baseflow periods, both prior to and after the



major discharge peaks observed from January to April 2016 (Figure 4.4a). We hypothesize that the higher DBC concentration spikes observed during the low-discharge periods may suggest that shallow groundwater feeding the Altamaha River system at baseflow may occasionally transport significant amounts of DBC derived from historical charcoal deposits depending on seasonal weather conditions.

Mineral rich soils, which are relatively abundant throughout the Altamaha River watershed particularly in the Georgia Piedmont regions (Bhatti et al., 2009; Shi et al., 2001), have been shown to stabilize BC in deeper soil horizons, particularly those enriched with iron complexes (Glaser et al., 2000). In the Altamaha River, ultisols dominate the soil profiles in the upper watershed while spodosols become abundant in the lower watershed (U.S. Department of Agriculture). Santos et al. (2017) reported significant leaching of DBC from deep soil horizons, consisting primarily of iron rich spodosols, with DBC composition comparable to that of aged charcoal. Dissolved black carbon composition in the Altamaha River was described as a measure of polycondensed character using the BPCA ratio (defined in section 4.4.2). The DBC composition during baseflow remained relatively consistent with a BPCA ratio of  $\sim 1.1$  indicating a BPCA distribution similar to that of leachable DBC from deep soil charcoal deposits (Abiven et al., 2011). The relative consistency in DBC composition under baseflow conditions coupled with leaching of DBC from deeper soils horizons as described by Santos et al. (2017) further supports the hypothesis that more oxidized DBC sourced from charcoal is transported via groundwater from deeper soil horizons to the Altamaha River.

#### *4.5.3 Sources and Export of DBC during High Flow Regimes*

During the wet season, a peak in DBC concentration (0.47 ppm) and the highest DBC fluxes (49 Mg/day) were observed. Similar to DOC, the relationship between high discharge and increasing DBC concentrations has been attributed to flushing of upper soil layers in tropical environments (Dittmar et al., 2012). However, both DBC concentration and flux were highest in February 2016 in comparison to DOC, which exhibited its greatest flux in January 2016 (Figure 4.3b). Medeiros et al. (2015) showed that DOM composition in the Altamaha-Doboy-Sapelo estuary is strongly modulated by river discharge and that changes in the Altamaha River flow at monthly time scales significantly influence the organic matter distribution in the entire estuarine system. While it is currently unclear why the time lag between DOC and DBC is observed in comparison to other studies, this time lag may be an indication that while high DOC is released from flushing of upper organic rich soil layers, soil saturation and percolation to deeper soil layers may be required for release of DBC into the system. We further note that our sampling period in January 2016 occurred about half way through the falling limb of this high discharge event and thus, it is possible that an initial pulse of DBC occurred prior to our sample collection. However, a considerable shift to lower BPCA ratios observed in January 2016 (Figure 4.4c) may be indicative of systematic changes within the watershed that lead to a less polycondensed DBC pool. For instance, a less polycondensed DBC signature has been linked to biogeochemical processes such as photodegradation (Stubbins et al., 2012) and interactions with iron precipitates (Riedel et al., 2012). Black carbon also has a high affinity for iron rich soils (Glaser et al., 2000). Thus for the Altamaha River watershed, in particular where mineral rich soils are

abundant (Bhatti et al., 2009; Shi et al., 2001) and total iron concentrations within the Altamaha River are around 25  $\mu\text{M}$  (Xie et al., 2004), increased suspended sediment yields because of higher discharge may induce interaction between DBC and iron rich particulates, leading to a less polycondensed DBC pool. On the other hand, the less polycondensed DBC character may indicate that DBC exported in January 2016 is not primarily derived from charcoal sources typically found in the deeper soil layers, but may be derived from anthropogenic sources such as combustion of fossil fuel (Ding et al. 2015).

Since DBC composition has also been linked to land-use (e.g., urban and agricultural vs. natural; Wagner et al., 2015b), the observed seasonal shifts in BPCA ratios may be an indication of temporal variations in DBC source that are driven by regional shifts in heavy rainfall events throughout the watershed with variable land-use regimes. The most intense storm events leading to the first high water discharge peak in January 2016 occurred primarily in urban and agricultural areas within the upper watershed of the Altamaha River system (Figure 4.2a,b). For example, the Atlanta Metropolitan Area and neighboring agricultural areas received numerous days of heavy rainfall events in late December, in some cases receiving upwards of 10 cm per day (Figure 4.2b). For DOC, heavy storm events can induce the release of humic rich material from agricultural areas (Eckard et al., 2017; Glendell & Brazier, 2014; Vidon et al., 2008). However, the less polycondensed DBC character as indicated by a lower BPCA ratio (0.53) coupled with the low concentrations (0.28 ppm) and DBC flux (28.60 Mg/day) observed in January 2016 may likely be the result of enhanced DBC contributions primarily originating from anthropogenically impacted areas (e.g., urban

and agricultural) in the upper watershed. This hypothesis is supported by the fact that the leachable fraction of fossil-fuel derived BC from soot material is less polycondensed in character compared to DBC derived for natural land covers (Ding et al., 2015). While atmospheric deposition may be an important transport route for the distribution of BC in highly urban areas (Mari et al., 2017), surface runoff, particular in urban areas, may also be an important transport mechanism for combustion-derived products (O'Malley et al., 1996)

Peak DBC concentration (Figure 4.4a) and flux (Figure 4.4b) were observed in February 2016. We have suggested this time lag between peak DOC (January 2016) and the highest export of DBC (February 2016) may be a result of soil percolation and release of DBC from deeper soil layers. However, when compared to January 2016, heavy rainfall events regionally shift to predominantly downstream areas (Figure 4.1, 4.2b) in which natural land cover (forest and wetlands) is more dominant over urban and agricultural land use (Schaefer & Alber, 2007; Weston et al., 2009). Thus, the peak DBC concentrations observed in February 2016 may be an indication that precipitation-induced changes in regional hydrological flowpaths further incorporate organic rich soil layers from the forested and wetland areas, leading to higher abundances of leachable components from BC deposited in these regions. Flood plain areas within Georgia's Coastal Plain, which are rich in natural wetland and forested areas, are large sources of organic matter to the main river channel (Cuffney, 1988; Webster & Meyer, 1997) and thus, a peak in DOC concurrent to DBC in February 2016 could have been expected. However, a lag between peak DBC and DOC concentrations has been observed in previous studies (Wagner et al., 2015a) suggesting there may be some significant

hydrological variability in DBC and DOC mobilization mechanisms. More extensive higher resolution sampling should be performed to further elucidate the lag between peak DBC and DOC concentrations observed during high discharge seasons.

Few rainfall events throughout the watershed in March 2016 (Figure 4.2b-d) led to low water discharge concurrent with a decrease in DBC concentrations (Figure 4.4a) and flux (Figure 4.4b). In April 2016, heavy rain events are again observed in the central region of the watershed where higher proportions of natural land cover are dominant (Figure 4.1, 4.2a,c). It may be expected that flushing of upper soil layers in this region of the watershed with natural land cover would lead to a more polycondensed DBC pool. However, DBC concentrations only slightly increased from March to April 2016 (Figure 4.4a) and a considerable decrease in the BPCA ratio (Figure 4.4c) from 1.17 to 0.69 was observed suggesting a less polycondensed pool of DBC exported from the Altamaha River in April 2016. The reason for the less polycondensed pool of DBC is unclear, however; the state of Georgia experiences most of its prescribed forest management burnings in the month of March (Tian et al., 2008) and leachable DBC from fresh chars are generally less abundant and less polycondensed compared to aged chars (Abiven et al., 2011). Significant leaching of DBC has also been reported for recently generated pine char (Wagner et al., 2017b), and thus, deposition of fresh char into upper soil layers in March 2016 from prescribed fires may lead to leaching of less polycondensed DBC during the April 2016 storm events. However, while numerous studies have suggested a lack of a direct relationship between DBC export and fire activity (Ding et al., 2013; Myers-Pigg et al., 2015), the immediate post fire response

with respect to DBC and local hydrology remains to be determined (Wagner et al., 2015a).

#### *4.5.4 Decoupling Between DOC and DBC*

Several recent studies have reported on the coupling between DOC and DBC in fluvial systems, both globally (Jaffé et al., 2013) and on regional and temporal scales (Dittmar et al., 2012; Stubbins et al., 2015). As such, while we hypothesized that this relationship would also be observed across temporal scales in the present study, a linear relationship between DOC and DBC was not observed ( $r = 0.00$ ,  $p > 0.05$ ). Therefore, it is possible that this correlation becomes periodically uncoupled across the hydrogram on large watershed scales. For instance, Myers-Pigg et al. (2017) showed that coupling between low-temperature pyrogenic carbon and bulk DOC in the Yenisei River, a large Arctic river, was disrupted under high flow conditions. Xu et al. (2016) further noted the seasonal decoupling between DBC and DOC in the Huanghe River while also highlighting the importance of local point sources on DBC export. In the Altamaha River, regional shifts in monthly rainfall events and sources of organic matter throughout the watershed likely contribute to the temporal decoupling of DBC and DOC through flushing of soil layers in areas with varying degrees of natural and anthropogenic influence. Distinct differences in the composition of DOM exported during storm events have been observed among watersheds with varying degrees of natural and anthropogenic land covers (Hood et al., 2006, Hu et al., 2016) further supporting the hypothesis that the decoupling between DBC and DOC may be a function of both river hydrology and watershed land use.

While DBC and DOC were not correlated, DBC typically represented between 2 and 8% of the bulk DOC pool, well within the range reported on a global scale of 0.1 to 17.5% (Jaffé et al. 2013). There was however no significant difference (students t-test,  $p = 0.05$ ) between the relative contributions of DBC to the bulk DOC pool during the wet ( $3.8 \pm 1.3\%$ ) and dry season ( $5.2 \pm 1.1\%$ ) Based on monthly flux estimates, DBC represented 4.9 Gg/yr of the 128 Gg/yr DOC exported from the Altamaha River during the sampling period. Roughly 80% of both the total DOC and DBC export were during the wet season (DOC: 106 Gg/yr; DBC: 3.8 Gg/yr) compared to the dry season (DOC: 22 Gg/yr; DBC: 1.1 Gg/yr) further suggesting that high discharge events lead to extensive pulsing and mobilization of OC in fluvial systems (Raymond et al., 2016). These hydrological shifts in sources and export of both DOC and DBC in response to storm events are particularly important for the fate and transport of organic material to coastal systems when considering the intensity of storm events is expected to rise with increasingly warmer atmospheric temperatures (Knutson et al., 2010).

#### *4.5.5 Hydrological Controls on the Export of POC and PBC*

Though not statistically significantly correlated with water discharge ( $r = 0.48$ ,  $p > 0.05$ ), POC was positively correlated to DOC ( $r = 0.85$ ,  $p < 0.01$ ) with each following similar seasonal trends (Figure 4.3a,d). Similar to DOC, seasonal variation in POC sources were also evident, notably due to shifts in  $\delta^{13}\text{C}$  throughout the sampling period (Figure 4.3f). At base flow, POC was generally more enriched in  $^{13}\text{C}$  (Figure 4.3f). Shifts to a less negative  $\delta^{13}\text{C}$  signature were most prominent when salinity measurements above zero were recorded (Figure 4.3f) indicating some degree of estuarine influence at the sampling location under baseflow conditions. This shift in  $\delta^{13}\text{C}$  signature would

imply some mixed sources of POC that may include phytoplankton, or C<sub>4</sub> vegetation that is commonly found in Atlantic coastal marshes such as *Spartina*, both of which carry a less negative  $\delta^{13}\text{C}$  signature compared to upland C<sub>3</sub> vegetation (Peterson et al., 1985). During the high water discharge period, the  $\delta^{13}\text{C}$  signature was generally more negative than that observed in the dry season (Figure 4.3f). Particulate organic carbon typically rises in response to water discharge as a result of sediment remobilization and erosional inputs of POC from terrestrial sources (Voss et al., 2015), which would be expected to have more negative  $\delta^{13}\text{C}$  values because of higher yields of C<sub>3</sub> vegetation (Peterson et al., 1985).

Similar to DOC, POC concentrations peaked at 1.32 ppm in April 2016 (Figure 4.3d) coinciding with a more negative  $\delta^{13}\text{C}$  value (-30.78‰, Figure 4.3f). Although peak fluxes were still observed in January 2016 concurrent to the largest discharge peak, the more negative  $\delta^{13}\text{C}$  and higher observed POC concentrations in April 2016 suggests a significant input of allochthonous organic material to the river during this time. River main channels in Georgia receive significant input of organic matter from flood plain sources, particularly through high loads of suspended particulates from litter fall (Cuffney, 1988; Webster & Meyer, 1997). Furthermore, Weston et al. (2009) has shown that the most significant OC inputs to the Altamaha River occur within the lower watershed. Thus, the observed higher DOC and POC concentrations in April 2016 can likely be attributed to allochthonous sources mobilized from the flood plains by the heavier rain events in more downstream regions of the watershed.

The seasonal distribution observed for PBC was quite different from POC and the two were not statistically significantly correlated ( $r = 0.00$ ,  $p > 0.05$ ). Although POC and



PBC are not directly coupled, the PBC flux (1.6 Gg/yr) represented about 14% of the total POC flux (11.4 Gg/yr) exported from the Altamaha River throughout the sampling period. As expected, significant export of both PBC and POC were observed during the wet season (PBC: 1.3 Gg/yr; POC: 9.2 Gg/yr) and was significantly higher compared to the dry season (PBC: 0.3 Gg/yr; POC: 2.2 Gg/yr), which agrees with the suggestion that there is enhanced mobilization and export of particulate material under high flow conditions. However, there was no significant difference in the seasonal contributions of PBC to the bulk POC pool (Students t-test,  $p = 0.05$ ; dry:  $15.3 \pm 9.2\%$ ; wet:  $14.8 \pm 9.8\%$ ). The roughly 14% contribution of PBC to POC is in the same order of values reported for other large rivers, such as the Mississippi River (16-17%; Mitra et al., 2002) and a variety of Chinese rivers ( $22 \pm 11\%$ ; Xu et al., 2016). While only limited information is available with respect to the relationship between PBC and POC, the decoupling of these two organic matter pools comes contrary to reports which show a positive relationship between PBC and POC export in two Chinese rivers (Wang et al., 2016). Similarly, a positive correlation between PBC and suspended solids, which are generally related to POC (Lewis et al., 1995), has been reported (Wagner et al., 2015a). The reason for this disconnect between POC and PBC in the Altamaha River is unclear, although it may be related to enhanced mobility of charcoal relative to bulk soil organic matter (Pyle et al., 2017) and possibly to variations in the sources of PBC throughout the hydrograph. PBC concentrations (Figure 4.4d) at base-flow prior to winter rain events were roughly 0.1 ppm and become diluted in November and December 2015 ( $< 1$  ppm) due to a number of low intensity rain events. Intense storm events that occurred in late December 2016 within the upper watershed (Figure 4.2b) give rise to an increase in water discharge

and an initial increase in PBC concentrations to a maximum of 0.26 ppm in January 2016 likely from mobilization through re-suspended sediments and/or introduction of PBC to the main stem through overland runoff. While PBC becomes diluted in response to continuous storm events throughout the remaining wet season, more concentrated values typical for base-flow conditions are slowly restored after the April 2016 storm events (Figure 4.4d).

#### *4.5.6 Seasonal Variability in PBC Source*

Sources of PBC during base flow appear to be linked to estuarine influences at the sampling location as previous discussed. Evidence for this hypothesis is presented in Figure 4.4d where PBC concentrations at base flow both pre- and post-winter storm events peak during periods where salt-water intrusions are evident. A similar pattern is also observed in the seasonal BPCA distributions where increases in PBC-BPCA ratio from  $< 1$  to *ca.* 1.25 are observed during base flow during periods of salinity intrusions (Figure 4.4f). The BPCA ratio was used for PBC (defined in section 4.4.2) to assess the relative degree of polycondensed character (Wiedemeier et al., 2015). However, similar to DBC, using BPCA ratios solely as a means of source should be exercised with caution as the biogeochemical controls on PBC degradation during riverine transport is not well understood. Nonetheless, the higher PBC-BPCA ratio observed during baseflow when saline intrusions are evident suggests significant estuarine influence that leads to a more polycondensed source of PBC. While fire activity within Atlantic coastal marshes is generally uncommon (Turner, 1988), lightning induced fires have been previously recorded in Georgia's coastal marshes (Kathryn & Bratton, 1988) and as such may likely be a source of PBC (and DBC). Thus, and in agreement with the  $\delta^{13}\text{C}$  values of the POC,

we hypothesize that higher PBC values of a more highly polycondensed nature observed during periods of tidal influence at the sampling location during baseflow may be in part derived from historical fire activity within the Georgia coastal *Spartina* marsh system.

The PBC-BPCA ratio is lowest during baseflow from October to December 2015 ( $< 0.4$ , Figure 4.4f), which is immediately prior to the winter storm events and a time in which there does not appear to be significant estuarine influence at the sampling location (Figure 4.4f). The low PBC-BPCA ratio would imply a significantly less polycondensed PBC signal during this period from October to December 2015. While this is a period of low water discharge, we note that one of the four main tributaries to the Altamaha River (Figure 4.1), the Oconee River, contributes consistently between 65 and 80% of the water discharge to the Altamaha River (from October to December 2015) compared to *ca.* 40% throughout the rest of the sampling period. The Oconee River tributary has extensive agricultural activity, particularly in the upper watershed (Schaefer & Alber, 2007). We would expect that low temperature burning practices, which are typically applied for agricultural management, would generate less polycondensed PBC compared to other PBC sources (Masiello, 2004). Thus, we hypothesize that shifts to less polycondensed PBC during this time may be linked to changes in sources that include significant agricultural influence. However, further research is needed to confirm this hypothesis.

In addition to the estuarine influences during low discharge, the onset of the winter storm events in early January 2016 also lead to a more polycondensed signature for the PBC exported from the Altamaha River watershed (Figure 4.4f). Considering contributions from the Atlanta Metropolitan Area and the significant rain events in the upper watershed in late December 2015 (Figure 4.2b), an enhancement of anthropogenic

PBC characterized by a more polycondensed signature would be expected (Masiello, 2004; Roth et al., 2012). Seasonal shifts in PBC source are likely highly variable among watersheds globally and have been linked to watershed activity. For instance, roughly 27% of PBC exported from the Mississippi River is derived from fossil fuel combustion (Mitra et al., 2002) compared to roughly 50% in significantly anthropogenically impacted Chinese rivers (Wang et al., 2016). In a highly polluted estuary, Mari et al. (2017) noted significant contributions of anthropogenically derived PBC delivered by atmospheric deposition during baseflow compared to riverine inputs during high flow. Wang et al. (2016) reported seasonal variation in PBC source noting that in winter high flow months, as much as 75% of the PBC exported from these rivers was derived from fossil fuel combustion. Fossil fuel consumption in the United States, particularly in the residential sector, increases more than 3-fold during winter months (U.S. EIA, 2017) and in the state of Georgia, coal represents nearly 30% of the state's energy consumption among all sectors (Georgia Environmental Finance Authority, 2016). In addition, atmospheric elemental carbon (i.e. BC) concentrations in the Atlanta area range from  $0.5 \mu\text{g}/\text{m}^3$  to  $\sim 2.5 \mu\text{g}/\text{m}^3$  and are seasonally variable with higher concentrations in winter months (Li et al., 2009). Thus, it is reasonable to suspect that the export of PBC with an enhanced polycondensed signature during the winter storm events may be linked to anthropogenic activity. However, the PBC-BPCA ratio (Figure 4.4f) reaches a maximum of  $\sim 1.25$  in January 2016 indicating a slight enrichment of B5CA and B6CA. While the observed BPCA maximum of  $\sim 1.25$  is similar to that of wood char/wildfire derived sources, fossil fuel derived PBC are most predominately enriched in B6CA (Roth et al., 2012). This may indicate that increased fireplace usage/wood burning in the watershed during winter

months (Li et al., 2009) may influence the PBC-BPCA signature during this time. Thus, while PBC mobilized during the initial high intensity rain events cannot be conclusively linked to fossil fuels alone, sources are likely a mix of both biomass burning and fossil fuel derived PBC, similar to that observed in Chinese rivers (Wang et al., 2016).

#### *4.5.7 Seasonal Coupling of PBC and DBC*

A primary objective of the present study was to comparatively assess in-stream dynamics of DBC and PBC on a watershed scale. An observed coupling behavior between these two pyrogenic carbon pools would greatly assist in the efforts to constrain current pyrogenic carbon budgets. However, only a limited number of studies are available which simultaneously measure both DBC and PBC export from fluvial systems. Consequently, the relationship between PBC and DBC has not been properly elucidated.

We estimated the yearly flux of BC from the Altamaha River to the Atlantic Ocean to be 6.5 Gg/yr with roughly 75% exported in the dissolved phase (4.9 Gg/yr) compared to the particulate phase (1.6 Gg/yr). These estimates are similar in magnitude to those from the Huanghe River (PBC: ~12 Gg/yr, DBC: ~1.7 Gg/yr; Xu et al., 2016); however, are much lower than for the Changjiang River (PBC: ~200 Gg/yr, DBC: ~47 Gg/yr; Xu et al., 2016) and the Mississippi River (PBC: ~500 Gg/yr; Mitra et al., 2002). Given that the relative contributions of BC to the bulk OC pool in the Altamaha River are similar in the aforementioned rivers above, the higher BC export from the Chinese rivers and the Mississippi River would be expected considering the sizable difference in watershed drainage areas.

Wagner et al. (2015a) reported that recent wildfire activity within a watershed could have an immediate impact on PBC export only, but not with DBC. The post-

wildfire increase in PBC export may contribute to the observed decoupling of DBC and PBC during riverine transport to coastal systems (Wagner et al., 2015a). Wang et al. (2016) have also reported the decoupling of PBC and DBC in large Chinese rivers, which appears to be linked to the mobilization and transport of BC from different sources (i.e. biomass burning vs. fossil-fuels) throughout the watershed. Our results are generally consistent with this study as DBC and PBC were decoupled across the hydrograph ( $r = 0.08$ ,  $p > 0.05$ ), and similarly is likely attributed to the seasonal variability in sources for each of these two pyrogenic carbon pools. On the other hand, we note that the decoupling between DBC and PBC in the Altamaha River appears to be driven by the high intensity storm events from January to April 2016 as a statistically significant positive relationship was observed between DBC and PBC under baseflow conditions ( $r = 0.78$ ,  $p < 0.05$ ). While this is the first study to report seasonal coupling and decoupling of high temperature BC, temporal coupling between dissolved and particulate low temperature pyrogenic carbon has also been reported in Arctic systems (Myers-Pigg et al., 2017). However, the decoupling of DBC and PBC in other temperate watersheds (Wagner et al., 2015, Wang et al., 2016) suggest that this phenomenon may be dependent on individual watershed dynamics, although it is currently unclear what processes are driving the coupled/decoupled BC relationships observed in these systems.

The magnitude of PBC and DBC exported from terrestrial to coastal systems suggest pyrogenic carbon contributes significantly to ocean carbon cycling (Santín et al., 2016) and the coupling of these BC phases suggests there may be a biogeochemical mechanism linking PBC and DBC during the transport to the ocean. While photochemical degradation of DBC is thought to be significant sink for ocean DBC

(Stubbins et al. 2012), photooxidation of PBC may be a source of DBC in aquatic systems (Roebuck et al. 2017). Furthermore, sorption mechanisms are considered a significant sink for DBC (Coppola et al., 2014) with 16 Tg/yr DBC lost in coastal systems through sorption to sinking particles (Santín et al., 2016). PBC is efficiently sequestered to sediments in coastal systems (Fang et al. 2016) where its storage is estimated at 1440 Pg (Santín et al. 2016). Currently, the exact mechanisms driving the temporal coupling between PBC and DBC remain unclear, particularly in the Altamaha River where there appears to be disparate sources of DBC and PBC under baseflow conditions. In order to fully understand the potential link between DBC and PBC in fluvial systems, it is necessary to gain a better understanding of the sources, age, and mechanisms driving the mobility of pyrogenic carbon throughout the aquatic environment. In addition, relative contributions and mobility of pyrogenic carbon across the entire combustion continuum should be further investigated with efforts to understand sources, sinks, and interactions between both dissolved and particulate phases. These efforts would lead to a better understanding of pyrogenic carbon cycling and to help better constrain current pyrogenic carbon budgets.

#### **4.6 Conclusions**

We present in this report a comprehensive study outlining the hydrological controls on the seasonal export of organic matter and associated BC in the Altamaha River, Georgia, USA. Our data suggests that the hydrological controls on BC mobilization may be more complex than previously observed. Under baseflow, groundwater appears to transport DBC derived from charcoal deposited in deeper soil horizons to the Altamaha River, whereas high intensity rain events throughout the

watershed with varying degrees of natural and anthropogenic land cover appear to influence DBC composition and export during high flow regimes. While PBC export was also linked to seasonal hydrology, sources appeared to be highly variable throughout the sampling period. Salt-water intrusion under low discharge conditions suggested an estuarine source of more polycondensed PBC, whereas similar to DBC, PBC export throughout the remaining sampling period was linked to surface runoff and changes in water sources from within areas of the watershed with variable land use. Seasonal dynamics also suggests that PBC and DBC may be coupled during baseflow, although further research is needed to corroborate this finding. As wildfire frequency continues to rise with on-going climate change, we can expect that production and export of BC from terrestrial to marine systems will also continue to increase. The Altamaha River may be particularly impacted with a series of droughts over that last decade (Medeiros et al., 2015), which likely increases this regions vulnerability to enhanced fire activity. The environmental implications for this are still not well understood, but an increasing export of BC from terrestrial systems may have a significant impact on both aquatic food web dynamics and the oceanic microbial loop as pyrogenic carbon is generally considered highly bio-recalcitrant. Thus, a more complete understanding of BC mobilization with seasonal hydrology is critical for elucidating both short and long-term contributions of riverine BC and its implications for global carbon cycling. While BPCA ratios have been previously linked to BC source, further incorporation of radio- and stable- isotopes in characterizing individual BPCA components would provide useful information relating seasonality to BC sources and export from fluvial systems (Hanke et al., 2017; Wagner et al., 2017a).



## 4.7 References

- Abiven, S., Hengartner, P., Schneider, M.P.W., Singh, N., Schmidt, M.W.I. (2011). Pyrogenic carbon soluble fraction is larger and more aromatic in aged charcoal than in fresh charcoal. *Soil Biology and Biochemistry*, 43, 1615-1617.
- Bhatti, A.M., Rundquist, D., Schalles, J., Ramirez, L., Nasu, S. (2009). A comparison between above-water surface and subsurface spectral reflectances collected over inland waters. *Geocarto International*, 24, 133-141.
- Bianchi, T.S., Filley, T., Dria, K., Hatcher, P.G. (2004). Temporal variability in sources of dissolved organic carbon in the lower Mississippi River. *Geochimica et Cosmochimica Acta*, 68, 959-967.
- Bird, M.I., Wynn, J.G., Saiz, G., Wurster, C.M., McBeath, A. (2015). The pyrogenic carbon cycle. *Annual Review of Earth and Planetary Sciences*, 43, 273-298.
- Buringh, P. (1984). Organic Carbon in Soils of the World, in: Woodwell, G.M. (Ed.), The role of terrestrial vegetation in the global carbon cycle: Measurement by Remote Sensing. John Wiley & Sons, New York, pp. 91-109.
- Cai, W. J. (2011). Estuarine and coastal ocean carbon paradox: CO<sub>2</sub> sinks or sites of terrestrial carbon incineration? *Annual Review of Marine Science*, 3, 123-145.
- Coppola, A.I., Ziolkowski, L.A., Masiello, C.A., Druffel, E.R.M. (2014). Aged black carbon in marine sediments and sinking particles. *Geophysical Research Letters*, 41, 2427-2433.
- Creed, I.F., McKnight, D.M., Pellerin, B.A., Green, M.B., Bergamaschi, B.A., Aiken, G.R., ..., Stackpoole, S.M. (2015). The river as a chemostat: fresh perspectives on dissolved organic matter flowing down a river continuum. *Canadian Journal of Fisheries and Aquatic Sciences*, 72 (8), 1272-1285.
- Cuffney, T.F. (1988). Input, movement and exchange of organic matter within a subtropical coastal black water river-flood plain system. *Freshwater Biology*, 19, 305-320.
- Dai, J., Sun, M. Y. (2007). Organic matter sources and their use by bacteria in the sediments of the Altamaha estuary during high and low discharge periods. *Organic Geochemistry*, 38, 1-15.
- Dhillon, G.S., Inamdar, S. (2014). Storm event patterns of particulate organic carbon (POC) for large storms and differences with dissolved organic carbon (DOC). *Biogeochemistry*, 118, 61-81.
- Ding, Y., Yamashita, Y., Dodds, W.K., Jaffé, R. (2013). Dissolved black carbon in grassland streams: Is there an effect of recent fire history? *Chemosphere*, 90, 2557-2562.

- Ding, Y., Yamashita, Y., Jones, J., Jaffé, R. (2015). Dissolved black carbon in boreal forest and glacial rivers of central Alaska: assessment of biomass burning versus anthropogenic sources. *Biogeochemistry*, 123, 15-25.
- Dittmar, T. (2008). The molecular level determination of black carbon in marine dissolved organic matter. *Organic Geochemistry*, 39, 396-407.
- Dittmar, T., de Rezende, C.E., Manecki, M., Niggemann, J., Coelho Ovalle, A.R., Stubbins, A., Bernardes, M.C. (2012). Continuous flux of dissolved black carbon from a vanished tropical forest biome. *Nature Geoscience*, 5, 618-622.
- Dittmar, T., Koch, B., Hertkorn, N., Kattner, G. (2008). A simple and efficient method for the solid-phase extraction of dissolved organic matter (SPE-DOM) from seawater. *Limnology and Oceanography: Methods*, 6, 230-235.
- Eckard, R.S., Pellerin, B.A., Bergamaschi, B.A., Bachand, P.A.M., Bachand, S.M., Spencer, R.G.M., Hernes, P.J. (2017). Dissolved organic matter compositional change and biolability during two storm runoff events in a small agricultural watershed. *Journal of Geophysical Research: Biogeosciences*, doi: 10.1002/2017JG003935
- Fellman, J.B., Hood, E., Edwards, R.T., D'Amore, D.V. (2009). Changes in the concentration, biodegradability, and fluorescent properties of dissolved organic matter during stormflows in coastal temperate watersheds. *Journal of Geophysical Research: Biogeosciences*, 114, doi: 10.1029/2008JG000790
- Flannigan, M.D., Krawchuk, M.A., de Groot, W.J., Wotton, B.M., Gowman, L.M. (2009). Implications of changing climate for global wildland fire. *International Journal of Wildland Fire*, 18, 483-507.
- Georgia Environmental Finance Authority. (2016). 2016 Georgia Energy Report. [https://gefa.georgia.gov/sites/gefa.georgia.gov/files/related\\_files/document/Georgia-Energy-Report-2016.pdf](https://gefa.georgia.gov/sites/gefa.georgia.gov/files/related_files/document/Georgia-Energy-Report-2016.pdf)
- Glaser, B., Balashov, E., Haumaier, L., Guggenberger, G., Zech, W. (2000). Black carbon in density fractions of anthropogenic soils of the Brazilian Amazon region. *Organic Geochemistry*, 31, 669-678.
- Glendell, M., Brazier, R.E. (2014). Accelerated export of sediment and carbon from a landscape under intensive agriculture. *Science of The Total Environment*, 476-477, 643-656.
- Goldberg, E.D. (1985). *Black Carbon in the environment: Properties and Distribution*, 1 ed. John Wiley & Sons Inc, New York.
- Hanke, U.M., Reddy, C.M., Braun, A.L.L., Coppola, A.I., Haghypour, N., McIntyre, C.P., ... Eglinton, T.I. (2017). What on earth have we been burning? Deciphering sedimentary records of pyrogenic carbon. *Environmental Science & Technology*, 51, 12972-12980.

- Hedges, J.I., Cowie, G.L., Richey, J.E., Quay, P.D., Benner, R., Strom, M., Forsberg, B.R. (1994). Origins and processing of organic matter in the Amazon River as indicated by carbohydrates and amino acids. *Limnology and Oceanography*, 39, 743-761.
- Hockaday, W.C., Grannas, A.M., Kim, S., Hatcher, P.G. (2006). Direct molecular evidence for the degradation and mobility of black carbon in soils from ultrahigh-resolution mass spectral analysis of dissolved organic matter from a fire-impacted forest soil. *Organic Geochemistry*, 37, 501-510.
- Holmes, R.M., McClelland, J.W., Peterson, B.J., Tank, S.E., Bulygina, E., Eglinton, T.I., ... Zimov, S.A. (2012). Seasonal and annual fluxes of nutrients and organic matter from large rivers to the arctic ocean and surrounding seas. *Estuaries and Coasts*, 35, 369-382.
- Hood, E., Gooseff, M.N., Johnson, S.L. (2006). Changes in the character of stream water dissolved organic carbon during flushing in three small watersheds, Oregon. *Journal of Geophysical Research: Biogeosciences*, 111, doi: 10.1029/2005JG000082
- Hu, Y., Lu, Y., Edmonds, J.W., Liu, C. Wang, S. Das, O., ... , Zheng, C. (2016). Hydrological and land use control of watershed exports of dissolved organic matter in a large arid river basin in northwestern China. *Journal of Geophysical Research: Biogeosciences*, 121, 466-478.
- Huguet, A., Vacher, L., Relexans, S., Saubusse, S., Froidefond, J.M., Parlanti, E. (2009). Properties of fluorescent dissolved organic matter in the Gironde Estuary. *Organic Geochemistry*, 40, 706-719.
- Inamdar, S., Singh, S., Dutta, S., Levia, D., Mitchell, M., Scott, D., ... McHale, P. (2011). Fluorescence characteristics and sources of dissolved organic matter for stream water during storm events in a forested mid-Atlantic watershed. *Journal of Geophysical Research: Biogeosciences*, 116 (G3). doi: 10.1029/2011JG001735
- Jaffé, R., Ding, Y., Niggemann, J., Vähätalo, A.V., Stubbins, A., Spencer, R.G.M., ... Dittmar, T. (2013). Global charcoal mobilization from soils via dissolution and riverine transport to the oceans. *Science*, 340, 345-347.
- Jeong, J.-J., Bartsch, S., Fleckenstein, J.H., Matzner, E., Tenhunen, J.D., Lee, S.D., ... Park, J.H. (2012). Differential storm responses of dissolved and particulate organic carbon in a mountainous headwater stream, investigated by high-frequency, in situ optical measurements. *Journal of Geophysical Research: Biogeosciences*, 117, doi: 10.1029/2012JG001999
- Kathryn, L.D., Bratton, S.P. (1988). Vegetation response and regrowth after fire on Cumberland Island national seashore, Georgia. *Castanea*, 53, 47-65.
- Knutson, T.R., McBride, J.L., Chan, J., Emanuel, K., Holland, G., Landsea, C., ... , Sugi, M. (2010). Tropical cyclones and climate change. *Nature Geoscience*, 3, 157-163.

- Krawchuck, M., Moritz, M., Parisien, M.-A., Van Dorn, J., Hayhoe, K. (2009). Global pyrogeography: the current and future distribution of wildfire. *PLoS ONE*, 4(4): e5102, doi: 10.1371/journal.pone.0005102
- Lee, S., Baumann, K., Schauer, J.J., Sheesley, R.J., Naeher, L.P., Meinardi, ... Clements, M. (2005). Gaseous and particulate emissions from prescribed burning in Georgia. *Environmental Science & Technology*, 39, 9049-9056.
- Lewis, W.M.J., Hamilton, S.K., Soaunders, J.F. (1995). Rivers of North South America, in: Cushing, C., Cummins, K. (Eds.), *Ecosystems of the World: Rivers*. Elsevier, New York, pp. 219-256.
- Leorri, E., Mitra, S., Irabien, J.M., Zimmerman, A.R., Blake, W.H., Cearreta, A. (2014). A 700 year record of combustion-derived pollution in northern Spain: Tools to identify the Holocene/Anthropocene transition in coastal sediments. *Science of the Total Environment*, 470-471, 240-247.
- Li, Z., Sjodin, A., Porter, E.N., Patterson, D.G., Needham, L.L., Lee, S., ..., Mulholland, J.A. (2009). Characterization of PM<sub>2.5</sub>-bound polycyclic aromatic hydrocarbons in Atlanta. *Atmospheric Environment*, 43, 1043-1050.
- Mari, X., Van, T.C., Guinot, B., Brune, J., Lefebvre, J.P., Raimbault, P., ... Niggemann, J. (2017). Seasonal dynamics of atmospheric and river inputs of black carbon, and impacts on biogeochemical cycles in Halong Bay, Vietnam. *Elementa Science of the Anthropocene*, 75, doi: 10.1525/elementa.1255
- Marques, J.S.J., Dittmar, T., Niggemann, J., Almeida, M.G., Gomez-Saez, G.V., Rezende, C.E. (2017). Dissolved black carbon in the headwaters-to-ocean continuum of Paraíba Do Sul River, Brazil. *Frontiers in Earth Science*, 5 (11). doi: 10.3389/feart.2017.00011
- Masiello, C.A. (2004). New directions in black carbon organic geochemistry. *Marine Chemistry*, 92, 201-213.
- Maurice, P.A., Cabaniss, S.E., Drummond, J., Ito, E. (2002). Hydrogeochemical controls on the variations in chemical characteristics of natural organic matter at a small freshwater wetland. *Chemical Geology*, 187, 59-77.
- Medeiros, P.M., Seidel, M., Dittmar, T., Whitman, W.B., Moran, M.A. (2015). Drought-induced variability in dissolved organic matter composition in a marsh-dominated estuary. *Geophysical Research Letters*, 42, 6446-6453.
- Medeiros, P.M., Sikes, E.L., Thomas, B., Freeman, K.H. (2012). Flow discharge influences on input and transport of particulate and sedimentary organic carbon along a small temperate river. *Geochimica et Cosmochimica Acta*, 77, 317-334.

- Mitra, S., Bianchi, T.S., McKee, B.A., Sutula, M. (2002). Black carbon from the Mississippi River: Quantities, sources, and potential implications for the global carbon cycle. *Environmental Science & Technology*, 36, 2296-2302.
- Moody, J.A., Martin, D.A. (2001). Initial hydrologic and geomorphic response following a wildfire in the Colorado Front Range. *Earth Surface Processes and Landforms*, 26, 1049-1070.
- Myers-Pigg, A.N., Louchouart, P., Amon, R.M.W., Prokushkin, A., Pierce, K., Rubtsov, A. (2015). Labile pyrogenic dissolved organic carbon in major Siberian Arctic rivers: Implications for wildfire-stream metabolic linkages. *Geophysical Research Letters*, 42, 377-385.
- Myers-Pigg, A.N., Louchouart, P., Teisserenc, R. (2017). Flux of dissolved and particulate low-temperature pyrogenic carbon from two high-latitude rivers across the spring freshet hydrograph. *Frontiers in Marine Science*, 4, doi: 10.3389/fmars.2017.00038
- O'Malley, V.P., Abrajano, T.A., Hellou, J. (1996). Stable carbon isotopic apportionment of individual polycyclic aromatic hydrocarbons in St. John's Harbour, Newfoundland. *Environmental Science & Technology*, 30 (2), 634-639.
- Ohno, T. (2002). Fluorescence inner-filtering correction for determining the humification index of dissolved organic matter. *Environmental Science & Technology*, 36, 742-746.
- Peterson, B.J., Howarth, R.W., Garritt, R.H. (1985). Multiple stable isotopes used to trace the flow of organic matter in estuarine food webs. *Science*, 227, 1361-1363.
- Preston, C.M., Schmidt, M.W.I. (2006). Black (pyrogenic) carbon: a synthesis of current knowledge and uncertainties with special consideration of boreal regions. *Biogeosciences*, 3, 397-420.
- Pyle, L.A., Magee, K.L., Gallagher, M.E., Hockaday, W.C., Masiello, C.A. (2017). Short-term changes in physical and chemical properties of soil charcoal support enhanced landscape mobility. *Journal of Geophysical Research: Biogeosciences*, 122, 3098-3107.
- Qualls, R.G., Haines, B.L. (1991). Geochemistry of dissolved organic nutrients in water percolating through a forest ecosystem. *Soil Science Society of America Journal*, 55, 1112-1123.
- Raymond, P. A., Saiers, J. E. (2010). Event controlled DOC export from forested watersheds. *Biogeochemistry*, 100, 197-209.
- Raymond, P. A., Spencer, R.G.M. (2015). Riverine DOM. *Biogeochemistry of Marine Dissolved Organic Matter* (2<sup>nd</sup> Ed.). Boston, MA: Academic Press

- Raymond, P.A., Saiers, J.E., Sobczak, W.V. (2016). Hydrological and biogeochemical controls on watershed dissolved organic matter transport: pulse-shunt concept. *Ecology*, 97 (1), 5-16.
- Riedel, T., Biester, H., Dittmar, T. (2012). Molecular fractionation of dissolved organic matter with metal salts. *Environmental Science & Technology*, 46, 4419-4426.
- Roebuck, J.A., Podgorski, D.C., Wagner, S., Jaffé, R. (2017). Photodissolution of charcoal and fire-impacted soil as a potential source of dissolved black carbon in aquatic environments. *Organic Geochemistry*, 112, 16-21.
- Roth, P.J., Lehndorff, E., Brodowski, S., Bornemann, L., Sanchez-García, L., Gustafsson, Ö., Amelung, W. (2012). Differentiation of charcoal, soot and diagenetic carbon in soil: Method comparison and perspectives. *Organic Geochemistry*, 46, 66-75.
- Sanberg, D., Ottmar, R., Peterson, J., Core, J. (2002). Wildland fire in ecosystems: effects of fire on air, in: United States Department of Agriculture, F.S., Rocky Mountain Research Station (Ed.), Ogden, UT, p. 79p.
- Santín, C., Doerr, S.H., Kane, E.S., Masiello, C.A., Ohlson, M., de la Rosa, J.M., ... Dittmar, T. (2016). Towards a global assessment of pyrogenic carbon from vegetation fires. *Global Change Biology*, 22, 76-91.
- Santos, F., Wagner, S., Rothstein, D., Jaffé, R., Miesel, J.R. (2017). Impact of a historical fire event on pyrogenic carbon stocks and dissolved pyrogenic carbon in spodosols in Northern Michigan. *Frontiers in Earth Science*, 5, doi: 10.3389/feart.2017.00080
- Schaefer, S.C., Alber, M. (2007). Temporal and spatial trends in nitrogen and phosphorus inputs to the watershed of the Altamaha River, Georgia, USA. *Biogeochemistry*, 86, 231-249.
- Schneider, M.P.W., Hilf, M., Vogt, U.F., Schmidt, M.W.I. (2010). The benzene polycarboxylic acid (BPCA) pattern of wood pyrolyzed between 200 °C and 1000 °C. *Organic Geochemistry*, 41, 1082-1088.
- Shen, Y., Chapell, F.H., Strom, E.W., Benner, R. (2015). Origins and bioavailability of dissolved organic matter in groundwater. *Biogeochemistry*, 122 (1), 61-78.
- Shi, W., Sun, M.-Y., Molina, M., Hodson, R.E. (2001). Variability in the distribution of lipid biomarkers and their molecular isotopic composition in Altamaha estuarine sediments: implications for the relative contribution of organic matter from various sources. *Organic Geochemistry*, 32, 453-467.
- Spencer, R.G.M., Hernes, P.J., Dinga, B., Wabakanhanzi, J.N., Drake, T.W., Six, J. (2016). Origins, seasonality, and fluxes of organic matter in the Congo River. *Global Biogeochemical Cycles*, 30, 1105-1121.

- Spencer, R.G.M., Hernes, P.J., Ruf, R., Baker, A., Dyda, R.Y., Stubbins, A., Six, J. (2010). Temporal controls on dissolved organic matter and lignin biogeochemistry in a pristine tropical river, Democratic Republic of Congo. *Journal of Geophysical Research: Biogeosciences*, 115, doi: 10.1029/2009JG001180
- Stubbins, A., Niggemann, J., Dittmar, T. (2012). Photo-lability of deep ocean dissolved black carbon. *Biogeosciences*, 9, 1661-1670.
- Stubbins, A., Spencer, R.G.M., Mann, P.J., Holmes, R.M., McClelland, J.W., Niggemann, J., Dittmar, T. (2015). Utilizing colored dissolved organic matter to derive dissolved black carbon export by arctic rivers. *Frontiers in Earth Science*, 3, doi: 10.3389/feart.2015.00063
- Tian, D., Wang, Y., Bergin, M., Hu, Y., Liu, Y., Russell, A.G. (2008). Air quality impacts from prescribed forest fires under different management practices. *Environmental Science & Technology*, 42, 2767-2772.
- Turner, M.G. (1988). Multiple disturbances in a *Spartina alterniflora* salt marsh: are they additive? *Bulletin of the Torrey Botanical Club*, 115, 196-202.
- United States Energy Information Administration (2017), December 2017: Monthly Energy Review. <https://www.eia.gov/totalenergy/data/monthly/pdf/mer.pdf>
- United States Environmental Protection Agency (1998), Interim Air Quality Policy on Wildland and Prescribed Fires, Washington DC.
- Ussiri, D.A.N., Johnson, C.E. (2004). Sorption of Organic Carbon fractions by spodosol mineral horizons. *Soil Science Society of America Journal*, 68, 253-262.
- Vidon, P., Wagner, L.E., Soyeux, E. (2008). Changes in the character of DOC in streams during storms in two Midwestern watersheds with contrasting land uses. *Biogeochemistry*, 88, 257-270.
- Voss, B.M., Peucker-Ehrenbrink, B., Eglinton, T.I., Spencer, R.G.M., Bulygina, E., Galy, V., ... Luymes, R. (2015). Seasonal hydrology drives rapid shifts in the flux and composition of dissolved and particulate organic carbon and major and trace ions in the Fraser River, Canada. *Biogeosciences*, 12, 5597-5618.
- Wagner, S., Brands, J., Goranov, A. I., Drake, T. W, Spencer, R. G. M., Stubbins, A. (2017a). Online quantification and compound-specific stable isotopic analysis of black carbon in environmental matrices via liquid chromatography-isotope ratio mass spectrometry. *Limnology & Oceanography: Methods*, 15 (12), doi: 10.1002/lom3.10219
- Wagner, S., Cawley, K., Rosario-Ortiz, F., Jaffé, R. (2015a). In-stream sources and links between particulate and dissolved black carbon following a wildfire. *Biogeochemistry*, 124, 145-161.

- Wagner, S., Ding, Y., Jaffé, R. (2017b). A new perspective on the apparent solubility of dissolved black carbon. *Frontiers in Earth Science*, 5, doi: 10.3389/feart.2017.00075
- Wagner, S., Jaffé, R. (2015). Effect of photodegradation on molecular size distribution and quality of dissolved black carbon. *Organic Geochemistry*, 86, 1-4.
- Wagner, S., Riedel, T., Niggemann, J., Vähätalo, A.V., Dittmar, T., Jaffé, R. (2015b). Linking the molecular signature of heteroatomic dissolved organic matter to watershed characteristics in world rivers. *Environmental Science & Technology*, 49, 13798-13806.
- Wang, X., Xu, C., Druffel, E.M., Xue, Y., Qi, Y. (2016). Two black carbon pools transported by the Changjiang and Huanghe Rivers in China. *Global Biogeochemical Cycles*, 30, 1778-1790.
- Webster, J.R., Meyer, J.L. (1997). Organic matter budgets for streams: a synthesis. *Journal of the North American Benthological Society*, 16, 141-161.
- Weishaar, J.L., Aiken, G.R., Bergamaschi, B.A., Fram, M.S., Fujii, R., Mopper, K. (2003). Evaluation of specific ultraviolet absorbance as an indicator of the chemical composition and reactivity of dissolved organic carbon. *Environmental Science & Technology*, 37, 4702-4708.
- Weston, N.B., Hollibaugh, J.T., Joye, S.B. (2009). Population growth away from the coastal zone: Thirty years of land use change and nutrient export in the Altamaha River, GA. *Science of The Total Environment*, 407, 3347-3356.
- Wiedemeier, D.B., Abiven, S., Hockaday, W.C., Keiluweit, M., Kleber, M., Masiello, C.A., ... Schmidt, M.W.I. (2015). Aromaticity and degree of aromatic condensation of char. *Organic Geochemistry*, 78, 135-143.
- Wiedemeier, D.B., Hilf, M.D., Smittenberg, R.H., Haberle, S.G., Schmidt, M.W.I. (2013). Improved assessment of pyrogenic carbon quantity and quality in environmental samples by high-performance liquid chromatography. *Journal of Chromatography A*, 1304, 246-250.
- Williams, C.J., Yamashita, Y., Wilson, H.F., Jaffé, R., Xenopoulos, M.A. (2010). Unraveling the role of land use and microbial activity in shaping dissolved organic matter characteristics in stream ecosystems. *Limnology and Oceanography*, 55, 1159-1171.
- Wilson, H.F., Xenopoulos, M.A. (2008). Effects of agricultural land use on the composition of fluvial dissolved organic matter. *Nature Geoscience*, 2, 37-41.
- Xie, H., Zafiriou, O., Cai, W., Zepp, R., Wang, Y. (2004). Photooxidation and its effects on the carboxyl content of dissolved organic matter in two coastal rivers in the Southeastern United States. *Environmental Science & Technology*, 38, 4113-4119.



Xu, C., Xue, Y., Qi, Y., Wang, X. (2016). Quantities and Fluxes of dissolved and particulate black carbon in the Changjiang and Huanghe Rivers, China. *Estuaries and Coasts*, 39, 1617-1625.

Yamashita, Y., Kloeppe, B.D., Knoepp, J., Zausen, G.L., Jaffé, R. (2011). Effects of watershed history on dissolved organic matter characteristics in headwater streams. *Ecosystems*, 14, 1110-1122.

Yoon, B., Raymond, P.A. (2012). Dissolved organic matter export from a forested watershed during Hurricane Irene. *Geophysical Research Letters*, 39. doi: 10.1029/2012GL052785

Zigah, P.K., Minor, E.C., Werne, J.P. (2012). Radiocarbon and stable-isotope geochemistry of organic and inorganic carbon in Lake Superior. *Global Biogeochemical Cycles*, 26. doi: 10.1029/2011GB004132

Ziolkowski, L.A., Chamberlin, A.R., Greaves, J., Druffel, E.R.M. (2011). Quantification of black carbon in marine systems using the benzene polycarboxylic acid method: a mechanistic and yield study. *Limnology and Oceanography: Methods*, 9, 140-140.

## CHAPTER V

### LAND USE CONTROLS ON THE SPATIAL VARIABILITY OF DISSOLVED BLACK CARBON IN A SUBTROPICAL WATERSHED

(Modified from *Roebuck et al. 2018, Environmental Science & Technology*)

## 5.1 Abstract

Rivers are large sources of terrestrially derived dissolved organic carbon (DOC) to coastal oceans. The DOC exported from rivers can be a reflection of its respective watershed geomorphology and land use activity. Thus, anthropogenic shifts in watershed land use can significantly alter the DOC signature through changes in its molecular composition and chemical reactivity. A significant fraction of DOC exported from rivers contains a thermogenic signature consisting of a collection of highly condensed aromatic compounds typically formed through biomass burning and fossil fuel combustion. This pyrogenic material has otherwise been termed dissolved black carbon (DBC). While DOC and DBC exported from riverine systems are generally coupled, the direct effects of watershed land use on DBC quality are not well understood. In this study, samples were collected throughout the Altamaha River, Georgia, southeastern USA, a large watershed characterized by a high diversity in land use activity. DBC was characterized using the benzenepolycarboxylic acid method and ultrahigh-resolution mass spectrometry (FTICR-MS) and further correlated with watershed land cover. We show clear trends suggesting that DBC exported from areas of natural land cover contains a higher degree of polycondensed character in comparison to DBC exported from areas with higher anthropogenic influence. Furthermore, FTICR-MS revealed that a significant fraction of the pyrogenic carbon contains some degree of heteroatomic functionality with the pyrogenic signature becoming enriched in low molecular weight dissolved black nitrogen (DBN) and dissolved black sulfur (DBS) in response to higher anthropogenic activity. Even as global land use practices continue to change, this study demonstrates on a localized scale that land use changes from the headwaters to ocean continuum can

influence the export of pyrogenic carbon, which may have further implications for global carbon and nutrient cycling.

## **5.2 Introduction**

Black carbon (BC) is a carbonaceous residue of thermogenically altered organic material formed through incomplete combustion of biomass and from anthropogenic activities, such as fossil fuel combustion<sup>1</sup>. BC is comprised of a large collection of organic compounds ranging across a combustion continuum from small anhydrosugars formed at low temperatures (< 300°C) to highly condensed polycyclic aromatic compounds formed under higher temperature combustion conditions<sup>2</sup>. In comparison to bulk organic matter (OM), the highly polycondensed fraction of the BC spectrum is considered to be highly recalcitrant and resistant to biological degradation<sup>3</sup>. Thus, BC is ubiquitous throughout both terrestrial and marine environments. However, while a majority of BC becomes incorporated and stored in soils and sediments over long time scales, a significant portion of this material can be mobilized and transported throughout the aquatic environment as dissolved BC (DBC)<sup>4-6</sup>. Each year, rivers export an average of 27 Tg DBC globally, which equates to about 10% of the total dissolved organic carbon (DOC) pool, making rivers an important means for transport and biogeochemical cycling of DBC<sup>7</sup>.

Rivers are intrinsically connected with the terrestrial environment and thus, the DOC and subsequent DBC exported from fluvial systems can be strongly reflective of watershed dynamics and the anthropogenic activities from within<sup>8</sup>. For instance, the majority of dissolved organic matter (DOM) exported from small headwater streams will be most reflective of local allochthonous inputs and may undergo further bio- and photo-

chemical transformations during downstream transport<sup>9-11</sup>. However, elevated nutrient inputs from agricultural activity and heightened urbanization throughout a watershed have been directly linked to shifts in DOM quality and bioavailability leading to significant transformations in molecular composition that is more nitrogen rich and reflective of autochthonous in-stream activity<sup>12-14</sup>. Similar transformations are also observed for combustion derived material in which pyrogenic DOM exported to coastal oceans from agriculturally influenced watersheds is enriched in nitrogen functionality<sup>15</sup>.

Contrary to bulk DOC, however, direct relationships between DBC export and composition with changes in watershed land use have yet to be determined. With charcoal and aerosols from wildfires being the most significant source of BC to the environment<sup>5, 16</sup>, it may be expected that watersheds with high degrees of burn activity in forested areas would yield higher exports of DBC. While some studies have suggested there is no direct correlation between watershed short-term fire history and DBC export<sup>17, 18</sup>, watersheds will continue to export DBC even decades after a major burn event<sup>19</sup>. Furthermore, it may also be expected that loss of natural landscapes in light of increasing anthropogenic activity would result in a decrease in DBC source. However, evidence has been presented to suggest an increase in DBC export from addition of biochars as soil amendments in agricultural areas<sup>20</sup>. With more than 40% of earth's land mass now developed for agricultural purposes and with an ever increasing urbanization to accommodate long term population growth<sup>21</sup>, a better understanding of changing DBC dynamics with respect to catchment land use and its effects on long term carbon cycling and river quality is of increasing importance.

While numerous studies have assessed the influence of catchment land use on bulk DOC properties and export<sup>22-25</sup>, only little information is available on the effects on land use with respect to pyrogenic carbon<sup>8, 15, 20</sup>. For this study, we aim to address the knowledge gap by characterizing DBC on a watershed scale and assessing shifts in DBC quality with respect to catchment land use. While no method has been developed which can quantitatively detect DBC across the entire range of the combustion continuum, the benzenepolycarboxylic acid (BPCA) method can provide not only quantitative, but also qualitative compositional information with respect to the highly polycondensed fraction of the pyrogenic carbon spectrum<sup>26</sup>. Ultrahigh-resolution Fourier transform ion cyclotron resonance mass spectrometry (FTICR-MS) is also appropriate for characterization of complex DOM mixtures, which include DBC<sup>27</sup>, as it is capable of resolving thousands of individual molecular masses to which molecular formula are assigned<sup>28, 29</sup>. These molecular formulae are mostly represented as compounds with carbon, hydrogen, and oxygen (C, H, & O) with some containing heteroatomic functionalities (nitrogen, N; sulfur, S, & phosphorus, P), and they can be further categorized into compound groups which best describe their degree of saturation, oxidation and aromaticity by using a modified aromaticity index ( $AI_{\text{mod}}$ )<sup>30, 31</sup>.

Together, we used the quantitative BPCA method along with the molecular characterization of the DOM via FTICR-MS to characterize DBC exported throughout the Altamaha River, a large subtropical watershed located within the state of Georgia, southeastern USA. This watershed is characterized by varying degrees of natural land use, urbanization (Atlanta Metropolitan Area), and agriculture consisting mainly of poultry, beef, and soy and hay production<sup>32</sup>. Because soil BC source and formation

temperature might influence DBC composition<sup>33</sup>, we hypothesized that DBC exported from natural landscapes would exhibit a more polycondensed signature that is most typically reflective of wildfire derived pyrogenic carbon. We further investigated conservative behavior to establish sources of DBC throughout the Altamaha River watershed in concert with changes in land cover. Additionally, in concurrence with Wagner et al.<sup>15</sup>, we hypothesized that the shifts in watershed land use will significantly influence the molecular level DBC signature through incorporation of heteroatomic functionalities.

### **5.3 Methods**

#### *5.3.1 Site Description*

The Altamaha River is located entirely within the state of Georgia, USA draining *ca.* 36,000 km<sup>2</sup> (~25%) of the Georgian land mass, making it one of the largest drainage basins in the Eastern United States (Figure 5.1). Its two largest tributaries, the Ocmulgee River and Oconee River, each having their source in the Piedmont regions at the foothills of Appalachia, converge in the Southern Coastal Plains near Lumber City to form the Altamaha River. Together, these two tributaries contribute about 75% of the total water flow from the Altamaha River to the Atlantic Ocean. The Altamaha River exhibits an average water discharge of 400 m<sup>3</sup>/s and has an annual maximum in the early spring.

The Altamaha River remains relatively undisturbed in comparison to other watersheds along the eastern seaboard. However, it was recognized as an endangered river<sup>34</sup> as increasing anthropogenic activities within the watershed are expected to contribute significantly to augment eutrophication within its estuary. In a thirty-year period from 1970 to 2000, population doubled within the watershed from *ca.* 1.2 million

to *ca.* 2.5 million people<sup>35</sup>. The most notable increase was within the Georgia Piedmont region, which was primarily due to the Atlanta Metropolitan Area and other urban developments, an arrangement counter to general patterns in which population densities are highest in coastal regions<sup>35</sup>. The Altamaha River drains a significant portion of the urban Atlanta area and its suburbs primarily by means of the Ocmulgee River tributary, although a much smaller fraction is also drained within the Oconee River tributary. Agricultural land use is highest in the upper Altamaha River watershed and generally declines throughout the watershed. Primary agricultural activities throughout the watershed include poultry, beef, soy, and hay production<sup>32</sup>. The lower watershed consists primarily of natural forested areas and pristine wetlands with a much lower degree of anthropogenic activity.

### *5.3.2 Sample Collection*

A total of 42 samples were collected primarily along the Oconee River tributary within the Altamaha River watershed between May 23, 2016 and May 27, 2016 (Figure 5.1). Samples were also collected at the mouth of each of the other three main tributaries (Figure 5.1). These sites were selectively chosen to represent a wide array land use types throughout a gradient of small streams in the upper headwaters to larger rivers downstream. Of these sites, 19 were at USGS gauge stations in which water discharge data was collected. When possible, 1 L samples were collected from the riverbank directly into clean high-density polyethylene (HDPE) bottles. Bottles were pre-treated by soaking subsequently in 2 M HCl and 2 M NaOH each for 24 hours followed by rinsing with ultrapure water. Bottles were rinsed 3 times with sample water before final collection. Otherwise, samples were collected by dispensing a 5-gallon bucket over a



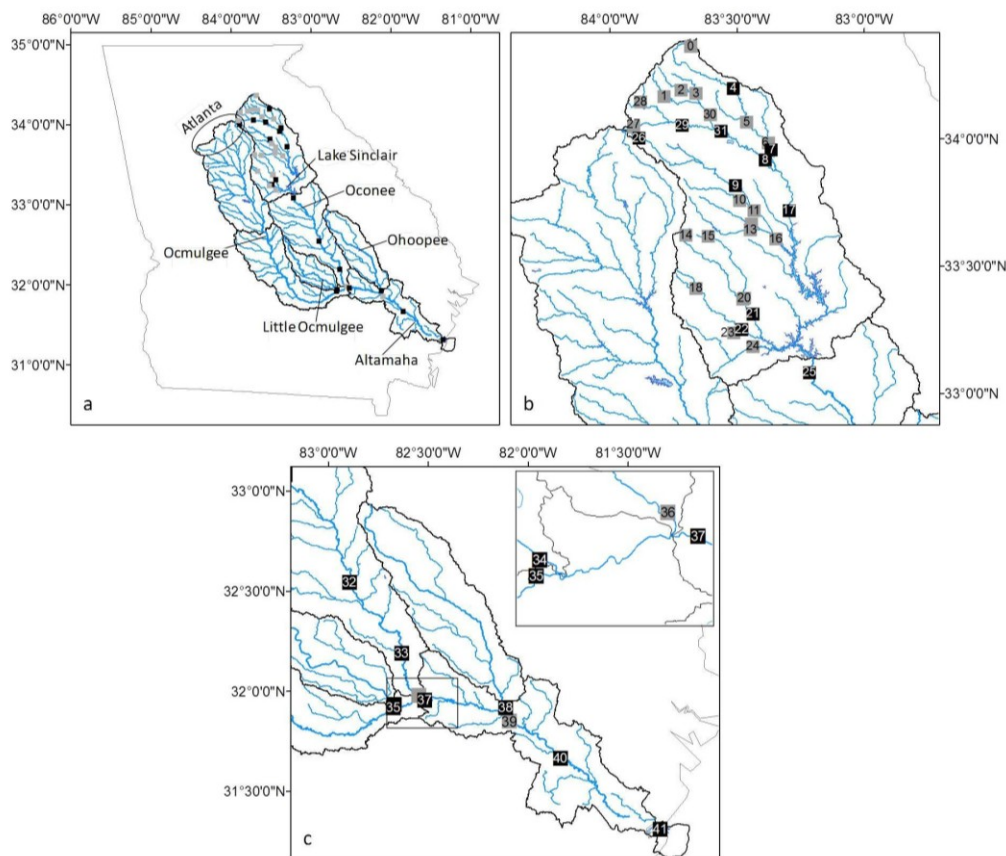


**Figure 5.1:** (a) Map of Altamaha River watershed displaying the 41 sample locations primarily from the Oconee River drainage basin. (b) Upper Oconee River sample locations and sample number listed in Table S1. (c) Lower Oconee River and Altamaha River main stem sample locations and sample number listed in Table S1. In all cases, the black boxes represent USGS stations and samples that were analyzed by the BPCA method and by FTICR-MS ( $n = 18$ ). The grey boxes represent all non-USGS stations and were characterized by FTICR-MS only ( $n = 23$ ).

bridge followed by transfer of water to clean HDPE bottles. The collection bucket was pre-rinsed at least three times with river water prior to each collection. Samples were stored on ice during transport back to the laboratory. Samples were filtered on the same day of collection (generally within 12 hours or less) through a  $0.7 \mu\text{m}$  pre-combusted ( $500^\circ\text{C}$ , 5.5 hours) Whatman glass fiber filter (GFF). DOC was analyzed on filtered river samples using a Shimadzu TOC-V CSH total organic carbon analyzer upon acidification and purging to remove inorganic carbon. Accuracy and precision were determined with

TOC quality control standards from ERA (Demand, WasteWarR, Lot#516, ERA) and were 100.3%.

### 5.3.3 Dissolved Black Carbon Analysis

DBC was extracted from water samples as part of the bulk DOC using a solid phase extraction (SPE) technique previously described by Dittmar et al.<sup>36</sup>. All samples were extracted by SPE on the same day of collection. DBC analysis was only performed on the 19 samples collected at USGS gauge stations.

Briefly, Agilent Bond Elut PPL cartridges (1 g) were conditioned consecutively with methanol and acidified ultrapure water (HCl, pH 2). The samples (~1L) were then gravity fed into the cartridge followed by rinsing again with acidified ultrapure water and drying under a stream of nitrogen gas. Samples were then eluted from the cartridge in methanol and stored at -20 °C until DBC and molecular analysis.

Quantification of DBC was carried out using the benzenepolycarboxylic (BPCA) method described by Dittmar<sup>26</sup> with thermal oxidation conditions optimized by Ding et al.<sup>17</sup>. For each sample, in triplicate, aliquots of methanol eluent containing *ca.* 0.2 mg DOC were dried under a stream of nitrogen gas in pre-combusted (500 °C for 5.5 hours) glass ampoules. The dried samples were redissolved in 0.5 mL concentrated nitric acid and flame sealed within the glass ampoules. Samples were thermo-chemically oxidized at 160 °C for 6 hours with remaining nitric acid removed by a stream of nitrogen gas<sup>17</sup>.

Thermo-chemical oxidation of DBC generates a collection tri-, tetra-, penta-, and hexa-substituted BPCAs (B3CA, B4CA, B5CA, and B6CA) which are directly proportional to DBC concentration. The newly generated BPCAs were re-dissolved in mobile phase buffer A (4 mM tert-butyl ammonium bromide, 50 mM sodium acetate,

10% methanol). High performance liquid chromatography (HPLC), coupled with a photodiode array detection (Surveyor, Thermo Scientific), was used to separate and quantify individual BPCAs. Separation was carried out on a Sunfire C<sub>18</sub> reverse phase column (3.1 μm, 2.1 x 150 mm, Waters Corporation) using an elution gradient consisting of mobile phase buffer A, and mobile phase buffer B (100% methanol). Complete separation conditions are described by Dittmar<sup>26</sup>. Quantification of DBC was achieved based on individual BPCA concentrations using a conversion factor reported by Dittmar<sup>26</sup>. The average coefficient of variation for all triplicate analyses was less than 5%.

#### 5.3.4 Development of Conservative Mixing Model for the Altamaha River

Modified from Marques et al.<sup>1</sup>, a conservative mixing model was developed for the Altamaha River to assess sources and sinks of DBC along the river continuum. Water discharge information was available from the USGS at 19 sample locations throughout the watershed in which subsequent DBC concentrations were measured. Due to very strong correlations with drainage area ( $r = 0.98$ ,  $p < 0.01$ ) and DOC ( $r = 0.98$ ,  $p < 0.01$ ) respectively, water discharge and DBC concentrations were extrapolated for the remaining 22 sample locations using the following equations:

$$\text{Log}Q = \log(\text{DA}) \cdot 0.425 - 2.185$$

$$Q = 10^{\text{DA} \cdot 0.425 - 2.185}$$

$$[\text{DBC}] = [\text{DOC}] \cdot 0.064 - 0.066$$

where Q is the water discharge (m<sup>3</sup>/s) and DA is the drainage area (km<sup>2</sup>). DBC fluxes (F<sub>DBC</sub>) were calculated as follows:

$$F_{\text{DBC}} = Q \cdot [\text{DBC}]$$

To assess sources and sinks along the river continuum, DBC fluxes were compared with those expected from ideal conservative behavior. Deviations from the theoretical, conservative DBC flux ( $F_{\text{DBC,cons.}}$ ) would suggest the presence of sources or sinks for DBC within the river continuum. For instance, a  $F_{\text{DBC}} > F_{\text{DBC,cons}}$  would indicate an additional source of DBC to the region. The  $F_{\text{DBC,cons}}$  at any given location was calculated as the additive flux of the most recent upstream sampling location along with the flux of any contributing tributaries to that location:

$$F_{\text{DBC,cons}} = F_{\text{DBC, most adjacent station}} + \Sigma F_{\text{DBC, contributing upstream tributaries}}$$

For instance,  $F_{\text{DBC,cons}}$  for sample #37 is equal to the sum of DBC fluxes for samples #34, 35, and 36 (Figure 5.1c). Given the number of samples and the spatial variability of said samples throughout the watershed, a 11 point model was developed in reference to the Altamaha river continuum (Figure 5.3).

### 5.3.5 Ultrahigh Resolution Mass Spectrometry

The DOM methanol extracts were diluted to a DOC concentration of 5 mg C/L in a methanol water mixture of 1:1 (v/v). The samples were analyzed as described in Seidel et al.<sup>37</sup> with ultrahigh-resolution mass spectrometry using a solariX XR FTICR-MS (Bruker Daltonik GmbH, Bremen, Germany) connected to a 15 Tesla superconducting magnet. The diluted extracts were infused at a rate of 2  $\mu\text{L}/\text{min}$  into the electrospray source (ESI; Apollo II ion source, Bruker Daltonik GmbH, Bremen, Germany) with the capillary voltage set to 4 kV in negative mode. 200 scans were accumulated in a mass window from 150 to 2000 Da and molecular formulae were assigned with the following restrictions:  $^{12}\text{C}_{1-130}{}^1\text{H}_{1-200}{}^{16}\text{O}_{1-50}{}^{14}\text{N}_{0-4}{}^{32}\text{S}_{0-2}{}^{31}\text{P}_{0-1}$  to masses above the method detection limit<sup>20</sup>. Molecular masses that were detected in less than three samples were removed

prior to further analysis. The samples were normalized to the sum of FTICR-MS signal intensities. The modified aromaticity index ( $AI_{\text{mod}}$ )<sup>30, 31</sup> and intensity-weighted molar ratios were calculated for each sample. Condensed aromatic compounds were defined by an  $AI_{\text{mod}} \geq 0.67$  and having greater than 14 carbon atoms. The elemental compositions of these compounds were represented by CHO, CHON, CHOS, CHOP, CHONS, CHONP, and CHOSP. Because the total number of CHOP, CHONS, CHONP and CHOSP represented on average less than 3% of the detected condensed aromatic molecular formulae, we limit this study to only include compounds categorized as CHO, CHON, or CHOS.

### *5.3.6 Statistical Analysis*

A geographical information systems (GIS) IMG data file containing Georgia land cover information from the year 2008 was obtained from Georgia GIS Data Clearinghouse, initially provided by the National Resources Spatial Analysis Laboratory, University of Georgia. ArcMap version 10.3 was used to calculate land cover contributions and drainage area for each sampling location. The initial 13 different land cover types for this dataset were condensed to four for this study, which include the following: forested area, wetlands, agriculture, and urban land use (Figure 5.2). Land use at each site was calculated as a function of the entire upstream catchment area respective to each sampling location. Percent urban land use was log-transformed to achieve a normal distribution.

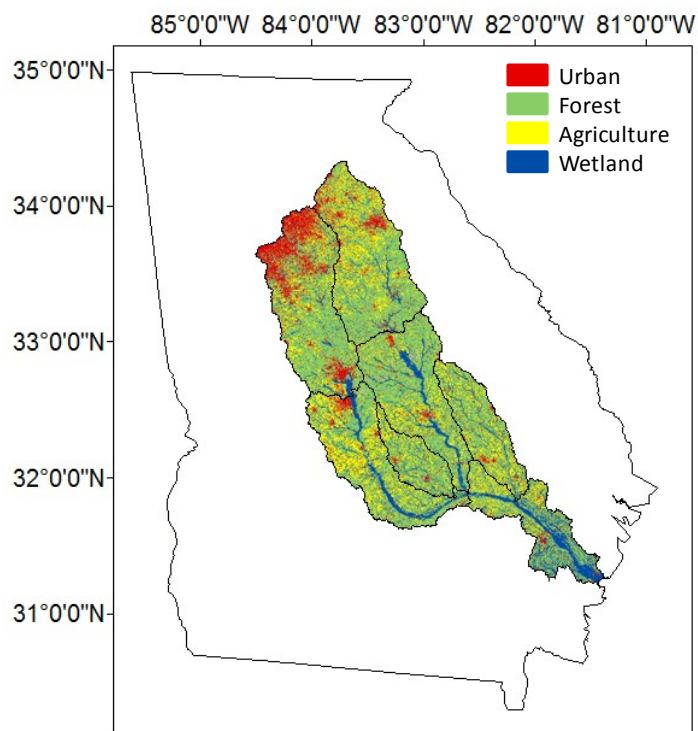


**Figure 5.2:** Map displaying land cover characteristics throughout the Altamaha River watershed.

Statistical analyses were performed using JMP version 12.0. The overall significance of a relationship between any two parameters was determined through linear correlations using Pearson’s product-moment correlation coefficient ( $r$ ). Hierarchical Cluster Analysis was performed on the percent-normalized BPCA concentrations with Ward’s method by using the squared Euclidean distance to determine similarity in BPCA distribution among sampled rivers. Principal Component Analysis (PCA) was performed on the percent-normalized BPCA concentrations and on the mean centered normalized peak intensities for all identified DBC formula detected throughout the Altamaha River, respectively.

## 5.4 Results

DBC was measured at 19 active USGS gauge stations throughout the Altamaha River watershed, primarily within the Oconee River sub-basin (Figure 5.1, Appendix 5.3). DBC concentrations were highly variable throughout the watershed ranging from 0.1 ppm up to 5.0 ppm and were highly correlated with DOC ( $r = 0.98$ ,  $p < 0.01$ ), a trend consistent with previous observations in world rivers<sup>7</sup>. In general, DBC concentrations were lowest in the upper watershed and higher in downstream areas (Figure 5.3a). Water discharge ranged from  $<0.1 \text{ m}^3/\text{s}$  to  $221 \text{ m}^3/\text{s}$  throughout the watershed and the associated DBC flux ranging from  $<1 \text{ mg/s}$  in the upper watershed to *ca.*  $48,000 \text{ mg/s}$  at the river mouth (Appendix 5.4). Water discharge was correlated to DBC concentration ( $r = 0.52$ ,  $p < 0.05$ ). In this study, DBC concentrations were strongly and inversely correlated with urban land use ( $r = -0.60$ ,  $p < 0.01$ ), but had a strong positive correlation with wetland cover ( $r = 0.87$ ,  $p < 0.01$ ).

BPCA distributions were used to describe the relative DBC composition. The BPCA ratio is defined as the relative abundance of B6CA and B5CA with respect to B4CA and B3CA where a higher ratio implies a higher degree of DBC polycondensed character (Schneider et al., 2010; Ziolkowski et al., 2011). For three samples, no detectable B5CA or B6CA was observed leading to a ratio of 0.00 (Appendix 5.4). Otherwise, the BPCA ratio ranged from 0.22 to 1.03 where higher values were generally observed in downstream areas (Figure 5.3b). The BPCA ratio was also highly correlated to land use increasing as a function of natural land cover (wetland:  $r = 0.87$ ,  $p < 0.01$ ) and decreasing as a function of anthropogenic land cover (urban:  $r = -0.63$ ,  $p < 0.01$ ).

Molecular characterization by FTICR-MS yielded a total of 16,477 detectable molecular formula among all samples. However, the total number of molecular formula detected in individual samples ranged from *ca.* 6500 to 9500 (Appendix 5.5). Polycondensed aromatic formulas ( $AI_{\text{mod}} > 0.67$ ,  $C > 14$ ) including DBC and heteroatomic DBC represented on average  $\sim 7.5\%$  of the total molecular formula (Appendix 5.5). The BPCA ratio was strongly correlated with the intensity weighted average molecular weight for the condensed aromatic region ( $m/z_{\text{w-dbc}}$ ,  $r = 0.81$ ,  $p < 0.01$ ). Roughly, 57% of the detected molecular formula assigned to the condensed aromatic region contained one or more heteroatoms including N and S (Appendix 5.5). Condensed aromatic formulae containing N were also strongly correlated to land use increasing in areas with higher agriculture activity ( $r = 0.42$ ,  $p < 0.01$ ) and decreasing in areas with higher forested ( $r = -0.40$ ,  $p < 0.01$ ) and wetland cover ( $r = -0.51$ ,  $p < 0.01$ ).

## **5.5 Discussion**

### *5.5.1 DBC Fluxes and Conservative Mixing Along the Altamaha River Continuum*

DBC concentrations varied significantly along the Altamaha River continuum with concentrations more than a magnitude higher in the lower watershed compared to the upper headwaters (Figure 5.3a). An increase in BPCA ratio was also observed along the river continuum suggesting a more polycondensed DBC signature in downstream regions (Figure 5.3b). The increase in DBC concentrations in the Altamaha River downstream areas was coupled with an increase in DBC flux (Appendix 5.4). However, two exceptions to this general downstream pattern are observed from within the Little Ocmulgee River and Ochopee River (Figure 5.1), which are the two smaller sub-basins of the Altamaha River. Concurrent to their smaller drainage area are significantly lower



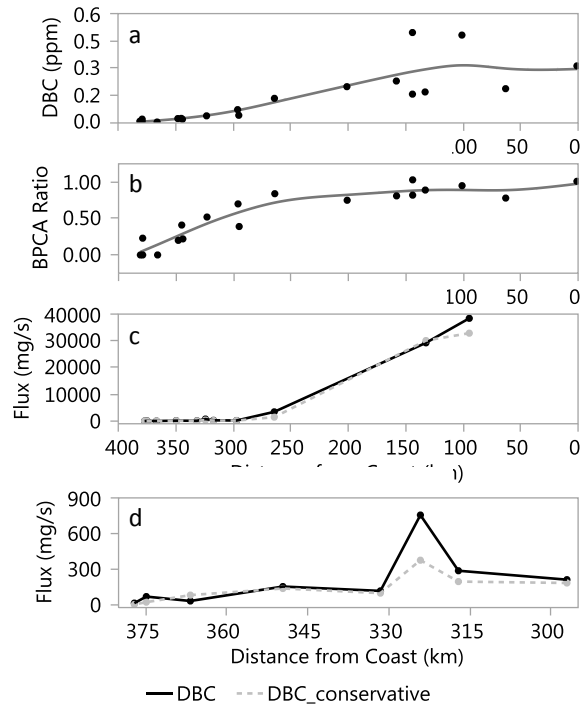


**Figure 5.3:** Spatial distribution of (a) DBC and (b) DBC composition (BPCA ratio) within the Altamaha River. Smoothing lines (grey) were added to follow general changes in data from the upper watershed to the coastal region. (c) DBC fluxes within the Altamaha River in comparison to conservative estimates where a DBC flux > conservative estimates indicates a source of DBC and a DBC flux < conservative estimates indicates a DBC sink. (d) The conservative mixing model displayed in 5.3c, however only showing the expanded scale between 380 and 250 km from the coastal region

water discharges, which in turn lead to lower DBC fluxes when compared to the larger Oconee River sub-basin (Appendix 5.4). Nevertheless, the general increase in DBC fluxes along the river continuum coupled with the increasing BPCA ratios may suggest either of two possibilities. Regarding concentration, (a) there are considerable source changes throughout the Altamaha River watershed that significantly influence downstream export of DBC, and/or (b) that DBC is most strongly associated with the more refractory pool of DOC that has survived upstream mineralization processes and is becoming enriched downstream. With regards to composition (i.e. BPCA ratio change),

(a) sources in the upper watershed might be more strongly influenced by urban DBC sources such as fossil fuels<sup>38</sup>, and/or (b) the less polycondensed fraction of the DBC is more reactive and selectively removed along the river continuum.

To further assess potential sources of DBC throughout the Altamaha River watershed, a DBC conservative mixing model was developed for the Altamaha River with slight modification from Marques et al.<sup>8</sup> and DBC fluxes were compared with those expected from conservative mixing behavior (Figure 5.3c,d). We note this model was developed in part with extrapolated DBC and discharge data, as detailed in section 5.3.4, and is thus limited with respect to the assumption of linearity and the consistency of a strong relationship between DBC with DOC and between discharge with drainage area. As presented in Figure 5.3c and Figure 5.3d, DBC fluxes were generally consistent with conservative estimates suggesting that higher DBC concentrations (Figure 5.3a) observed in the mid-lower reaches of the Altamaha River compared to those upstream may result through conservative accumulation of DBC downstream as suggested above. This coupled with higher BPCA ratios (Figure 5.3b) might imply significant source related shifts, where DBC with higher BPCA ratios accumulated downstream is enriched in wildfire derived DBC, compared to the DBC derived from fossil fuel combustion that may be expected from the highly urban areas upstream<sup>33, 38</sup>. This hypothesis is discussed in further detail below. When comparing to other watersheds, the conservative behavior of DBC in the Altamaha River highlights the importance of unique watershed dynamics in transporting DBC from upper headwaters to coastal areas. For instance, in a similar study, Marques et al.<sup>8</sup> attributed upstream sources of DBC in the Paraíba Do Sul River, Brazil to old slash and burn practices in the region followed by a downstream sink of

DBC due to photodegradation (as noted by shifts in BPCA distribution patterns). In comparison to the Altamaha River, however, the increasing BPCA ratios in the lower reaches of the watershed coupled with high turbidity in this region<sup>39</sup> does not suggest photodegradation to be a substantial downstream sink for DBC in this system.

Nonetheless, source related shifts in DBC accumulated in the downstream areas could be the result of a combined effect of photo-degradation and source strength as evident based on the higher BPCA ratios observed. The latter explanation is more likely due to noticeable differences in land cover between the upper and lower watershed.

#### *5.5.2 Land Use Controls on DBC Concentration and Composition*

DBC concentrations and respective BPCA ratios were significantly related to changes in land use throughout the Altamaha River watershed. However, DBC concentrations were most strongly correlated with bulk DOC concentrations ( $r = 0.98$ ,  $p < 0.01$ ) suggesting strong intermolecular associations between the respected DBC and DOC pools<sup>7</sup>. Thus, it is unclear if there is a direct relationship between DBC concentrations and changes in respective land cover, but rather an indirect relationship driven by changes in DOC concentrations with respect to land cover. However, the source related changes in DBC composition as noted by BPCA distribution would be expected when considering there is major BC compositional variation observed with respect to source change or formation temperature<sup>2, 33</sup>.

The upper portion of the Altamaha River watershed is the most anthropogenically impacted region within the basin (Figure 5.1) consisting of areas draining both the urban influences of the Atlanta Metropolitan Area as well as drainage areas from primarily agricultural and farming regions, which consist primarily of poultry and beef, corn, soy,

and hay production<sup>32</sup>. This distinction between the upper and lower watershed with respect to DBC is highlighted with a cluster analysis performed using percent-normalized BPCA concentrations (Appendix 5.1) that clearly shows clustering of samples between two groups that represent the upper and lower watershed. Because of the clear spatial differentiation in land use type throughout the watershed, the clustering of these samples provides clear indication that BPCA composition may be driven by watershed land cover and/or land use.

Among the small rivers and streams sampled, the lowest DBC concentrations were observed in 3 rivers with the highest urban influence (Stations 26, 29, & 31, Appendix 5.3 and Appendix 5.4), each collecting waters primarily from the Atlanta metropolitan region. These samples also had no detectable representation of penta- and hexa-substituted BPCAs (B5CA, B6CA in Appendix 5.4) suggesting that the DBC has a lower degree of polycondensed aromaticity. This overall general trend is still highlighted on watershed scale in which a strong inverse relationship is observed between urban land use and both DBC concentrations ( $r = -0.74$ ,  $p < 0.01$ ) and BPCA ratio ( $r = -0.72$ ,  $p < 0.01$ ). The low BPCA ratio, and in particular samples lacking representation of B5CA and B6CA, would suggest the DBC in samples with significant urban influence are mainly from anthropogenic sources. However, using BPCA ratio as a sole indicator of DBC source should be exercised with caution considering the potential effects of photodegradation on the BPCA distribution<sup>40, 41</sup>. Nonetheless, the low BPCA ratios in urban areas are probably indicative of a source primarily derived from fossil fuel combustion<sup>38, 42</sup>. Deposition of aerosols can be sources of DBC to fluvial systems<sup>43</sup> and the soot particles formed from fossil fuel combustion represent a source of highly

polycondensed BC<sup>44</sup>. The leachable fraction of this material contain primarily less polycondensed DBC, as reflected by a predominately B3CA and B4CA signature<sup>38</sup>.

The low aromaticity DBC signature was not limited to urban land use. In fact, the BPCA ratio was also inversely correlated with agricultural land cover ( $r = -0.52$ ,  $p < 0.05$ ) suggesting that in general, anthropogenically impacted areas are represented by a less polycondensed DBC signature. The lower BPCA ratios in agricultural areas though may come as a surprise considering the common practice of burning agricultural croplands and use of pyrogenic carbon as soil amendments<sup>45</sup>. Between 8 and 11% of global fires can be attributed to agricultural practices and charcoal can represent between 10 and 35% of U.S. agricultural soils<sup>44,46</sup>. Furthermore, the release of DBC is enhanced when biochars are added to soils for agricultural purpose<sup>20</sup>. However, more condensed BC and increasing biochar aromaticity has repeatedly been observed to increase as a function of charring temperature<sup>33</sup>. Because biochar production and farm management burning are most favored at lower temperatures<sup>47</sup>, the formation of less polycondensed BC (and therefore subsequent DBC) is likely more notable in agricultural areas, which may explain the observed inverse correlation between BPCA ratios and agricultural land cover ( $r = -0.52$ ,  $p < 0.05$ ) within the Altamaha River watershed.

The anthropogenic influences in the Oconee River sub-basin of the Altamaha River watershed are reduced downstream with natural forest and wetlands prevailing as the dominant land cover. Downstream samples (below Lake Sinclair, Figure 5.1) average about 68% natural land cover in comparison to upstream samples, which have a much higher anthropogenic influence (~50% with some samples >80%, Appendix 5.3). DBC concentrations increased considerably in downstream samples and were coupled with an

increase in the BPCA ratio, suggesting a downstream source of a more polycondensed DBC pool (Appendix 5.3 and Appendix 5.4). BPCA ratios were positively correlated with natural forest area ( $r = 0.58$ ,  $p < 0.05$ ) suggesting a predominately wildfire derived DBC source from forested areas. Roughly a million acres of Georgia forests are burned yearly for forest management purposes<sup>48</sup>, and a 50 year survey of fire history dating up to the year 2007 suggests the state experiences an average between 8,000 and 12,000 small wildfires annually<sup>49</sup>. The extensive annual burning of Georgia forests would suggest a significant source of DBC in watersheds throughout the state, which likely includes sources of DBC to the Altamaha River as well. The higher temperature wildfire derived burning of forested biomass leads to the formation of more polycondensed BC as noted due to an enrichment of B5CA and B6CA formation upon thermal oxidation<sup>33</sup> further supporting the observed positive correlation of BPCA ratios with forest area coverage ( $r = 0.58$ ,  $p < 0.05$ ) within the Altamaha River.

The observed increases in DBC and BPCA ratio with increasing natural land cover was not limited to forested area as wetlands were also very strongly associated with more polycondensed DBC ( $r = 0.87$ ,  $p < 0.01$ ). This association is further highlighted with a principal component analysis where a clear separation of BPCAs was observed along principal component 1 (PC1) in which the more substituted BPCAs fell negatively along PC1 and the least substituted BPCAs falling positively along PC1 (Appendix 5.2). Wetland cover was both inversely and strongly related to PC1 ( $r = -0.80$ ,  $p < 0.01$ ) further confirming the association between wetlands with polycondensed DBC. The importance of DBC export to coastal areas from wetlands has been previously noted for large ecosystems such as the Florida Everglades, in which case BC from watershed burning

activities is deposited in wetland soils and released as DBC after aging<sup>50</sup>. Wetlands in the Altamaha River watershed however would not be considered nearly as large-scale as the Florida Everglades, but are rather integrated throughout the lower watershed primarily within the riparian areas of the Oconee River and Altamaha River. These riparian wetlands areas are further surrounded by natural forest area, which experience frequent burning activity<sup>48</sup>. Due to their waterlogged nature, the impact of burning in the surrounding areas may lead to accumulation of BC within the wetland soils, inducing the release and transport of more polycondensed DBC throughout the Altamaha River<sup>50, 51</sup>.

### 5.5.3 Land Use Controls on Molecular Composition of DBC

Using FTICR-MS, we identified *ca.* 1500 individual molecular formulas within the Altamaha River watershed containing a combustion derived/polycondensed aromatic signature (DBC, A.I.  $\geq 0.67$ , C  $\geq 15$ ). Most individual samples contained between *ca.* 400 to 700 DBC molecular formula (*ca.* 5% - 10% of the total formula detected). The percent of DBC molecular formulas detected were also highly correlated to individual BPCA concentrations (normalized to DOC; B3CA:  $r = 0.92$ ,  $p < 0.01$ ; B4CA:  $r = 0.93$ ,  $p < 0.01$ ; B5CA:  $r = 0.87$ ,  $p < 0.01$ ; B6CA:  $r = 0.77$ ,  $p < 0.01$ ) suggesting a similar source of thermogenic material for both the BPCAs and the polycondensed aromatic compounds detected by FTICR-MS. These DBC signatures were not limited to CHO compounds, however, but also contained heteroatoms such as nitrogen and/or sulfur, which is more commonly referred to as dissolved black nitrogen (DBN)<sup>52, 53</sup> or dissolved black sulfur (DBS)<sup>54</sup>, respectively. In the Altamaha River, an average of about 43% of the polycondensed aromatic molecular formulas were characterized as CHO compounds, while the other 57% contain CHO and one or more heteroatoms (Appendix 5.5).

Changes in watershed land use can have significant impacts on the molecular composition of organic matter transported through river systems. For instance, increasing cropland has been routinely linked to higher nitrogen inputs into local rivers, which leads to a higher proportion of low molecular weight, nitrogen-containing DOM that is characteristic of autochthonous DOM production<sup>13, 14, 55, 56</sup>. A recent study found that in 10 large global river systems, the pyrogenic DOM signature is enriched in nitrogen for watersheds most impacted with agricultural activities, indicating that agricultural burning practices may enhance the production of charcoal containing nitrogen and may enhance the export of DBN<sup>15</sup>. Molecular structures containing nitrogen and sulfur have also been linked to urbanization through high loads in wastewater<sup>57</sup> and septic influenced aquatic systems<sup>58</sup>.

In order to elucidate the impacts of land use on the molecular composition and export of DBC on a smaller, localized watershed scale, principal component analysis was performed on the intensity-mean centered DBC molecular formulae (Figure 5.4). PCA loading and score plots are presented in Figure 5.4a and Figure 5.4b, respectively with PC1 representing 45.1% of explained variation and PC2 explaining 10.2% of the explained variation. As shown in Figure 5.4b, a clear separation in elemental composition of DBC compounds was observed along both principal component 1 (PC1) and principal component 2 (PC2). CHO-DBC compounds cluster predominately around negative PC1 whereas heteroatomic DBC cluster more positively with PC1. This is further evident with a strong positive correlation between PC1 and intensity weighted DBN ( $N_{w-dbc}$ ,  $r = 0.62$ ,  $p < 0.01$ ). Clustering of pyrogenic DOM based on heteroatom composition has been previously reported in world rivers and found to be directly related to changes in



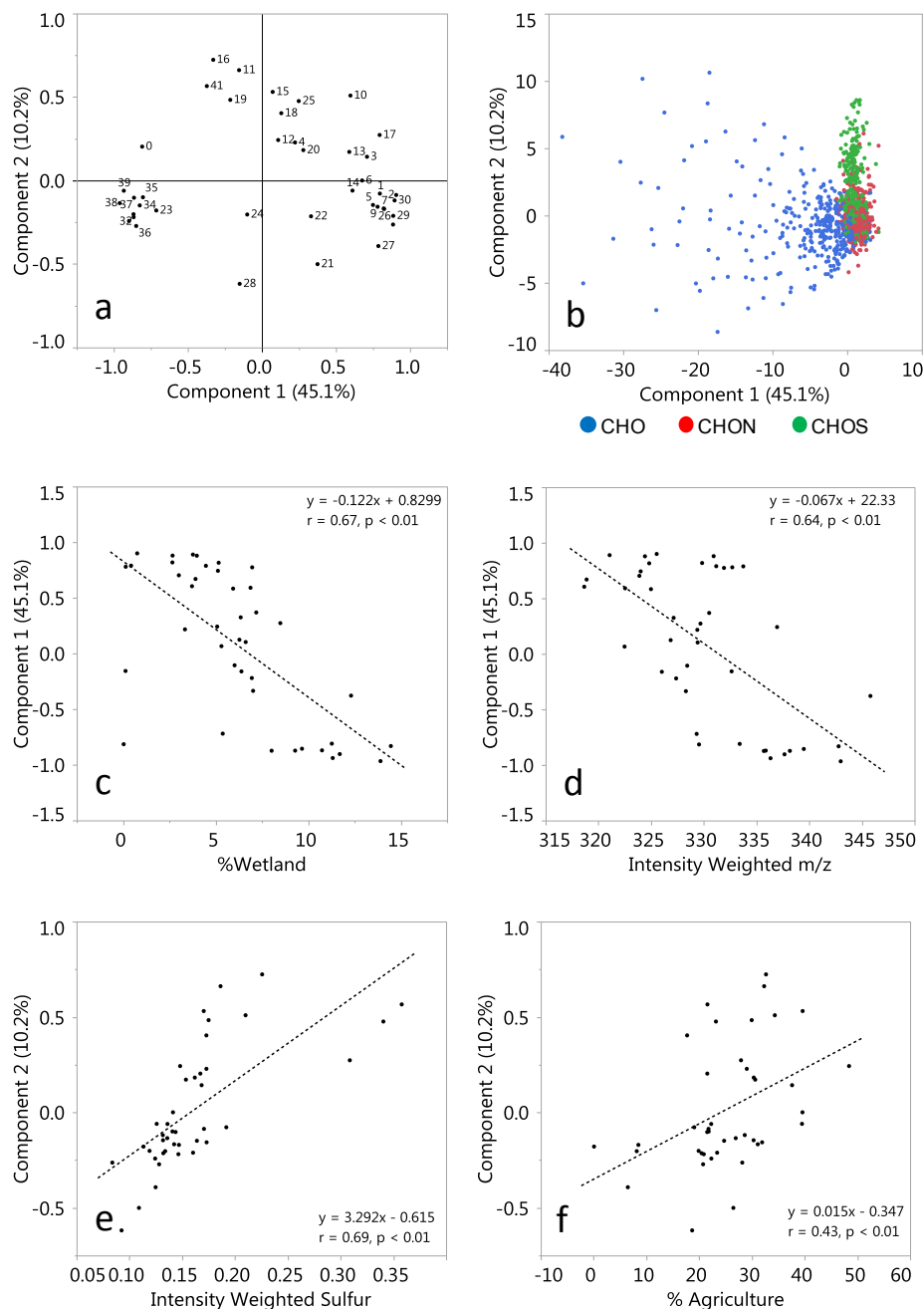


**Figure 5.4:** A principal component (PC) analysis of the intensity mean-centered DBC molecular formulae as determined by FTICR-MS analysis. (a) Loading plots displaying sample locations in PC space. (b) Score plot representing the distribution of molecular formulas in PC space with each highlighted in accordance with molecular composition. Graphs (c) and (d) represent linear correlations of PC1 with percent wetland cover and intensity weighted m/z, respectively. Graphs (e) and (f) represent linear correlations of PC2 with intensity weighted sulfur and percent agriculture, respectively.

watershed land use<sup>15</sup>. For the Altamaha River, PC1 was negatively related to wetland ( $r = -0.67$ ,  $p < 0.01$ , Figure 5.4c) and forest area ( $r = -0.38$ ,  $p < 0.05$ ) but positively related to urban land cover ( $r = 0.39$ ,  $p < 0.05$ ) indicating an enrichment in DBN with anthropogenic activity. These correlations in general support global trends reported by Wagner et al.<sup>15</sup>, but on a smaller watershed scale, in that anthropogenic activity enhances the heteroatomic DBC signature in fluvial systems. In agreement with the observed correlation of PC1 with ‘natural’ (negative PC1) vs. urban (positive PC1) land use, PC1 was also correlated with the  $m/z_{w-dbc}$  (Figure 5.4d,  $r = -0.64$ ,  $p < 0.01$ ),  $O/C_{w-dbc}$  ( $r = -0.36$ ,  $p < 0.05$ ), and  $H/C_{w-dbc}$  ( $r = 0.85$ ,  $p < 0.01$ ). This agrees with the expectation that DBC exported from natural land covers is higher in average molecular weight. This is also consistent with our previous results using BPCA ratios, that indicate a more polycondensed DBC signature from natural land covers compared to a less polycondensed DBC signature in more the anthropogenically impacted areas of the watershed. Furthermore, this pattern suggests that DBN exported from anthropogenically impacted areas is also generally lower in average molecular weight in comparison to their CHO only counterparts. This hypothesis is further supported by a strong inverse correlation between  $m/z_{w-dbc}$  and  $N_{w-dbc}$  ( $r = -0.76$ ,  $p < 0.01$ ).

The positive relation between PC1 with both urban land use and  $N_{w-dbc}$  may be an indication that nitrogen in the pyrogenic DOM pool may be in part fossil fuel combustion derived. Evidence to support this hypothesis has been reported by Yang et al.<sup>59</sup> who have shown the release of nitrogen containing polycyclic aromatic hydrocarbons (PAH) from coal combustion. Thus, we hypothesize that similar mechanisms driving the inclusion of nitrogen into PAHs would be similar for the more condensed aromatic fraction of the

pyrogenic carbon spectrum as described in this study. The relationship of DBN with land use has also been related to agricultural practices in comparison to urbanization<sup>15</sup>. While PC1 was not directly related to agricultural land cover, a strong correlation between  $N_{w-dbc}$  and agriculture ( $r = 0.42$ ,  $p < 0.01$ ) further suggests a link between DBN export and agricultural activity. In general, nitrogen inputs from agricultural areas have typically been associated with enhanced production of low molecular weight DOM derived from instream autochthonous sources<sup>13, 14</sup>. However, for pyrogenic OM, nitrogen has been shown to become incorporated into charred material during burning activity where it may be leached as DBN<sup>60</sup>. As previously discussed, charring temperature can significantly influence pyrogenic OM composition<sup>33</sup>, and thus the low temperature burning for agricultural management may enhance the production and leaching of low molecular weight DBN in comparison to higher temperature, wildfire derived char.

Heteroatomic DBC is not limited to DBN as preliminary evidence by FTICR-MS has been reported suggesting the existence of condensed aromatic compounds in aquatic systems that contain some degree of sulfur functionality<sup>54</sup>. The presence of DBS is evident throughout the Altamaha River as roughly 28% of the identified condensed aromatic compounds contain at least one sulfur atom (Appendix 5.5). However, the intensity-weighted average of DBS ( $S_{w-dbc}$ ) is much lower in comparison to  $N_{w-dbc}$  (Appendix 5.5) suggesting the relative abundance of these DBS compounds in fluvial systems is quite low in comparison to DBN compounds. In the PCA presented in Figure 5.4b, DBS molecular formulae cluster positively along PC1 similar to DBN, but also cluster more positively along PC2. In fact, PC2 is strongly correlated with both  $S_{w-dbc}$  (Figure 5.4e,  $r = 0.63$ ,  $p < 0.01$ ) and agricultural land cover (Figure 5.4f,

$r = 0.43, p < 0.01$ ) suggesting sulfur from agricultural sources may become incorporated into the pyrogenic DOM pool within a watershed. Studies within the agricultural areas of the Florida Everglades suggests that DOM becomes enriched in sulfur moieties in areas where there is increased sulfate enrichment, with DBS accounting for a small fraction of the detected sulfur containing compounds<sup>54, 61</sup>. Mechanisms for addition of sulfur into the pyrogenic carbon spectrum are currently unknown. A strong inverse relationship between PC2 and  $O/C_{w-dbc}$  ( $r = -0.85, p < 0.01$ ) suggests that DBS is associated with less oxygenated DBC and in a more reduced state. This would support a hypothesis of abiotic sulfurization in low oxygen and reducing environments, which has been previously observed for bulk DOM in sulfide rich conditions such as marine hydrothermal systems<sup>62</sup> and sulfidic intertidal flat sediments<sup>37</sup>. However, it is not unreasonable to hypothesize that sulfur can also be directly incorporated into charred materials through fire activity similar to that of nitrogen<sup>60</sup>. However, evidence to support this hypothesis is currently not available and would require further investigation. Regardless, the link between DBS and agricultural land cover in the Altamaha River suggests the existence of an important, but still unrecognized mechanism for integration of sulfur functionality within the condensed aromatic spectrum. The incorporation of these compounds into aquatic systems may have further unrecognized biogeochemical implications in relation to carbon, nitrogen, and sulfur cycling and their influence on global climate change, which warrants further investigation.

#### *5.5.4 Environmental Implications and Future Directions*

We show in this study that compositional shifts in DBC, implying variations in source and quality, are directly impacted by watershed land use. As the population and

agricultural activities continue to increase in the watershed, long-term shifts in the molecular composition and potentially the reactivity of DBC is to be expected. The long-term consequence for these changes are not well understood, but shifts in DBC composition throughout fluvial systems and export to coastal oceans could have significant impacts on both carbon and nutrient cycling, and may have further implications for on-going global climate change trends. Additional studies should continue to focus on the effects of land use with respect to DBC composition in large watersheds while further incorporating other environmental drivers that may influence DBC composition such as climatology, wildfire history, and river biogeochemistry. Furthermore, hydrological controls on DBC export have been previously observed in fluvial systems<sup>18, 19, 63</sup>. However, temporal variability and hydrological controls on DBC composition and export with respect to land use have yet to be determined and warrant further study.

## 5.6 References

1. Goldberg, E. D., *Black Carbon in the Environment: Properties and Distribution*. 1 ed.; John Wiley & Sons Inc: New York, 1985.
2. Masiello, C. A., New directions in black carbon organic geochemistry. *Mar. Chem.* **2004**, *92*, (1–4), 201-213.
3. Kuzyakov, Y.; Bogomolova, I.; Glaser, B., Biochar stability in soil: Decomposition during eight years and transformation as assessed by compound-specific <sup>14</sup>C analysis. *Soil Biol. Biochem.* **2014**, *70*, 229-236.
4. Hockaday, W. C.; Grannas, A. M.; Kim, S.; Hatcher, P. G., Direct molecular evidence for the degradation and mobility of black carbon in soils from ultrahigh-resolution mass spectral analysis of dissolved organic matter from a fire-impacted forest soil. *Org. Geochem.* **2006**, *37*, (4), 501-510.

5. Santín, C.; Doerr, S. H.; Kane, E. S.; Masiello, C. A.; Ohlson, M.; de la Rosa, J. M.; Preston, C. M.; Dittmar, T., Towards a global assessment of pyrogenic carbon from vegetation fires. *Global Change Biol.* **2016**, *22*, (1), 76-91.
6. Roebuck, J. A.; Podgorski, D. C.; Wagner, S.; Jaffé, R., Photodissolution of charcoal and fire-impacted soil as a potential source of dissolved black carbon in aquatic environments. *Org. Geochem.* **2017**, *112*, 16-21.
7. Jaffé, R.; Ding, Y.; Niggemann, J.; Vähätalo, A. V.; Stubbins, A.; Spencer, R. G. M.; Campbell, J.; Dittmar, T., Global charcoal mobilization from soils via dissolution and riverine transport to the oceans. *Science* **2013**, *340*, (6130), 345-347.
8. Marques, J. S. J.; Dittmar, T.; Niggemann, J.; Almeida, M. G.; Gomez-Saez, G. V.; Rezende, C. E., Dissolved black carbon in the headwaters-to-ocean continuum of Paraíba Do Sul River, Brazil. *Front. Earth Sci.* **2017**, *5*, (11), doi: 10.3389/feart.2017.00011.
9. Lu, Y.; Bauer, J. E.; Canuel, E. A.; Yamashita, Y.; Chambers, R. M.; Jaffé, R., Photochemical and microbial alteration of dissolved organic matter in temperate headwater streams associated with different land use. *J. Geophys. Res. Biogeosci.* **2013**, *118*, (2), 566-580.
10. Obernosterer, I.; Benner, R., Competition between biological and photochemical processes in the mineralization of dissolved organic carbon. *Limnol. Oceanogr.* **2004**, *49*, (1), 117-124.
11. Vannote, R. L.; Minshall, G. W.; Cummins, K. W.; Sedell, J. R.; Cushing, C. E., The river continuum concept. *Can. J. Fish. Aquat. Sci.* **1980**, *37*, (1), 130-137.
12. Parr, T. B.; Cronan, C. S.; Ohno, T.; Findlay, S. E. G.; Smith, S. M. C.; Simon, K. S., Urbanization changes the composition and bioavailability of dissolved organic matter in headwater streams. *Limnol. Oceanogr.* **2015**, *60*, (3), 885-900.
13. Williams, C. J.; Yamashita, Y.; Wilson, H. F.; Jaffé, R.; Xenopoulos, M. A., Unraveling the role of land use and microbial activity in shaping dissolved organic matter characteristics in stream ecosystems. *Limnol. Oceanogr.* **2010**, *55*, (3), 1159-1171.
14. Wilson, H. F.; Xenopoulos, M. A., Effects of agricultural land use on the composition of fluvial dissolved organic matter. *Nature Geosci.* **2008**, *2*, (1), 37-41.
15. Wagner, S.; Riedel, T.; Niggemann, J.; Vähätalo, A. V.; Dittmar, T.; Jaffé, R., Linking the molecular signature of heteroatomic dissolved organic matter to watershed characteristics in world rivers. *Environ. Sci. Technol.* **2015**, *49*, (23), 13798-13806.

16. Jones, M. W.; Quine, T. A.; de Rezende, C. E.; Dittmar, T.; Johnson, B.; Manecki, M.; Marques, J. S. J.; de Aragão, L. E. O. C., Do regional aerosols contribute to the riverine export of dissolved black carbon? *J. Geophys. Res. Biogeosci.* **2017**, *122*, (11), 2925-2938.
17. Ding, Y.; Yamashita, Y.; Dodds, W. K.; Jaffé, R., Dissolved black carbon in grassland streams: Is there an effect of recent fire history? *Chemosphere* **2013**, *90*, (10), 2557-2562.
18. Wagner, S.; Cawley, K.; Rosario-Ortiz, F.; Jaffé, R., In-stream sources and links between particulate and dissolved black carbon following a wildfire. *Biogeochemistry* **2015**, *124*, (1-3), 145-161.
19. Dittmar, T.; de Rezende, C. E.; Manecki, M.; Niggemann, J.; Coelho Ovalle, A. R.; Stubbins, A.; Bernardes, M. C., Continuous flux of dissolved black carbon from a vanished tropical forest biome. *Nature Geosci.* **2012**, *5*, (9), 618-622.
20. Riedel, T.; Iden, S.; Geilich, J.; Wiedner, K.; Durner, W.; Biester, H., Changes in the molecular composition of organic matter leached from an agricultural topsoil following addition of biomass-derived black carbon (biochar). *Org. Geochem.* **2014**, *69*, 52-60.
21. Foley, J. A.; DeFries, R.; Asner, G. P.; Barford, C.; Bonan, G.; Carpenter, S. R.; Chapin, F. S.; Coe, M. T.; Daily, G. C.; Gibbs, H. K.; Helkowski, J. H.; Holloway, T.; Howard, E. A.; Kucharik, C. J.; Monfreda, C.; Patz, J. A.; Prentice, I. C.; Ramankutty, N.; Snyder, P. K., Global consequences of land use. *Science* **2005**, *309*, (5734), 570-574.
22. Fuß, T.; Behounek, B.; Ulseth, A. J.; Singer, G. A., Land use controls stream ecosystem metabolism by shifting dissolved organic matter and nutrient regimes. *Freshwater Biol.* **2017**, *62*, (3), 582-599.
23. Graeber, D.; Gelbrecht, J.; Pusch, M. T.; Anlanger, C.; von Schiller, D., Agriculture has changed the amount and composition of dissolved organic matter in Central European headwater streams. *Sci. Total Environ.* **2012**, *438*, 435-446.
24. Molinero, J.; Burke, R. A., Effects of land use on dissolved organic matter biogeochemistry in piedmont headwater streams of the Southeastern United States. *Hydrobiologia* **2009**, *635*, (1), 289-308.
25. Yamashita, Y.; Kloeppel, B. D.; Knoepp, J.; Zausen, G. L.; Jaffé, R., Effects of watershed history on dissolved organic matter characteristics in headwater streams. *Ecosystems* **2011**, *14*, (7), 1110-1122.
26. Dittmar, T., The molecular level determination of black carbon in marine dissolved organic matter. *Org. Geochem.* **2008**, *39*, (4), 396-407.

27. Dittmar, T.; Koch, B. P., Thermogenic organic matter dissolved in the abyssal ocean. *Mar. Chem.* **2006**, *102*, (3), 208-217.
28. Kujawinski, E. B., Electrospray Ionization Fourier Transform Ion Cyclotron Resonance Mass Spectrometry (ESI FT-ICR MS): Characterization of complex environmental mixtures. *Environ. Forensics* **2002**, *3*, (3), 207-216.
29. Sleighter, R. L.; Hatcher, P. G., The application of electrospray ionization coupled to ultrahigh resolution mass spectrometry for the molecular characterization of natural organic matter. *J. Mass Spectrom.* **2007**, *42*, (5), 559-574.
30. Koch, B. P.; Dittmar, T., From mass to structure: an aromaticity index for high-resolution mass data of natural organic matter. *Rapid Commun. Mass Sp.* **2006**, *20*, (5), 926-932.
31. Koch, B. P.; Dittmar, T., From mass to structure: an aromaticity index for high-resolution mass data of natural organic matter. *Rapid Commun. Mass Sp.* **2016**, *30*, (1), 250-250.
32. Schaefer, S. C.; Alber, M., Temporal and spatial trends in nitrogen and phosphorus inputs to the watershed of the Altamaha River, Georgia, USA. *Biogeochemistry* **2007**, *86*, (3), 231-249.
33. Schneider, M. P. W.; Hilf, M.; Vogt, U. F.; Schmidt, M. W. I., The benzene polycarboxylic acid (BPCA) pattern of wood pyrolyzed between 200 °C and 1000 °C. *Org. Geochem.* **2010**, *41*, (10), 1082-1088.
34. National Oceanic and Atmospheric Administration., *NOAA's Estuarine Eutrophication Survey Volume 1: South Atlantic Region*; Silver Spring MD, 1996.
35. Weston, N. B.; Hollibaugh, J. T.; Joye, S. B., Population growth away from the coastal zone: Thirty years of land use change and nutrient export in the Altamaha River, GA. *Sci. Total Environ.* **2009**, *407*, (10), 3347-3356.
36. Dittmar, T.; Koch, B.; Hertkorn, N.; Kattner, G., A simple and efficient method for the solid-phase extraction of dissolved organic matter (SPE-DOM) from seawater. *Limnol. Oceanogr. Methods* **2008**, *6*, (6), 230-235.
37. Seidel, M.; Beck, M.; Riedel, T.; Waska, H.; Suryaputra, I. G. N. A.; Schnetger, B.; Niggemann, J.; Simon, M.; Dittmar, T., Biogeochemistry of dissolved organic matter in an anoxic intertidal creek bank. *Geochim. Cosmochim. Acta* **2014**, *140*, (Supplement C), 418-434.



38. Ding, Y.; Yamashita, Y.; Jones, J.; Jaffé, R., Dissolved black carbon in boreal forest and glacial rivers of central Alaska: assessment of biomass burning versus anthropogenic sources. *Biogeochemistry* **2015**, *123*, (1), 15-25.
39. Witte, W. G.; Whitlock, C. H.; Harriss, R. C.; Usry, J. W.; Poole, L. R.; Houghton, W. M.; Morris, W. D.; Gurganus, E. A., Influence of dissolved organic materials on turbid water optical properties and remote-sensing reflectance. *J. Geophys. Res. Oceans* **1982**, *87*, (C1), 441-446.
40. Stubbins, A.; Niggemann, J.; Dittmar, T., Photo-lability of deep ocean dissolved black carbon. *Biogeosciences* **2012**, *9*, (5), 1661-1670.
41. Wagner, S.; Jaffé, R., Effect of photodegradation on molecular size distribution and quality of dissolved black carbon. *Org. Geochem.* **2015**, *86*, 1-4.
42. Khan, A. L.; Jaffé, R.; Ding, Y.; McKnight, D. M., Dissolved black carbon in Antarctic lakes: Chemical signatures of past and present sources. *Geophys. Res. Lett.* **2016**, *43*, (11), 5750-5757.
43. Mari, X.; Van, T. C.; Guinot, B.; Brune, J.; Lefebvre, J.-P.; Raimbault, P.; Dittmar, T.; Niggemann, J., Seasonal dynamics of atmospheric and river inputs of black carbon, and impacts on biogeochemical cycles in Halong Bay, Vietnam. *Elementa* **2017**, *75*, doi: 10.1525/elementa.255.
44. Roth, P. J.; Lehndorff, E.; Brodowski, S.; Bornemann, L.; Sanchez-García, L.; Gustafsson, Ö.; Amelung, W., Differentiation of charcoal, soot and diagenetic carbon in soil: Method comparison and perspectives. *Org. Geochem.* **2012**, *46*, 66-75.
45. Woolf, D.; E., A. J.; Street-Perrott, F. A.; Lehmann, J.; Joseph, S., Sustainable biochar to mitigate global climate change. *Nat. Commun.* **2010**, *1*, (56), doi: 10.1038/ncomms1053.
46. Korontzi, S.; McCarty, J.; Loboda, T.; Kumar, S.; Justice, C., Global distribution of agricultural fires in croplands from 3 years of Moderate Resolution Imaging Spectroradiometer (MODIS) data. *Global Biogeochem. Cycles* **2006**, *20*, (2), doi: 10.1029/2005GB002529.
47. McHenry, M. P., Agricultural bio-char production, renewable energy generation and farm carbon sequestration in Western Australia: Certainty, uncertainty and risk. *Agric. Ecosyst. Environ.* **2009**, *129*, (1), 1-7.
48. Tian, D.; Wang, Y.; Bergin, M.; Hu, Y.; Liu, Y.; Russell, A. G., Air quality impacts from prescribed forest fires under different management practices. *Environ. Sci. Technol.* **2008**, *42*, (8), 2767-2772.

49. Georgia Forestry Commission., *The Historic 2007 Georgia Wildfires: Learning from the Past - Planning for the Future*; 2007.
50. Ding, Y.; Cawley, K. M.; da Cunha, C. N.; Jaffé, R., Environmental dynamics of dissolved black carbon in wetlands. *Biogeochemistry* **2014**, *119*, (1), 259-273.
51. Abiven, S.; Hengartner, P.; Schneider, M. P. W.; Singh, N.; Schmidt, M. W. I., Pyrogenic carbon soluble fraction is larger and more aromatic in aged charcoal than in fresh charcoal. *Soil Biol. Biochem.* **2011**, *43*, (7), 1615-1617.
52. Ding, Y.; Watanabe, A.; Jaffé, R., Dissolved black nitrogen (DBN) in freshwater environments. *Org. Geochem.* **2014**, *68*, 1-4.
53. Wagner, S.; Dittmar, T.; Jaffé, R., Molecular characterization of dissolved black nitrogen via electrospray ionization Fourier transform ion cyclotron resonance mass spectrometry. *Org. Geochem.* **2015**, *79*, 21-30.
54. Hertkorn, N.; Harir, M.; Cawley, K. M.; Schmitt-Kopplin, P.; Jaffé, R., Molecular characterization of dissolved organic matter from subtropical wetlands: a comparative study through the analysis of optical properties, NMR and FTICR/MS. *Biogeosciences* **2016**, *13*, (8), 2257-2277.
55. Carpenter, S. R.; Caraco, N. F.; Correll, D. L.; Howarth, R. W.; Sharpley, A. N.; Smith, V. H., Nonpoint pollution of surface waters with phosphorus and nitrogen. *Ecol. Appl.* **1998**, *8*, (3), 559-568.
56. Mattsson, T.; Kortelainen, P.; Laubel, A.; Evans, D.; Pujo-Pay, M.; Räike, A.; Conan, P., Export of dissolved organic matter in relation to land use along a European climatic gradient. *Sci. Total Environ.* **2009**, *407*, (6), 1967-1976.
57. Gonsior, M.; Zwartjes, M.; Cooper, W. J.; Song, W.; Ishida, K. P.; Tseng, L. Y.; Jeung, M. K.; Rosso, D.; Hertkorn, N.; Schmitt-Kopplin, P., Molecular characterization of effluent organic matter identified by ultrahigh resolution mass spectrometry. *Water Res.* **2011**, *45*, (9), 2943-2953.
58. Arnold, W. A.; Longnecker, K.; Kroeger, K. D.; Kujawinski, E. B., Molecular signature of organic nitrogen in septic-impacted groundwater. *Environ. Sci. Process. Impacts* **2014**, *16*, (10), 2400-2407.
59. Yang, X.; Liu, S.; Xu, Y.; Liu, Y.; Chen, L.; Tang, N.; Hayakawa, K., Emission factors of polycyclic and nitro-polycyclic aromatic hydrocarbons from residential combustion of coal and crop residue pellets. *Environ. Pollut.* **2017**, *231*, (Part 2), 1265-1273.
60. Knicker, H., How does fire affect the nature and stability of soil organic nitrogen and carbon? A review. *Biogeochemistry* **2007**, *85*, (1), 91-118.

61. Poulin, B. A.; Ryan, J. N.; Nagy, K. L.; Stubbins, A.; Dittmar, T.; Orem, W.; Krabbenhoft, D. P.; Aiken, G. R., Spatial dependence of reduced sulfur in Everglades dissolved organic matter controlled by sulfate enrichment. *Environ. Sci. Technol.* **2017**, *51*, (7), 3630-3639.
62. Gomez-Saez, G. V.; Niggemann, J.; Dittmar, T.; Pohlabein, A. M.; Lang, S. Q.; Noowong, A.; Pichler, T.; Wörmer, L.; Bühring, S. I., Molecular evidence for abiotic sulfurization of dissolved organic matter in marine shallow hydrothermal systems. *Geochim. Cosmochim. Acta* **2016**, *190*, (Supplement C), 35-52.
63. Myers-Pigg, A. N.; Louchouart, P.; Teisserenc, R., Flux of dissolved and particulate low-temperature pyrogenic carbon from two high-latitude rivers across the spring freshet hydrograph. *Front. Mar. Sci.* **2017**, *4*, (38), doi: 10.3389/fmars.2017.00038.

## CHAPTER VI

### CHARACTERIZATION OF DISSOLVED ORGANIC MATTER ALONG A RIVER CONTINUUM: LINKING WATERSHED LAND USE TO THE RIVER CONTINUUM

#### CONCEPT

(In preparation for *Environmental Science & Technology*)

## 6.1 Abstract

About 250 Tg of dissolved organic carbon are annually transported from inland waters to coastal systems making rivers a critical link in the carbon cycle between terrestrial and marine environments. During transport through fluvial systems, various degradation pathways selectively remove or transform labile material effectively altering the composition of dissolved organic matter (DOM) exported to the ocean. The River Continuum Concept (RCC) has been historically used as a model to predict the fate and quality of OM along a river continuum. However, conversion of natural landscapes for urban and agricultural practices can also alter the sources and quality of DOM exported from fluvial systems, and the RCC may be significantly limited in predicting DOM quality in anthropogenically impacted watersheds. Here, we studied DOM dynamics in the Altamaha River watershed in Georgia, USA, a system where headwater streams are highly impacted by anthropogenic activity. The primary goal of this study was to quantitatively assess the importance of both the RCC and land use as environmental drivers controlling DOM composition. Forty-two samples were collected throughout the watershed and DOM was characterized with optical properties and high-resolution mass spectrometry. Using multivariate statistics, we were able to explain a significant portion of the spatial variability in DOM composition as a function of both the RCC and watershed land use. This study highlights the importance of incorporating land use among other controls into the RCC for predicting DOM composition during downstream transport to coastal systems.

## 6.2. Introduction

Dissolved organic matter (DOM) contains the largest pool of recyclable carbon transported throughout terrestrial systems where the global export of dissolved organic carbon (DOC) from rivers is estimated at roughly 0.25 Pg per year<sup>1</sup>. The role of DOM in aquatic systems is quite diverse, but critical for riverine health and ecosystem functions. For instance, chromophoric DOM (CDOM) is a light attenuator that can both regulate primary production<sup>2</sup> and protect aquatic organisms from harmful radiation<sup>3</sup>. In addition, DOM serves as a primary energy source for microbial heterotrophs in fueling ecosystem respiration<sup>4-5</sup> and also alters the solubility and transport of metals and organic pollutants<sup>6</sup>. As such, DOM is also as a significant source of CO<sub>2</sub> evasion from aquatic systems<sup>5, 7-8</sup> and thus a critical component within the global carbon cycle.

While DOM exported from rivers has been most prominently linked to terrestrial sources (allochthonous), such as humic acids generated from decomposed plant material<sup>9-10</sup>, it may also be derived from in-stream sources (autochthonous)<sup>11</sup>. The composition of DOM is a leading factor in its general reactivity<sup>12</sup> and during transport, DOM may be exposed to a variety of in-stream processes that may ultimately alter its composition and fate. Such processes may include photodegradation<sup>13</sup>, flocculation and interaction with metals<sup>14-16</sup>, and microbial respiration<sup>5, 17</sup>. As DOM has become increasingly linked with terrestrial ecosystem processes and its role in global carbon cycling has become more evident, there is an increasing a need for a better understanding of riverine dynamics that control the fate and transport of DOM in fluvial systems.

The River Continuum Concept (RCC) was established nearly four decades ago providing a general paradigm for fluvial ecosystem functions and predicting systematic

biological responses with an increasing river continuum<sup>18</sup>. The original hypothesis suggests that the relative chemical diversity of DOM is highest in the upper headwaters where contributions are primarily derived from terrestrial sources. With longitudinal succession, selective labile components are removed through various pathways, and sources of DOM shift primarily to an autochthonous signature as light availability increases (less canopy cover, wider rivers) and photosynthesis exceeds ecosystem respiration. This generally leads to a decrease in DOM molecular diversity with increasing stream order<sup>18</sup>. With modern advancements in DOM characterization, others have generally confirmed the original RCC hypothesis by noting a higher number of molecular formulae (as detected with high resolution mass spectrometry) in lower stream orders<sup>19</sup>. This is accompanied by a less aromatic and less reactive DOM pool with decreasing distance to coastal regions<sup>20-21</sup>, which is the result of a variety of degradation processes as well as a disconnect between DOM and the terrestrial landscape downstream<sup>22</sup>. Since its inception, limitations to the RCC have been highlighted and adaptations to this paradigm have been introduced with efforts to acknowledge a variety of anthropogenic and hydrological stressors on aquatic systems such as serial discontinuity<sup>23</sup>, the influence of floodplain sources<sup>24</sup>, and the impacts of seasonal high discharge storm driven events<sup>25</sup>. However, DOM composition has also been very closely linked with watershed land use<sup>26-27</sup>, a parameter for which the original RCC has been constrained to natural, undisturbed systems.

Globally, watershed activity is rapidly changing as urbanization continues to increase in response to population growth, and now more than 40% of earth's land mass has been developed for agricultural purposes<sup>28</sup>. Sources of DOM exported from

headwater streams have routinely been linked to the presence of natural covers<sup>29</sup>. However, headwater urban streams are increasingly disconnected hydrologically from riparian zones as channelization and drainage networks are engineered and thus, greatly altering these streams from their natural states<sup>30-31</sup>. In response, storm drains, ditches, and leaky sewers and septic systems increase both carbon and nutrient loads while also increasing the transport of pollutants (hydrocarbons, metals, pesticides) downstream<sup>32</sup>. Furthermore, high export of nutrients (fertilizers) from both urban and agricultural watersheds fuel autotrophic activity in streams leading to significant source related shifts in DOM composition<sup>33-34</sup>. Thus, as DOM sources and composition have been extensively linked to watershed land cover, there is a need to further integrate the controls of land use into classic paradigms such as the RCC to better predict the fate and quality of DOM exported from fluvial systems.

The Altamaha River, which was selected for this study and is located entirely within the state of Georgia, USA, is a prime example in which an effort to understand ecosystem controls on DOM sources and composition as predicted by the RCC may be significantly inhibited due watershed land use. The Altamaha River watershed is also of interest as anthropogenic activities, such as urbanization and agriculture, are elevated in the upper watershed, and generally decrease in the lower watershed being replaced by a prevalence of more natural forested and wetland ecosystems<sup>35</sup>. Thus, it can be hypothesized that DOM quality in the upper watershed may be more autochthonously derived/impacted in this system compared to the lower watershed.

In this study, the Altamaha River was extensively sampled from headwaters to mouth over a gradient of low to high stream orders with a high degree of variability in



land cover. DOM was characterized using modern analytical techniques (ultra-high resolution mass spectrometry and fluorescence spectroscopy) with the primary objective to assess the relative importance of both land use and the RCC as environmental drivers of DOM composition in the Altamaha River. Our results provide new insights into the contributions of anthropogenically impacted watersheds on stream ecosystem functions and the need for considering land use with traditional paradigms in predicting the fate and quality of DOM exported to coastal systems.

### **6.3. Methods**

#### *6.3.1 Sample Locations and Collection*

With a drainage basin of roughly 36,000 km<sup>2</sup>, the Altamaha River drains primarily by means of the Ocmulgee River and Oconee River tributaries (Figure 5.1), each developing within the Georgia Piedmont Region at the foothills of Appalachia. The headwaters of each of these tributaries drain highly anthropogenically impacted areas, with the Ocmulgee River draining primarily from the Atlanta Metropolitan Area and the Oconee River draining areas with enhanced agricultural activity<sup>36</sup> (soy, hay, poultry; Figure 6.1a). Nutrient exports are highest in the upper watershed, as would be expected in anthropogenically impacted systems, and decrease downstream<sup>36</sup>.

A total of forty-two samples were collected throughout the Altamaha River watershed primarily within the Oconee River tributary, representing the spatially longest possible transect within this system (Figure 6.1b). A single sample was also collected at the mouth of each of the other three primary tributaries to the Altamaha River (Ocmulgee River, Little Ocmulgee River, and Ohoopsee River; Figure 6.1b with more detailed information in Figure 5.1). Sample locations were selected with a diverse set of land use

activity including both natural and anthropogenic disturbances while also representing a gradient of low order headwater streams to larger, high order rivers downstream (Figure 6.1b). Samples were classified and assigned to a stream order group based up the Strahler classification system<sup>37</sup>, which includes low order small streams (stream order 1-3, n = 14), medium order small rivers (stream order 4-6, n = 11), and high order large rivers (stream order > 6, n = 11).

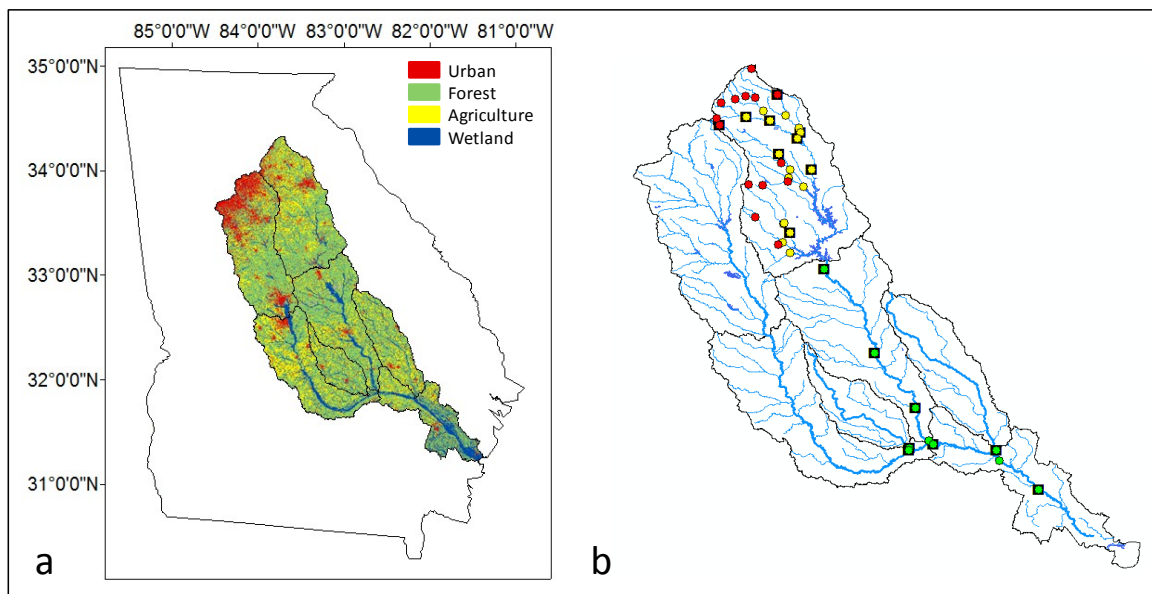


**Figure 6.1:** Map of Altamaha River (a) land use and (b) sample locations categorized by stream order. Red, yellow, and green circles note small, medium, and high stream orders, respectively. Black boxes note USGS monitoring stations.

When possible, 1 L samples were collected directly along the river banks in actively flowing sections of the rivers and placed into clean high-density polyethylene (HDPE) bottles. Otherwise, samples were collected by dispensing a 5-gallon bucket from a bridge followed by transfer to a clean HDPE bottle. This bucket was pre-rinsed three times with river water prior to sample collection. In all cases, HDPE bottles were pre-treated with 2 M HCl and 2 M NaOH for 24 hours each and rinsed with ultrapure water.

These bottles were also pre-rinsed three times with sample water prior to final collection. Samples were stored in the dark on ice during transport back to the laboratory.

All samples were filtered on the same day of collection (generally less than 12 hours) through a pre-combusted (500 °C, 5 hours) 0.7 µm Whatman glass fiber filter (GFF). DOM was further extracted from river samples using a solid phase extraction technique previously described by Dittmar, et al.<sup>38</sup>. Briefly, Agilent Bond Elut PPL cartridges were conditioned with methanol followed by ultra-pure water (pH 2). Roughly 1 liter of samplers were loaded onto the cartridge followed by another rinse with ultra pure water (pH 2). The cartridges were then dried under a stream of N<sub>2</sub> gas followed by elution of DOM in 10 mL of methanol and stored at -20 °C until further analysis. The extraction efficiency for these samples was 73 ± 8%.

### *6.3.2 Water Quality Analyses*

Surface water samples were collected and filtered on location for DOC and total dissolved nitrogen (TDN) analyses. Samples were filtered through pre-combusted 0.7 µm GFF filters and stored at 4 °C in the dark until further analysis. Samples for DOC determinations were acidified and purged to remove inorganic carbon followed by analysis on a Shimadzu TOC-V CSH total organic carbon analyzer. TOC quality control standards from ERA (Demand, WasteWarR, Lot#516) were used to determine accuracy and precision, which were 100.3%. TDN was analyzed with the ASTM D 5176-91 protocol (doi: 10.1520/D5176-91R03), which is the “Standard Test Method for Total Chemically Bound Nitrogen in Water by Pyrolysis and Chemiluminescence Detection”. Turbidity was measured on site with a LaMotte 2020 turbidimeter.

### *6.3.3 Optical Properties and Parallel Factor Analysis*

UV absorbance scans and fluorescence excitation-emission matrices (EEM) were collected simultaneously using an Aqualog (Horiba Scientific) equipped with a 150-W continuous output Xenon lamp. Fluorescence spectra were corrected for inner filter effects<sup>39</sup> and normalized to Raman scatter units. The specific UV absorbance (SUVA), calculated by dividing the absorbance at 254 nm by DOC concentration, was used as a representation of DOM aromaticity<sup>40</sup>. The humification index (HIX) was calculated as a ratio of the area of emission wavelengths 435-480/300-345 (excitation 254) and was used as a proxy for DOM complexity and condensed nature<sup>41</sup>. The biological index (BIX) was calculated as a ratio of emission wavelengths 380/430 (excitation 310) to indicate contributions of recently produced DOM<sup>42</sup>. The fluorescence index (FI), calculated as the ratio of emission wavelengths 470/520 (excitation 370) was used as an indicator for DOM of microbial origin<sup>43</sup>. EEMs were further characterized with parallel factor analysis (PARAFAC) as observed in Figure 6.2. The model was derived and split-half validated using the DrEEMs tool box<sup>44</sup> in Matlab 15b and PARAFAC components were compared with those logged within in the OpenFluor database. To minimize concentration effects, PARAFAC components are reported in relative abundance for each sample.

### *6.3.4 Ultra-High Resolution Mass Spectrometry*

Methanol extracts containing isolated DOM were diluted in 1:1 methanol/water to a final concentration of 5 mg C/l. Samples were analyzed by ultrahigh resolution mass spectrometry as described by Seidel, et al.<sup>45</sup> using a solariX XR FTICR-MS (Bruker Daltonik GmbH, Bremen, Germany) connected to a 15 Tesla superconducting magnet. Samples were infused into the electrospray source (ESI; Apollo II ion source, Bruker

Daltonik GmbH, Bremen, Germany) in negative mode at  $2 \mu\text{L min}^{-1}$ . 200 scans were collected with a mass window from 150 to 2000 Da. Molecular formulae above the detection limit<sup>46</sup> were assigned under the following constraints:  $^{12}\text{C}_{1-30} \text{}^{1}\text{H}_{1-200} \text{}^{16}\text{O}_{1-50} \text{}^{14}\text{N}_{0-4} \text{}^{32}\text{S}_{0-2} \text{}^{31}\text{P}_{0-1}$ . Molecular mass were removed for further analysis when detected in less than 3 samples. Samples were normalized to the sum of FTICR-MS signal intensities. A modified aromaticity index<sup>47-48</sup> and intensity weighted molar ratios calculated for each sample (Appendix 6.3). Molecular formulae were further categorized into molecular compound classes as described by Seidel, et al.<sup>45</sup> and are described as follows: (1)  $\text{AI}_{\text{mod}} > 0.67$ , less than 15 carbons, (2) condensed aromatics 15 or more carbons, (3) condensed aromatics compounds with heteroatoms, (4) polyphenols, (5), highly unsaturated compounds, (6) unsaturated aliphatics, (7), saturated fatty acids, (8) saturated fatty acids with heteroatoms, (9) carbohydrate-like, (10) carbohydrate-like with heteroatoms, and (11) peptide-like. Molecular compound classes are further presented as their relative intensity weighted contributions to each sample (Appendix 6.4).

### *6.3.5 Statistical Analysis and Land Use*

A geographical information systems (GIS) IMG data file containing Georgia land use information was obtained from the Georgia GIS Data Clearinghouse, which was originally provided by the National Resources Spatial Analysis Laboratory, University of Georgia. The initial land cover types were condensed to 4 major categories (urban, agriculture, forest, and wetlands, Figure 6.1a) and relative contributions of each land use type was calculated in ArcMap version 10.3. Land use at each sample location was derived as a function of the entire upstream catchment area.

JMP version 12.0 was primarily used for statistical applications. One way analysis of variance (ANOVA) followed by Tukey's honest significance difference (HSD) test were used to assess the variability and significance among variables distributed with respect to stream order. The Pearson's product-moment correlation coefficient ( $r$ ) was further used to assess the overall significance of a relationship between any two parameters. Percent urban land use, %C2, and turbidity measurements were log normalized to meet assumptions of a normal distribution. Redundancy analysis (RDA) was performed in XLSTAT to assess the spatial variability in DOM composition as a function of both land use and stream order. For RDA, PARAFAC and FTICR-MS data were constrained on the y-matrices with land use and stream order constrained to the x-matrices (predictor variables).

#### **6.4 Results**

Forty-two samples were collected throughout the Altamaha River watershed and separated into three groups based upon the Strahler stream order classification system<sup>37</sup>. These include low order streams (stream order 1-3,  $n = 14$ ), medium order small rivers (stream order 4-6,  $n = 17$ ), and high order rivers (stream order  $> 6$ ,  $n = 11$ ). Land use throughout the watershed was highly variable (Appendix 6.1, Figure 6.1a) consisting of both anthropogenic (urban:  $17.1\% \pm 14.5\%$ ; agriculture:  $54.5\% \pm 13.4\%$ ) and natural (forested:  $25.4\% \pm 9.4\%$ ; wetlands:  $6.10\% \pm 3.7\%$ ) sources. However, anthropogenic activity was generally highest in the upper watershed (Figure 6.1a; above lake Sinclair as displayed in Figure 5.1) averaging  $\sim 50\%$  of the relative land cover contributions compared to downstream samples (Figure 6.1a; below Lake Sinclair as displayed in

Figure 5.1) where anthropogenic activity was not as prominent, averaging ~32% of the respective activity in the lower watershed (Appendix 6.1).

Concurrent with land use trends, TDN was highest in the upper watershed and decreased along the river continuum (Appendix 6.2). This was coupled with a positive correlation between TDN and anthropogenic activity (urban:  $r = 0.54$ ,  $p < 0.01$ ; agriculture:  $r = 0.43$ ,  $p < 0.05$ ) compared to an inverse correlation observed between TDN and natural land covers (forest:  $r = -0.52$ ,  $p < 0.01$ ; wetland:  $r = -0.50$ ,  $p < 0.01$ ). In contrast, DOC increased along the river continuum and was very strongly correlated with increasing proportions of wetland cover ( $r = 0.78$ ,  $p < 0.01$ ) throughout the watershed. DOC concentrations however could not be linked to other land use regimes within this system.

While DOC quantitatively could only be linked to wetlands, DOC composition on the other hand could be linked to wetland cover and to other land use regimes as well. For instance, SUVA, which is generally an indicator of DOM aromaticity, increases along the river continuum with a positive correlation with wetland area ( $r = 0.51$ ,  $p < 0.01$ ) and an inverse correlation urban activity ( $r = -0.34$ ,  $p < 0.05$ ). The HIX, which gives a general indication of the degree of humification within the DOM pool, was also higher in the lower watershed with positive correlations to natural land cover (wetland:  $r = 0.85$ ,  $p < 0.01$ ; forest:  $r = 0.35$ ,  $p < 0.05$ ) and a negative correlation with urban land use ( $r = -0.53$ ,  $p < 0.01$ ). Other optical properties such as the BIX and FI, both of which are general indicators of increased microbial DOM sources, were highest in the upper watershed compared to SUVA and HIX (Appendix 6.2). The higher BIX in the upper watershed was coupled with a positive correlation with anthropogenic activity (urban:

$r = 0.38, p < 0.05$ ; agriculture:  $r = 0.32, p < 0.05$ ) and an inverse correlation with natural land cover (forest:  $r = -0.47, p < 0.01$ ; wetland:  $r = -0.58, p < 0.05$ ). Similarly, the FI was positively correlated to agricultural activity ( $r = 0.42, p < 0.05$ ) and inversely correlated to wetlands ( $r = -0.58, p < 0.01$ ).

A five component PARAFAC model was validated (Figure 6.2) with three terrestrial-like humic components (C1, C2, & C4), a microbial humic-like component (C3), and a protein-like component (C5). Clear spatial variation was observed among PARAFAC components (C1-C5) throughout the Altamaha River watershed. The relative abundance of the terrestrial components C2 and C4 were significantly enhanced in high stream order rivers (Tukey's HSD,  $p < 0.05$  for both C2 and C4) compared to small and medium order rivers upstream (Figure 6.3a,b), whereas microbial humic-like C3 and protein-like C5 were enriched in small and medium order rivers (Tukey's HSD,  $p < 0.05$  for both C3 and C5) compared to high order rivers downstream (Figure 6.3c,d). No significant difference was observed in the distribution of terrestrial humic like C1 among respective stream order categories (Tukey's HSD,  $p > 0.05$ ); however, C1 was still correlated to changes in land cover throughout the watershed (urban:  $r = -0.48, p < 0.01$ , wetlands:  $r = 0.56, p < 0.01$ ). Relative abundances of C2 and C4 were also positively correlated to wetlands (C2:  $r = 0.78, p < 0.01$ ; C4:  $r = 0.61, p < 0.01$ ) with C2 also positively correlated to forested areas ( $r = 0.36, p < 0.05$ ) and negatively correlated to urbanization ( $r = -0.48, p < 0.01$ ). While the relative contributions of microbial humic like C3 and protein-like C5 were both highest in the upper watershed, clear distinctions in source was observed as C3 was more closely linked to agricultural activity ( $r = 0.35,$



**Table 6.1:** Pearson's product-moment correlation coefficient (*r*) showing correlations between watershed land use with water quality parameters, EEM-PARAFAC components, and FTICR-MS molecular compound classes that are significant at  $p < 0.01$  and  $p < 0.05$ .

	Urban	Forest	Agriculture	Wetland
DOC	-	-	-	<b>0.79</b>
TDN	<b>0.54</b>	<b>-0.52</b>	<i>0.43</i>	<b>-0.50</b>
Turbidity	-	-	-	<b>0.88</b>
C1	<b>-0.48</b>	-	-	<b>0.56</b>
C2	<b>-0.47</b>	<i>0.37</i>	-	<b>0.78</b>
C3	-	-	<i>0.36</i>	<b>-0.45</b>
C4	-	-	-	<b>0.61</b>
C5	<b>0.50</b>	-	-	<b>-0.88</b>
BC CHO <C15	<b>-0.46</b>	<i>0.37</i>	-	<b>0.72</b>
BC CHO >=C15	<i>-0.40</i>	-	-	<b>0.74</b>
BC CHOX	<i>-0.32</i>	-	<i>0.40</i>	<b>0.49</b>
Polyphenols	<b>-0.49</b>	-	-	<b>0.78</b>
Highly unsaturated	-	-	-	<i>-0.36</i>
Unsaturated aliphatics	<i>0.36</i>	-	<i>0.31</i>	<b>-0.70</b>
Saturated FA CHO	-	-	-	-
Saturated FA CHOX	-	-	-	<b>-0.62</b>
Sugars CHO	-	-	-	-
Sugars CHOX	<i>0.38</i>	-	-	<i>-0.40</i>
Peptides	<i>0.37</i>	<i>-0.33</i>	<i>0.37</i>	<b>-0.71</b>
m/z <sub>w</sub>			<b>-0.53</b>	
C <sub>w</sub>			<b>-0.60</b>	
H <sub>w</sub>	<b>0.48</b>			<b>-0.78</b>
O <sub>w</sub>			<b>-0.44</b>	<i>0.38</i>
N <sub>w</sub>		<b>-0.47</b>	<b>0.65</b>	<b>-0.47</b>
S <sub>w</sub>	<b>0.47</b>	<i>-0.35</i>		<i>-0.31</i>
P <sub>w</sub>	<b>0.45</b>			<b>-0.51</b>
O/C <sub>w</sub>			<i>-0.31</i>	<b>0.45</b>
H/C <sub>w</sub>	<b>0.45</b>			<b>-0.82</b>
Almod <sub>w</sub>	<b>-0.46</b>			<b>0.78</b>
DBE <sub>w</sub>	<i>-0.36</i>		<i>-0.32</i>	<b>0.73</b>

$p < 0.05$ ) compared to C5 which was strongly correlated to urbanization ( $r = 0.50$ ,  $p < 0.01$ ).

Using FTICR-MS, we were able to identify 16,477 individual molecular formulae throughout the Altamaha River watershed. Individual samples in general contained *ca.* 6,500 to 9,500 detected molecular formulae and there was no significant difference in the number of molecular formula detected among low, medium, and high stream orders (ANOVA, Tukey's HSD,  $p > 0.05$ ). There were 3,698 molecular formulae ubiquitous to all samples and another 7,846 molecular formula that, while not ubiquitous in all samples, were detected in samples among all three stream order groups. Together, these molecular formulae represented on average *ca.* 99% of the relative intensity. To better assess compositional differences between samples, molecular formulae were assigned to molecular compound classes based upon their elemental ratios as defined by Seidel, et al.<sup>45</sup> (See methods section 6.3.4). The most significant differences in molecular composition between stream order groups were observed among peptides and unsaturated aliphatics, both of which had higher relative contributions in low and medium stream orders compared to high stream orders (ANOVA, Tukey's HSD,  $p < 0.05$ ; Figure 6.3g,h). On the other hand, polycondensed aromatics and polyphenols were more abundant in high stream orders compared to low and medium stream orders (ANOVA, Tukey's HSD,  $p < 0.05$ , Figure 6.3e,f). The compositional differences based on these compound classes, were highly related to land use. In particular, contributions from wetlands could significantly explain some of the degree of variability in 9 out of the 11 assigned molecular compound classes (Table 6.1). Compound classes representing highly aromatic compounds such as polycondensed aromatics and polyphenols were

positively correlated to wetlands (polycondensed aromatics:  $r = 0.74$ ,  $p < 0.01$ ; polyphenols:  $r = 0.78$ ,  $p < 0.01$ ) and inversely correlated to urbanization (polycondensed aromatics:  $r = -0.40$ ,  $p < 0.05$ ; polyphenols:  $r = -0.49$ ,  $p < 0.01$ ). Compound classes generally representing non-aromatic molecules and molecular formula containing heteroatoms however, were negatively correlated to natural land cover and were more associated with anthropogenic activity (Table 6.1). For instance, both unsaturated aliphatics and peptides were correlated to both urbanization (unsaturated aliphatics:  $r = 0.36$ ,  $p < 0.05$ ; peptides:  $r = 0.37$ ,  $p < 0.05$ ) and as well as agricultural activity (unsaturated aliphatics:  $r = 0.31$ ,  $p < 0.05$ ; peptides:  $r = 0.37$ ,  $p < 0.05$ ). Furthermore, the intensity weighted nitrogen average ( $N_w$ ) was positively correlated with agriculture ( $r = 0.65$ ,  $p < 0.01$ ) while the intensity weighted sulfur ( $S_w$ ) was positively correlated with urban land use ( $r = 0.47$ ,  $p < 0.01$ ).

## 6.5. Discussion

### 6.5.1 Identification of PARAFAC Components

PARAFAC components C1 and C2 are among the most ubiquitous components identified within aquatic environments and generally represent high molecular weight humic like compounds of terrestrial origin<sup>49-50</sup>. These components are routinely identified in a number of aquatic systems ranging from tropical and subtropical wetlands<sup>51-53</sup>, boreal lakes<sup>54</sup>, large arctic rivers<sup>55</sup> and coastal marine systems<sup>56-57</sup>. Of the 5 validated PARAFAC components identified in the Altamaha River, C4 was perhaps the most unique component as it has not been identified as robustly in aquatic systems compared to the other components, which is noted by a limited number matches within the OpenFluor database. However, components with similar spectral character have been

reported as terrestrially derived humic/fulvic acid like components<sup>49, 58</sup>. On the other hand, comparable (but not identical) components previously identified exhibiting similar broad range emission spectra observed with C4 have also been linked with DOM photochemistry suggesting these components may represent photo-products<sup>59</sup> and/or photo-refractory DOM components<sup>60</sup>.

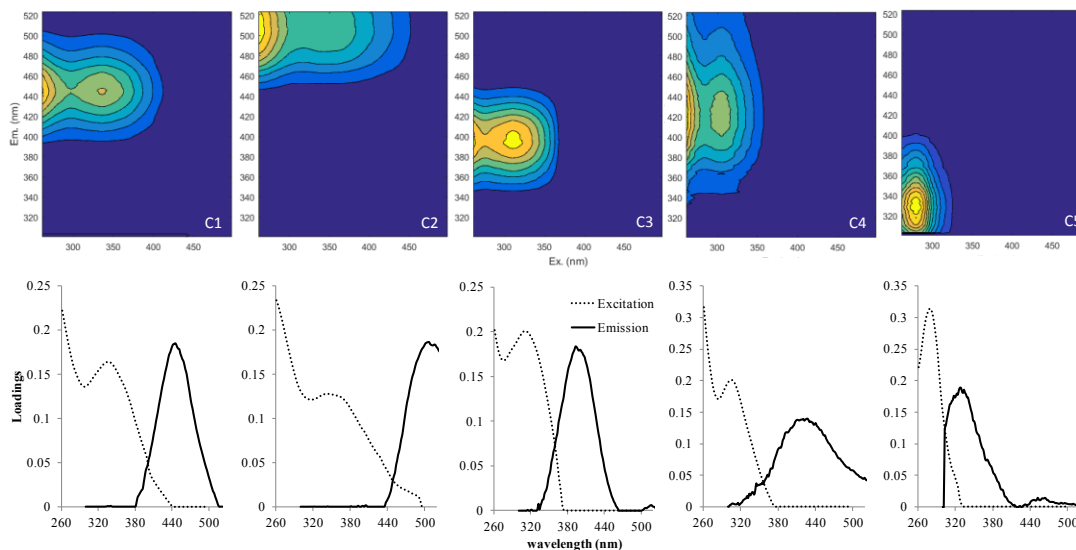


**Figure 6.2:** A 5-component PARAFAC model for the Altamaha River displaying 3 terrestrial humic like components (C1, C2, & C4), a microbial humic like component (C3) and protein-like component (C5). 3D-EEMs are displayed on the top row and loading plots are displayed on the bottom row.

The more blue-shifted C3 has been associated with lower molecular weight DOM derived from biological activity<sup>52, 61-62</sup> and has commonly been observed in wastewater and agriculturally impacted aquatic systems<sup>49, 63</sup>. Protein-like C5 is also commonly found in both terrestrial and marine environments<sup>64</sup> and has been routinely linked to autochthonous DOM sources and high bioavailability in watersheds with increasing anthropogenic activity<sup>33, 65-67</sup>.

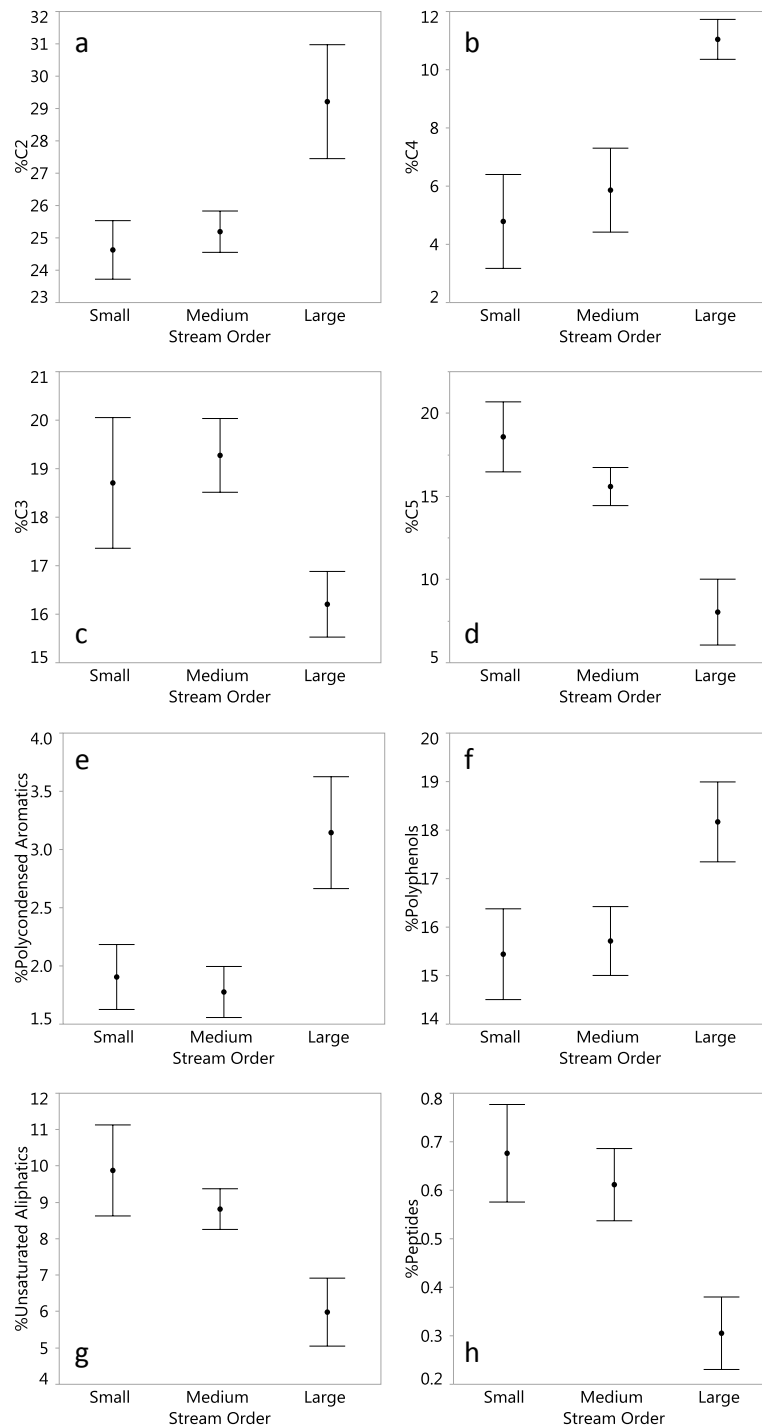


**Figure 6.3:** Distribution of EEM-PARAFAC components and FTICR-MS molecular compound classes as a function of stream in the Altamaha River. (a-b), terrestrial components C2 and C4, respectively (c-d) microbial and protein like components C3 and C5, respectively (e) condensed aromatic compounds, (f) polyphenols, (g) unsaturated aliphatics, and (h) peptides

### *6.5.2 Shifts in DOM Composition along the Altamaha River Continuum*

The River Continuum Concept (RCC) by definition was developed as a model to predict the fate of organic matter transported from headwaters to high order rivers. Its prediction is that detrital sources of organic matter fluctuate from heterotrophic environments (stream order 1-3) to autotrophic (stream order 4-6), and back to heterotrophic (stream order 7 and above). For DOC, considered part of the detrital OM pool, headwater streams will generate a molecularly complex, allochthonous pool of DOM. Downstream, molecular diversity decreases as larger rivers become increasingly disconnected from the terrestrial environment and in-situ stream processes remove selective labile components<sup>18</sup>. Since the incorporation of new analytical techniques for characterization of riverine DOM, specifically FTICR-MS, this concept has been recently revisited and there is agreement with the RCC that a more diverse set of molecular formula (as noted by the total number of molecular formulae detected) are observed in low order streams<sup>19</sup>. For the Altamaha River, we were unable to detect evidence for such molecular diversity changes, as the differences in the total number of molecular formula among low, medium, and high stream orders were statistically insignificant (ANOVA,  $p > 0.05$ ). However, while previous studies were focused on mainly undisturbed systems<sup>19</sup>, the Altamaha River watershed is quite different in that the upper headwaters is considered to be highly disturbed due to intense agricultural development and urbanization<sup>35</sup>. Because headwater streams are tightly connected to the terrestrial environment, their structure and function are likely to be highly vulnerable and disproportionately affected by increasing anthropogenic activity compared to higher order rivers<sup>68</sup>. For instance, urbanized headwaters are engineered to include significant

drainage networks and channelization, a process that may induce low order streams to behave more similarly to high order streams<sup>30</sup>. In addition, DOM composition in headwater streams have been found to be strongly influenced not only by urbanization, but also agricultural practices<sup>69-71</sup> and forest management<sup>26</sup>. Thus, we hypothesize that DOM sources and in-situ processing may be enhanced in anthropogenically impacted headwaters, which may further explain the lack of significant variability in molecular diversity observed along the Altamaha River continuum.

Because a high number of molecular formulas (11,544 of 16,455) were detected among all stream orders that represented a high proportion of the relative abundance (~99%), we further assessed the effects of stream order (i.e. the RCC) as a function of changes in DOM composition (EEM-PARAFAC and FTICR-MS compound classes) throughout the river continuum. The removal of labile components downstream as predicted by the RCC not only suggest that molecular diversity decreases downstream, but also suggest that DOM will become more refractory and less reactive during downstream transport<sup>18, 22</sup> which further indicate significant shifts in molecular composition downstream. For instance, Massicotte, et al.<sup>20</sup> indicated on a global scale that DOM becomes profoundly less reactive downstream as noted by decreases in DOM aromaticity (SUVA), which can likely be attributed to various degradation/removal processes as well as a diminished connectivity between aquatic systems and the surrounding terrestrial environment. However, we show clear trends of an increasingly aromatic DOM pool downstream as noted by significantly higher proportions of terrestrial humic-like PARAFAC components C2 and C4 coupled with higher proportions of polyphenols and polycondensed aromatic compounds in higher stream orders

compared to low and medium stream orders (Figure 6.3, ANOVA & Tukey's HSD,  $p < 0.05$  in all cases). This increased proportion of terrestrial material downstream is likely a function of a number of factors that may include a reoccurring source downstream (i.e. land use as discussed below) and/or a significant reduction in in-stream biogeochemical processes that are subject to remove highly aromatic compounds. For instance, DOM degradation from photochemical processes is likely to be reduced in the lower watershed due to higher turbidity (Appendix 6.2). However, with higher turbidity, it may be expected that a variety of DOM sorption process with mineral surfaces are enhanced<sup>14, 72-73</sup>, particularly in the Altamaha River where soils are rich with iron and contribute significantly to the particulate material<sup>74-75</sup>. However, the observed continuous input of highly aromatic, terrestrial-like material coupled with higher turbidity may also indicate that removal of high molecular weight DOM through sorption mechanisms may also be limited in this system with respect to increases in sources downstream.

On the contrary, in-stream processing may be enhanced in the upper Altamaha River watershed where lower turbidity may allow for greater photodegradation of aromatic DOM<sup>13</sup>. A combination of enhanced light availability from lower turbidity and higher nutrient loads from agricultural and urban areas in the upper watershed may also lead to higher contributions of microbial related processes (production/respiration) on DOM composition<sup>33-34, 76</sup>. This is noted with increased contributions of microbial humic like component C3 and protein like component C5 in the upper watershed along with a higher relative abundance of peptides and unsaturated aliphatic compounds as detected by FTICR-MS (Figure 6.3). There was no significant difference (ANOVA, Tukey's HSD,  $p < 0.05$ , Figure 6.3), however, between low and medium stream orders for these



molecular compound classes. It may be expected that higher tree cover would limit light availability in small order streams and in turn, limit photochemical processes and autotrophic activity. Thus, significant changes in DOM composition between small and medium order streams would have been hypothesized. However, tree cover decreases in anthropogenically impacted systems<sup>77</sup>, an observation which was also observed in the Altamaha River where tree cover for sampling locations within the small stream order group were highly variable (data not shown). Thus, the lack of a significant difference in molecular compound classes in low and medium stream orders may indicate to some degree a similar behavior in DOM sources and/or in-stream processing as enhanced anthropogenic activity may induce small order streams to behave more similarly to higher order streams<sup>30</sup>.

It is well understood that a variety of in-stream biogeochemical processes can have a significant impact on DOM composition<sup>12</sup>. However, the relative contributions of in-stream processing with stream order on DOM composition are not well understood. In some cases, stream order has shown to have little effect on predicting stream DOM composition<sup>78</sup>, whereas in others, clear processing and degradation of DOM has been observed along an increasing stream order gradient<sup>71, 79</sup>. For this study, we show clear compositional shifts in DOM composition with respect to increasing stream order indicating that in-stream processing of DOM (microbial/photochemical/etc) may have significant influence on DOM composition in the Altamaha River; however, the evident anthropogenic disturbances in the upper watershed (urban Atlanta, agricultural activity) likely contribute significantly to the quality of DOM exported downstream as well.

### 6.5.3 Land Use Controls on DOM Composition

General patterns show clear downstream shifts in DOM composition represented by a higher degree of aromaticity as noted by the enrichment of polycondensed aromatic and polyphenolic like compounds (Figure 6.3). The enrichment of this material could suggest that selective biologically labile material is removed or altered during downstream transport and/or a reduction in photochemical degradation potential with increasing turbidity in the lower watershed. Alternatively, this clear shift in composition may reflect a shift in DOM sources downstream. Longitudinal shifts in DOM quality have been linked to clear shifts in watershed land cover<sup>80</sup>, but more specifically to watershed connectivity with wetlands<sup>81-82</sup>. In the Mississippi River, loss of wetlands downstream generally resulted DOM becoming less aromatic in character<sup>83</sup>. In fact, wetlands are generally considered good predictors of DOC concentration<sup>84-85</sup> as well as DOM composition where a higher proportion of aromatic, humic like material are sourced from areas with high degrees of wetland cover<sup>29, 86</sup>. An enrichment of wetlands is observed in the lower Altamaha River watershed (Figure 6.1a; below Lake Sinclair as presented in Figure 5.1) where, in general, 10-15% of the land cover can be attributed to wetlands, whereas generally less than 6% wetland cover is observed in the upper watershed (Figure 6.1a, Appendix 6.1). Wetlands also appear to be good predictors of DOM composition in the Altamaha River as they can be significantly linked to the distribution of all 5 PARAFAC components as well as 9 of the 11 molecular compound classes established by FTICR-MS (Table 6.1). Consistent with other reports<sup>29, 83</sup>, it is evident that an enrichment of aromatic, humic like DOM is linked to the distribution of wetlands throughout the watershed as wetlands were positively correlated with humic

like PARAFAC components C1 ( $r = 0.56$ ,  $p < 0.01$ ), C2 ( $r = 0.78$ ,  $p < 0.01$ ), and C4 ( $r = 0.61$ ,  $p < 0.01$ ) as well MS groups representing condensed aromatic compounds ( $r = 0.74$ ,  $p < 0.01$ ) and polyphenols ( $r = 0.78$ ,  $p < 0.01$ )

On the contrary, in the upper watershed, anthropogenic activity is much more prominent compared to the lower watershed as noted by the presence of the Atlanta Metropolitan Area as well as an abundant display of agricultural activity (Figure 6.1a, Appendix 6.1). In the upper watershed, there is an enrichment of DOM that is more characteristically derived from autochthonous sources. This is notable with an enrichment of microbial humic like and protein like PARAFAC components C3 and C5 along with and enrichment in FTICR-MS molecular compound classes represented by unsaturated aliphatics and peptides (Figure 6.3). The enrichment of autochthonously derived DOM in both urban and agricultural areas has been linked to higher nutrient loads<sup>87-89</sup> which fuel primary productivity<sup>34</sup> and production of more bioavailable DOM<sup>33, 67, 71</sup>. In the Altamaha River, TDN concentrations are highest in the upper watershed with positive correlations to both urban ( $r = 0.54$ ,  $p < 0.01$ ) and agricultural activity ( $r = 0.43$ ,  $p < 0.05$ ) suggesting higher nutrient availability in these areas, which is consistent with other reports previously mentioned.

While higher TDN concentrations are evident in both urban and agricultural areas, it appears that each of these land cover types contributes individually with respect to DOM composition throughout the Altamaha River watershed. For instance, a positive correlation was observed between agriculture and microbial humic like PARAFAC component C3 ( $r = 0.36$ ,  $p < 0.05$ ), while no correlation was observed between C3 and urban activity ( $r = 0.19$ ,  $p > 0.05$ ). Clear distinctions between urban and agriculture in

relation to the identified FTICR-MS molecular compound classes was not observed as both urban and agriculture were positively correlated with both unsaturated aliphatics and peptides (Table 6.1). However, DOM derived from agricultural activity within the watershed can clearly be distinguished from urban activity due to an enrichment in N functionality ( $r = 0.65$ ,  $p < 0.01$ ) within the detected DOM molecular formulae, an observation consistent with a report by Wagner et al.<sup>90</sup> who suggested an enrichment of nitrogen globally within the DOM pool in watersheds influenced by high degrees of agricultural activity. Our results are generally consistent with other studies as well that suggest that agricultural activity enhances the export of dissolved organic nitrogen along with a greater contribution of autochthonously derived DOM<sup>66, 76</sup>. However, there is a need to recognize that the effects of agricultural land use on DOM composition is not completely clear as contrasting reports have also suggested that agriculturally impacted watersheds export a higher degree of aromatic, structurally complex material<sup>71, 91-92</sup>. Others however have reported that the relationship between DOM composition and agriculture is driven by seasonality where autochthonous DOM sources are enhanced at low river flow compared to an export of terrestrially derived DOM at high river flow<sup>93</sup>, an observation that is generally consistent globally irrespective of land use<sup>94</sup>. We note our sampling period occurred at the onset of the dry season and discharge conditions within the watershed were at baseflow. Thus, we hypothesize that the enrichment of autochthonous DOM in agricultural areas of the Altamaha River watershed are driven by the enhanced nutrient inputs within the upper watershed coupled with low flow conditions, which presumably increase light availability (due to low sediment resuspension) and autochthonous activity.

In urban areas of the catchment, DOM can be clearly distinguished from agriculturally influenced DOM due to an enrichment in protein-like PARAFAC component C5 ( $r = 0.50$ ,  $p < 0.01$ ). Small urban streams are particularly vulnerable to increasing eutrophication and autotrophic production as leaky sewer and septic systems release nutrients that are transported in the groundwater to headwater streams<sup>34, 95-96</sup>. Thus, higher contributions of protein-like fluorescence and autochthonously derived, low molecular weight DOM are often observed in urban-influenced streams<sup>33, 67, 97</sup>. However, high degrees of protein like fluorescence in wastewaters<sup>65</sup> further indicates the influence of humans as contributing sources of protein-like DOM in urban-influenced watersheds. We also note an enrichment of sulfur moieties within the DOM pool as a function of urban land use ( $r = 0.47$ ,  $p < 0.01$ ), a property of DOM that has been linked to wastewater treatment<sup>98</sup>. In some instances, addition of sulfate fertilizers as agricultural amendments have also been suggested to result in an enrichment of dissolved organic sulfur in agricultural systems<sup>99-100</sup>. However, the relationship with sulfur in the Altamaha River was limited to urban areas highlighting the influence of wastewater treatment and other potential point sources from the Atlanta region on DOM composition in this system.

#### *6.5.4 Spatial Variability in DOM Composition: Land Use vs Stream Order (RCC)*

The data presented in the previous sections show clear trends in DOM composition throughout the Altamaha River watershed relating to both stream order (RCC) and watershed land use. There are particularly evident shifts from autochthonously derived DOM in the anthropogenically impacted upper watershed (low stream orders) to more aromatic humic-like material present in the lower watershed (high stream order) where a natural land cover is more persistent. We used redundancy analysis

(RDA) to further integrate these two environmental drivers of DOM composition in order to assess the relative contributions of both land use and stream order on the spatial variability of DOM composition in the Altamaha River. For both EEM-PARAFAC (Figure 6.4) and FTICR-MS molecular compound classes (Figure 6.5), RDA generally confirmed trends previously discussed relating to spatial shifts in DOM compositions as functions of both stream order and land use. Using RDA, 57% of the total spatial variability of DOM composition represented by EEM-PARAFAC (Figure 6.4) can be explained as a combined function of stream order and land use as noted along RDA1 (51%) and RDA2 (6%). Of this 57% explained variability, we determined that land use contributed to a higher fraction of this variability (31%) compared to stream order (26%). Similarly, RDA could explain 45% of the spatial variability in DOM composition represented as FTICR-MS molecular compound classes (Figure 6.5), with land use again estimated at a higher contribution (25%) compared to stream order (20%).

RDA for PARAFAC components (Figure 6.4) displays a clear separation of natural and anthropogenic land use on RDA1. Low order urban streams cluster positively along RDA1 and negatively with RDA2 along with protein like C5 compared to agricultural streams which are displayed positively along both RDA1 and RDA2 along with microbial humic like C3. Conversely, a cluster of high stream order with wetlands negatively along RDA1 coupled with terrestrial humic like components C1, C2, and C4 also falling negatively along RDA1. There does appear however, to be a small degree of separation between high stream orders and wetlands along PC2 with C4 being more closely linked to high stream orders compared to C1 being linked more closely to natural land use. This observation may be further indication of ongoing in-stream processes

within the watershed as we have noted previously that C4 displays similar characteristics as fluorophores in other systems that have been linked to in-stream photochemical processes<sup>59-60</sup>. While DOM processing through photochemistry is expected to decrease in the lower watershed due to increasing turbidity, the association of C4 with higher stream order compared to land use indicates to a small extent that photochemical alteration of DOM in the lower Altamaha River watershed might still be pertinent.

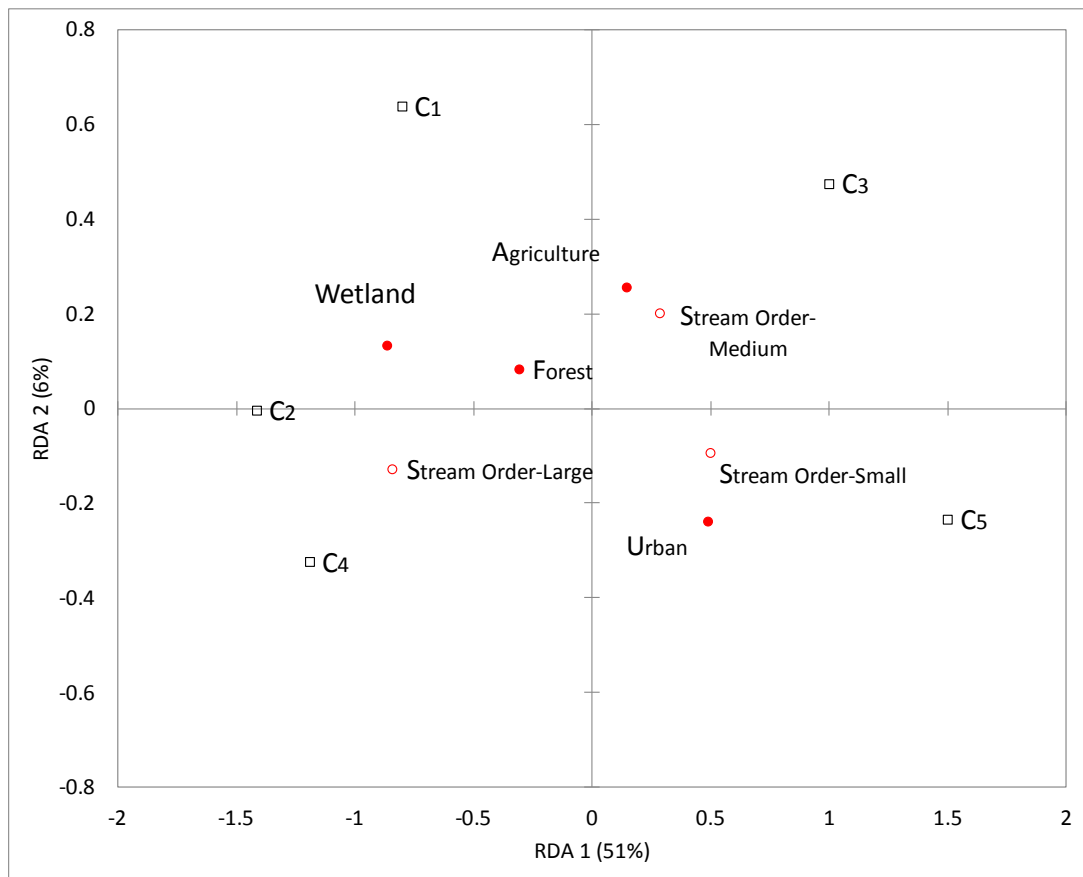


**Figure 6.4:** Redundancy analysis using stream order (i.e. RCC) and land use as predictor variables for the spatial distribution of EEM-PARAFAC components in the Altamaha River watershed. PARAFAC components are represented as open black boxes, stream order as open red circles, and land use as solid red circles.

Similar observations describing spatial distributions in DOM composition as defined by FTICR-MS were also observed using RDA. Highly aromatic terrestrial like material such as polycondensed aromatic compounds and polyphenols clustered positively along RDA1 in association to high stream orders and wetlands. Anthropogenic land use is clearly separated from natural land use where high urban activity is associated

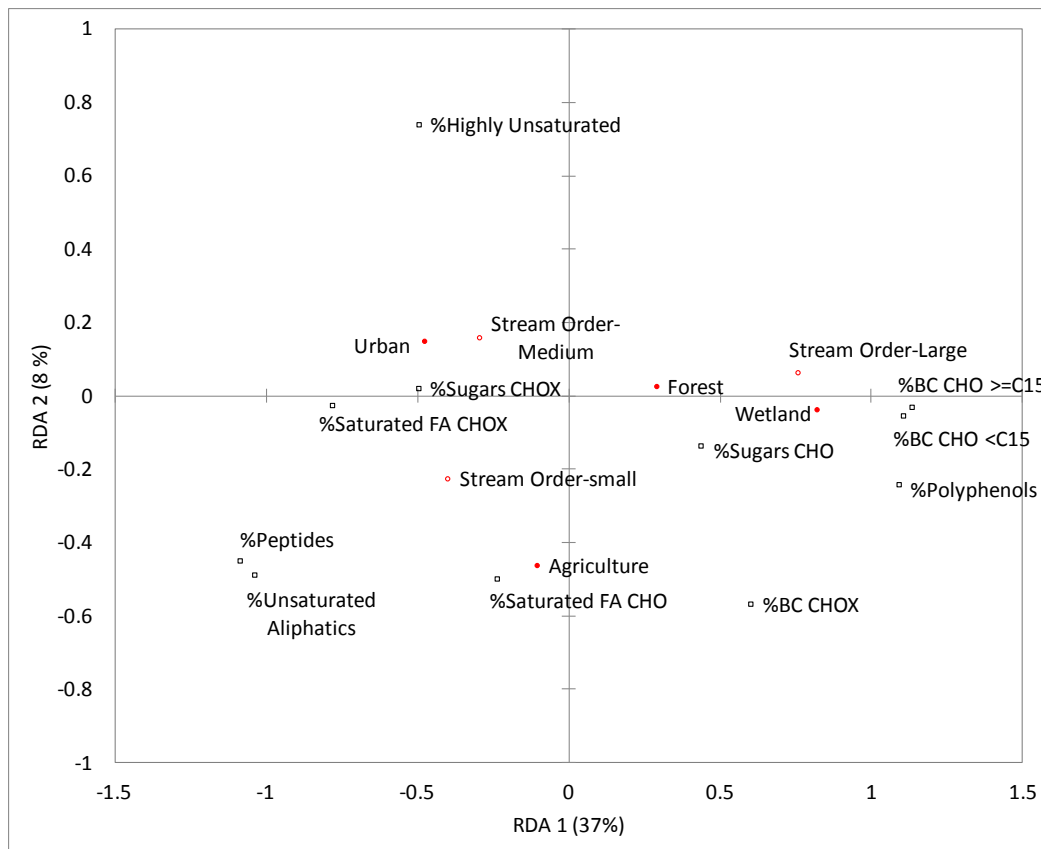


**Figure 6.5:** Redundancy analysis using stream order (i.e. RCC) and land use as predictor variables for the spatial distribution of FTICR-MS molecular compound classes in the Altamaha River watershed. FTICR-MS groups are represented as open black boxes, stream order as open red circles, and land use as solid red circles.

negatively on RDA1. Agricultural activity is further separated from urbanization along negative RDA2. Peptides and unsaturated aliphatics cluster negatively along both RDA1 and RDA2 indicating some links between both urban and agricultural activity. Saturated



fatty acids are mostly associated with small agricultural streams (Figure 6.5), an observation consistent with previous reports of higher proportions of fatty acids linked to agricultural soils<sup>101</sup>. Highly unsaturated compounds, which have been linked to lignin degradation products<sup>102</sup>, were more associated medium order urban streams. The presence of this material in medium size stream orders may indicate to some extent the degradation of lignin like material being transported within the upper watershed<sup>103</sup>.

We were able to show with RDA that a combination of both watershed land use and the traditional RCC could explain roughly 50% of the spatial variability of DOM composition in the Altamaha River watershed as described by both EEM-PARAFAC and FTICR-MS. Just as watershed land use has been described as good predictors of DOM composition in other systems<sup>83-85</sup>, it also explained a higher degree of variability in the Altamaha River watershed compared stream order, highlighting the need to further consider the controls of land use on DOM composition in future adaptations of the RCC. However, about 50% of the variability in the data remains unexplained within this system, which is likely related to other environmental drivers of DOM composition in fluvial networks. For instance, Kothawala, et al.<sup>78</sup> has suggested that land cover in boreal streams could explain 49% the observed DOM composition while an additional 8% could be explained by seasonality. Furthermore, water residence time, precipitation, and discharge (groundwater versus high flow), soil type and temperature have all also been linked to DOM composition in a variety of systems<sup>21, 71, 104-108</sup>. Thus, we would suspect that a portion of this remaining 50% of unexplained variability in DOM composition within the Altamaha River watershed could also be explained with soil dynamics and/or as a function of river hydrology.

The RCC has been used as a paradigm for decades to predict ecosystem function including the fate and transport of DOM from headwater streams along increasing flow paths during transport to coastal systems. However, the number of environmental factors that regulate fluvial ecosystem dynamics has led to a variety of adaptations to the RCC addressing both spatial and hydrological limitations within this concept. We have further shown in this study that land use also contributes significantly in respect to the RCC in predicting DOM composition in large, anthropogenically influenced watersheds. As DOM dynamics are unique and vary over both spatial and temporal scales, future research should continue to integrate both land use and other environmental drivers of DOM composition (i.e. seasonality, soil type) into traditional models such as the RCC in an effort to improve our understanding of DOM cycling in fluvial networks and continued response to on-going urban and agricultural development and climate change.

## 6.6 References

1. Cai, W.-J., Estuarine and coastal ocean carbon paradox: CO<sub>2</sub> sinks or sites of terrestrial carbon incineration? *Annu. Rev. Mar. Sci.* **2011**, *3* (1), 123-145.
2. Markager, S.; Stedmon, C.; Conan, P., Effects of DOM in marine ecosystems. In *Dissolved Organic Matter (DOM) in Aquatic Ecosystems: A study of European Catchments and Coastal Waters*, Søndergaard, M.; Thomas, D. N., Eds. 2004; pp 37-42.
3. Hader, D. P.; Helbling, E. W.; Williamson, C. E.; Worrest, R. C., Effects of UV radiation on aquatic ecosystems and interactions with climate change. *Photoch. Photobio. Sci.* **2011**, *10* (2), 242-260.
4. del Giorgio, P. A.; Williams, P., The global significance of respiration in aquatic ecosystems: from sing cells to the biosphere. In *Respiration in Aquatic Ecosystems*, Del Giorgio, P. A.; Williams, P., Eds. Oxford University Press: Oxford, 2005; pp 267-303.
5. Battin, T. J.; Kaplan, L. A.; Findlay, S.; Hopkinson, C. S.; Marti, E.; Packman, A. I.; Newbold, J. D.; Sabater, F., Biophysical controls on organic carbon fluxes in fluvial networks. *Nat. Geosci.* **2008**, *1*, 95-100.

6. Aiken, G. R.; Gilmour, C. C.; Krabbenhoft, D. P.; Orem, W., Dissolved organic matter in the Florida Everglades: implications for ecosystem restoration. *Crit. Rev. Env. Sci. Tec.* **2011**, *41* (Sup1), 217-248.
7. Raymond, P. A.; Hartmann, J.; Lauerwald, R.; Sobek, S.; McDonald, C.; Hoover, M.; Butman, D.; Striegl, R. G.; Mayorga, E.; Humborg, C.; Pirkko, K.; Dürr, H.; Meybeck, M.; Ciais, P.; Guth, P., Global carbon dioxide emissions from inland waters. *Nature* **2013**, *503*, 355-359.
8. Cole, J. J.; Prairie, Y. T.; Caraco, N. F.; McDowell, W. H.; Tranvik, L. J.; Striegl, R. G.; Duarte, C. M.; Kortelainen, P.; Downing, J. A.; Middelburg, J. J.; Melack, J., Plumbing the global carbon cycle: integrating inland waters into the terrestrial carbon budget. *Ecosystems* **2007**, *10* (1), 172-185.
9. Bianchi, T. S.; Filley, T.; Dria, K.; Hatcher, P. G., Temporal variability in sources of dissolved organic carbon in the lower Mississippi river. *Geochim. Cosmochim. Acta* **2004**, *68* (5), 959-967.
10. Hedges, J. I.; Cowie, G. L.; Richey, J. E.; Quay, P. D.; Benner, R.; Strom, M.; Forsberg, B. R., Origins and processing of organic matter in the Amazon River as indicated by carbohydrates and amino acids. *Limnol. Oceanogr.* **1994**, *39* (4), 743-761.
11. Massicotte, P.; Frenette, J.-J., Spatial connectivity in a large river system: resolving the sources and fate of dissolved organic matter. *Ecol. Appl.* **2011**, *21* (7), 2600-2617.
12. Kothawala, D. N.; Stedmon, C. A.; Müller, R. A.; Weyhenmeyer, G. A.; Köhler, S. J.; Tranvik, L. J., Controls of dissolved organic matter quality: evidence from a large-scale boreal lake survey. *Glob. Change Biol.* **2014**, *20* (4), 1101-1114.
13. Amon, R. M. W.; Benner, R., Photochemical and microbial consumption of dissolved organic carbon and dissolved oxygen in the Amazon River system. *Geochim. Cosmochim. Acta* **1996**, *60* (10), 1783-1792.
14. Philippe, A.; Schaumann, G. E., Interactions of dissolved organic matter with natural and engineered inorganic colloids: a review. *Environ. Sci. Technol.* **2014**, *48* (16), 8946-8962.
15. Yamashita, Y.; Jaffé, R., Characterizing the interactions between trace metals and dissolved organic matter using excitation–emission matrix and parallel factor analysis. *Environ. Sci. Technol.* **2008**, *42* (19), 7374-7379.
16. von Wachenfeldt, E.; Tranvik, L. J., Sedimentation in boreal lakes—the role of flocculation of allochthonous dissolved organic matter in the water column. *Ecosystems* **2008**, *11* (5), 803-814.

17. Amon, R. M. W.; Benner, R., Bacterial utilization of different size classes of dissolved organic matter. *Limnol. Oceanogr.* **1996**, *41* (1), 41-51.
18. Vannote, R. L.; Minshall, G. W.; Cummins, K. W.; Sedell, J. R.; Cushing, C. E., The river continuum concept. *Can. J. Fish. Aquat. Sci.* **1980**, *37* (1), 130-137.
19. Mosher, J.; Kaplan, L.; Podgorski, D.; McKenna, A.; Marshall, A., Longitudinal shifts in dissolved organic matter chemogeography and chemodiversity within headwater streams: a river continuum reprise. *Biogeochemistry* **2015**, *124* (1-3), 371-385.
20. Massicotte, P.; Asmala, E.; Stedmon, C.; Markager, S., Global distribution of dissolved organic matter along the aquatic continuum: Across rivers, lakes and oceans. *Sci. Total Environ.* **2017**, *609*, 180-191.
21. Weyhenmeyer, G. A.; Fröberg, M.; Karlton, E.; Khalili, M.; Kothawala, D.; Temnerud, J.; Tranvik, L. J., Selective decay of terrestrial organic carbon during transport from land to sea. *Glob. Change Biol.* **2012**, *18* (1), 349-355.
22. Creed, I. F.; McKnight, D. M.; Pellerin, B. A.; Green, M. B.; Bergamaschi, B. A.; Aiken, G. R.; Burns, D. A.; Findlay, S. E. G.; Shanley, J. B.; Striegl, R. G.; Aulenbach, B. T.; Clow, D. W.; Laudon, H.; McGlynn, B. L.; McGuire, K. J.; Smith, R. A.; Stackpoole, S. M., The river as a chemostat: fresh perspectives on dissolved organic matter flowing down the river continuum. *Can. J. Fish. Aquat. Sci.* **2015**, *72* (8), 1272-1285.
23. Ward, J. V.; Stanford, J. A., The serial discontinuity concept of lotic ecosystems. In *Dynamics of Lotic Ecosystems*, Fontain, T. D.; Bartell, S. M., Eds. Ann Arbor Science: Ann Arbor, 1983; pp 29-42.
24. Junk, J. W.; Bayley, P. B.; Sparks, R. E., The flood pulse concept in river flood plain systems. *Can. J. Fish. Aquat. Sci.* **1989**, *106*, 110-127.
25. Raymond, P. A.; Saiers, J. E.; Sobczak, W. V., Hydrological and biogeochemical controls on watershed dissolved organic matter transport: pulse-shunt concept. *Ecology* **2016**, *97* (1), 5-16.
26. Yamashita, Y.; Kloeppel, B. D.; Knoepp, J.; Zausen, G. L.; Jaffé, R., Effects of watershed history on dissolved organic matter characteristics in headwater streams. *Ecosystems* **2011**, *14* (7), 1110-1122.
27. Cawley, K. M.; Campbell, J.; Zwilling, M.; Jaffé, R., Evaluation of forest disturbance legacy effects on dissolved organic matter characteristics in streams at the Hubbard Brook Experimental Forest, New Hampshire. *Aquat. Sci.* **2014**, *76* (4), 611-622.

28. Foley, J. A.; DeFries, R.; Asner, G. P.; Barford, C.; Bonan, G.; Carpenter, S. R.; Chapin, F. S.; Coe, M. T.; Daily, G. C.; Gibbs, H. K.; Helkowski, J. H.; Holloway, T.; Howard, E. A.; Kucharik, C. J.; Monfreda, C.; Patz, J. A.; Prentice, I. C.; Ramankutty, N.; Snyder, P. K., Global consequences of land use. *Science* **2005**, *309* (5734), 570-574.
29. Lambert, T.; Teodoru, C. R.; Nyoni, F. C.; Bouillon, S.; Darchambeau, F.; Massicotte, P.; Borges, A. V., Along-stream transport and transformation of dissolved organic matter in a large tropical river. *Biogeosciences* **2016**, *13* (9), 2727-2741.
30. Elmore, A. J.; Kaushal, S. S., Disappearing headwaters: patterns of stream burial due to urbanization. *Front. Ecol. Environ.* **2008**, *6* (6), 308-312.
31. Groffman, P. M.; Boulware, N. J.; Zipperer, W. C.; Pouyat, R. V.; Band, L. E.; Colosimo, M. F., Soil nitrogen cycle processes in urban riparian zones. *Environ. Sci. Technol.* **2002**, *36* (21), 4547-4552.
32. Paul, M. J.; Meyer, J. L., Streams in the urban landscape. *Annu. Rev. Ecol. Syst.* **2001**, *32* (1), 333-365.
33. Parr, T. B.; Cronan, C. S.; Ohno, T.; Findlay, S. E. G.; Smith, S. M. C.; Simon, K. S., Urbanization changes the composition and bioavailability of dissolved organic matter in headwater streams. *Limnol. Oceanogr.* **2015**, *60* (3), 885-900.
34. Finlay, J. C., Stream size and human influences on ecosystem production in river networks. *Ecosphere* **2011**, *2* (8), 1-21.
35. Weston, N. B.; Hollibaugh, J. T.; Joye, S. B., Population growth away from the coastal zone: Thirty years of land use change and nutrient export in the Altamaha River, GA. *Sci. Total Environ.* **2009**, *407* (10), 3347-3356.
36. Schaefer, S. C.; Alber, M., Temporal and spatial trends in nitrogen and phosphorus inputs to the watershed of the Altamaha River, Georgia, USA. *Biogeochemistry* **2007**, *86* (3), 231-249.
37. Strahler, A. N., Quantitative analysis of watershed geomorphology. *Eos, Transactions American Geophysical Union* **1957**, *38* (6), 913-920.
38. Dittmar, T.; Koch, B.; Hertkorn, N.; Kattner, G., A simple and efficient method for the solid-phase extraction of dissolved organic matter (SPE-DOM) from seawater. *Limnol. Oceanogr-Meth.* **2008**, *6* (6), 230-235.
39. Ohno, T., Fluorescence inner-filtering correction for determining the humification index of dissolved organic matter. *Environ. Sci. Technol.* **2002**, *36* (4), 742-746.

40. Weishaar, J. L.; Aiken, G. R.; Bergamaschi, B. A.; Fram, M. S.; Fujii, R.; Mopper, K., Evaluation of specific ultraviolet absorbance as an indicator of the chemical composition and reactivity of dissolved organic carbon. *Environ. Sci. Technol.* **2003**, *37* (20), 4702-4708.
41. Zsolnay, A.; Baigar, E.; Jimenez, M.; Steinweg, B.; Saccomandi, F., Differentiating with fluorescence spectroscopy the sources of dissolved organic matter in soils subjected to drying. *Chemosphere* **1999**, *38* (1), 45-50.
42. Huguet, A.; Vacher, L.; Relexans, S.; Saubusse, S.; Froidefond, J. M.; Parlanti, E., Properties of fluorescent dissolved organic matter in the Gironde Estuary. *Org. Geochem.* **2009**, *40* (6), 706-719.
43. Jaffé, R.; McKnight, D.; Maie, N.; Cory, R.; McDowell, W. H.; Campbell, J. L., Spatial and temporal variations in DOM composition in ecosystems: The importance of long-term monitoring of optical properties. *J. Geophys. Res. Biogeosci.* **2008**, *113* (G4), doi: 10.1029/2008JG000683.
44. Murphy, K. R.; Stedmon, C. A.; Graeber, D.; Bro, R., Fluorescence spectroscopy and multi-way techniques. PARAFAC. *Anal. Methods.* **2013**, *5*, 6557-6566.
45. Seidel, M.; Beck, M.; Riedel, T.; Waska, H.; Suryaputra, I. G. N. A.; Schnetger, B.; Niggemann, J.; Simon, M.; Dittmar, T., Biogeochemistry of dissolved organic matter in an anoxic intertidal creek bank. *Geochim. Cosmochim. Acta* **2014**, *140* (Supplement C), 418-434.
46. Riedel, T.; Dittmar, T., A method detection limit for the analysis of natural organic matter via Fourier Transform Ion Cyclotron Resonance Mass Spectrometry. *Anal. Chem.* **2014**, *86* (16), 8376-8382.
47. Koch, B. P.; Dittmar, T., From mass to structure: an aromaticity index for high-resolution mass data of natural organic matter. *Rapid Commun. Mass. Sp.* **2016**, *30* (1), 250-250.
48. Koch, B. P.; Dittmar, T., From mass to structure: an aromaticity index for high-resolution mass data of natural organic matter. *Rapid Commun. Mass. Sp.* **2006**, *20* (5), 926-932.
49. Stedmon, C. A.; Markager, S., Resolving the variability in dissolved organic matter fluorescence in a temperate estuary and its catchment using PARAFAC analysis. *Limnol. Oceanogr.* **2005**, *50* (2), 686-697.
50. Coble, P. G.; Del Castillo, C. E.; Avril, B., Distribution and optical properties of CDOM in the Arabian Sea during the 1995 Southwest Monsoon. *Deep Sea Res. Part II Top. Stud. Oceanogr.* **1998**, *45* (10), 2195-2223.

51. Cawley, K. M.; Wolski, P.; Mladenov, N.; Jaffé, R., Dissolved organic matter biogeochemistry along a transect of the Okavango Delta, Botswana. *Wetlands* **2012**, *32* (3), 475-486.
52. Yamashita, Y.; Scinto, L. J.; Maie, N.; Jaffé, R., Dissolved organic matter characteristics across a subtropical wetland's landscape: application of optical properties in the assessment of environmental dynamics. *Ecosystems* **2010**, *13* (7), 1006-1019.
53. Zurbrügg, R.; Suter, S.; Lehmann, M. F.; Wehrli, B.; Senn, D. B., Organic carbon and nitrogen export from a tropical dam-impacted floodplain system. *Biogeosciences* **2013**, *10* (1), 23-38.
54. Kellerman, A. M.; Kothawala, D. N.; Dittmar, T.; Tranvik, L. J., Persistence of dissolved organic matter in lakes related to its molecular characteristics. *Nature Geosci.* **2015**, *8* (6), 454-457.
55. Walker, S. A.; Amon, R. M. W.; Stedmon, C. A., Variations in high-latitude riverine fluorescent dissolved organic matter: A comparison of large Arctic rivers. *J. Geophys. Res. Biogeosci.* **2013**, *118* (4), 1689-1702.
56. Cawley, K. M.; Ding, Y.; Fourqurean, J.; Jaffé, R., Characterising the sources and fate of dissolved organic matter in Shark Bay, Australia: a preliminary study using optical properties and stable carbon isotopes. *Mar. Freshw. Res.* **2012**, *63* (11), 1098-1107.
57. Jørgensen, L.; Stedmon, C. A.; Kragh, T.; Markager, S.; Middelboe, M.; Søndergaard, M., Global trends in the fluorescence characteristics and distribution of marine dissolved organic matter. *Mar. Chem.* **2011**, *126* (1-4), 139-148.
58. Cory, R. M.; McKnight, D. M., Fluorescence spectroscopy reveals ubiquitous presence of oxidized and reduced quinones in dissolved organic matter. *Environ. Sci. Technol.* **2005**, *39* (21), 8142-8149.
59. Stedmon, C. A.; Markager, S.; Tranvik, L.; Kronberg, L.; Slätis, T.; Martinsen, W., Photochemical production of ammonium and transformation of dissolved organic matter in the Baltic Sea. *Mar. Chem.* **2007**, *104* (3), 227-240.
60. Chen, M.; Jaffé, R., Photo- and bio-reactivity patterns of dissolved organic matter from biomass and soil leachates and surface waters in a subtropical wetland. *Water Res.* **2014**, *61*, 181-190.
61. Yamashita, Y.; Jaffé, R.; Maie, N.; Tanoue, E., Assessing the dynamics of dissolved organic matter (DOM) in coastal environments by excitation emission matrix fluorescence and parallel factor analysis (EEM-PARAFAC). *Limnol. Oceanogr.* **2008**, *53* (5), 1900-1908.

62. Stedmon, C. A.; Markager, S.; Bro, R., Tracing dissolved organic matter in aquatic environments using a new approach to fluorescence spectroscopy. *Mar. Chem.* **2003**, *82* (3–4), 239-254.
63. Fellman, J. B.; Hood, E.; Spencer, R. G. M., Fluorescence spectroscopy opens new windows into dissolved organic matter dynamics in freshwater ecosystems: A review. *Limnol. Oceanogr.* **2010**, *55* (6), 2452-2462.
64. Jaffé, R.; Cawley, K. M.; Yamashita, Y., Applications of excitation emission matrix fluorescence with parallel factor analysis (EEM-PARAFAC) in assessing environmental dynamics of natural dissolved organic matter (DOM) in aquatic environments: a review. In *Advances In the Physicochemical Characterization of Dissolved Organic Matter: Impact on Natural and Engineered Systems*, Rosario-Ortiz, F., Ed. American Chemical Society: 2014; pp 22-73.
65. Baker, A.; Inverarity, R., Protein-like fluorescence intensity as a possible tool for determining river water quality. *Hydrol. Process.* **2004**, *18* (15), 2927-2945.
66. Williams, C. J.; Yamashita, Y.; Wilson, H. F.; Jaffé, R.; Xenopoulos, M. A., Unraveling the role of land use and microbial activity in shaping dissolved organic matter characteristics in stream ecosystems. *Limnol. Oceanogr.* **2010**, *55* (3), 1159-1171.
67. Hosen, J. D.; McDonough, O. T.; Febria, C. M.; Palmer, M. A., Dissolved organic matter quality and bioavailability changes across an urbanization gradient in headwater streams. *Environ. Sci. Technol.* **2014**, *48* (14), 7817-7824.
68. Hynes, H., The stream and its valley. *Verh. Internat. Verein. Limnol.* **1975**, *19*, 1-15.
69. Lu, Y. H.; Bauer, J. E.; Canuel, E. A.; Chambers, R. M.; Yamashita, Y.; Jaffé, R.; Barrett, A., Effects of land use on sources and ages of inorganic and organic carbon in temperate headwater streams. *Biogeochemistry* **2014**, *119* (1), 275-292.
70. Lu, Y.; Bauer, J. E.; Canuel, E. A.; Yamashita, Y.; Chambers, R. M.; Jaffé, R., Photochemical and microbial alteration of dissolved organic matter in temperate headwater streams associated with different land use. *J. Geophys. Res. Biogeosci.* **2013**, *118* (2), 566-580.
71. Shang, P.; Lu, Y.; Du, Y.; Jaffé, R.; Findlay, R. H.; Wynn, A., Climatic and watershed controls of dissolved organic matter variation in streams across a gradient of agricultural land use. *Sci. Total Environ.* **2018**, *612*, 1442-1453.
72. Kothawala, D. N.; Roehm, C.; Blodau, C.; Moore, T. R., Selective adsorption of dissolved organic matter to mineral soils. *Geoderma* **2012**, *189–190*, 334-342.
73. Du, Y.; Ramirez, C. E.; Jaffé, R., Fractionation of dissolved organic matter by coprecipitation with iron: effects of composition. *Environ. Process.* **2018**, *5* (1), 5-21.



74. Bhatti, A. M.; Rundquist, D.; Schalles, J.; Ramirez, L.; Nasu, S., A comparison between above-water surface and subsurface spectral reflectances collected over inland waters. *Geocarto Int.* **2009**, *24* (2), 133-141.
75. Shi, W.; Sun, M.-Y.; Molina, M.; Hodson, R. E., Variability in the distribution of lipid biomarkers and their molecular isotopic composition in Altamaha estuarine sediments: implications for the relative contribution of organic matter from various sources. *Org. Geochem.* **2001**, *32* (4), 453-467.
76. Wilson, H. F.; Xenopoulos, M. A., Effects of agricultural land use on the composition of fluvial dissolved organic matter. *Nature Geosci.* **2008**, *2* (1), 37-41.
77. Nowak, D. J.; Greenfield, E. J., Tree and impervious cover change in U.S. cities. *Urban For. Urban Gree.* **2012**, *11* (1), 21-30.
78. Kothawala, D. N.; Ji, X.; Laudon, H.; Ågren, A. M.; Futter, M. N.; Köhler, S. J.; Tranvik, L. J., The relative influence of land cover, hydrology, and in-stream processing on the composition of dissolved organic matter in boreal streams. *J. Geophys. Res. Biogeosci.* **2015**, *120* (8), 1491-1505.
79. Hutchins, R. H. S.; Aukes, P.; Schiff, S. L.; Dittmar, T.; Prairie, Y. T.; del Giorgio, P. A., The optical, chemical, and molecular dissolved organic matter succession along a boreal soil-stream-river continuum. *J. Geophys. Res. Biogeosci.* **2017**, *122* (11), 2892-2908.
80. Ward, N. D.; Krusche, A. V.; Sawakuchi, H. O.; Brito, D. C.; Cunha, A. C.; Moura, J. M. S.; da Silva, R.; Yager, P. L.; Keil, R. G.; Richey, J. E., The compositional evolution of dissolved and particulate organic matter along the lower Amazon River—Óbidos to the ocean. *Mar. Chem.* **2015**, *177*, 244-256.
81. Battin, T. J., Dissolved organic matter and its optical properties in a blackwater tributary of the upper Orinoco river, Venezuela. *Org. Geochem.* **1998**, *28* (9), 561-569.
82. Mladenov, N.; McKnight, D. M.; Macko, S. A.; Norris, M.; Cory, R. M.; Ramberg, L., Chemical characterization of DOM in channels of a seasonal wetland. *Aquat. Sci.* **2007**, *69* (4), 456-471.
83. Duan, S.; He, Y.; Kaushal, S. S.; Bianchi, T. S.; Ward, N. D.; Guo, L., Impact of wetland decline on decreasing dissolved organic carbon concentrations along the Mississippi River continuum. *Front. Mar. Sci.* **2017**, *3* (280), doi: 10.3380/fmars.2016.00280.
84. Gergel, S. E.; Turner, M. G.; Kratz, T. K., Dissolved organic carbon as an indicator of the scale of watershed influence on lakes and rivers. *Ecol. Appl.* **1999**, *9* (4), 1377-1390.

85. D'Amore, D. V.; Edwards, R. T.; Biles, F. E., Biophysical controls on dissolved organic carbon concentrations of Alaskan coastal temperate rainforest streams. *Aquat. Sci.* **2016**, *78* (2), 381-393.
86. Hanley, K. W.; Wollheim, W. M.; Salisbury, J.; Huntington, T.; Aiken, G., Controls on dissolved organic carbon quantity and chemical character in temperate rivers of North America. *Global Biogeochem. Cycles* **2013**, *27* (2), 492-504.
87. Carpenter, S. R.; Caraco, N. F.; Correll, D. L.; Howarth, R. W.; Sharpley, A. N.; Smith, V. H., Nonpoint pollution of surface waters with phosphorus and nitrogen. *Ecol. Appl.* **1998**, *8* (3), 559-568.
88. Kaushal, S. S.; Belt, K. T., The urban watershed continuum: evolving spatial and temporal dimensions. *Urban Ecosyst.* **2012**, *15* (2), 409-435.
89. Fuß, T.; Behounek, B.; Ulseth, A. J.; Singer, G. A., Land use controls stream ecosystem metabolism by shifting dissolved organic matter and nutrient regimes. *Freshw. Biol.* **2017**, *62* (3), 582-599.
90. Wagner, S.; Riedel, T.; Niggemann, J.; Vähätalo, A. V.; Dittmar, T.; Jaffé, R., Linking the molecular signature of heteroatomic dissolved organic matter to watershed characteristics in world rivers. *Environ. Sci. Technol.* **2015**, *49* (23), 13798-13806.
91. Graeber, D.; Gelbrecht, J.; Pusch, M. T.; Anlanger, C.; von Schiller, D., Agriculture has changed the amount and composition of dissolved organic matter in Central European headwater streams. *Sci. Total Environ.* **2012**, *438*, 435-446.
92. Eckard, R. S.; Pellerin, B. A.; Bergamaschi, B. A.; Bachand, P. A. M.; Bachand, S. M.; Spencer, R. G. M.; Hernes, P. J., Dissolved organic matter compositional change and biolability during two storm runoff events in a small agricultural watershed. *J. Geophys. Res. Biogeosci.* **2017**, doi: 10.1002/2017JG003935.
93. Hu, Y.; Lu, Y.; Edmonds, J. W.; Liu, C.; Wang, S.; Das, O.; Liu, J.; Zheng, C., Hydrological and land use control of watershed exports of dissolved organic matter in a large arid river basin in northwestern China. *J. Geophys. Res. Biogeosci.* **2016**, *121* (2), 466-478.
94. Spencer, R. G. M.; Hernes, P. J.; Dinga, B.; Wabakanghanzi, J. N.; Drake, T. W.; Six, J., Origins, seasonality, and fluxes of organic matter in the Congo River. *Global Biogeochem. Cycles* **2016**, *30* (7), 1105-1121.
95. Kaushal, S. S.; Lewis Jr, W. M.; McCutchan Jr, J. H., Land use change and nitrogen enrichment of a rocky mountain watershed. *Ecol. Appl.* **2006**, *16* (1), 299-312.
96. Kaushal, S. S.; Groffman, P. M.; Band, L. E.; Elliott, E. M.; Shields, C. A.; Kendall, C., Tracking nonpoint source nitrogen pollution in human-impacted watersheds. *Environ. Sci. Technol.* **2011**, *45* (19), 8225-8232.

97. McElmurry, S. P.; Long, D. T.; Voice, T. C., Stormwater dissolved organic matter: influence of land cover and environmental factors. *Environ. Sci. Technol.* **2014**, *48* (1), 45-53.
98. Gonsior, M.; Zwartjes, M.; Cooper, W. J.; Song, W.; Ishida, K. P.; Tseng, L. Y.; Jeung, M. K.; Rosso, D.; Hertkorn, N.; Schmitt-Kopplin, P., Molecular characterization of effluent organic matter identified by ultrahigh resolution mass spectrometry. *Water Res.* **2011**, *45* (9), 2943-2953.
99. Hertkorn, N.; Harir, M.; Cawley, K. M.; Schmitt-Kopplin, P.; Jaffé, R., Molecular characterization of dissolved organic matter from subtropical wetlands: a comparative study through the analysis of optical properties, NMR and FTICR/MS. *Biogeosciences* **2016**, *13* (8), 2257-2277.
100. Poulin, B. A.; Ryan, J. N.; Nagy, K. L.; Stubbins, A.; Dittmar, T.; Orem, W.; Krabbenhoft, D. P.; Aiken, G. R., Spatial dependence of reduced sulfur in Everglades dissolved organic matter controlled by sulfate enrichment. *Environ. Sci. Technol.* **2017**, *51* (7), 3630-3639.
101. Jandl, G.; Leinweber, P.; Schulten, H.-R.; Ekschmitt, K., Contribution of primary organic matter to the fatty acid pool in agricultural soils. *Soil Biol. Biochem.* **2005**, *37* (6), 1033-1041.
102. Stenson, A. C.; Marshall, A. G.; Cooper, W. T., Exact masses and chemical formulas of individual Suwannee River fulvic acids from Ultrahigh Resolution Electrospray Ionization Fourier Transform Ion Cyclotron Resonance Mass Spectra. *Anal. Chem.* **2003**, *75* (6), 1275-1284.
103. Spencer, R. G. M.; Stubbins, A.; Hernes, P. J.; Baker, A.; Mopper, K.; Aufdenkampe, A. K.; Dyda, R. Y.; Mwamba, V. L.; Mangangu, A. M.; Wabakanghanzi, J. N.; Six, J., Photochemical degradation of dissolved organic matter and dissolved lignin phenols from the Congo River. *J. Geophys. Res. Biogeosci.* **2009**, *114* (G3), doi: 10.1029/2009JG000968.
104. Kellerman, A. M.; Dittmar, T.; Kothawala, D. N.; Tranvik, L. J., Chemodiversity of dissolved organic matter in lakes driven by climate and hydrology. *Nat. Commun.* **2014**, *5*, doi: 10.1038/ncomms4804.
105. Spencer, R. G. M.; Hernes, P. J.; Ruf, R.; Baker, A.; Dyda, R. Y.; Stubbins, A.; Six, J., Temporal controls on dissolved organic matter and lignin biogeochemistry in a pristine tropical river, Democratic Republic of Congo. *J. Geophys. Res. Biogeosci.* **2010**, *115* (G3), doi: 10.1029/2009JG001180.

106. Inamdar, S.; Singh, S.; Dutta, S.; Levia, D.; Mitchell, M.; Scott, D.; Bais, H.; McHale, P., Fluorescence characteristics and sources of dissolved organic matter for stream water during storm events in a forested mid-Atlantic watershed. *J. Geophys. Res. Biogeosci.* **2011**, *116* (G3), doi: 10.1029/2011JG001735.
107. Fellman, J. B.; Hood, E.; Edwards, R. T.; D'Amore, D. V., Changes in the concentration, biodegradability, and fluorescent properties of dissolved organic matter during stormflows in coastal temperate watersheds. *J. Geophys. Res. Biogeosci.* **2009**, *114* (G1), doi: 10.1029/2008JG000790.
108. Yamashita, Y.; Maie, N.; Briceño, H.; Jaffé, R., Optical characterization of dissolved organic matter in tropical rivers of the Guayana Shield, Venezuela. *J. Geophys. Res. Biogeosci.* **2010**, *115* (G1), doi: 10.1029/2009JG0009987.

## CHAPTER VII

## CONCLUSIONS

In coming decades, the production of black carbon (BC) is expected to increase with projections of more frequent, high impact wildfires as a response to on-going climate change trends. While a majority of this material will likely be sequestered in soils over millennial scales, oxidation of particulate charcoal over much shorter time scales induces the release and transport of dissolved BC (DBC) in fluvial systems. Soil microbial processes have been previously recognized as a primary mechanism for BC oxidation. However, incubation experiments suggests that photodissolution of particulate charcoal may be a previously unrecognized source of DBC to aquatic systems. The global contributions of photodissolution as a source of DBC are still unknown, and future studies should continue to derive the relative contributions with respect to soil microbial oxidation processes.

While photodissolution of particulate charcoal may be a considerable source of DBC, photochemical degradation has also been identified as a pertinent sink for more polycondensed DBC fractions. Systems with high light availability display a less polycondensed signature compared to other regions where light is attenuated with a high presence of chromophoric dissolved organic matter. In contrast, rivers with high turbidity and particulates largely comprised of metal oxide complexes also displayed a less polycondensed DBC signature, suggesting in-situ reactions with metal complexes may also be sinks for more polycondensed DBC fractions. The ultimate fate of DBC within these systems is quite diverse as photodegradation of DBC may lead to production of more biologically labile constituents as well as evasion of CO<sub>2</sub> from aquatic systems; whereas, the removal of DBC through co-precipitation mechanisms with iron oxides may further lead to the sequestration and burial of BC in riverine and ocean sediments. Thus,

in-stream biogeochemical processing of DBC likely affects the long-term reactivity and may have significant implications for global cycling of DBC.

Mobilization of BC is complex and likely involves a number of factors. However, mobilization of particulate BC (PBC) under high flow regimes is apparent, and in some instances, sources of PBC under low flow regimes at the mouth of a river may be linked to tidal influences and fire history in coastal regions. On the other hand, the release of DBC from soils has been linked to seasonal discharge regimes where flushing of organic rich soils during high discharge events enrich DBC in fluvial systems. While groundwater is expected to transport less polycondensed DBC fractions, this may not be a ubiquitous case as groundwater may also transport DBC with sources characteristic of older deep soil chars in some systems. DBC exported from a large watershed during high flow regimes however displayed a signature characteristic of anthropogenically derived sources and was connected to seasonal high intensity precipitation events in urban and agricultural areas. Thus, the need to further relate the controls of both land use and seasonal hydrology on DBC export to coastal systems is warranted.

DBC composition was significantly impacted by watershed land use. In urban and agricultural areas, DBC was less polycondensed and lower in molecular weight compared to DBC sources from natural wetlands. Furthermore, the incorporation of both nitrogen and sulfur within DBC could be linked to anthropogenic activity. In particular, DBC from agricultural systems was enriched with sulfur suggesting the burning of agricultural areas with sulfate amendments may lead to an enrichment of dissolved black sulfur (DBS). Similarly, dissolved black nitrogen (DBN) was strongly linked with anthropogenic activity and is likely derived from the use of fertilizers and burning of farmlands. The

impact of DBN and DBS on pyrogenic carbon reactivity and transport in fluvial systems is relatively unknown, however it is expected that downstream transport of DBN and DBS may have significant implications for both carbon and nutrient cycling.

Similarly, the controls of land use were shown to significantly influence bulk dissolved organic matter (DOM) composition with an enrichment of highly aromatic terrestrial-like material from areas with of more natural influence compared to areas of high anthropogenic activity where an enrichment of autochthonous-like DOM was observed. The coupling of land use with stream order as a proxy for the River Continuum Concept (RCC) could explain roughly 50% of the spatial variability in DOM composition in a watershed with anthropogenically impacted headwaters. While paradigms such as the RCC have been historically used to predict DOM composition along a river continuum, the need to incorporate other environmental controls of DOM composition, such as land use, into these paradigms is highlighted.

With an increasing number of fires across the global landscape and natural systems being converted for anthropogenic purposes, sources and transformations of both DBC and bulk DOM are expected to follow and are likely to have significant implications for fluvial ecosystem functions, aquatic food web dynamics, and carbon and nutrient cycling. While a better understanding of DBC export has been achieved in recent years, a number of questions as previously mentioned still remain. The relative global contributions of photodissolution as a source of DBC to aquatic systems are still to be determined. Shifts in land use can significantly alter DBC composition; however, methods to directly quantify the contributions of DBN and DBS are still unavailable and thus, fluxes of these components from fluvial to coastal systems are unknown. It is also



apparent that a number of environmental controls can influence both DBC and bulk DOM composition, and there is still a need to integrate these controls to provide the most accurate assessments in predicting both DOM and DBC composition in fluvial networks. Addressing these knowledge gaps will better assist in the ultimate goals of constraining BC budgets and understanding the role of BC in global carbon cycling.

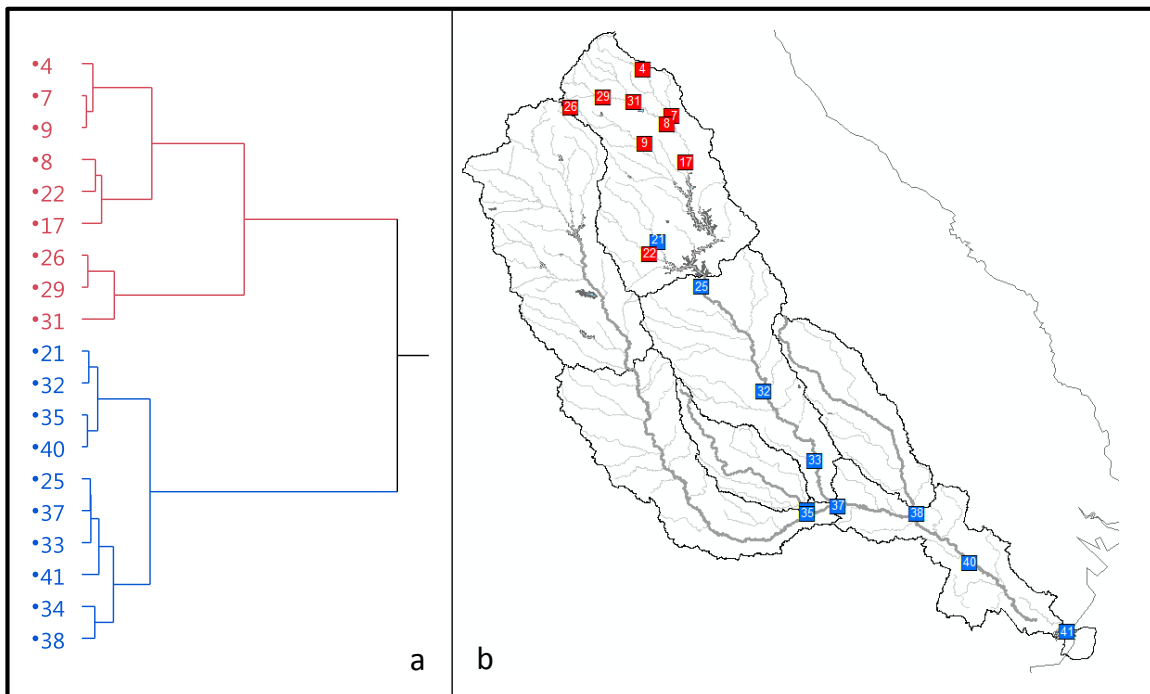
## APPENDICES

**Appendix 4.1: Altamaha River monthly sampling information and data**

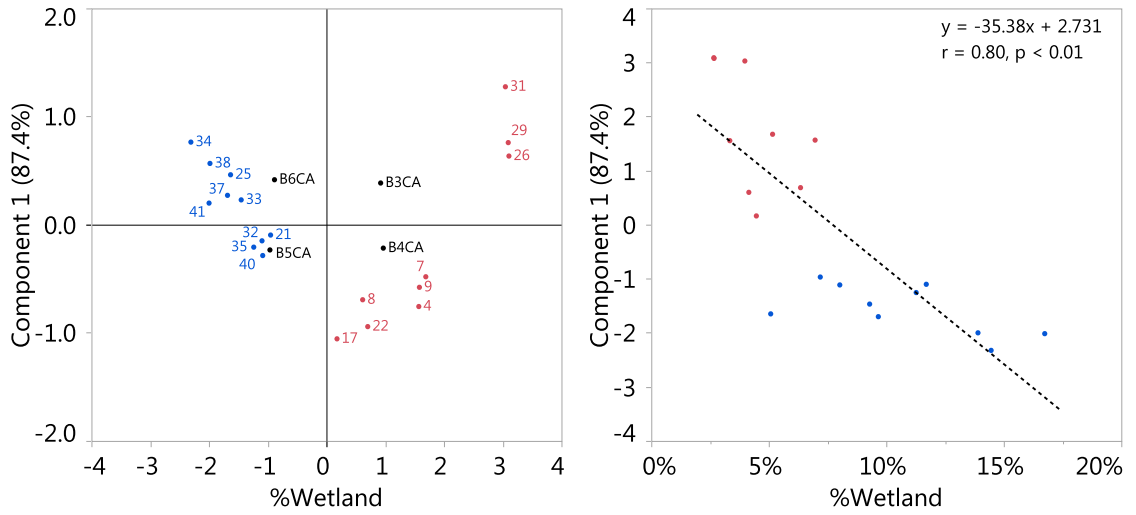
<b>Sample Date</b>	<b>Time</b>	<b>Salinity</b>	<b>DOC (ppm)</b>	<b>BIX</b>	<b>SUVA</b>	<b>POC (ppm)</b>	<b>δ<sup>13</sup>C</b>	<b>DBC (ppm)</b>	<b>BPCA Ratio (DBC)</b>	<b>PBC (ppm)</b>	<b>BPCA (PBC)</b>
09/15/2015	11:49	2.36	6.900	0.53	3.5580	0.46	-26.33	0.302	1.050	0.117	1.13
10/13/2015	13:05	0.1	7.384	0.48	3.3518	0.74	-28.08	0.430	1.437	0.102	0.33
11/10/2015	13:30	0.1	6.424	0.54	3.5554	0.7	-27.91	0.328	1.138	0.049	0.27
12/14/2015	14:20	0	8.176	0.50	3.9371	0.65	-27.39	0.288	0.906	0.006	0.21
01/19/2016	13:20	0	10.139	0.49	6.2531	0.8	-27.23	0.227	0.529	0.255	1.18
02/16/2016	13:35	0	9.731	0.47	5.1249	0.87	-27.31	0.468	1.092	0.067	0.89
03/15/2016	13:40	0	7.491	0.50	5.6281	0.52	-26.74	0.367	1.170	0.047	0.83
04/10/2016	14:45	0	12.615	0.46	4.5914	1.32	-30.78	0.389	0.688	0.071	0.57
05/09/2016	12:25	0	6.855	0.53	4.7794	0.65	-28.74	0.331	1.091	0.067	0.65
06/05/2016	14:50	0	6.231	0.57	4.7025	0.66	-27.91	0.313	1.014	0.084	0.51
07/11/2016	15:15	3.65	6.187	0.59	3.0886	0.61	-25.86	0.374	1.043	0.098	1.25
08/14/2016	16:28	2.22	6.159	0.63	3.0839	0.63	-26.57	0.448	1.027	0.192	1.35
09/11/2016	16:43	1.75	7.763	0.57	2.9991	0.73	-26.86	0.429	1.005	0.154	1.18

**Appendix 4.2:** Altamaha River monthly discharge and flux data

<b>Sample Date</b>	<b>Discharge (m<sup>3</sup>/s)</b>	<b>Flux DOC (Mg/day)</b>	<b>Flux DBC (Mg/day)</b>	<b>Flux PBC (Mg/day)</b>	<b>Flux POC (Mg/day)</b>
09/15/2015	101	60.21	2.64	1.02	4.01
10/13/2015	227	144.82	8.43	2.00	14.51
11/10/2015	251	139.31	7.11	1.06	15.18
12/14/2015	324	228.88	8.06	0.17	18.20
01/19/2016	1298	1137.06	25.46	28.60	89.72
02/16/2016	1210	1017.32	48.93	7.00	90.95
03/15/2016	696	450.47	22.07	2.83	31.27
04/10/2016	760	829.44	25.58	4.67	86.79
05/09/2016	269	159.32	7.69	1.56	15.11
06/05/2016	156	83.98	4.22	1.13	8.90
07/11/2016	100	49.71	3.01	0.79	4.90
08/14/2016	75	39.91	2.90	1.24	4.08
09/11/2016	87	58.35	3.22	1.16	5.49



**Appendix 5.1:** Cluster analysis for 19 Altamaha River samples using relative BPCA distributions including (a) a dendrogram displaying two distinct clusters and (b) a map displaying samples color-coded respective to each cluster. Sample number and locations are presented in Appendix 5.3.



**Appendix 5.2:** Principal Component (PC) Analysis using the relative BPCA distributions including (a) BPCA loading plot and sample score plot displaying location of individual samples in PC space, and (b) a strong inverse linear correlation between PC1 and wetland land cover. Samples are color coded according to their clusters (Appendix 5.1).

**Appendix 5.3:** Sample information including date of collection, geographic location, and land cover in the Altamaha River.

Sample	Date	Time	USGS	Latitude	Longitude	Drainage Area (km <sup>2</sup> )	Urban	Forested	Agriculture	Wetland
0 North Oconee 1	5/23/2016	10:30	-	34.364997	-83.683652	5	29.85%	48.68%	21.47%	0.01%
1 Walnut Creek	5/23/2016	11:40	-	34.169425	-83.786935	65	25.76%	54.83%	19.00%	0.41%
2 Allen Creek	5/23/2016	12:10	-	34.192889	-83.719469	49	23.32%	54.24%	21.70%	0.74%
3 Pond Fork	5/23/2016	12:30	-	34.180702	-83.661236	70	13.16%	46.31%	37.54%	2.99%
4 North Oconee 2	5/23/2016	13:15	2217615	34.200278	-83.515833	266	11.14%	56.58%	28.96%	3.32%
5 North Oconee 3	5/23/2016	14:05	-	34.067354	-83.46302	460	11.82%	52.83%	30.25%	5.10%
6 Sandy Creek	5/23/2016	14:30	-	33.986217	-83.377379	168	12.46%	44.14%	39.51%	3.89%
7 North Oconee 4	5/23/2016	15:15	2217770	33.958922	-83.366834	742	14.23%	49.59%	31.04%	5.14%
8 Middle Oconee	5/23/2016	16:10	2217500	33.918535	-83.39001	1176	24.02%	43.93%	27.92%	4.13%
9 Apalachee River 1	5/24/2016	7:45	2219000	33.817588	-83.506017	397	19.45%	41.74%	31.86%	6.95%
10 Jack's Creek	5/24/2016	8:15	-	33.760295	-83.490974	135	14.70%	44.17%	34.27%	6.86%
11 Apalachee River 2	5/24/2016	9:15	-	33.718955	-83.434228	609	16.63%	44.75%	32.25%	6.37%
12 Big Sandy Creek	5/24/2016	10:00	-	33.667263	-83.444624	160	5.85%	39.21%	48.34%	6.60%
13 Hard Labor Creek	5/24/2016	10:15	-	33.644459	-83.448126	213	8.36%	55.16%	30.56%	5.92%
14 Little River 1	5/24/2016	11:00	-	33.623104	-83.701162	15	16.04%	40.84%	39.42%	3.70%
15 Rice Creek	5/24/2016	11:30	-	33.618404	-83.612916	2	40.57%	14.60%	39.54%	5.29%
16 Lake Sinclair	5/24/2016	13:00	-	33.608733	-83.348184	1101	12.17%	48.23%	32.60%	7.00%
17 Oconee 1	5/24/2016	13:45	2218300	33.7207	-83.295596	2404	19.13%	48.56%	27.86%	4.45%
18 Murder Creek 1	5/25/2016	8:30	-	33.414878	-83.661196	62	4.50%	71.59%	17.65%	6.26%
19 Little River 2	5/25/2016	9:15	-	33.372838	-83.4773	354	6.44%	56.74%	29.89%	6.93%
20 Big Indian Creek	5/25/2016	9:30	-	33.37587	-83.471547	213	8.11%	53.14%	30.28%	8.47%
21 Little River 3	5/25/2016	10:45	2220900	33.314021	-83.437109	693	6.71%	59.71%	26.41%	7.17%
22 Murder Creek	5/25/2016	11:00	2221525	33.252355	-83.481276	496	5.58%	67.70%	20.39%	6.33%
23 Kinder Road Creek	5/25/2016	11:15	-	33.239448	-83.513049	0.22	8.30%	86.34%	0.01%	5.36%
24 Cedar Creek	5/25/2016	11:45	-	33.186449	-83.437009	391	4.50%	81.40%	8.10%	6.00%
25 Oconee 2	5/25/2016	14:00	2223000	33.083772	-83.21479	7632	11.61%	60.22%	23.11%	5.06%
26 Apalachee River 3	5/26/2016	7:00	2218565	34.004475	-83.886019	20	60.63%	28.32%	8.41%	2.64%
27 Little Mulberry River	5/26/2016	7:15	-	34.049803	-83.905672	5	78.52%	14.95%	6.41%	0.12%
28 Mulberry Creek 1	5/26/2016	7:45	-	34.147221	-83.878812	3	26.80%	54.49%	18.60%	0.11%
29 Mulberry Creek 2	5/26/2016	8:30	2217297	34.055111	-83.717134	290	29.60%	44.41%	23.34%	2.65%
30 Middle Oconee 2	5/26/2016	9:00	-	34.095939	-83.606152	356	19.07%	48.61%	28.57%	3.75%
31 Middle Oconee 3	5/26/2016	9:45	2217475	34.031833	-83.563299	790	23.05%	44.89%	28.10%	3.96%
32 Oconee 3	5/27/2016	9:10	2223500	32.544611	-82.894587	11138	9.40%	62.77%	19.83%	8.00%
33 Oconee 4	5/27/2016	9:45	2224500	32.191291	-82.63319	13478	8.93%	60.99%	20.81%	9.27%
34 Little Ocmulgee	5/27/2016	10:30	2215900	31.935204	-82.670643	2083	5.75%	55.15%	24.66%	14.44%
35 Ocmulgee	5/27/2016	10:45	2215500	31.919878	-82.674063	13733	17.60%	49.41%	21.74%	11.25%

36 Oconee 5	5/27/2016	11:45	-	31.980866	-82.546458	13798	8.81%	60.87%	20.68%	9.64%
37 Altamaha 2	5/27/2016	12:10	2224940	31.957744	-82.517106	29614	12.70%	55.13%	21.45%	10.72%
38 Ohoopee	5/27/2016	13:00	2225500	31.920484	-82.112638	3483	6.74%	52.52%	26.86%	13.88%
39 Altamaha 2	5/27/2016	13:45	-	31.854456	-82.093861	34280	11.84%	54.65%	22.21%	11.30%
40 Altamaha 3	5/27/2016	15:30	2226000	31.666591	-81.838942	35121	11.74%	54.34%	22.24%	11.68%
41 Altamaha 4	6/5/2016	14:45	2226160	31.337816	-81.449939	36866	11.59%	54.62%	21.50%	12.29%



**Appendix 5.4** Quantitative and compositional BPCA data along with DOC and flux information for 18 samples collected at USGS stations throughout the Altamaha River.

Sample	DOC (ppm)	DBC (ppm)	%DBC	BPCA Ratio	Discharge (m <sup>3</sup> /s)	Flux DBC (mg/s)
4. North Oconee 2	1.29	0.02	1.67	0.23	2.35	49.35
7. North Oconee 4	1.50	0.02	1.62	0.20	6.34	152.16
8. Middle Oconee	1.58	0.03	1.61	0.41	8.89	222.25
9. Apalachee River 1	1.62	0.02	1.21	0.22	3.09	61.80
17. Oconee 1	1.45	0.04	2.66	0.52	19.37	755.43
21. Little River 3	2.08	0.07	3.52	0.70	2.88	210.24
22. Murder Creek	1.77	0.04	2.40	0.39	2.18	91.56
25. Oconee 2	2.90	0.14	4.65	0.84	25.57	3451.95
26. Apalachee River 3	1.54	0.01	0.56	0.00	0.08	0.72
29. Mulberry Creek 2	1.63	0.01	0.47	0.00	1.56	12.48
31. Middle Oconee 3	1.50	0.01	0.35	0.00	6.09	30.45
32. Oconee 3	3.87	0.20	5.14	0.75	52.30	10407.70
33. Oconee 4	4.19	0.23	5.49	0.81	75.66	17401.80
34. Little Ocmulgee	7.65	0.50	6.48	1.03	0.40	198.40
35. Ocmulgee	3.10	0.16	5.10	0.82	105.54	16675.32
37. Altamaha 5	3.53	0.17	4.81	0.89	193.32	32864.40
38. Ohoopee	9.70	0.48	4.97	0.95	7.47	3600.54
40. Altamaha 3	4.20	0.19	4.48	0.78	221.78	41694.64
41. Altamaha 4	6.23	0.31	5.02	1.01	156.00	48828.00

**Appendix 5.5:** Molecular parameters for polycondensed aromatic compounds ( $A.I.mod \geq 0.67$ ,  $C \geq 15$ ) as determined by FTICR-MS for samples collected throughout the Altamaha River. A (-) indicates that sample information is not available

Sample Name	Total Formula	DBC Formula	m/z <sub>w-dbc</sub>	C <sub>w-dbc</sub>	H <sub>w-dbc</sub>	O <sub>w-dbc</sub>	N <sub>w-dbc</sub>	S <sub>w-dbc</sub>	O/C <sub>w-dbc</sub>	H/C <sub>w-dbc</sub>	Almod <sub>w-dbc</sub>	CHO <sub>DBC</sub> (%)	CHON <sub>DBC</sub> (%)	CHOS <sub>DBC</sub> (%)
0 North Oconee 1	8020	704 (8.78)	329.51	19.09	10.97	5.08	0.27	0.17	0.27	0.58	0.73	291 (41.34)	211 (29.97)	187 (26.56)
1 Walnut Creek	8977	480 (5.35)	331.14	19.11	11.37	5.05	0.32	0.19	0.27	0.60	0.72	186 (38.75)	145 (30.21)	137 (28.54)
2 Allen Creek	8540	518 (6.07)	325.49	18.83	11.06	4.95	0.33	0.17	0.27	0.59	0.72	206 (39.77)	169 (32.63)	131 (25.29)
3 Pond Fork	8311	548 (6.59)	323.85	18.66	10.97	4.96	0.37	0.17	0.27	0.59	0.72	219 (39.96)	181 (33.03)	138 (25.18)
4 North Oconee 2	8728	682 (7.81)	329.35	19.02	11.04	5.04	0.35	0.17	0.27	0.58	0.73	251 (36.80)	224 (32.84)	187 (27.42)
5 North Oconee 3	8048	468 (5.82)	323.97	18.55	11.02	5.12	0.37	0.13	0.28	0.60	0.72	192 (41.03)	163 (34.83)	106 (22.65)
6 Sandy Creek	6223	343 (5.51)	318.84	18.36	10.94	4.96	0.33	0.14	0.28	0.60	0.72	159 (46.36)	104 (30.32)	76 (22.16)
7 North Oconee 4	8056	486 (6.03)	324.78	18.58	10.98	5.13	0.38	0.14	0.28	0.59	0.72	196 (40.33)	169 (34.77)	116 (23.87)
8 Middle Oconee	-	-	-	-	-	-	-	-	-	-	-	-	-	-
9 Apalachee River 1	7941	508 (6.40)	331.88	19.05	11.16	5.20	0.30	0.17	0.28	0.59	0.72	207 (40.75)	152 (29.92)	143 (28.15)
10 Jack's Creek	8180	587 (7.18)	322.49	18.77	11.02	4.72	0.35	0.21	0.26	0.59	0.73	225 (38.33)	185 (31.52)	160 (27.26)
11 Apalachee River 2	8887	733 (8.25)	325.98	18.94	11.09	4.85	0.35	0.19	0.26	0.59	0.73	265 (36.15)	251 (34.24)	196 (26.74)
12 Big Sandy Creek	9243	753 (8.15)	329.38	19.01	11.14	5.04	0.40	0.15	0.27	0.59	0.73	271 (35.99)	270 (35.86)	179 (23.77)
13 Hard Labor Creek	8787	641 (7.29)	324.95	18.77	11.04	4.99	0.34	0.15	0.27	0.59	0.72	252 (39.31)	217 (33.85)	158 (24.65)
14 Little River 1	7659	482 (6.29)	318.62	18.41	10.85	4.88	0.41	0.13	0.27	0.59	0.73	209 (43.36)	171 (35.48)	93 (19.29)
15 Rice Creek	7682	571 (7.43)	322.44	18.74	11.13	4.83	0.33	0.17	0.26	0.60	0.72	223 (39.05)	181 (31.70)	150 (26.27)
16 Lake Sinclair	8469	740 (8.74)	328.26	19.09	11.02	4.82	0.34	0.23	0.26	0.58	0.73	262 (35.41)	241 (32.57)	213 (28.78)
17 Oconee 1	7071	452 (6.39)	333.71	19.51	11.40	4.71	0.28	0.31	0.25	0.59	0.72	168 (37.17)	109 (24.12)	170 (37.61)
18 Murder Creek 1	8109	624 (7.70)	326.82	18.92	11.03	5.00	0.30	0.17	0.27	0.58	0.73	254 (40.71)	190 (30.45)	167 (26.76)
19 Little River 2	8127	670 (8.24)	327.34	18.95	11.00	4.97	0.34	0.17	0.27	0.58	0.73	255 (38.06)	217 (32.39)	179 (26.72)
20 Big Indian Creek	8967	712 (7.94)	329.64	19.01	11.07	5.06	0.37	0.16	0.27	0.59	0.73	263 (36.94)	247 (34.69)	182 (25.56)
21 Little River 3	9387	706 (7.52)	330.47	18.89	11.01	5.29	0.40	0.11	0.29	0.59	0.73	279 (39.52)	268 (37.96)	133 (18.84)
22 Murder Creek	7415	518 (6.99)	327.10	18.74	10.92	5.23	0.30	0.13	0.29	0.59	0.73	233 (44.98)	156 (30.12)	119 (22.97)
23 Kinder Road Creek	6965	549 (7.88)	329.28	18.90	10.89	5.33	0.27	0.11	0.29	0.58	0.73	257 (46.98)	162 (29.51)	115 (20.95)
24 Cedar Creek	7669	579 (7.55)	328.39	18.88	10.99	5.23	0.28	0.13	0.28	0.58	0.73	253 (43.70)	173 (29.88)	140 (24.18)
25 Oconee 2	6459	501 (7.76)	336.91	19.57	11.10	4.92	0.16	0.34	0.26	0.57	0.73	196 (39.12)	88 (17.56)	206 (41.12)
26 Apalachee River 3	9275	606 (6.53)	329.80	19.08	11.25	5.05	0.36	0.15	0.27	0.59	0.72	231 (38.12)	210 (34.65)	151 (24.92)
27 Little Mulberry River	8662	546 (6.30)	332.66	19.02	11.04	5.32	0.36	0.12	0.29	0.58	0.73	235 (43.04)	193 (35.35)	98 (17.95)
28 Mulberry Creek 1	7896	583 (7.38)	332.60	19.00	10.96	5.45	0.31	0.09	0.29	0.58	0.73	271 (46.48)	192 (32.93)	97 (16.64)
29 Mulberry Creek 2	8895	565 (6.35)	330.89	19.01	11.14	5.15	0.35	0.16	0.28	0.59	0.72	217 (38.41)	182 (32.21)	150 (26.55)
30 Middle Oconee 2	7710	413 (5.36)	321.03	18.47	11.07	4.97	0.39	0.13	0.28	0.60	0.72	174 (42.13)	145 (35.11)	89 (21.55)
31 Middle Oconee 3	7679	374 (4.87)	324.38	18.58	11.04	5.21	0.38	0.08	0.29	0.60	0.72	176 (47.06)	140 (37.43)	56 (14.97)
32 Oconee 3	8406	796 (9.47)	335.66	19.21	10.98	5.45	0.29	0.12	0.29	0.57	0.73	331 (41.58)	253 (31.78)	173 (21.73)
33 Oconee 4	8940	852 (9.53)	338.13	19.36	11.04	5.44	0.28	0.15	0.29	0.57	0.73	334 (39.20)	259 (30.40)	209 (24.53)
34 Little Ocmulgee	6826	664 (9.73)	342.75	19.63	11.13	5.56	0.19	0.16	0.29	0.57	0.73	307 (46.23)	148 (22.29)	186 (28.01)

35 Ocmulgee	8651	780 (9.02)	333.36	19.14	10.98	5.33	0.28	0.14	0.28	0.58	0.73	320 (41.03)	242 (31.03)	195 (25.00)
36 Oconee 5	8937	847 (9.48)	339.45	19.45	11.08	5.48	0.29	0.13	0.29	0.57	0.73	342 (40.38)	270 (31.88)	196 (23.14)
37 Altamaha 2	8909	871 (9.78)	335.84	19.27	11.01	5.37	0.29	0.14	0.29	0.57	0.73	340 (39.04)	276 (31.69)	217 (24.91)
38 Ohoopce	8008	923 (11.53)	342.95	19.60	10.95	5.65	0.22	0.14	0.30	0.56	0.73	377 (40.85)	257 (27.84)	237 (25.68)
39 Altamaha 2	8274	832 (10.06)	336.29	19.29	10.98	5.43	0.26	0.14	0.29	0.57	0.73	341 (41.99)	252 (30.29)	209 (25.12)
40 Altamaha 3	8659	837 (9.67)	337.62	19.31	10.94	5.53	0.25	0.12	0.29	0.57	0.73	349 (41.70)	246 (29.39)	197 (23.54)
41 Altamaha 4	7824	739 (9.45)	345.77	20.28	11.39	4.84	0.21	0.36	0.25	0.57	0.73	267 (36.13)	162 (21.92)	274 (37.05)

**Appendix 6.1:** List of sample locations, date, time, stream order category, geographical coordinates, and land use characteristics in the Altamaha River. An (\*) indicates a USGS monitoring station

Sample	Date	Time	Stream Order	Latitude	Longitude	Urban	Forested	Agriculture	Wetland
0 North Oconee 1	5/23/2016	10:30	Small	34.364997	-83.683652	29.85%	48.68%	21.47%	0.01%
1 Walnut Creek	5/23/2016	11:40	Small	34.169425	-83.786935	25.76%	54.83%	19.00%	0.41%
2 Allen Creek	5/23/2016	12:10	Small	34.192889	-83.719469	23.32%	54.24%	21.70%	0.74%
3 Pond Fork	5/23/2016	12:30	Small	34.180702	-83.661236	13.16%	46.31%	37.54%	2.99%
*4 North Oconee 2	5/23/2016	13:15	Small	34.200278	-83.515833	11.14%	56.58%	28.96%	3.32%
5 North Oconee 3	5/23/2016	14:05	Medium	34.067354	-83.46302	11.82%	52.83%	30.25%	5.10%
6 Sandy Creek	5/23/2016	14:30	Medium	33.986217	-83.377379	12.46%	44.14%	39.51%	3.89%
*7 North Oconee 4	5/23/2016	15:15	Medium	33.958922	-83.366834	14.23%	49.59%	31.04%	5.14%
*8 Middle Oconee	5/23/2016	16:10	Medium	33.918535	-83.39001	24.02%	43.93%	27.92%	4.13%
*9 Apalachee River 1	5/24/2016	7:45	Medium	33.817588	-83.506017	19.45%	41.74%	31.86%	6.95%
10 Jack's Creek	5/24/2016	8:15	Small	33.760295	-83.490974	14.70%	44.17%	34.27%	6.86%
11 Apalachee River 2	5/24/2016	9:15	Medium	33.718955	-83.434228	16.63%	44.75%	32.25%	6.37%
12 Big Sandy Creek	5/24/2016	10:00	Medium	33.667263	-83.444624	5.85%	39.21%	48.34%	6.60%
13 Hard Labor Creek	5/24/2016	10:15	Small	33.644459	-83.448126	8.36%	55.16%	30.56%	5.92%
14 Little River 1	5/24/2016	11:00	Small	33.623104	-83.701162	16.04%	40.84%	39.42%	3.70%
15 Rice Creek	5/24/2016	11:30	Small	33.618404	-83.612916	40.57%	14.60%	39.54%	5.29%
16 Lake Sinclair	5/24/2016	13:00	Medium	33.608733	-83.348184	12.17%	48.23%	32.60%	7.00%
*17 Oconee 1	5/24/2016	13:45	Medium	33.7207	-83.295596	19.13%	48.56%	27.86%	4.45%
18 Murder Creek 1	5/25/2016	8:30	Small	33.414878	-83.661196	4.50%	71.59%	17.65%	6.26%
19 Little River 2	5/25/2016	9:15	Medium	33.372838	-83.4773	6.44%	56.74%	29.89%	6.93%
20 Big Indian Creek	5/25/2016	9:30	Medium	33.37587	-83.471547	8.11%	53.14%	30.28%	8.47%
*21 Little River 3	5/25/2016	10:45	Medium	33.314021	-83.437109	6.71%	59.71%	26.41%	7.17%
*22 Murder Creek	5/25/2016	11:00	Medium	33.252355	-83.481276	5.58%	67.70%	20.39%	6.33%
23 Kinder Road Creek	5/25/2016	11:15	Small	33.239448	-83.513049	8.30%	86.34%	0.01%	5.36%
24 Cedar Creek	5/25/2016	11:45	Medium	33.186449	-83.437009	4.50%	81.40%	8.10%	6.00%
*25 Oconee 2	5/25/2016	14:00	Large	33.083772	-83.21479	11.61%	60.22%	23.11%	5.06%
*26 Apalachee River 3	5/26/2016	7:00	Small	34.004475	-83.886019	60.63%	28.32%	8.41%	2.64%
27 Little Mulberry River	5/26/2016	7:15	Small	34.049803	-83.905672	78.52%	14.95%	6.41%	0.12%
28 Mulberry Creek 1	5/26/2016	7:45	Small	34.147221	-83.878812	26.80%	54.49%	18.60%	0.11%
*29 Mulberry Creek 2	5/26/2016	8:30	Medium	34.055111	-83.717134	29.60%	44.41%	23.34%	2.65%
30 Middle Oconee 2	5/26/2016	9:00	Medium	34.095939	-83.606152	19.07%	48.61%	28.57%	3.75%
*31 Middle Oconee 3	5/26/2016	9:45	Medium	34.031833	-83.563299	23.05%	44.89%	28.10%	3.96%
*32 Oconee 3	5/27/2016	9:10	Large	32.544611	-82.894587	9.40%	62.77%	19.83%	8.00%
*33 Oconee 4	5/27/2016	9:45	Large	32.191291	-82.63319	8.93%	60.99%	20.81%	9.27%
*34 Little Ocmulgee	5/27/2016	10:30	Large	31.935204	-82.670643	5.75%	55.15%	24.66%	14.44%

*35 Ocmulgee	5/27/2016	10:45	Large	31.919878	-82.674063	17.60%	49.41%	21.74%	11.25%
36 Oconee 5	5/27/2016	11:45	Large	31.980866	-82.546458	8.81%	60.87%	20.68%	9.64%
*37 Altamaha 2	5/27/2016	12:10	Large	31.957744	-82.517106	12.70%	55.13%	21.45%	10.72%
*38 Ohoopce	5/27/2016	13:00	Large	31.920484	-82.112638	6.74%	52.52%	26.86%	13.88%
39 Altamaha 2	5/27/2016	13:45	Large	31.854456	-82.093861	11.84%	54.65%	22.21%	11.30%
*40 Altamaha 3	5/27/2016	15:30	Large	31.666591	-81.838942	11.74%	54.34%	22.24%	11.68%
*41 Altamaha 4	6/5/2016	14:45	Large	31.337816	-81.449939	11.59%	54.62%	21.50%	12.29%

**Appendix 6.2:** Measurements of water quality parameters, optical properties, and relative contributions of PARAFAC components at each sampling location in the Altamaha River. A (-) indicates measurements are not available.

Sample	DOC (ppm)	TDN (ppm)	Turbidity	HIX	BIX	FI	SUVA	%C1	%C2	%C3	%C4	%C5
0 North Oconee 1	1.247	0.911	7.22	3.47	0.57	1.56	3.40	30.87	25.13	14.45	6.11	23.44
1 Walnut Creek	1.133	0.690	7.83	3.47	0.63	1.58	4.55	29.68	23.34	16.39	6.63	23.96
2 Allen Creek	1.432	1.312	9.04	4.17	0.72	1.65	4.20	30.87	22.22	20.14	3.82	22.95
3 Pond Fork	1.318	1.359	8.59	5.44	0.67	1.59	4.51	34.54	25.14	20.13	4.23	15.96
4 North Oconee 2	1.288	1.243	14.00	3.81	0.65	1.61	5.15	32.97	24.97	17.71	4.92	19.42
5 North Oconee 3	1.470	1.155	27.00	4.35	0.65	1.63	5.29	32.99	23.66	18.96	3.99	20.39
6 Sandy Creek	1.921	0.402	11.50	3.55	0.70	1.56	3.54	30.91	23.65	17.81	12.14	15.48
7 North Oconee 4	1.496	0.815	24.60	4.53	0.67	1.63	5.35	34.01	24.72	19.40	6.19	15.67
8 Middle Oconee	1.579	1.348	14.10	4.13	0.70	1.61	4.45	33.00	23.51	20.05	5.88	17.55
9 Appalachian River 1	1.616	1.026	21.60	4.84	0.63	1.62	4.95	34.48	26.21	18.36	8.39	12.56
10 Jack's Creek	1.699	1.460	17.40	5.07	0.65	1.73	4.40	37.81	23.80	22.88	0.01	15.51
11 Appalachian River 2	1.518	0.930	17.10	5.49	0.63	1.60	5.02	33.13	24.62	17.99	6.85	17.42
12 Big Sandy Creek	1.278	0.890	16.90	6.02	0.62	1.62	5.85	35.35	26.56	19.48	4.65	13.96
13 Hard Labor Creek	1.791	0.453	12.50	5.03	0.67	1.59	4.03	33.08	24.91	18.97	7.52	15.53
14 Little River 1	1.527	10.637	10.20	4.24	0.70	1.81	4.09	36.92	22.24	21.49	0.01	19.35
15 Rice Creek	2.382	0.908	25.30	4.96	0.66	1.60	5.89	33.12	24.87	18.93	9.43	13.65
16 Lake Sinclair	1.725	0.718	31.70	5.54	0.64	1.56	4.36	32.40	24.55	17.76	9.35	15.93
17 Oconee 1	1.450	1.430	22.00	5.35	0.68	1.60	4.69	33.46	23.84	20.02	4.85	17.83
18 Murder Creek 1	1.509	0.492	10.90	5.44	0.61	1.54	4.50	33.05	26.11	16.98	6.31	17.55
19 Little River 2	1.775	0.804	26.70	5.78	0.62	1.58	4.15	34.54	26.05	18.82	6.30	14.28
20 Big Indian Creek	2.081	0.541	24.50	6.28	0.64	1.61	5.20	35.03	25.95	19.68	6.66	12.69
21 Little River 3	2.077	0.640	19.40	6.02	0.63	1.57	4.43	33.72	25.37	18.67	7.64	14.60
22 Murder Creek	1.768	0.425	24.60	5.96	0.63	1.58	4.74	34.66	25.83	18.59	6.02	14.91
23 Kinder Road Creek	0.752	0.134	9.46	4.55	0.58	1.58	4.86	35.27	28.11	16.18	2.69	17.76
24 CedarCreek	1.948	0.221	23.70	6.15	0.62	1.63	5.26	36.29	26.86	19.70	5.43	11.73
25 Oconee 2	2.903	0.547	19.60	5.08	0.61	1.49	5.09	31.93	25.48	16.34	12.72	13.52
26 Appalachian River 3	1.535	0.760	12.00	4.38	0.66	1.55	5.22	31.93	24.78	18.41	7.78	17.10
27 Little Mulberry River	1.178	1.925	2.66	3.39	0.70	1.53	3.15	30.08	23.34	17.91	4.92	23.75
28 Mulberry Creek 1	1.187	1.343	5.00	4.28	0.58	1.57	3.76	36.01	25.82	21.32	2.66	14.19
29 Mulberry Creek 2	1.628	1.346	14.00	4.23	0.68	1.61	3.78	34.08	27.63	17.38	3.60	17.31
30 Middle Oconee 2	1.515	1.574	15.50	5.04	0.71	1.68	4.15	36.21	25.05	23.21	0.01	15.53
31 Middle Oconee 3	1.498	1.356	21.00	4.33	0.69	1.65	4.66	35.06	24.20	21.78	1.72	17.24
32 Oconee 3	3.868	0.524	26.70	8.25	0.55	1.47	5.42	35.65	28.86	16.56	11.15	7.78
33 Oconee 4	4.193	0.504	39.80	8.16	0.55	1.49	5.10	35.80	28.68	16.78	11.12	7.62
34 Little Ocmulgee	7.653	0.408	10.20	14.38	0.47	1.41	4.96	37.69	32.81	14.28	11.01	4.20
35 Ocmulgee	3.104	0.552	40.40	7.00	0.58	1.51	4.75	34.36	27.68	17.13	11.22	9.61
36 Oconee 5	4.473	0.523	37.00	7.75	0.56	1.48	4.93	35.69	28.66	16.76	10.99	7.90

37 Altamaha 2	3.529	0.759	38.60	6.92	0.57	1.49	4.97	34.46	27.68	16.97	11.08	9.80
38 Ohoopee	9.695	0.606	7.73	15.38	0.46	1.40	5.22	38.79	33.93	14.75	8.75	3.78
39 Altamaha 2	4.365	0.620	43.20	7.34	0.55	1.48	4.99	35.29	29.17	16.17	10.96	8.41
40 Altamaha 3	4.202	0.606	43.10	7.83	0.55	1.47	4.87	35.30	29.16	16.31	11.43	7.81
41 Altamaha 4	6.231	-	-	6.37	0.57	1.48	4.70	32.50	27.83	14.85	14.26	10.57

**Appendix 6.3:** FTICR-MS weighted molecular parameters for each sampling location in the Altamaha River. A (-) indicates measurements are not available.

Sample	m/z <sub>w</sub>	C <sub>w</sub>	H <sub>w</sub>	O <sub>w</sub>	N <sub>w</sub>	S <sub>w</sub>	P <sub>w</sub>	O/C <sub>w</sub>	H/C <sub>w</sub>	Aimod <sub>w</sub>	DBE <sub>w</sub>
0 North Oconee 1	346.190	18.135	21.14	6.45	0.22	0.05	0.01	0.36	1.15	0.37	8.68
1 Walnut Creek	360.221	18.442	22.57	6.95	0.21	0.07	0.02	0.38	1.22	0.32	8.28
2 Allen Creek	345.163	17.858	21.86	6.49	0.20	0.08	0.01	0.37	1.22	0.32	8.04
3 Pond Fork	352.739	18.051	21.36	6.85	0.27	0.06	0.01	0.38	1.17	0.35	8.51
4 North Oconee 2	351.684	18.070	21.24	6.80	0.26	0.06	0.01	0.38	1.16	0.35	8.59
5 North Oconee 3	353.379	18.001	21.43	6.95	0.26	0.05	0.01	0.39	1.18	0.34	8.42
6 Sandy Creek	347.374	17.777	21.24	6.78	0.25	0.04	0.01	0.38	1.18	0.34	8.29
7 North Oconee 4	357.084	18.115	21.49	7.10	0.25	0.05	0.01	0.40	1.17	0.34	8.50
8 Middle Oconee	-	-	-	-	-	-	-	-	-	-	-
9 Appalachian River 1	360.614	18.349	21.77	7.14	0.23	0.05	0.01	0.39	1.17	0.34	8.58
10 Jack's Creek	337.618	17.511	20.85	6.27	0.27	0.09	0.01	0.36	1.18	0.35	8.22
11 Appalachian River 2	345.460	17.917	20.84	6.54	0.26	0.06	0.01	0.37	1.15	0.37	8.63
12 Big Sandy Creek	355.792	18.244	21.14	6.93	0.28	0.05	0.01	0.38	1.14	0.36	8.82
13 Hard Labor Creek	354.905	18.192	21.39	6.93	0.25	0.05	0.01	0.38	1.16	0.35	8.62
14 Little River 1	332.196	17.049	20.65	6.24	0.29	0.11	0.01	0.37	1.20	0.33	7.87
15 Rice Creek	345.234	17.802	20.71	6.64	0.27	0.05	0.01	0.38	1.15	0.36	8.59
16 Lake Sinclair	340.318	17.832	20.79	6.28	0.25	0.07	0.01	0.36	1.15	0.37	8.57
17 Oconee 1	350.510	17.933	21.39	6.75	0.23	0.10	0.02	0.38	1.18	0.34	8.36
18 Murder Creek 1	349.943	18.060	21.30	6.74	0.22	0.05	0.01	0.38	1.17	0.35	8.53
19 Little River 2	347.457	17.893	20.73	6.70	0.26	0.05	0.01	0.38	1.14	0.37	8.67
20 Big Indian Creek	352.808	17.986	20.83	6.95	0.27	0.05	0.01	0.39	1.14	0.36	8.71
21 Little River 3	361.523	18.302	21.30	7.26	0.26	0.05	0.01	0.40	1.15	0.35	8.78
22 Murder Creek	356.014	18.107	21.09	7.11	0.22	0.04	0.01	0.39	1.15	0.35	8.68
23 Kinder Road Creek	360.875	18.509	21.40	7.13	0.17	0.04	0.01	0.39	1.14	0.37	8.90
24 CedarCreek	356.621	18.193	21.06	7.14	0.19	0.03	0.01	0.39	1.14	0.36	8.76
25 Oconee 2	350.979	18.096	21.20	6.80	0.16	0.06	0.02	0.38	1.16	0.36	8.59
26 Appalachian River 3	363.842	18.498	21.76	7.21	0.23	0.06	0.01	0.39	1.16	0.34	8.74
27 Little Mulberry River	363.502	18.551	22.17	7.10	0.23	0.07	0.02	0.39	1.18	0.33	8.59
28 Mulberry Creek 1	363.500	18.492	21.42	7.25	0.21	0.05	0.01	0.39	1.14	0.36	8.89
29 Mulberry Creek 2	362.155	18.319	21.67	7.22	0.25	0.07	0.01	0.40	1.17	0.34	8.61
30 Middle Oconee 2	352.643	18.010	21.54	6.86	0.27	0.06	0.01	0.38	1.18	0.34	8.38
31 Middle Oconee 3	354.329	17.774	21.25	7.05	0.24	0.13	0.01	0.40	1.19	0.33	8.28
32 Oconee 3	356.877	18.159	20.40	7.19	0.20	0.05	0.01	0.40	1.11	0.38	9.06
33 Oconee 4	360.967	18.297	20.52	7.32	0.20	0.05	0.01	0.40	1.11	0.38	9.14
34 Little Ocmulgee	367.035	18.559	20.50	7.56	0.14	0.04	0.01	0.41	1.09	0.38	9.39
35 Ocmulgee	356.287	18.208	20.71	7.06	0.20	0.06	0.01	0.39	1.12	0.37	8.96



36 Oconee 5	361.213	18.327	20.48	7.32	0.20	0.05	0.01	0.40	1.10	0.38	9.19
37 Altamaha 2	356.632	18.221	20.63	7.10	0.20	0.05	0.01	0.39	1.12	0.37	9.01
38 Ohoopce	355.167	18.062	19.35	7.25	0.17	0.04	0.01	0.40	1.06	0.41	9.47
39 Altamaha 2	352.759	18.048	20.14	7.03	0.19	0.05	0.01	0.39	1.10	0.39	9.08
40 Altamaha 3	362.917	18.380	20.49	7.39	0.19	0.05	0.01	0.40	1.10	0.38	9.23
41 Altamaha 4	358.086	18.538452	20.86733	6.92	0.13	0.08	0.02	0.38	1.11	0.38	9.18

**Appendix 6.4:** Relative intensity weighted contributions of each FTICR-MS molecular compound class at each sample locations in the Altamaha River. A (-) indicates measurements are not available. Classes are defined as follows: (1)  $AI_{mod} > 0.67$ , less than 15 carbons, (2) condensed aromatics 15 or more carbons, (3) condensed aromatics compounds with heteroatoms, (4) polyphenols, (5), highly unsaturated compounds, (6) unsaturated aliphatics, (7), saturated fatty acids, (8) saturated fatty acids with heteroatoms, (9) carbohydrate-like, (10) carbohydrate-like with heteroatoms, and (11) peptide-like.

Sample	Group 1	Group 2	Group 3	Group 4	Group 5	Group 6	Group 7	Group 8	Group 9	Group 10	Group 11
0 North Oconee 1	3.919	2.891	2.97	17.70	61.16	10.05	0.00	0.39	0.15	0.14	0.63
1 Walnut Creek	2.178	1.208	1.68	13.32	66.64	13.41	0.00	0.40	0.06	0.23	0.89
2 Allen Creek	2.223	1.329	1.84	13.00	67.20	13.07	0.00	0.24	0.07	0.12	0.91
3 Pond Fork	2.843	1.675	2.64	15.81	66.14	9.67	0.05	0.27	0.08	0.15	0.69
4 North Oconee 2	3.170	2.029	2.88	16.32	64.84	9.58	0.07	0.25	0.08	0.12	0.65
5 North Oconee 3	2.735	1.542	2.27	15.32	66.53	10.15	0.03	0.33	0.09	0.12	0.88
6 Sandy Creek	2.934	1.505	2.29	15.70	65.85	10.64	0.00	0.41	0.06	0.06	0.55
7 North Oconee 4	2.506	1.448	2.21	15.05	68.14	9.59	0.00	0.24	0.07	0.08	0.66
8 Middle Oconee	-	-	-	-	-	-	-	-	-	-	-
9 Appalachee River 1	2.542	1.566	2.06	14.86	68.52	9.56	0.00	0.19	0.07	0.11	0.52
10 Jack's Creek	2.891	1.777	3.09	16.17	63.71	11.21	0.01	0.18	0.08	0.10	0.78
11 Appalachee River 2	3.337	2.259	3.24	17.47	63.66	9.01	0.00	0.14	0.07	0.13	0.68
12 Big Sandy Creek	3.009	2.124	3.02	16.81	66.33	7.71	0.00	0.16	0.07	0.11	0.66
13 Hard Labor Creek	2.838	1.869	2.49	15.80	67.73	8.38	0.00	0.18	0.08	0.08	0.56
14 Little River 1	2.516	1.638	2.76	14.29	63.61	13.48	0.00	0.44	0.12	0.10	1.05
15 Rice Creek	3.139	2.054	2.98	17.79	64.02	9.18	0.00	0.09	0.07	0.06	0.62
16 Lake Sinclair	3.479	2.416	3.54	18.10	61.15	10.11	0.01	0.24	0.08	0.14	0.72
17 Oconee 1	2.618	1.294	2.49	14.66	68.23	9.46	0.00	0.24	0.07	0.19	0.74
18 Murder Creek 1	3.128	2.102	2.51	16.01	65.77	9.44	0.00	0.24	0.09	0.10	0.61
19 Little River 2	3.416	2.264	3.15	17.31	64.80	8.15	0.00	0.15	0.08	0.13	0.55
20 Big Indian Creek	3.006	2.047	2.92	16.64	66.61	7.90	0.00	0.10	0.09	0.09	0.60
21 Little River 3	2.749	2.014	2.49	15.59	68.33	7.95	0.00	0.20	0.08	0.05	0.55
22 Murder Creek	3.139	1.950	2.27	15.85	68.49	7.58	0.00	0.18	0.08	0.06	0.40
23 Kinder Road Creek	3.876	2.703	2.25	16.98	65.17	7.69	0.00	0.65	0.11	0.12	0.44
24 CedarCreek	3.344	2.125	2.11	16.36	68.21	7.28	0.00	0.10	0.09	0.05	0.34
25 Oconee 2	3.531	1.857	2.58	16.22	66.11	8.81	0.00	0.18	0.09	0.17	0.45
26 Appalachee River 3	2.499	1.598	2.15	14.81	69.85	8.17	0.00	0.18	0.07	0.11	0.55
27 Little Mulberry River	2.341	1.513	1.91	12.78	71.88	8.33	0.00	0.40	0.08	0.16	0.61
28 Mulberry Creek 1	3.333	2.283	2.13	15.40	69.25	6.65	0.00	0.24	0.09	0.14	0.47
29 Mulberry Creek 2	2.376	1.421	2.06	13.98	71.29	7.90	0.00	0.19	0.06	0.12	0.61
30 Middle Oconee 2	2.316	1.242	2.15	14.33	69.93	8.92	0.00	0.16	0.05	0.11	0.79
31 Middle Oconee 3	2.245	1.200	1.76	13.39	71.30	9.15	0.00	0.26	0.07	0.10	0.53

32 Oconee 3	4.034	3.099	2.82	18.23	64.92	6.25	0.00	0.17	0.09	0.05	0.33
33 Oconee 4	3.873	3.004	2.81	17.91	66.01	5.79	0.00	0.12	0.09	0.08	0.31
34 Little Ocmulgee	4.219	3.227	2.30	18.35	67.25	4.35	0.00	0.05	0.07	0.10	0.09
35 Ocmulgee	3.595	2.843	2.70	17.54	65.68	6.94	0.00	0.17	0.08	0.08	0.39
36 Oconee 5	3.804	3.046	2.71	18.06	66.30	5.50	0.00	0.12	0.09	0.07	0.29
37 Altamaha 2	3.687	3.001	2.87	17.63	65.56	6.57	0.00	0.14	0.09	0.06	0.39
38 Ohoopce	5.480	4.604	3.06	20.81	61.29	4.31	0.00	0.06	0.11	0.10	0.18
39 Altamaha 2	4.300	3.447	2.94	18.76	64.01	5.89	0.00	0.11	0.14	0.07	0.33
40 Altamaha 3	4.051	3.322	2.69	18.19	65.75	5.43	0.00	0.10	0.10	0.09	0.29
41 Altamaha 4	4.041	2.66	3.10	18.91	64.31	6.49	0.00	0.09	0.09	0.19	0.13

## VITA

JESSE ALAN ROEBUCK, JR.

Born, Goldsboro, North Carolina

2006 - 2011                    B.S., Chemistry  
University of North Carolina Wilmington  
Wilmington, North Carolina

2011 - 2014                    M.S., Chemistry  
University of North Carolina Wilmington  
Wilmington, North Carolina

Teaching Assistant  
University of North Carolina Wilmington  
Wilmington, North Carolina

2014 - 2018                    Doctoral Candidate  
Florida International University,  
Miami, FL

Teaching Assistant  
Florida International University  
Miami, FL

## PUBLICATIONS AND PRESENTATIONS

Jesse Alan Roebuck, Jr., Patricia M. Medeiros, Maria L. Letourneau, and Rudolf Jaffé (in review). Hydrological controls on the seasonal variability of dissolved and particulate black carbon in the Altamaha River, GA. *Journal of Geophysical Research: Biogeosciences*

Jesse Alan Roebuck, Jr., Michael Seidel, Thorsten Dittmar, Rudolf Jaffé (in review). Land use controls on the spatial variability of dissolved black carbon in a sub-tropical watershed. *Environmental Science and Technology*

Jesse Alan Roebuck, Jr., Michael Gonsior; Yingxun Du; Phillippe Schmitt-Kopplin; Alex Enrich-Prast, Rudolf Jaffe (in review). Biogeochemical controls on the fate and transport of dissolved black carbon in the Amazon River. *Aquatic Sciences*

Jesse Alan Roebuck, Jr., Patricia Medeiros, Maria L. Letourneau, and Rudolf Jaffé (February 2018). Presented a poster entitled “Hydrological controls on the seasonal variability of dissolved and particulate black carbon in the Altamaha River, GA” at the ASLO Ocean Sciences Meeting in Portland, OR.

Jesse Alan Roebuck, Jr., Michael Gonsior, Alex Enrich-Prast, and Rudolf Jaffé (June 2017). Presented a talk entitled “Environmental Dynamics of Dissolved Black Carbon in the Amazon River” at the Florida Annual Meeting and Exposition hosted by the American Chemical Society in Palm Harbor FL.

Jesse Alan Roebuck, Jr., David C. Podgorski, Sasha J. Wagner, and Rudolf Jaffé. 2017. Photodissolution of char and fire-impacted soil as a potential source of dissolved black carbon in aquatic environments. *Organic Geochemistry*. 112, 16-21

Jesse Alan Roebuck, Jr., David C. Podgorski, Sasha Wagner, and Rudolf Jaffé (February 2017). Presented a paper entitled “Photodissolution of Char and Fire-impacted Soil as a Potential Source of Dissolved Black Carbon in Aquatic Environments” at the ASLO Aquatic Sciences Meeting in Honolulu, HI.

Jesse Alan Roebuck, Jr., Michael Gonsior, Alex Enrich-Prast, and Rudolf Jaffé (February 2016). Presented a poster entitled “Environmental Dynamics of Dissolved Black Carbon in the Amazon River” at the ASLO Ocean Sciences Meeting in New Orleans, LA.

Jesse Alan Roebuck, Jr., G. Brooks Avery, Robert J. Kieber, Stephen A. Skrabal, Ralph N. Mead, and David J. Felix. (2016). Biogeochemistry of Ethanol and Acetaldehyde in Freshwater Sediments. *Aquatic Geochemistry*. 22 (3), 177-195

G. Brooks Avery, Laura Foley, Angela L. Carroll, Jesse Alan Roebuck, Jr., Amanda Guy, Ralph N. Mead, Robert J. Kieber, Joan D. Willey, Stephen A. Skrabal, J. David Felix, Katherine M. Mullaugh, and John R. Helms. (2016). Surface Waters as a Sink and Source of Atmospheric Gas Phase Ethanol. *Chemosphere*. 144. 360-365

Robert J. Kieber, Amanda L. Guy, Jesse Alan Roebuck, Jr., Angela L. Carroll, Ralph N. Mead, S. Bart Jones, F. F. Giubbina, M. L. A. M. Campos, Joan D. Willey, and G. Brooks Avery. (2013). Determination of Ambient Ethanol Concentrations in Aqueous Environmental Matrixes by Two Independent Analyses. *Analytical Chemistry*. 85. 6095-6099